Study on Activation of Peroxo Compounds for Oxidative Degradation of Organic Contaminants and Inactivation of Bacteria in Water

THESIS

Submitted in partial fulfilment
of the requirements for the degree of
DOCTOR OF PHILOSOPHY
by

S. GOKULAKRISHNAN

Under the Supervision of
Prof. Halan Prakash

BIRLA INSTITUTE OF TECHNOLOGY AND SCIENCE
PILANI (RAJASTHAN) INDIA
2015

BIRLA INSTITUTE OF TECHNOLOGY AND SCIENCE
PILANI (RAJASTHAN)

CERTIFICATE

This is to certify that the thesis entitled "**Study on Activation of Peroxo Compounds for Oxidative Degradation of Organic Contaminants and Inactivation of Bacteria in Water"** and submitted by **S. GOKULAKRISHNAN** ID No. **2010PHXF017G** for award of Ph.D. degree of the Institute embodies original work done by him under my supervision.

Signature of the Supervisor:

Name: **Professor HALAN PRAKASH**

Designation: **Associate Professor, Department of Chemistry**

Date:17-07-2015

CONTENTS

ACKNOWLEDGEMENT

First and foremost, I thank my supervisor, Prof. Halan Prakash for his scholastic guidance that was fundamental to the successful completion of my research work.

I am thankful to Prof. Shyamalava Mazumdar, TIFR, Mumbai; Dr. Nitin Borkar, CEO, VerGo pharma, Goa; Dr. Subash, VerGo pharma, Goa; Dr. Kannan, NCBS, Bangalore and Dr. Rahul Mohan, NCAOR, Goa; for giving me the access to their facilities. I thank Prof. Suresh C. Pillai, Institute of Sligo, Ireland for his suggestions and help in getting XPS data.

I am grateful to Prof. Dinkar Sahal, ICGEB Delhi; and Prof. Srinivasan, Goa University, for their time and valuable suggestions.

I thank my Doctoral Advisory Committee members, Prof. Sunil Bhand and Prof. Meenal Kowshik, for their time, encouragement and valuable comments. I am thankful to Departmental Research Committee members for their useful reviews.

I thank my colleague Ms. Priyadarshini Parakh for her sincere support, suggestions, and active cooperation.

I thank Prof. K. E Raman, (former Director) and Prof. Sasikumar Punnekkat, (current Director) of BITS Pilani KK Birla Goa Campus for providing me the essential facilities for research. I am grateful to the Department of Chemistry for supporting interdisciplinary research, for providing opportunity to develop my teaching skills, for organising guest lectures, seminars and conferences that lifted my research interests, for providing a good environment to study, and facility to do research. I thank Prof. Raghu Nath Behera, Prof. Srikanth Mutnuri, Prof. Meenal Kowshik, and Prof. Meenakshi Raman for their lectures in my Ph.D course work. I thank the entire faculty for their kindly interaction and all my labmates for their support and friendship.

I am grateful to BITS Pilani KK Birla Goa Campus, Department of Biotechnology and Council of Scientific and Industrial Research for providing me financial support to complete my research work. I also thank Academic Research Division and Sponsored Research and Consultancy Division, BITS Pilani K K Birla Goa Campus for facilitating research activities.

I found no words to express my feelings to my beloved late mother for her indefinite love and constant blessings, and my family for their sincere love, sacrifice, support, encouragement and prayers.

Gokulakrishnan Subramanian

ABSTRACT

Activation of peroxo compounds such as persulphate and hydrogen peroxide generate stronger oxidants such as sulphate radical (2.43 V) and hydroxyl radical (2.73 V), respectively that readily degrade organic contaminants, and inactivate bacteria in water. While activation of peroxo compounds using transition metal ion Fe(II) is actively studied, the use of redox or photoredox active Ni(II), Ru(II) and Cu(II) metal complexes for the activation of peroxo compounds remains understudied.

In the present thesis, Nickel(II) hexaazamacrocylic complex was identified as a potential persulphate activator for the degradation of a variety of non biodegradable organic contaminants such as malachite green, ciprofloxacin, methyl orange, methylene blue and rhodamine B in a wide pH range (chapter 2). Importantly, the Nickel(II) hexaazamacrocylic complex was recovered using adsorbents such as activated carbon and amberlite, and reused in the homogeneous or heterogeneous forms for the activation of persulphate to degrade organic contaminant (chapter 3). Moreover, Ruthenium(II) trisbipyridyl complex was identified as a potential photochemical activator of persulphate. Very low concentration (1μM) of Ruthenium(II) trisbipyridyl complex activated persulphate upon visible light irradiation using energy efficient LED array as light source and caused the degradation of organic and bacterial contaminants in water (chapter 4). Copper based photo-Fenton like process under visible light irradiation activated hydrogen peroxide and caused effective inactivation of Gram negative and Gram positive bacteria. Importantly, effective disinfection of bacteria in water was achieved using very low concentration of Cu(II) ions i.e., ~20 times less than the permissible level of Cu(II) ions in drinking water (chapter 5). In addition, a new Copper(II) polypyridyl complex caused rapid photoinactivation of bacteria under visible light irradiation that is useful in water disinfection, as well as in photoantimicrobial chemotherapy (chapter 5). The findings of the present thesis revealed that Nickel(II), Ruthenium(II) and Copper(II) complexes are promising for the activation of peroxo compounds for the degradation of recalcitrant organic and bacterial contaminants in water.

Table of Content for Chapters

List of Tables

List of Figures

List of Tables and Figures in Supporting Information

List of Units, Symbols and Abbreviations

Units:

Å	Angstrom
µg	Microgram
ml	Millilitre
cm	Centimetre
eV	Electron volt
J	Joule
kV	Kilovolts
m/z	mass to charge ratio
mg	Milligram
mM	Millimolar
mm	Millimetre
mW	Milliwatt
ng	Nanogram
nm	nanometre
ppm	Parts Per Million
rpm	Revolutions per minute
V	volt
µl	Microlitre
µm	Micrometre
µM	Micromolar

Symbols:

°C	Degree Celsius
1/n	Freundlich constant indicative of intensity of adsorption
$^1O_2$	Singlet Oxygen
Ag	Silver
C	Final concentration
C_0	Initial concentration
C1	1,8-dimethyl-1,3,6,8,10,13-hexaazacyclotetradecane nickel (II) perchlorate
Co	Cobalt

Cu	Copper
Fe	Iron
H_2O_2	Hydrogen peroxide
K	Potassium
K_F	Adsorption capacity
K_F	Freundlich constant indicative of equilibrium adsorption capacity of the adsorbent
mAU	Milliampere units
m_d	Mass of desorbed complex into solution
Ni	Nickel
$O_2^{-\bullet}$	Superoxide anion
$OH^{\bullet}$	Hydroxyl radical
p	*p*- value (calculated probability)
q_e	Amount of substance adsorbed per unit weight of adsorbent at equilibrium
q_m	Freundlich maximum adsorption capacity
R^2	Correlation coefficient
Ru	Ruthenium
$SO_4^{\bullet-}$	Sulphate radical
wt%	Weight percent

Abbreviations:

5-NH_2-Phen	5-amino 1,10 phenanthroline
AAS	Atomic Absorption Spectroscopy
AC	Activated carbon
Am	Amberlite
ANOVA	Analysis of variance
AOP	Advanced oxidation process
BPA	Bisphenyl amine
bpy	2,2´ – bypyridine
BSA	Bovine Serum Albumin
CFU	Colony Forming Units
CPCB	Central Pollution Control Board
Cpf	Ciprofloxacin

DCP	Dichlorophenyl
DLBP	Dimethyl amino benophenone
DNA	Deoxyribonucleic acid
EDDS	Ethylenediamine-N,N'-disuccinic acid
EDTA	Ethylenediaminetetraacetic acid
FT – IR	Fourier Transform Infra Red
HTA	Hydroxy terephthalic acid
ISCO	*In situ* Chemical Oxidation
KPS	Potassium Persulpahte
LC – ESI – MS	Liquid Chromatography Electrospray Ionisation Mass Spectrometry
LED	Light emitting diode
LMG	Leuco malachite green
MB	Methylene blue
MG	Malachite green
MLCT	Metal to ligand charge transfer
MO	Methyl orange
NB	Nutrient broth
NIR	Near infrared
PACT	Photoantimicrobial Chemotherapy
PBS	Phosphate Buffered Saline
Phen	1, 10 phenanthroline
PS	Photosensitizer
PTFE	polytetrafluoroethylene
RhB	Rhodamine B
RP HPLC	Reverse phase high pressure liquid chromatography
RT	Retention time
SEM	Scanning Electron Microscopy
TA	Terephthalic acid
TIC	Total ion Chromatogram
TOC	Total Organic Carbon
UFLC	Ultra Fast Liquid Chromatography
UK	United Kingdom

US – EPA	United States –Environmental Protection Agency
US – FDA	United States Food and Drug Administration
UV	Ultraviolet
v/v	Volume/Volume
WHO	World Health Organisation
WWTP	Waste Water Treatment Plant
XPS	X – ray Photoelectron Spectroscopy

1. Introduction

1.1 The need to improve water quality:

Of the total water in earth, only ~ 0.77% is available for human use as fresh water resources in the form of lakes, rivers, and underground aquifers.[1, 2] These accessible fresh water resources are severely contaminated by human activities (anthropogenic contamination) leading to the depletion of water quality.[3] Manmade non biodegradable organic chemicals such as pharmaceuticals, personal care products, textile dyes and pesticides are entering water resources due to human activities, posing a threat to public health and environment.[4]

In general, domestic or municipal waste water (waste water from homes, laundries, hotels etc.,) is treated in wastewater treatment plants (WWTPs) that usually employ microbes to degrade organic contaminants.[5-8] It has been reported that certain non biodegradable contaminants such as pharmaceuticals, personal care products and pesticides are not eliminated by biological oxidation employed in WWTPs.[6-11] Consequently, these non-biodegradable contaminants are released in to fresh water bodies [9-12] (Figure 1.1) and termed as emerging pollutants.[10]

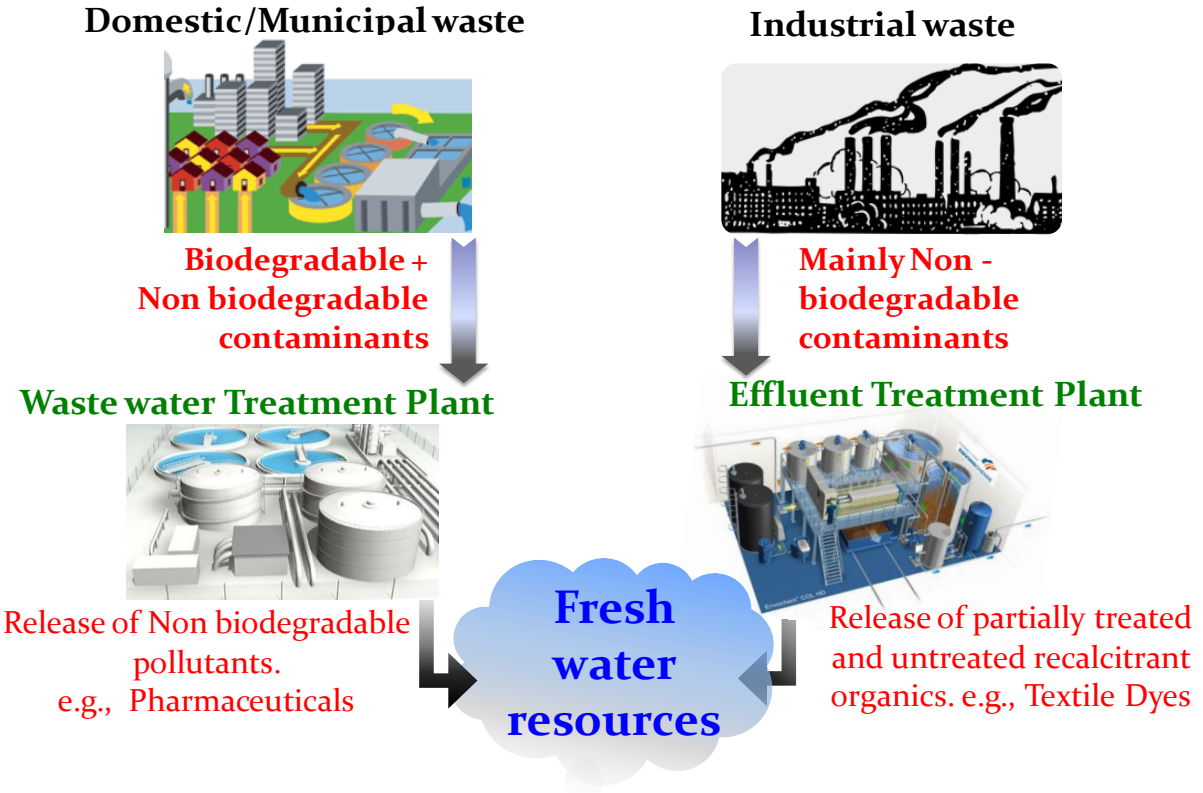

Figure 1.1 Contamination of fresh water resources by non-biodegradable contaminants from waste water treatment plants and industrial effluent treatment plants.

The US EPA (United States – Environmental Protection Agency) defines emerging

pollutants as new chemicals without regulatory status and which impact on environment and human health.[10] They are also called "micropollutants", because they are present in the aquatic environment in variable concentrations of ng L^{-1} to µg L^{-1} (eg. Ciprofloxacin, a broad spectrum antibiotic).[11, 13]

Moreover, the release of untreated or partially treated industrial effluents in to fresh water resources due to poor practice and lack of proper treatment methods at the industrial sites severely affects the water quality (Figure 1.1).[14] Thus, there is an urgent need for elimination of these persistent organic pollutants to improve the water quality. Chemical oxidative degradation methods are recognised as promising to improve the quality of waste water.

1.2 Non-biodegradable pollutants:

Chemicals with toxic properties, certain pharmaceuticals and dye pollutants are often not degraded into environmentally harmless products by natural process (such as microbial degradation) and termed as "Non-biodegradable" contaminants.[15]

For example, malachite green (MG), a biocide that is used to prevent the infection of fishes in fisheries is not effectively degraded by microbes (Figure 1.2).[16, 17] US FDA (United States – Food and Drug Association) nominated MG as a priority chemical for carcinogenicity and banned its use.[17] Although MG is not approved by the US FDA or the US EPA, it is extensively used as biocide in fish hatcheries; dye in textiles industries and as a colorant in food industries as it is relatively inexpensive, readily available, and highly efficacious.[16, 17] Previous research on microbial degradation of MG showed that MG is partially oxidised to other forms resulting in the decolourisation but not degradation.[18]

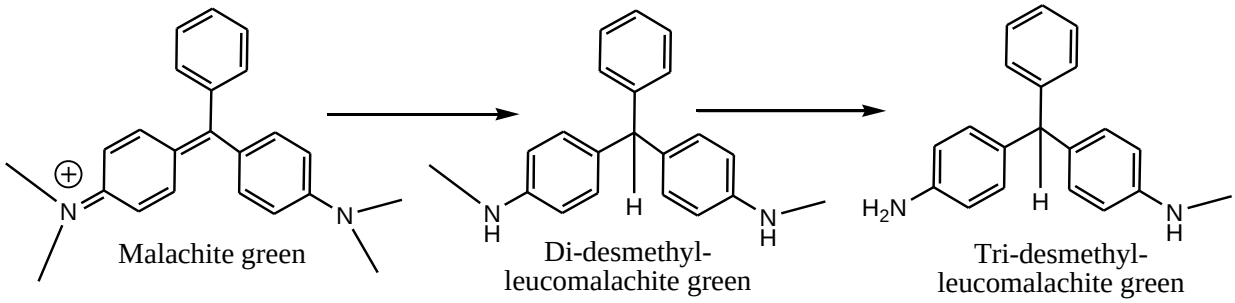

Figure 1.2 Structure of Malachite green and transformation products of MG on biological oxidation by *Pandoraea pulmonicola* YC32. [18]

It is important to note that MG and its partially oxidised products such as triphenyl amines that are not eliminated in biological oxidation are potentially harmful because of their

carcinogenic properties.[18]

Moreover, effluents from pharmaceutical companies and hospitals, unethical discharge of medical wastes or expired drugs by human beings are main sources of pharmaceutical pollution that contaminate fresh water supplies with pharmaceuticals.[6-8] It is important to note that pharmaceuticals such as antibiotics are designed to inhibit microbial cell growth and therefore not degraded by conventional biological oxidation.[7, 8, 19-21] The presence of even low concentration of antibiotics leads to the development of antibiotic resistance in bacteria that is dangerous to public health.[20]

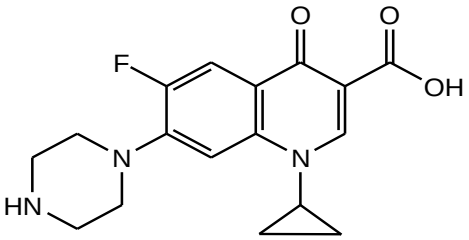

Figure 1.3 Structure of Ciprofloxacin

For example, Ciprofloxacin (Cpf) a broad spectrum fluoroquinolone antibiotic, is widely used in aquaculture and livestock husbandry, and prescribed for humans (Figure 1.3).[22] Previous research has revealed that Cpf that inhibit bacterial proliferation is non-biodegradable.[22, 23] It has been reported that in common WWTPs, most of the Cpf is not degraded but partly adsorbed on to activated sludge and the remaining escape from the treatment plants and contaminate water resources.[23, 24]

In addition, dye effluents from textile industries contain a variety of highly coloured dyes that absorb natural sunlight and affect light penetration into water bodies. Consequently, dye pollutants in water bodies impede photosynthesis and adversely affect the entire aquatic ecosystem.[25] It has been reported that the coloured dye effluents are also highly alkaline and ionic due to processing steps involved in dyeing industries and thus pose difficulty for degradation.[14, 25]

Methyl orange (MO, azo dye), methylene blue (MB, phenothiazine dye) and rhodamine B (RhB xanthine dye) are some common textile dyes. Importantly, MO, RhB and MB absorb visible light in the range of 350-580, 450-600 and 500-710 nm, respectively (Figure 1.4). Water contaminated with a mixture of these 3 dyes absorbs majority of the visible light radiation (350-710 nm), and could adversely affect the aquatic ecosystem. All above facts reveal that quality of water in fresh water sources is severely affected by a wide variety of non-biodegradable organic contaminants.

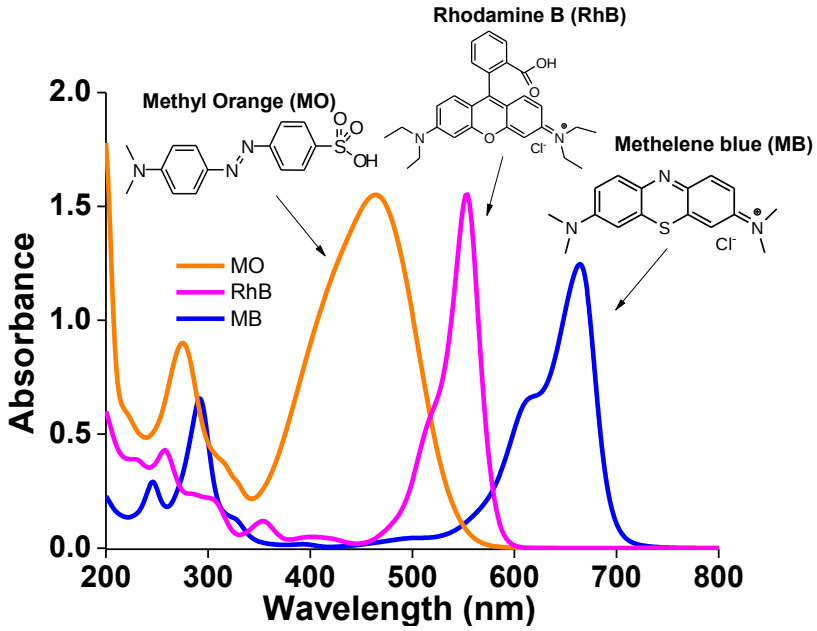

Figure 1.4 Structure and the absorption spectrum of dyes methyl orange (MO), rhodamine B (RhB) and methylene blue (MB).

Treatment technologies such as adsorption by activated carbon and other adsorbents do not degrade organic contaminants but transfer pollutants from one phase to another. In case of reverse osmosis, pollutants are not degraded, but concentrated and discharged as concentrated wastes.[26] There is a great demand for treatment process that effectively degrade recalcitrant (non biodegradable) organic pollutants and remove its toxicity. Advanced Oxidation Process (AOP) is recognised as a potential method for treatment of non-biodegradable toxic organic contaminants in to biodegradable products, and completely oxidise organic contaminants to CO_2, H_2O and inorganic ions, a process called mineralisation.

1.3 Advanced Oxidation Process:

Advanced oxidation process was first defined by Glaze in 1987 as near ambient temperature and pressure water treatment process which involve the generation of hydroxyl radicals in sufficient quantity that could effectively degrade organic pollutants.[27] Due to the ability of AOPs to degrade a variety of emerging non-biodegradable organic contaminants,[28, 29] AOP is termed as "*water treatment process of 21st century*".[30] Importantly, a recent approach is to use AOPs for partial oxidation of non biodegradable toxic organic pollutants to non-toxic biodegradable intermediates that could be degraded in the conventional biological treatment process employed in common WWTPs.[28,29] Peroxo compounds such as peroxydisulphate ($S_2O_8^{2-}$), commonly called as persulphate and hydrogen peroxide (H_2O_2) are used widely in AOPs as a source of sulphate and hydroxyl radicals, respectively. Sulphate and

hydroxyl radicals can completely degrade and mineralize recalcitrant organic contaminants. AOP that rely on hydroxyl radical as primary oxidant is called as hydroxyl radical based AOP or conventional AOP.[31] Recently, sulphate radical based AOP that rely on sulphate radical as primary oxidant, has been recognised as one of the powerful AOP.[32]

1.4 Activated persulphate for degradation of non-biodegradable organic contaminants and bacteria:

Persulphate ($S_2O_8^{2-}$) is a relatively stable solid white powder. It is a two electron oxidizing agent with a redox potential of (2.01V, reaction 1).[33] Persulphate can oxidise organic contaminants in three ways: (i) direct oxidation of organic contaminants by persulphate itself (reaction 1) (ii) by generation of sulphate radicals via homolytic or heterolytic cleavage of peroxo bond of persulphate, a process called 'activation' (reactions 2-3)[36] (iii) by producing another powerful oxidant, hydroxyl radical (2.8 V) formed by reaction of sulphate radicals in aqueous medium at neutral and alkaline pH (reactions 4-5).[33-37]

$$S_2O_8^{2-} + 2e^- \longrightarrow 2SO_4^{2-} \quad (2.01\ V) \qquad \text{.....(1)}$$

$$S_2O_8^{2-} \xrightarrow{UV} 2SO_4^{\bullet -} \quad \text{(Homolytic Cleavage)} \qquad \text{.....(2)}$$

$$S_2O_8^{2-} + M^{n+} \longrightarrow SO_4^{2-} + SO_4^{\bullet -} + M^{n+1} \quad \text{(Heterolytic Cleavage) ..(3)}$$

$$M = Fe^{2+} \text{ or } Ag^{+}$$

$$SO_4^{\bullet -} + H_2O \longrightarrow HSO_4^- + OH^{\bullet} \qquad \text{.....(4)}$$

$$OH^{\bullet} + S_2O_8^{2-} \longrightarrow HSO_4^- + SO_4^{\bullet -} + 1/_2\ O_2 \qquad \text{.....(5)}$$

Importantly, sulphate and hydroxyl radicals react readily with organic or microbial pollutants leading to their degradation and even mineralisation.[33, 36, 38] Persulphate can be activated by UV,[39] heat,[40] transition metal ions and metal complexes.[34, 41, 42] Among these activation strategies, activation of persulphate by using metal ions or metal complexes is widely preferred because it is relatively feasible, economic and effective.[34, 36, 38] Activation of persulphate by metal ion catalysis occurs by an oxidation – reduction reaction in which low valent metal ions M^{n+} act as reducing agents and get oxidised to higher valency (reaction 3).[42] Redox active transition metal ions such as Co(II), Fe(II), Cu(II), Ag(I), have been studied for activation of persulphate to degrade a variety of organic contaminants. [34, 41, 42]

1.5 Gap in literature:

1.5 (a) Metal complex based persulphate activation:

The redox chemistry of metal azamacrocyclic complexes has been extensively studied.[43]A variety of Nickel(II) azamacrocyclic complexes having different redox properties have already been reported. [43, 44] Nickel(II) hexaazamacrocyclic complex (C1), $[Ni(II)L]^{2+}$ (Figure 1.5A) forms an ion-pair complex with persulphate, followed by nickel ion assisted heterolytic cleavage of peroxo bond of persulphate leading to the generation of sulphate radical and trivalent nickel species (reactions 7-9).[45] However, reaction between persulphate and nickel(II) azamacrocyclic complex, and its effect on recalcitrant organic pollutants such as biocides, antibiotics and dyes has not been studied. Moreover, Ag(I) ion was shown to activate persulphate effectively.[42, 46, 47] The activation of persulphate by silver salts such as silver sulphate and silver nitrate, in which the Ag is in +1 oxidation state has been studied for the degradation of contaminants such as 2,4 –dichlorophenol and Triclosan using stoichiometric concentrations of Ag(I) and persulphate.[46, 47]

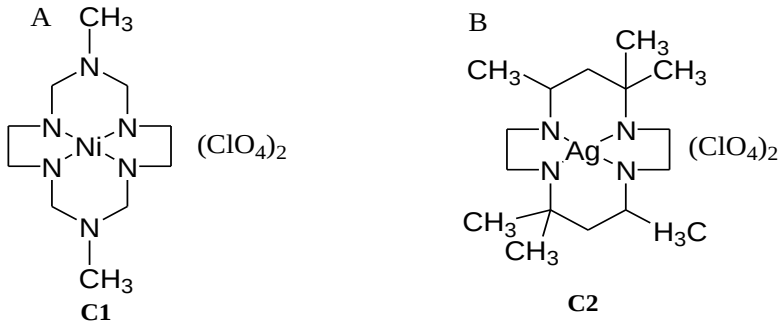

Figure 1.5 (A) Structure of 1,8-dimethyl-1,3,6,8,10,13-hexaazacyclotetradecane nickel (II) perchlorate, C1 and (B) 5,5,7,12,12,14-hexamethyltetraazacyotetradecanesilver(II) perchlorate, C2.

$$[Ni(II)L]^{2+} + S_2O_8^{2-} \rightleftharpoons \{Ni(II)L^{2+}, S_2O_8^{2-}\} \quad \text{.... (7)}$$

L = azamacrocyclic ligand; C1; ion-pair

$$\{Ni(II)L^{2+}, S_2O_8^{2-}\} \longrightarrow [Ni(III)L(SO_4)]^{+} + SO_4^{\bullet -} \text{.... (8)}$$

trivalent nickel 290 nm species

$$[Ni(II)L]^{2+} + SO_4^{\bullet -} \longrightarrow [Ni(III)L(SO_4)]^{+} \quad \text{.... (9)}$$

where, $[Ni(II)L]^{2+}$ = 1,8-dimethyl-1,3,6,8,10,13-hexaazacyclotetradecane nickel (II) perchlorate

Generally, Ag exists in +1 oxidation state. Divalent oxidation state of Ag is uncommon and highly unstable. Interestingly, tetra azamacrocyclic ligands stabilise Ag in +2 and +3

oxidation states.[48, 49] However activation of persulphate using a silver tetra azamacrocyclic complex has not been carried out.

1.5 (b) Recovery and reuse of homogeneous metal complex based persulphate activator:

It is important to note that, the transition metal ions and metal complexes used for persulphate based AOPs are leftover in water after the degradation of organic pollutants. The separation of such useful metal complex based persulphate activators from the treated water using common adsorbents employed in water remediation, and recycling these activators is imperative. The charge of the metal complex and the nature of the ligand could favour the adsorption of metal complex onto ion exchange resins (eg. Amberlite) and carbon based adsorbents (eg. activated carbon). Moreover, adsorptive immobilisation of a metal complex based persulphate activator could transform a homogeneous activator into heterogeneous form that is highly preferred in environmental catalysis. However, immobilisation of a redox active metal complex based persulphate activator onto adsorbents and their effect on organic contaminant degradation has not been studied.

1.5 (c) Visible light activation of persulphate using photoactive metal complex:

Persulphate has been studied as a sacrificial electron acceptor in tris(2,2′-bipyridyl)-ruthenium(II) bypyridine (Figure 1.6), ($[Ru(bpy)_3]^{2+}$) based photolytic water splitting for hydrogen production.[50]

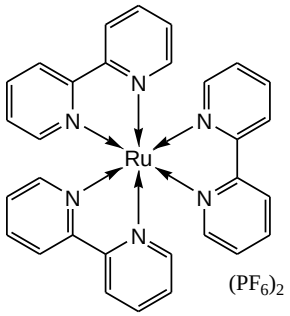

Figure 1.6 Structure of Tris(2,2′-bipyridyl)ruthenium(II) hexafluorophosphate complex.

Importantly, the electron transfer from the excited $[Ru(bpy)_3]^{2+}$* to $[S_2O_8]^{2-}$ occurs upon irradiation of $[Ru(bpy)_3]^{2+}$ in the range of 420-520 nm wavelength. Excited state $[Ru(bpy)_3]^{2+}$* transfer an electron to $[S_2O_8]^{2-}$ via MLCT that results in the heterolytic cleavage of peroxo bond of persulphate and formation of sulphate radical and $[Ru(bpy)_3]^{3+}$(reactions 10-12).[51, 52]

$$[Ru(bpy)_3]^{2+} + h\nu \longrightarrow [Ru(bpy)_3]^{2+*} \quad .....(10)$$

$$[Ru(bpy)_3]^{2+*} + [S_2O_8]^{2-} \longrightarrow [Ru(bpy)_3]^{3+} + SO_4^{2-} + SO_4^{\bullet -} .....(11)$$

$$[Ru(bpy)_3]^{2+} + SO_4^{\bullet -} \longrightarrow [Ru(bpy)_3]^{3+} + SO_4^{2-} \quad .....(12)$$

Both sulphate radical and $[Ru(bpy)_3]^{3+}$are strong oxidants capable of oxidising organic compounds.[53, 54] However, the effect of photochemical activation of persulphate using $[Ru(bpy)_3]^{2+}$ on recalcitrant organic contaminants has not been studied. Activation of persulphate by visible light irradiation using a photo redox active metal complex such as $[Ru(bpy)_3]^{2+}$ has not been carried out, although activation of persulphate by UV photolysis[39] has been studied for the degradation of organic contaminants. Few studies have shown that persulphate used in *in-situ chemical oxidation* (ISCO) process for the degradation of soil contaminants could retard the metabolic activity of indigenous soil microorganisms.[55] Moreover, it is important to note that oxidants such as sulphate and hydroxyl radicals generated by activation of persulphate in aqueous media could degrade organic contaminants,[38, 41, 42, 47, 56-59] as well as damage vital biomolecules such as DNA and cell membrane.[53, 54, 60-63] However, the direct effect of activated persulphate for simultaneous degradation of organic and microbial contaminants has also not been studied.

1.6 Activated hydrogenperoxide for elimination of bacterial pollutants:

H_2O_2 is widely used as disinfectant in water treatment, medical and domestic sanitation purposes.[64-66] Importantly, the activation of H_2O_2 i.e. cleavage of peroxo bond of H_2O_2 generate hydroxyl radical ($OH^{\bullet}$), reaction 13-14.[67]

$$H_2O_2 + 2H^+ + 2e^- \longrightarrow 2H_2O \ (1.78\ V) \quad .....(13)$$

$$2\ OH^{\bullet} + 2H^+ + 2e^- \longrightarrow 2H_2O \ (2.76\ V) \quad .....(14)$$

Hydroxyl radical ($OH^{\bullet}$) is the most powerful (2.6 V) of the reactive oxygen species that readily react with organic compounds including vital microbial cell components such as lipids, proteins, and DNA.[68, 69] Thus, strategies for activation of hydrogen peroxide to generate hydroxyl radical is actively studied for the inactivation of bacteria in water.[62, 70, 71]

UV irradiation and transition metal catalysis are two common strategies employed for H_2O_2 activation to inactivate bacteria in water.[67, 70] UV- H_2O_2 oxidation process is relatively costly because of the energy intensive UV lamps used as light source.[72] Moreover, it is generally inefficient for disinfection of turbid waters such as waste water because of the impairment of UV light penetration. On the other hand, activation of H_2O_2 using transition

metal ions is less expensive and effective for treatment of even turbid water. As a result, transition metal ions/complexes are preferred to activate H_2O_2 for remediation of waste water contaminated with organic and microbial pollutants.[62, 70, 73] Use of Fe(II) ions and H_2O_2, popularly known as Fenton process generate hydroxyl radicals. The first mechanistic proposal for the formation of $OH^{\bullet}$ radicals from H_2O_2 in the presence of the transition metal Fe(II) was formulated by Haber and Weiss.[74] This mechanism involves the one-electron oxidation of Fe(II) to Fe(III) accompanied by the homolytic O−O bond cleavage and generation of reactive hydroxyl radical (reaction 15-16).[75]

$$[Fe(II)(H_2O)_6]^{2+} + H_2O_2 \longrightarrow [Fe(III)(H_2O)_5(OH)]^{2+} + OH^{\bullet} + H_2O \quad .....(15)$$

$$[Fe(III)(H_2O)_5(OH)]^{2+} + H_2O_2 \longrightarrow [Fe(II)(H_2O)_6]^{2+} + HOO^{\bullet} \quad .....(16)$$

The above Fenton reaction at neutral pH generates iron sludge due to low solubility of Fe(III) species which is undesirable in Fenton based degradation process. [71]

1.6 (a) Gap in literature: Fenton-like process for water disinfection:

Reaction between Cu(I) species and H_2O_2 commonly known as copper based Fenton-like reaction generates hydroxyl radical (reaction 17). The hydroxyl radical formed in Fenton-like reaction (reaction 17) cause oxidative damage to bacteria, that is useful for water disinfection.[73, 78] Cu(II) species in presence of H_2O_2 may undergo slow reduction to Cu(I) state (reaction 18) that could generate hydroxyl radical due to Copper based Fenton-like reaction (reaction 17), and induce damage to biomolecules and bacteria.[70, 73, 76-78]

$$Cu(I) + H_2O_2 \longrightarrow Cu(II) + {}^{\bullet}OH + OH^{-} \quad .....(17)$$

$$Cu(II) + H_2O_2 \longrightarrow Cu(I) + {}^{\bullet}HO_2 + H^{+} \quad .....(18)$$

It is important to note that Cu(II) complexes of amino acids, peptides and proteins photoreduce to Cu(I) state that undergo copper based Fenton-like reaction to produce hydroxyl radical (reaction 17).[76,77,81] Cu(II) ions are known to bind bacterial cell surface.[58,82] These facts indicate that irradiation of bacterial cell components such as proteins and peptides bound to Cu(II) ions in presence of H_2O_2 could enhance the inactivation of bacteria by activation of H_2O_2. Nevertheless, the effect of visible light irradiation on copper based Fenton-like reaction for inactivation of bacteria is not known.

1.7 Metal complexes in Photo-antimicrobial chemotherapy (PACT):

Photo-antimicrobial chemotherapy (PACT) involves the use of light and photosensitizer to kill pathogenic microbes.[83, 84, 85] A photosensitizer (PS) molecule absorbs energy in the form of light and gets excited from its ground state. In this excited state, the PS can cause a chemical change in the neighbouring molecule via two pathways called Type I and Type II photochemical reaction (Figure 1.7).[83, 84, 85] The type I pathway involves an electron transfer step between the triplet PS and a nearby substrate with generation of radical species. The type II pathway involves an electronic energy transfer process from the triplet PS to molecular oxygen leading to generation of highly reactive singlet oxygen. [83, 84, 85] Thus, irradiation of a PS at appropriate wavelength leads to the formation of cytotoxic species (reactive oxygen species such as singlet oxygen ($^1O_2$), superoxide ion and free radicals) which could oxidize intracellular molecules and thereby destroy cells (Figure 1.7). [83,84, 85]

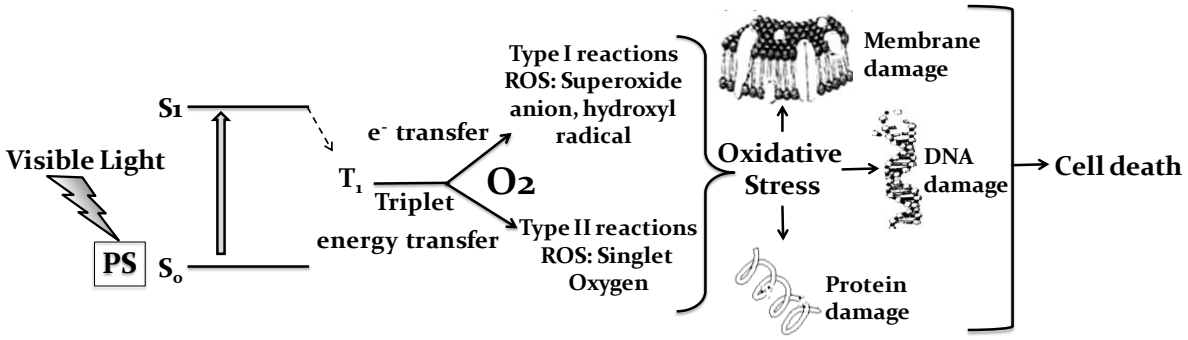

Figure 1.7 Illustration of the mechanism of photoantimicrobial chemotherapy (PACT). S_0 – PS at the ground state, S_1 - exited state PS, T_1 PS at triplet state, e^- - electron.

Usually, PS is injected into the target area, where it accumulates and is exposed to light of a specific wavelength. This reaction induces the production of reactive oxygen species (ROS) that causes oxidative damage to the target bacterial cells leading to its death. [83,84, 85] The key advantage of PACT is that the microbes cannot develop resistance against PACT.[83-85]

Earlier, it has been shown that Ru(II) polypyridyl complexes with membrane binding ligands were able to photoinactivate *Escherichia coli* efficiently, indicating the potential of transition metal complexes as effective photoantimicrobial agents.[86] It is important to note that Copper(II) polypyridyl complexes are photoactive in nature and upon irradiation generate reactive oxygen species such as superoxide anion and singlet oxygen[79, 80, 87, 88] that are detrimental to bacteria. Nevertheless, photoantibacterial activities of Copper(II) polypyridyl complexes remains unexplored. Study on the effect of photoactive Copper(II) complexes on bacteria is important to develop efficient PACT agents, and would also be useful to disinfect water contaminated with microbes.

1.7 (a) Gap in literature: Visible light emitting diodes as light source for degradation of organic and bacterial contaminants in water:

Light emitting diodes (LEDs) are emerging light sources with attractive properties such as low power input, high energy efficiency, and small size. These properties make them an effective alternate light source for photocatalytic water purification.[89, 90] Ultra violet light emitting diodes have been used to drive photochemical AOPs for degradation of organic and microbial pollutants.[89-91] Moreover, visible light emitting LEDs with different emission spectrum and light intensities are commercially available (Figure 1.8). However, the application of LEDs, in particular, visible light LEDs are underexplored for the photochemical AOPs.

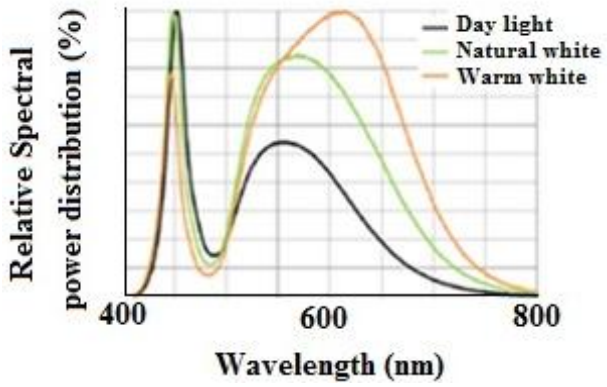

Figure 1.8 Emission spectrum of commercially available visible light LEDs (http://www.kwalityindia.com).

Visible light driven AOPs is particularly advantageous as visible light irradiation is harmless to human beings unlike UV irradiation. Moreover, visible light of natural sunlight could be useful in visible light driven AOPs. Thus in the present work, custom fabricated visible light- LED arrays have been used as the light source for driving the photochemical AOPs.

1.8 Objectives of present study:

Based on all the above facts, the main objectives of the present work are:

(a) To study the activation of peroxo compounds such as persulphate and hydrogen peroxide using redox active or photoredox active metal complexes.

(b) To study the effect of metal complex/metal ions activated peroxo compounds on non biodegradable organic contaminants in water.

(c) To study the effect of metal complex/metal ions activated peroxo compounds on bacterial contaminants, and vital biomolecules such as cell membrane and DNA.

1.9 Thesis Structure:

- **Chapter 1** provides an introduction to the activation of peroxo compounds, current literature review and existing gaps on the use of metal complexes or metal ions for activation of peroxo compounds.
- **Chapter 2** presents the activation of persulphate using Ni(II) hexa azamacrocyclic complex for degradation of a variety of recalcitrant organic contaminants in water.
- **Chapter 3** illustrates the adsorptive recovery and reuse of metal complex based persulphate activators using Ni(II) hexa azamacrocyclic complex and adsorbents such as activated carbon and amberlite.
- **Chapter 4** reveals the visible light induced photochemical activation of persulphate using Ru(II)tris bipyridyl complex for the degradation of organic as well as bacterial contaminants in water.
- **Chapter 5** examines the effect of Copper based photo Fenton-like process on bacterial inactivation.
- **Chapter 6** presents the key findings of this thesis and suggests future research.

1.10 References:

1. Gleick, P. H., *Water in crisis: a guide to the world's fresh water resources*. Oxford University Press, Inc.: **1993**.

2. Postel, S. L.; Daily, G. C.; Ehrlich, P. R., Human appropriation of renewable fresh water. *Science-AAAS-Weekly Paper Edition* **1996,** *271* (5250), 785-787.

3. Rhind, S., Anthropogenic pollutants: a threat to ecosystem sustainability? *Philosophical Transactions of the Royal Society B: Biological Sciences* **2009,** *364* (1534), 3391-3401.

4. Vorosmarty, C. J.; Mc Intyre, P. B.; Gessner, M. O.; Dudgeon, D.; Prusevich, A.; Green, P.; Glidden, S.; Bunn, S. E.; Sullivan, C. A.; Liermann, C. R.; Davies, P. M., Global threats to human water security and river biodiversity. *Nature* **2010,** *467* (7315), 555-561.

5. Michael, I.; Rizzo, L.; McArdell, C. S.; Manaia, C. M.; Merlin, C.; Schwartz, T.; Dagot, C.; Fatta-Kassinos, D., Urban wastewater treatment plants as hotspots for the release of antibiotics in the environment: A review. *Water Research* **2013,** *47* (3), 957-995.

6. Batt, A. L.; Kim, S.; Aga, D. S., Comparison of the occurrence of antibiotics in four full-scale wastewater treatment plants with varying designs and operations. *Chemosphere* **2007,** *68* (3), 428-435.

7. Miao, X.S.; Bishay, F.; Chen, M.; Metcalfe, C. D., Occurrence of antimicrobials in the final effluents of wastewater treatment plants in canada. *Environmental Science & Technology* **2004,** *38* (13), 3533-3541.

8. McArdell, C. S.; Molnar, E.; Suter, M. J. F.; Giger, W., Occurrence and fate of macrolide antibiotics in wastewater treatment plants and in the Glatt Valley Watershed, Switzerland.

Environmental Science & Technology **2003,** *37* (24), 5479-5486.

9. Kammerer, K.; Daughton, C. G., PPCPs in the Environment: Future research- beginning with the end always in mind. In *Pharmaceuticals in the Environment*, Springer Berlin Heidelberg: **2004**; pp 463-495.

10. Deblonde, T.; Cossu Leguille, C.; Hartemann, P., Emerging pollutants in wastewater: A review of the literature. *International Journal of Hygiene and Environmental Health* **2011,** *214* (6), 442-448.

11. Pal, A.; Gin, K. Y.H.; Lin, A. Y.C.; Reinhard, M., Impacts of emerging organic contaminants on freshwater resources: review of recent occurrences, sources, fate and effects. *Science of The Total Environment* **2010,** *408* (24), 6062-6069.

12. Fram, M. S.; Belitz, K., Occurrence and concentrations of pharmaceutical compounds in groundwater used for public drinking-water supply in California. *Science of The Total Environment* **2011,** *409* (18), 3409-3417.

13. Miralles Cuevas, S.; Arquas, A.; Maldonado, M. I.; Sanchez-Parez, J. A.; Malato Rodraguez, S., Combined nanofiltration and photo-Fenton treatment of water containing micropollutants. *Chemical Engineering Journal* **2013,** *224* (0), 89-95.

14. Lefebvre, O.; Moletta, R., Treatment of organic pollution in industrial saline wastewater: A literature review. *Water Research* **2006,** *40* (20), 3671-3682.

15. Moreno Casillas, H. A.; Cocke, D. L.; Gomes, J. A. G.; Morkovsky, P.; Parga, J. R.; Peterson, E., Electrocoagulation mechanism for COD removal. *Separation and Purification Technology* **2007,** *56* (2), 204-211.

16. Culp, S. J.; Mellick, P. W.; Trotter, R. W.; Greenlees, K. J.; Kodell, R. L.; Beland, F. A., Carcinogenicity of malachite green chloride and leucomalachite green in B6C3F1 mice and F344 rats. *Food and Chemical Toxicology* **2006,** *44* (8), 1204-1212.

17. Srivastava, S.; Sinha, R.; Roy, D., Toxicological effects of malachite green. *Aquatic Toxicology* **2004,** *66* (3), 319-329.

18. Chen, C. Y.; Kuo, J. T.; Cheng, C. Y.; Huang, Y. T.; Ho, I. H.; Chung, Y. C., Biological decolorization of dye solution containing malachite green by *Pandoraea pulmonicola* YC32 using a batch and continuous system. *Journal of Hazardous Materials* **2009,** *172* (2-3), 1439-1445.

19. Fatta Kassinos, D.; Meric, S.; Nikolaou, A., Pharmaceutical residues in environmental waters and wastewater: current state of knowledge and future research. *Analytical and Bioanalytical Chemistry* **2011,** *399* (1), 251-275.

20. Rizzo, L.; Manaia, C.; Merlin, C.; Schwartz, T.; Dagot, C.; Ploy, M. C.; Michael, I.; Fatta-Kassinos, D., Urban wastewater treatment plants as hotspots for antibiotic resistant bacteria and genes spread into the environment: A review. *Science of The Total Environment* **2013,** *447* (0), 345-360.

21. Snyder, S. A., Occurrence, treatment, and toxicological relevance of EDCs and pharmaceuticals in water. *Ozone: Science & Engineering* **2008,** *30* (1), 65-69.

22. Sun, S.P.; Guo, H.Q.; Ke, Q.; Sun, J.H.; Shi, S.H.; Zhang, M.L.; Zhou, Q., Degradation of

antibiotic Ciprofloxacin hydrochloride by photo-Fenton oxidation process. *Environmental Engineering Science* **2008,** *26* (4), 753-759.

23. Vasconcelos, T. A. G.; Henriques, D. M.; Kanig, A.; Martins, A. F.; Kammerer, K., Photo-degradation of the antimicrobial ciprofloxacin at high pH: identification and biodegradability assessment of the primary by-products. *Chemosphere* **2009,** *76* (4), 487-493.

24. Watkinson, A. J.; Murby, E. J.; Costanzo, S. D., Removal of antibiotics in conventional and advanced wastewater treatment: Implications for environmental discharge and wastewater recycling. *Water Research* **2007,** *41* (18), 4164-4176.

25. Anjaneyulu, Y.; Sreedhara Chary, N.; Samuel Suman Raj, D., Decolourization of industrial effluents "Available Methods and Emerging Technologies" - A Review. *Reviews in Environmental Science and Bio/Technology* **2005,** *4* (4), 245-273.

26. Zhang, M.; An, T.; Fu, J.; Sheng, G.; Wang, X.; Hu, X.; Ding, X., Photocatalytic degradation of mixed gaseous carbonyl compounds at low level on adsorptive TiO_2/SiO_2 photocatalyst using a fluidized bed reactor. *Chemosphere* **2006,** *64* (3), 423-431.

27. Glaze, W. H.; Kang, J.W.; Chapin, D. H., The chemistry of water treatment processes involving ozone, Hydrogen Peroxide and Ultraviolet Radiation. *Ozone: Science & Engineering* **1987,** *9* (4), 335-352.

28. Comninellis, C.; Kapalka, A.; Malato, S.; Parsons, S. A.; Poulios, I.; Mantzavinos, D., Advanced oxidation processes for water treatment: advances and trends for R&D. *Journal of Chemical Technology and Biotechnology* **2008,** *83* (6), 769-776.

29. Andreozzi, R.; Caprio, V.; Insola, A.; Marotta, R., Advanced oxidation processes (AOP) for water purification and recovery. *Catalysis Today* **1999,** *53* (1), 51-59.

30. Munter, R., Advanced oxidation processes- current status and prospects. *Proceedings of Estonian Academy Sciences-Chemistry* **2001,** *50* (2), 59-80.

31. Grebel, J. E.; Pignatello, J. J.; Mitch, W. A., Effect of halide ions and carbonates on organic contaminant degradation by hydroxyl radical-based advanced oxidation processes in saline waters. *Environmental Science & Technology* **2010,** *44* (17), 6822-6828.

32. Deng, Y.; Ezyske, C. M., Sulfate radical-advanced oxidation process (SR-AOP) for simultaneous removal of refractory organic contaminants and ammonia in landfill leachate. *Water Research* **2011,** *45* (18), 6189-6194.

33. Yuan, S.; Liao, P.; Alshawabkeh, A. N., Electrolytic Manipulation of Persulfate Reactivity by Iron Electrodes for Trichloroethylene Degradation in Groundwater. *Environmental Science & Technology* **2013,** *48* (1), 656-663.

34. Xiong, X.; Sun, B.; Zhang, J.; Gao, N.; Shen, J.; Li, J.; Guan, X., Activating persulfate by Fe (0) coupling with weak magnetic field: Performance and mechanism. *Water Research* **2014,** *62*, 53-62.

35. Fang, G. D.; Gao, J.; Dionysiou, D. D.; Liu, C.; Zhou, D. M., Activation of Persulfate by Quinones: Free Radical Reactions and Implication for the Degradation of PCBs. *Environmental Science & Technology* **2013,** *47* (9), 4605-4611.

36. Ahn, S.; Peterson, T. D.; Righter, J.; Miles, D. M.; Tratnyek, P. G., Disinfection of ballast

water with iron activated persulfate. *Environmental Science & Technology* **2013,** *47* (20), 11717-11725.

37. Liu, H. Z.; Bruton, T. A.; Doyle, F. M.; Sedlak, D. L., In situ chemical oxidation of contaminated groundwater by persulfate: Decomposition by Fe(III)- and Mn(IV)-containing oxides and aquifer materials. *Environmental Science & Technology* **2014,** *48* (17), 10330-10336.

38. Ahmed, M. M.; Chiron, S., Solar photo-Fenton like using persulphate for carbamazepine removal from domestic wastewater. *Water Res.,* **2014,** *48* (0), 229-236.

39. He, X.; de la Cruz, A. A.; O'Shea, K. E.; Dionysiou, D. D., Kinetics and mechanisms of cylindrospermopsin destruction by sulfate radical-based advanced oxidation processes. *Water Research* **2014,** *63* (0), 168-178.

40. Waldemer, R. H.; Tratnyek, P. G.; Johnson, R. L.; Nurmi, J. T., Oxidation of chlorinated ethenes by heat-activated persulfate:- kinetics and products. *Environmental Science & Technology* **2006,** *41* (3), 1010-1015.

41. Rastogi, A.; Al Abed, S. R.; Dionysiou, D. D., Effect of inorganic, synthetic and naturally occurring chelating agents on Fe(II) mediated advanced oxidation of chlorophenols. *Water Research* **2009,** *43* (3), 684-694.

42. Anipsitakis, G. P.; Dionysiou, D. D., Radical generation by the interaction of transition metals with common oxidants. *Environmental Science & Technology* **2004,** *38* (13), 3705-3712.

43. Liang, X.; Sadler, P. J., Cyclam complexes and their applications in medicine. *Chemical Society Reviews* **2004,** *33* (4), 246-266.

44. Nag, K.; Chakravorty, A., Monovalent, trivalent and tetravalent nickel,. *Coordination Chemistry Reviews* **1980,** ***33***, 87.

45. Haines, R. I.; Rowley, J. E., Structure and kinetics of oxidation of amphiphilic Nickel(II) pentaazamacrocycles by peroxodisulfate and by a Nickel(III) pendant-arm macrocycle. *Journal of Inclusion Phenomena and Macrocyclic Chemistry* **2003,** *47* (1), 25-32-32.

46. Nfodzo, P.; Choi, H., Triclosan decomposition by sulfate radicals: effects of oxidant and metal doses. *Chemical Engineering Journal* **2011,** *174* (2), 629-634.

47. Anipsitakis, G. P.; Dionysiou, D. D., Transition metal/UV-based advanced oxidation technologies for water decontamination. *Applied Catalysis B: Environmental* **2004,** *54* (3), 155-163.

48. Barefield, E. K.; Mocella, M. T., Complexes of silver (II) and silver (III) with macrocyclic tetraaza ligands. *Inorganic Chemistry* **1973,** *12* (12), 2829-2832.

49. Clark, I.; Harrowfield, M. B., Electrochemistry and photochemistry of silver (II) complexes of macrocyclic amines. *Inorganic Chemistry* **1984,** *23* (23), 3740-3745.

50. Henbest, K.; Douglas, P.; Garley, M. S.; Mills, A., Persulphate quenching of the excited state of ruthenium(II) tris-bipyridyl dication: thermal reactions. *Journal of Photochemistry and Photobiology A: Chemistry* **1994,** *80* (1-3), 299-305.

51. Kaledin, A. L.; Huang, Z.; Geletii, Y. V.; Lian, T.; Hill, C. L.; Musaev, D. G., Insights into photoinduced electron eransfer between $[Ru(bpy)_3]^{2+}$ and $[S_2O_8]^{2-}$ in water: Computational and Experimental Studies. *The Journal of Physical Chemistry A* **2009,** *114* (1), 73-80.

52. Kaledin, A. L.; Huang, Z.; Yin, Q.; Dunphy, E. L.; Constable, E. C.; Housecroft, C. E.; Geletii, Y. V.; Lian, T.; Hill, C. L.; Musaev, D. G., Insights into photoinduced electron transfer between $[Ru(mptpy)_2]^{4+}$ and $[S_2O_8]^{2-}$: Computational and experimental studies. *The Journal of Physical Chemistry A* **2010,** *114* (21), 6284-6297.

53. Aboul Enein, A.; Schulte Frohlinde, D., Biological deactivation and single-strand breakage of plasmid DNA by photosensitization using Tris(2,2′- Bipyridyl)Ruthenium(II) and peroxydisulfate. *Photochemistry and Photobiology* **1988,** *48* (1), 27-34.

54. Tossi, A. B.; Garner, H., Photoinduced interaction of $Ru(bpy)_3^{2+}$ with nucleotides and nucleic acids in the presence of $S_2O_8^{2-}$: A transient conductivity study. *Journal of Photochemistry and Photobiology B: Biology* **1993,** *17* (2), 115-125.

55. Tsitonaki, A.; Smets, B. F.; Bjerg, P. L., Effects of heat-activated persulfate oxidation on soil microorganisms. *Water Research* **2008,** *42* (4-5), 1013-1022.

56. Antoniou, M. G.; Andersen, H. R., Comparison of UVC/$S_2O_8^{2-}$ with UVC/H_2O_2 in terms of efficiency and cost for the removal of micropollutants from groundwater. *Chemosphere* **2015,** *119,* S81-S88.

57. Antoniou, M. G.; de la Cruz, A. A.; Dionysiou, D. D., Degradation of microcystin-LR using sulfate radicals generated through photolysis, thermolysis and $e^{(-)}$ transfer mechanisms. *Applied Catalysis B-Environmental* **2010,** *96* (3-4), 290-298.

58. Rensing, C.; Grass, G., *Escherichia coli* mechanisms of copper homeostasis in a changing environment. *FEMS Microbiology Reviews* **2003,** *27* (2-3), 197-213.

59. Waldemer, R. H.; Tratnyek, P. G.; Johnson, R. L.; Nurmi, J. T., Oxidation of chlorinated ethenes by heat-activated persulfate: kinetics and products. *Environmental Science & Technology* **2007,** *41* (3), 1010-1015.

60. Muller, J. G.; Hickerson, R. P.; Perez, R. J.; Burrows, C. J., DNA damage from sulfite autoxidation catalyzed by a Nickel(II) peptide. *Journal of the American Chemical Society* **1997,** *119* (7), 1501-1506.

61. Lepentsiotis, V.; Domagala, J.; Grgic, I.; Van Eldik, R.; Muller, J. G.; Burrows, C. J., Mechanistic Information on the Redox Cycling of Nickel(II/III) Complexes in the presence of sulfur oxides and oxygen. Correlation with DNA damage experiments. *Inorganic Chemistry* **1999,** *38* (15), 3500-3505.

62. Cho, M.; Lee, Y.; Chung, H.; Yoon, J., Inactivation of *Escherichia coli* by photochemical reaction of Ferrioxalate at slightly acidic and near-neutral pHs. *Applied and Environmental Microbiology* **2004,** *70* (2), 1129-1134.

63. Gogniat, G. T.; Dukan, S., TiO_2 Photocatalysis causes DNA damage via Fenton reaction-generated hydroxyl radicals during the recovery period. *Applied and Environmental Microbiology* **2007,** *73* (23), 7740-7743.

64. Finnegan, M.; Linley, E.; Denyer, S. P.; McDonnell, G.; Simons, C.; Maillard, J. Y.,

Mode of action of hydrogen peroxide and other oxidizing agents: differences between liquid and gas forms. *Journal of antimicrobial chemotherapy* **2010**, 308.

65. Linley, E.; Denyer, S. P.; McDonnell, G.; Simons, C.; Maillard, J. Y., Use of hydrogen peroxide as a biocide: new consideration of its mechanisms of biocidal action. *Journal of antimicrobial chemotherapy* **2012,** *67* (7), 1589-1596.

66. Clifford, D. P.; Repine, J. E., Hydrogen peroxide mediated killing of bacteria. *Molecular and cellular biochemistry* **1982,** *49* (3), 143-149.

67. Mamane, H.; Shemer, H.; Linden, K. G., Inactivation of E. coli, B. subtilis spores, and MS2, T4, and T7 phage using UV/H_2O_2 advanced oxidation. *Journal of Hazardous Materials* **2007,** *146* (3), 479-486.

68. Wolcott, R. G.; Franks, B. S.; Hannum, D. M.; Hurst, J. K., Bactericidal potency of hydroxyl radical in physiological environments. *Journal of Biological Chemistry* **1994,** *269* (13), 9721-9728.

69. Watts, R. J.; Washington, D.; Howsawkeng, J.; Loge, F. J.; Teel, A. L., Comparative toxicity of hydrogen peroxide, hydroxyl radicals, and superoxide anion to *Escherichia coli*. *Advances in Environmental Research* **2003,** *7* (4), 961-968.

70. N. Juarez, J. I.; Pierzcha, K.; Sienkiewicz, A.; Kohn, T., Inactivation of MS2 coliphage in Fenton and Fenton-like systems: role of transition metals, hydrogen peroxide and sunlight. *Environmental Science & Technology* **2010,** *44* (9), 3351-3356.

71. Pignatello, J. J.; Oliveros, E.; MacKay, A., Advanced oxidation processes for organic contaminant destruction based on the Fenton reaction and related chemistry. *Critical reviews in environmental science and technology* **2006,** *36* (1), 1-84.

72. Jo, W.K.; Tayade, R. J., New generation energy efficient light source for photocatalysis: LEDs for environmental applications. *Industrial & Engineering Chemistry Research* **2014,** *53* (6), 2073-2084.

73. Nguyen, T. T. M.; Park, H. J.; Kim, J. Y.; Kim, H. E.; Lee, H.; Yoon, J.; Lee, C., Microbial inactivation by cupric ion in combination with H_2O_2: Role of reactive oxidants. *Environmental Science & Technology* **2013,** *47* (23), 13661-13667.

74. Haber, F.; Weiss, J., Uber die katalyse des hydroperoxydes. *Naturwissenschaften* **1932,** *20* (51), 948-950.

75. Novikov, A. S.; Kuznetsov, M. L.; Pombeiro, A. J.; Bokach, N. A.; Shulapin, G. B., Generation of Hydroxyl Radical from Hydrogen Peroxide Catalyzed by Aqua Complexes of the Group III Metals $[M\ (H_2O)_n]^{3+}$ (M= Ga, In, Sc, Y, or La): A Theoretical Study. *ACS Catalysis* **2013,** *3* (6), 1195-1208.

76. Lin, T. Y.; Wu, C. H., Activation of hydrogen peroxide in copper(II)/amino acid/H_2O_2 systems: effects of pH and copper speciation. *Journal of Catalysis* **2005,** *232* (1), 117-126.

77. Robbins, M. H.; Drago, R. S., Activation of hydrogen peroxide for oxidation by copper (II) complexes. *Journal of Catalysis* **1997,** *170* (2), 295-303.

78. Patikarnmonthon, N.; Nawapan, S.; Buranajitpakorn, S.; Charoenlap, N.; Mongkolsuk, S.; Vattanaviboon, P., Copper ions potentiate organic hydroperoxide and hydrogen peroxide

toxicity through different mechanisms in *Xanthomonas campestris*. *FEMS microbiology letters* **2010,** *313* (1), 75-80.

79. Fortner, A.; Wang, S.; Darbha, G. K.; Ray, A.; Yu, H.; Ray, P. C.; Kalluru, R. R.; Kim, C. K.; Rai, V.; Singh, J. P., Near infrared photo-induced DNA damage in the presence of copper-dppz complex: Evidence for the involvement of singlet oxygen. *Chemical physics letters* **2007,** *434* (1), 127-132.

80. Patra, A. K.; Bhowmick, T.; Roy, S.; Ramakumar, S.; Chakravarty, A. R., Copper(II) complexes of l-arginine as Netropsin mimics showing DNA cleavage activity in red light. *Inorganic Chemistry* **2009,** *48* (7), 2932-2943.

81. Hayase, K.; Zepp, R. G., Photolysis of copper(II)-amino acid complexes in water. *Environmental Science & Technology* **1991,** *25* (7), 1273-1279.

82. Moehl, W.; Motschi, H.; Schweiger, A., Magnetic resonance studies of copper(II) adsorbed on the surface of the bacterium *klebsiella pneumoniae*. *Langmuir* **1988,** *4* (3), 580-583.

83. Hamblin, M. R.; Hasan, T., Photodynamic therapy: a new antimicrobial approach to infectious disease? *Photochemical & Photobiological Sciences* **2004,** *3* (5), 436-450.

84. Jori, G.; Brown, S. B., Photosensitized inactivation of microorganisms. *Photochemical & Photobiological Sciences* **2004,** *3* (5), 403-405.

85. DeRosa, M. C.; Crutchley, R. J., Photosensitized singlet oxygen and its applications. *Coordination Chemistry Reviews* **2002,** *233*, 351-371.

86. Lei, W.; Zhou, Q.; Jiang, G.; Zhang, B.; Wang, X., Photodynamic inactivation of *Escherichia coli* by Ru (II) complexes. *Photochemical and Photobiological Sciences* **2011,** *10* (6), 887-890.

87. Patra, A. K.; Bhowmick, T.; Ramakumar, S.; Nethaji, M.; Chakravarty, A. R., DNA cleavage in red light promoted by copper(II) complexes of α-amino acids and photoactive phenanthroline bases. *Dalton Transactions* **2008,** (48), 6966-6976.

88. Tabassum, S.; Al Asbahy, W. M.; Afzal, M.; Arjmand, F.; Hasan Khan, R., Interaction and photo-induced cleavage studies of a copper based chemotherapeutic drug with human serum albumin: spectroscopic and molecular docking study. *Molecular BioSystems* **2012,** *8* (9), 2424-2433.

89. Ghosh, J. P.; Langford, C. H.; Achari, G., Characterization of an LED based photoreactor to degrade 4-chlorophenol in an aqueous medium using coumarin (C-343) sensitized TiO_2. *The Journal of Physical Chemistry A* **2008,** *112* (41), 10310-10314.

90. Maclean, M.; MacGregor, S. J.; Anderson, J. G.; Woolsey, G., Inactivation of bacterial pathogens following exposure to light from a 405-nanometer light-emitting diode array. *Applied and Environmental Microbiology* **2009,** *75* (7), 1932-1937.

91. Vilhunen, S.; Sarkka, H.; Sillanppa, M., Ultraviolet light-emitting diodes in water disinfection. *Environmental Science and Pollution Research* **2009,** *16* (4), 439-442.

Activation of persulphate by Nickel(II) hexaazamacrocyclic complex: Study on degradation of persistent organic pollutants

2.1 Abstract:

Nickel(II) hexaazamacrocyclic complex, (C1) forms an ion-pair complex with persulphate, followed by nickel ion assisted heterolytic cleavage of peroxo bond of persulphate leading to the generation of sulphate radical and trivalent nickel species (Chapter 1 Section 1.5a). However, reaction between persulphate and nickel azamacrocyclic complex and its effect on recalcitrant organic pollutants such as biocides, antibiotics and dyes has not been studied.

The present chapter is focused on activation of potassium persulphate (KPS) by redox active Nickel(II) hexaazamacrocyclic complex (C1) for degradation of certain non-biodegradable biocidal contaminants such as Malachite green (MG) and Ciprofloaxin (Cpf), and highly coloured textile dye pollutants such as Methyl Orange (MO), Rhodamine B (RhB) and Methylene blue (MB). The degradation intermediates of biocidal compounds MG and Cpf and the toxicity of MG and Cpf before and after the degradation were investigated. The performance of C1 activated KPS to degrade dyes MO, RhB and MB was evaluated in simulated natural water containing a variety of inorganic ions and organic content. This chapter addresses the gap in literature discussed under the section 1.5 (a) of chapter 1.

Graphical Abstract:

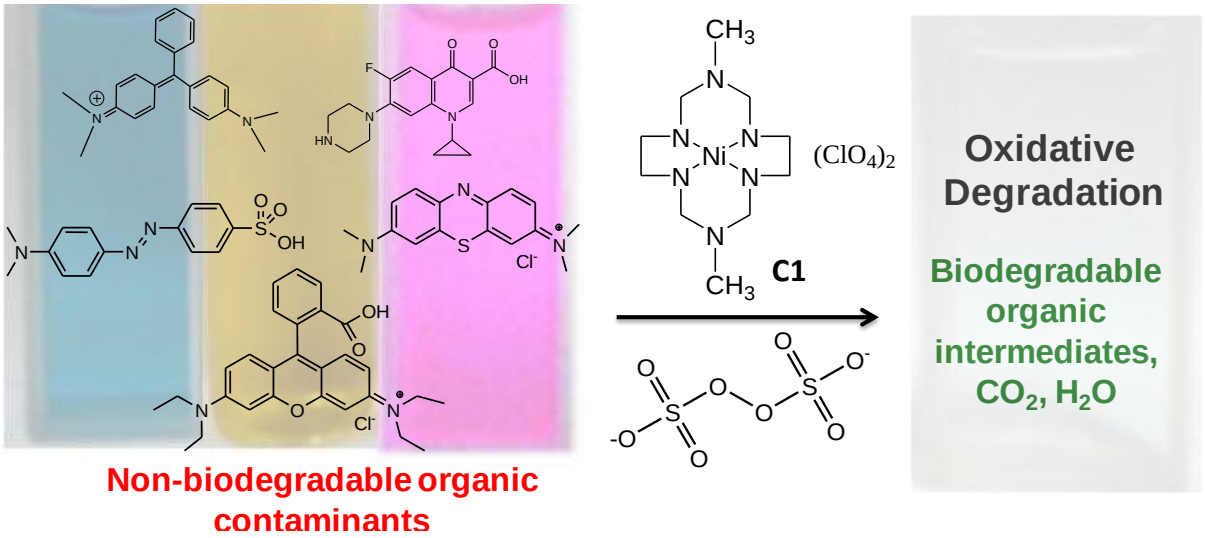

2.2 Experimental procedures and analysis:

2.2 (a) Reagents:

Nickel chloride hexahydrate ($NiCl_2.6H_2O$), Silver nitrate ($AgNO_3$), Potassium persulphate ($K_2S_2O_8$), Sulphuric acid (H_2SO_4), Sodium hydroxide (NaOH), Sodium chloride

(NaCl), Potassium iodide (KI), Potassium dichromate ($K_2Cr_2O_7$), Starch, Sodium thiosulphate ($Na_2S_2O_3$), Ethanol, Ammonium acetate (CH_3COONH_4), Tertiary butyl alcohol, Methyl orange (MO), Methylene blue (MB), and Rhodamine B (RhB) used, were of guaranteed analytical grade, from SD fine chemicals, India. Malachite green (MG) was obtained from Hi media, India and Ciprofloxacin (Cpf) was extracted from Ciptec™ – 250 mg, Cipla and purified by RP-HPLC. Complexes, 1,8-dimethyl-1,3,6,8,10,13-hexaazacyclotetradecane nickel(II) perchlorate (C1), and 5,5,7,12,12,14-hexamethyltetraazacyotetradecanesilver(II) perchlorate (C2) were prepared as reported earlier.[1, 2] Care must be taken as large amount of perchlorate salts could be explosive. For HPLC analysis, methanol (HPLC grade), acetonitrile (HPLC grade), ammonium acetate buffer (pH 4.5) and millipore water were used.

2.2 (b) Experimental procedure:

Stock solutions of MG, Cpf, MO, MB and RhB and complexes C1 and C2 were prepared using double distilled water. Freshly prepared KPS solution was used for all experiments. These stock solutions were diluted to get solutions of desired concentrations. All reactions were carried out at 27 ± 2 °C at pH 7 unless specified. pH was adjusted to desired value with help of pH meter (EU Tech) by adding 0.1 N H_2SO_4 or 0.1 N NaOH.

Degradation of MG, MO, MB and RhB was studied by following the decrease in the absorption maximum at 618 nm, 454 nm, 664 nm and 564 nm respectively, after specific time intervals using JASCO V-570 UV/VIS/NIR, while the degradation of Cpf was monitored by high-performance liquid chromatography (HPLC), using Shimadzu UFLC, equipped with a phenomenex C18 HPLC column (250 mm × 4.5 mm, 5 μm) and SPDM 20A Prominence diode array detector. Typically, reaction is carried out by addition of stock solutions of contaminant and KPS with and without C1 or C2 followed by thorough mixing and incubation for specified time intervals.

2.2 (c) HPLC analysis:

Degradation of MG, Cpf, MO, MB and RhB were monitored by high pressure liquid chromatography using Shimadzu UFLC, equipped with a phenomenex C18 HPLC column (250 mm × 4.5 mm, 5 μm) and SPDM 20A Prominence diode array detector. The measurements for the organic pollutants are as follows (Table 2.1).

Table 2.1 HPLC conditions for study of degradation of contaminants

Contaminants	Mobile Phase	Wavelength
MG	80:20 (v/v) ammonium acetate (pH 4.5)/acetonitrile	618 nm
Cpf	70:30 (v/v) ammonium acetate buffer (pH 4.5)/acetonitrile	275 nm
MO	70:30 (v/v) ammonium acetate buffer (pH 4.5)/acetonitrile	464 nm
MB	70:30 (v/v) ammonium acetate buffer (pH 4.5)/acetonitrile	660 nm
RhB	30:70 (v/v) ammonium acetate buffer (pH 4.5)/acetonitrile	554 nm

100 μL of sample was injected and the measurement was performed in isocratic mode with a flow rate of 1 ml/min.

2.2 (d) TOC analysis:

TOC was measured using Sievers 900 TOC analyser. An aliquot of 20 mL of sample was taken at specific time intervals from reaction mixture (100 mL) and injected in to TOC analyser. The results are expressed as TOC/ TOC_0 where TOC is Total organic carbon at time t, and TOC_0 is initial Total organic carbon. % reduction in TOC was obtained using the equation [TOC/ TOC_0] x 100.

2.2 (e) LC–ESI–MS analysis:

LC–ESI–MS analysis was performed using Thermo Finnigan LCQ Deca LC/MS/MS Electrospray quadrupole ion trap mass spectrometer. Surveyor LC was equipped with a C-18 column (150 mm × 2 mm). Nitrogen was used as sheath and auxiliary gas. Ion source conditions were: sheath gas flow rate ~7.5 L/min. Capillary temperature was maintained at 200 °C and capillary voltage was kept at 15 V. Ion-spray voltage and tube lens offset were maintained at +4.5 kV and −7 V respectively.

2.2 (f) Microbial assays:

Sterile distilled water and sterile glasswares were used. A reaction mixture (1 mL) containing appropriate concentration of MG or Cpf, KPS and C1 was prepared by adding appropriate volumes of respective stock solutions. This solution was mixed thoroughly and kept undisturbed for 60 min. After 60 min, 1 mL of 2X NB was added to the above solution followed by addition of *E. coli* cells (~10^6). The contents were mixed well and incubated in a shaking incubator for overnight at 37 °C. Appropriate controls were prepared using only MG or Cpf. 0.1 mL of above culture suspensions were spread plated on nutrient agar plates followed by overnight incubation at 37 °C.

All the experiments were performed thrice in duplicates. Origin Pro 8.0 software was used for data analysis.

2.3 Results and Discussion:

2.3.1 Degradation of Malachite green (MG)

2.3.1 (a) Degradation of MG by KPS, and C1 activated KPS:

Absorption spectra of MG showed three main peaks with absorption maxima at 618, 425 and 315 nm (Figure 2.1A). Absorbance of these bands decreased on addition of KPS to MG with a significant decrease in absorbance at 618 nm, until it became almost zero at ~60 min (Figure 2.1A). These spectral changes revealed ability of KPS to degrade MG. Earlier, disappearance of absorption band (500 to 700 nm) with peak at 618 nm was monitored to study degradation of MG by various methods.[3-5]

HPLC chromatogram of MG monitored at 618 nm showed a single sharp peak with retention time (RT) 4 min, which corresponds to MG (Figure 2.1B).[4] Addition of KPS to MG decreased the intensity of MG peak, and led to the formation of new peak with RT 1.8 min. MG peak at RT 4 min and peak observed at RT 3.5 min completely disappeared after 60 min of reaction, while peak at RT 1.8 min was reduced to negligible level (Figure 2.1B).

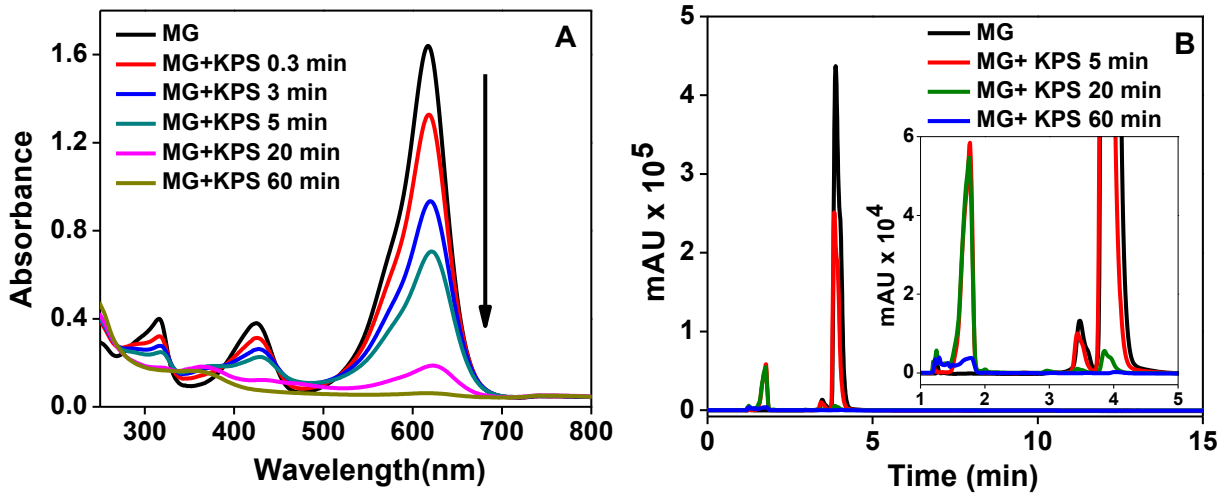

Figure 2.1 (A) Change in absorption spectrum of MG (10 mg/L) at different time intervals after addition of KPS (1 g/L) in water. (B) HPLC chromatogram of MG (10 mg/L) at different time intervals after addition of KPS (1 g/L). Figure 2.1 (B) Inset Magnified image (10X) of Figure 2.1B.

HPLC results clearly showed that KPS has ability to degrade MG to other species and peaks at RT 1.8 min and 3.5 min could correspond to the degradation products of MG. Absorption spectral changes of MG observed on addition of both KPS and C1 showed a rapid decrease in absorption at 618 nm within 20 mins (Figure 2.2A). Moreover, after 60 mins, a shoulder around 450 nm and also a peak around 290 nm were observed, which correspond to trivalent nickel species formed due to reaction between KPS and C1, as reported earlier.[6] The

corresponding HPLC profiles monitored at 618 nm also revealed that MG as well as the degraded products of MG were degraded within 20 mins on addition of KPS with C1 (Figure 2.2B).

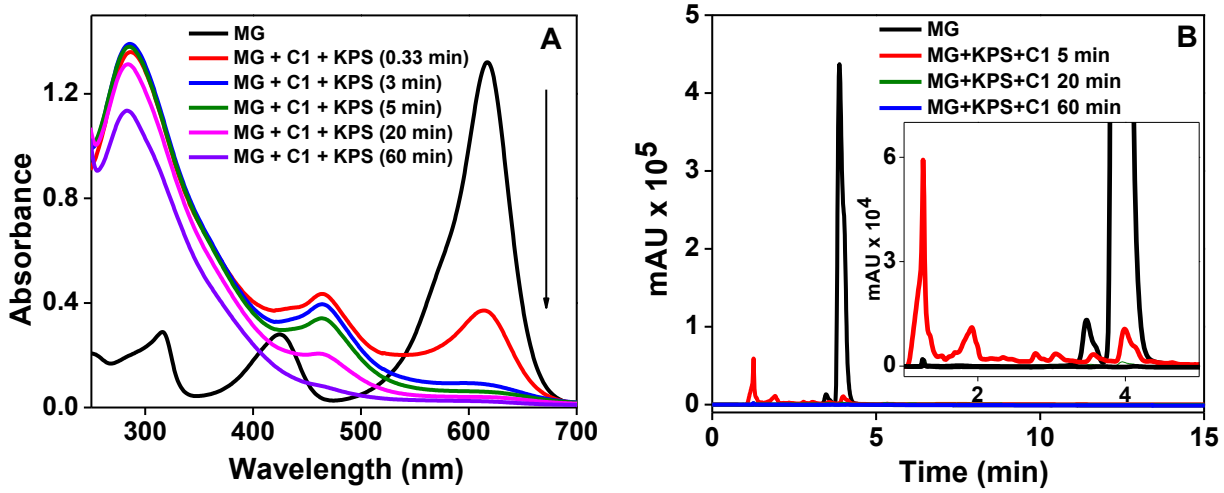

Figure 2.2 (A) Change in absorption spectrum of MG (10 mg/L) at different time intervals after addition of KPS (1 g/L) in presence of C1 (200 µM) in water. (B) HPLC chromatogram of MG (10 mg/L) at different time intervals after the addition of KPS (1 g/L) in presence of C1 (200 µM). Figure 2.2 (B) Inset Magnified image (10X) of Figure 2.2B.

Importantly, rate of degradation of MG by KPS alone was determined to be 0.11±0.011 min^{-1} where as the rate of rate of degradation of MG by KPS in presence of C1 was determined to be 0.93±0.05 min^{-1} (Figure 2.3, Table 2.2). These results revealed that C1 caused marked enhancement in the rate of degradation of MG by KPS (Table 2.2).

Table 2.2 Rate constants determined for degradation of MG by KPS under various conditions

Reaction	pH	Rate Constants (min^{-1})
MG+KPS	7	0.11 ± 0.01
MG+KPS+C1	7	0.93 ± 0.05
MG+KPS	3	0.20 ± 0.01
MG+KPS	9	0.23 ± 0.02
MG+KPS+C1	3	0.59 ± 0.02
MG+KPS+C1	9	0.63 ± 0.03
MG+KPS+ Ni(II) ions	7	0.12 ± 0.01
MG+KPS+ Fe(II) ions	3,7,9	Not determined[a]

[a] - Reaction incomplete

2.3.1 (b) Effect of pH:

Rates of degradation of MG at pH 3 and 9 were found to be almost similar, and slightly higher than neutral condition (Figure 2.3A). It is known that decomposition of KPS is enhanced by acid catalysis.[7] Moreover, base such as sodium hydroxide is also known to

activate decomposition of persulphate.[8] Increase in rate of degradation of MG by KPS at pH 3 and 9 (Table 2.2) in the present study is due to acid catalysis and base activation of KPS, respectively.

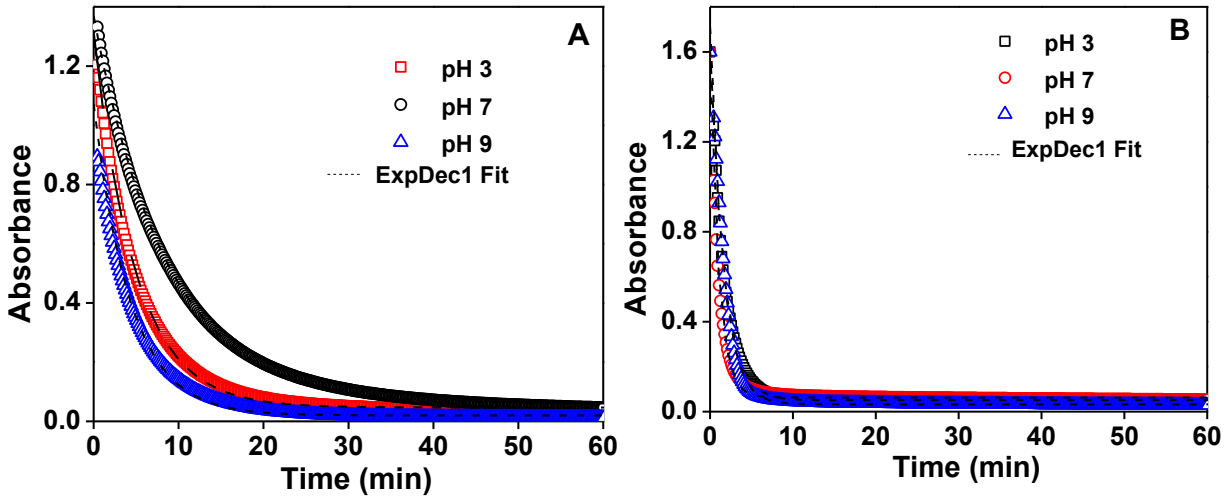

Figure 2.3 (A) Absorption changes with time at 618 nm for solutions having MG (10 mg/L) and KPS (1 g/L) at three different pH (pH 3, pH 7, pH 9) along with the corresponding exponential decay fit. (B) Absorption changes with time at 618 nm for solutions having MG (10 mg/L) and KPS (1 g/L) in presence of C1 (200 µM) at three different pH (pH 3, pH 7, pH 9) along with the corresponding exponential decay fit.

Rapid redox reaction between KPS and C1 generates highly reactive sulphate radicals (2.6 V) and oxidants such as trivalent nickel species.[6, 9] Thus, the rapid degradation of MG by KPS in presence of C1 is due to the activation of KPS by C1. Present results also show that degradation of MG by C1 activated KPS was faster and efficient than KPS activated by acid catalysis or base. Rates of degradation of MG by KPS in presence of C1 at pH 3, 7 and 9 were found to be almost similar (Figure 2.3B, Table 2.2). Earlier, it has been suggested that trivalent nickel species act as effective catalyst for oxidation process in aqueous neutral media and in alkaline media.[9, 10] It is known that stability of trivalent species is highest in acidic, lowest in alkaline and intermediate in neutral conditions, indicating that trivalent nickel species are highly stabilised under acidic conditions and not favourable for oxidation reactions.[9, 10] Although there is a slight variation in rate of degradation of MG by KPS in presence of C1 within pH range 3-9, it is important to note that MG is degraded effectively over a broad range of pH (Figure 2.3B).

2.3.1 (c) Effect of Nickel(II) and Iron(II) ions:

Rate of degradation of MG by KPS in presence of Ni(II) ions (200 µM) at pH 3-9 was similar to rate of degradation of MG by KPS alone (Figure 2.4A, Table 2.2). Moreover, degradation

of MG by KPS in presence Fe(II) ions (200 µM) at pH 3-9 showed relatively higher absorbance at 618 nm indicating that degradation was incomplete (Figure 2.4A).

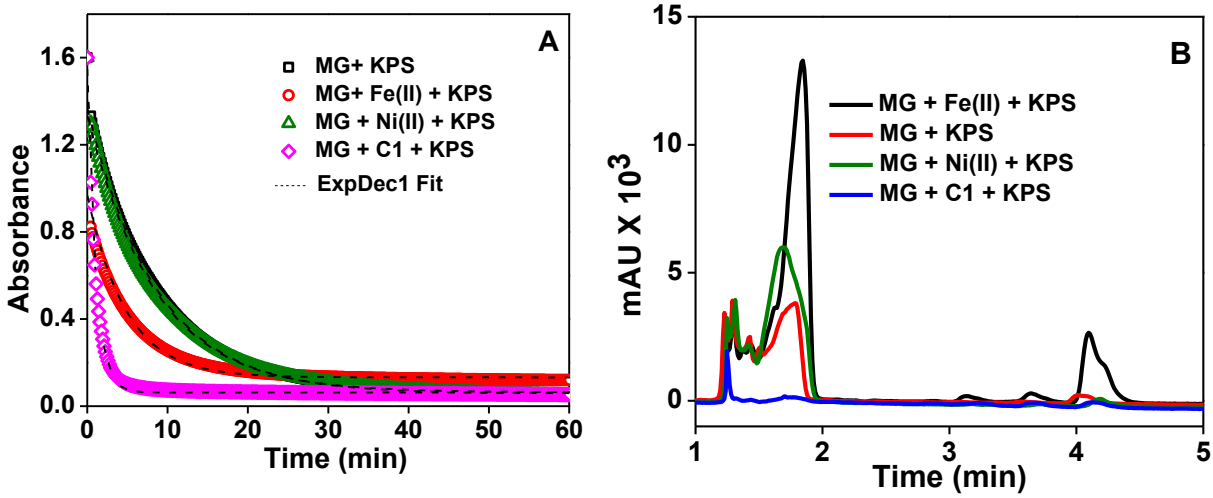

Figure 2.4 (A) Absorption changes with time at 618 nm for solutions having MG (10 mg/L) and KPS(1 g/L); MG (10 mg/L) and KPS (1 g/L) in presence of C1(200 µM); MG (10 mg/L) and KPS (1 g/L) in presence of Fe (II) (200 µM) and, MG (10 mg/L) and KPS (1 g/L) in presence of Ni(II) (200 µM); along with the corresponding exponential decay fit. **(b)** HPLC chromatogram of MG (10 mg/L) and KPS (1 g/L); MG (10 mg/L) and KPS (1 g/L) in presence of C1(200 µM); MG (10 mg/L) and KPS (1 g/L) in presence of Fe (II) (200 µM); MG (10 mg/L) and KPS (1 g/L) in presence of Ni(II) (200 µM) at time intervals.

HPLC chromatogram showed a peak at 4 min corresponding to MG, and peaks at 1.8 min and 3.5 min corresponding to N- demethylated species produced during degradation (Figure 2.4B).[4] These results clearly showed that in presence of Fe(II) ions or Ni(II) ions, both MG and N-demethylated species are not effectively degraded compared to degradation of MG by KPS in presence of C1. Based on absorption and HPLC results discussed above (Figure 2.4), order of degradation of MG under mentioned experimental conditions is as follows:

KPS: ferrous sulphate < KPS: nickel chloride ~ KPS < KPS: C1 (Table 2.2)

Effect of various parameters observed for degradation of MG by KPS and by KPS in presence of C1 followed a similar trend as observed for degradation of MG by Fenton processes and Ozonation.[3, 11] Importantly, the present results show that degradation of MG by KPS and by KPS in presence of C1 is effective over a wide pH range (3-9) while Fenton processes as well as Ozonation process are mainly effective under acidic conditions.

2.3.1 (d) Total organic carbon analysis:

TOC analysis results showed that treatment of MG (20 mg/L) with KPS (2 g/L) alone could remove 7% of TOC (Figure 2.5).

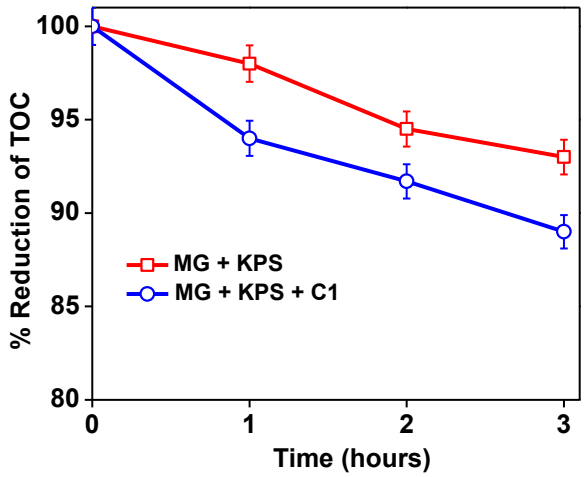

Figure 2.5 TOC reduction (%) of MG (20 mg/L) after the treatment with KPS (2 g/L) in absence and presence of C1 (400 µM).

On the other hand, treatment of MG (20 mg/L) with KPS (2 g/L) along with C1 (400 µM) could remove 11% of TOC within 3 h (Figure 2.5). This shows that treatment of MG with KPS alone and KPS with C1 not only results in degradation of MG but also in reduction of TOC.

2.3.1 (e) Antimicrobial activity of MG before and after degradation:

E. coli cells suspended in NB containing MG (untreated) were incubated overnight, and solution was found to be clear (Figure 2.6A).

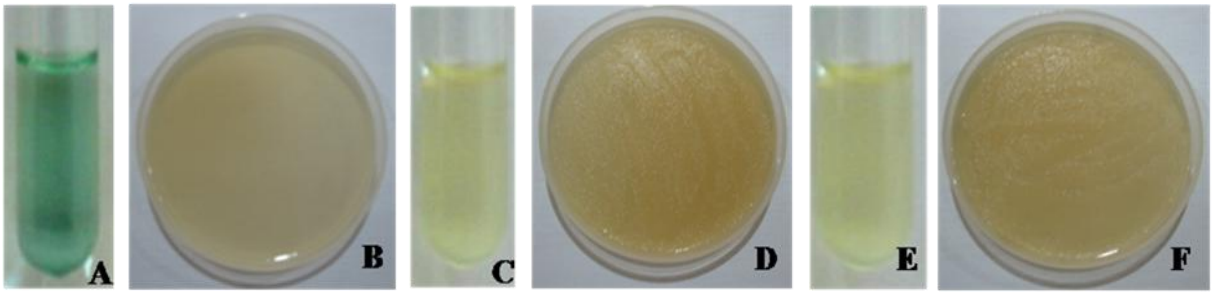

Figure 2.6 Photograph showing effect of MG (10 mg/L) on growth of *E. coli* (~10^6 cells) before and after treatment by KPS (1 g/L) and C1 (200 M). A, C and E tubes containing *E. coli* with MG, *E. coli* with MG after treatment by KPS and C1, and *E. coli.*, respectively. B, D and F are the plates corresponding to the tubes A, C and E respectively after overnight incubation

This solution when spread plated on NB agar and incubated overnight, did not show formation of any bacterial colonies (Figure 2.6B), revealing that MG alone is toxic to bacteria. On the other hand, when *E. coli* cells were suspended in NB, containing degraded MG (after treatment with KPS in presence of C1 for 60 min), solution was found to be turbid (Figure 2.6E). This solution, on agar plates displayed formation of numerous bacterial colonies (matt

growth) (Figure 2.6F).Thus, above results indicate that KPS and C1 system has propensity to remove antibacterial activity of MG and thereby aid conventional biological oxidation. Earlier, it has been shown that degradation of MG by ozonation processes[11] and decolourization of MG by dye-decolorizing bacterium (*Shewanella decolorationis* NTOU1)[12] showed reduction in antibacterial activity.

2.3.1 (f) Identification of transformation products by ESI – MS:

MG solution showed a single peak in total ion chromatogram (TIC), and its corresponding mass spectrum had a clear peak with 329 m/z (Appendix I Figure S.I 2.1). Degraded MG solution showed 3 peaks (A, B, C) in TIC plot, and corresponding mass spectra of these peaks revealed the formation of a variety of degraded intermediates (Appendix I Figure S.I 2.2). Earlier studies on degradation of MG mediated by hydroxyl radicals reported the formation of complex reaction mixture with N-demethylated intermediates of MG, DLBP (dimethylaminobenzophenone) and their hydroxyl adducts along with many other possible intermediates.[4, 13] Analysis of present mass spectral results clearly showed ions that could correspond to N-demethylated intermediates, hydroxyl adducts of N-demethylated intermediates and DLBP (Table 2.3). Interestingly, these results showed that persulphate mediated degradation of MG could form hydroxyl adducts. Sulphate radicals react with water to produce hydroxyl radicals that could react with aromatic ring to form hydroxyl adducts.[7,8]

Table 2.3 m/z values of degradation intermediates and tentative structures.

TIC peak[a]	Tentative structure		m/z
A	MG–3CH_2	A_1	287.16
A	DLBP + OH	A_2	242.11
A	DLBP–CH_2 + OH	A_3	228.50
A	DLBP + 2OH	A_4	257.11
A	BPA + HSO_4^-	A_5	266.00
A	BPA + CH_3 + OH	A_6	200.10
A	MG–4CH_2− NH + 4OH	A_7	322.11
B	MG–2CH_2− NH + 4OH	B_1	352.15
B	MG–4CH_2 + 2OH	B_2	305.13
C	LMG	C_1	331.00
C	MG–4CH_2− 2NH + 4OH	C_2	309.10
C	MG–2CH_2–NH	C_3	286.16

a Peaks and their corresponding RT: A (1.48–1.53 min), B (2.38–2.41 min) and C (3.61–3.65 min).

Moreover, sulphate radicals could directly attack the aromatic ring and form hydroxyl adducts. Thus, in the present study, formation of hydroxyl adducts of degradation intermediates could be attributed to both the sulphate radicals and secondary hydroxyl radicals generated upon activation of KPS by C1.

ESI-MS/MS analysis of MG showed following ions, 329.17 (MG); 285.12 (MG-$2CH_2$-NH_2); 251.20 (MG-C_6H_6); 237.11 (MG-C_6H_6-CH_2) and 208.28 (MG-C_6H_6-CH_2) (Figure 2.7), similar to earlier report.[4] Importantly, ESI-MS/MS of degradation intermediate A3 (DLBP-CH_2 + OH) with 228.5 m/z value showed a fragment ion with 149.10 m/z (A3-C_6H_6) (Figure 2.7).

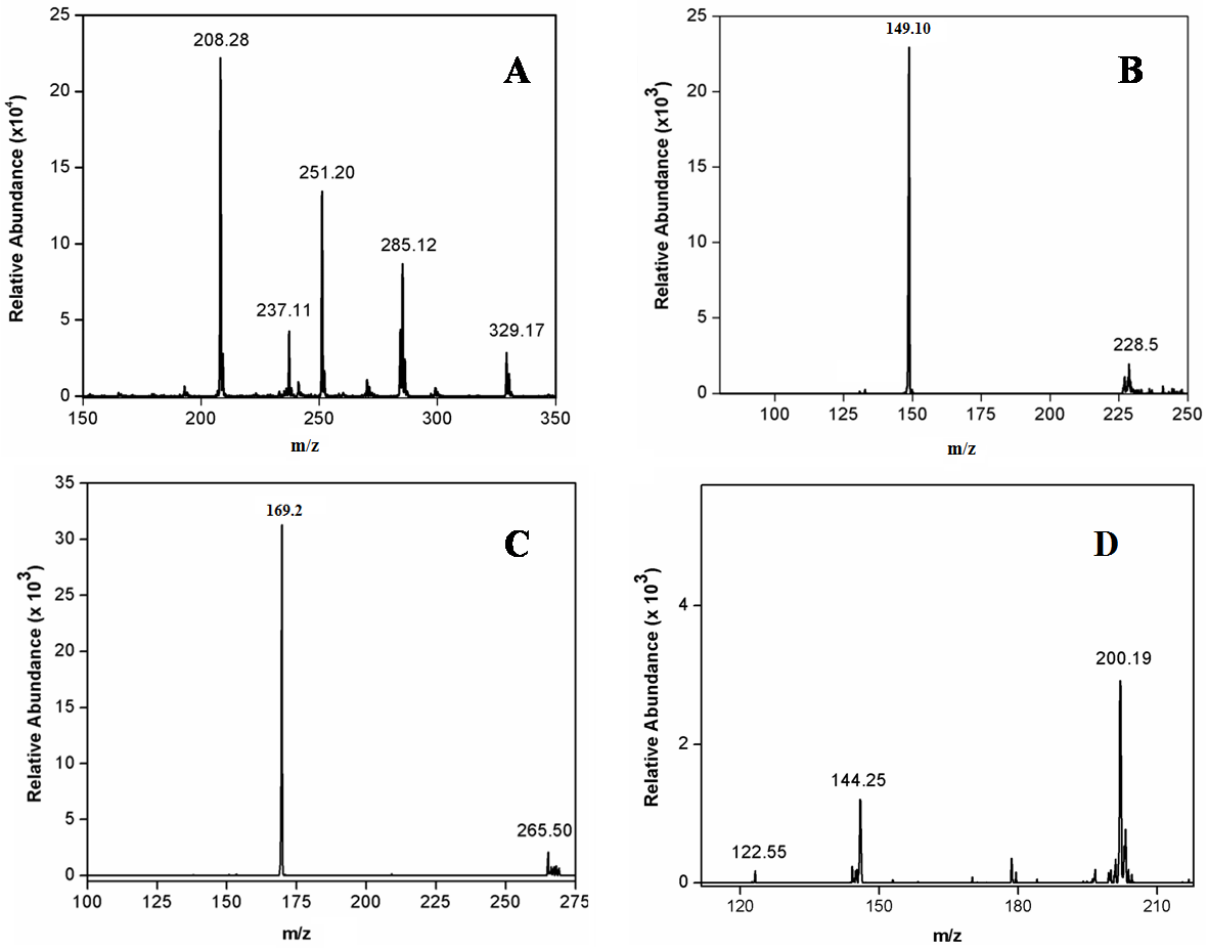

Figure 2.7 MS-MS analysis of MG and degradation intermediates: A3, A5 and A6.

Similar fragmentation has been reported for bezenophenone type molecule.[14] Thus, this result further supports the presence of degradation intermediate with hydroxyl adduct. Hydroxyl radicals could cause deamination of aromatic amines.[4, 13, 15, 16] Earlier, report on the oxidation of MG by persulphate suggested the formation of biphenyl amine (BPA) intermediates.[17] In addition, persulphate is known to react with aromatic amines to form aromatic amine sulphate adducts.[18, 19] A peak with 266m/z identified in the mass spectra could correspond to BPA sulphate adduct (A5) (Figure 2.7). ESI-MS/MS of this intermediate A5 (BPA +HSO_4), showed a fragment ion with 169.2m/z (A5-H_2SO_4) (Figure 2.7). In addition, intermediate A6 (BPA +CH_3 + OH) with 200.19 m/z showed following fragment ions;

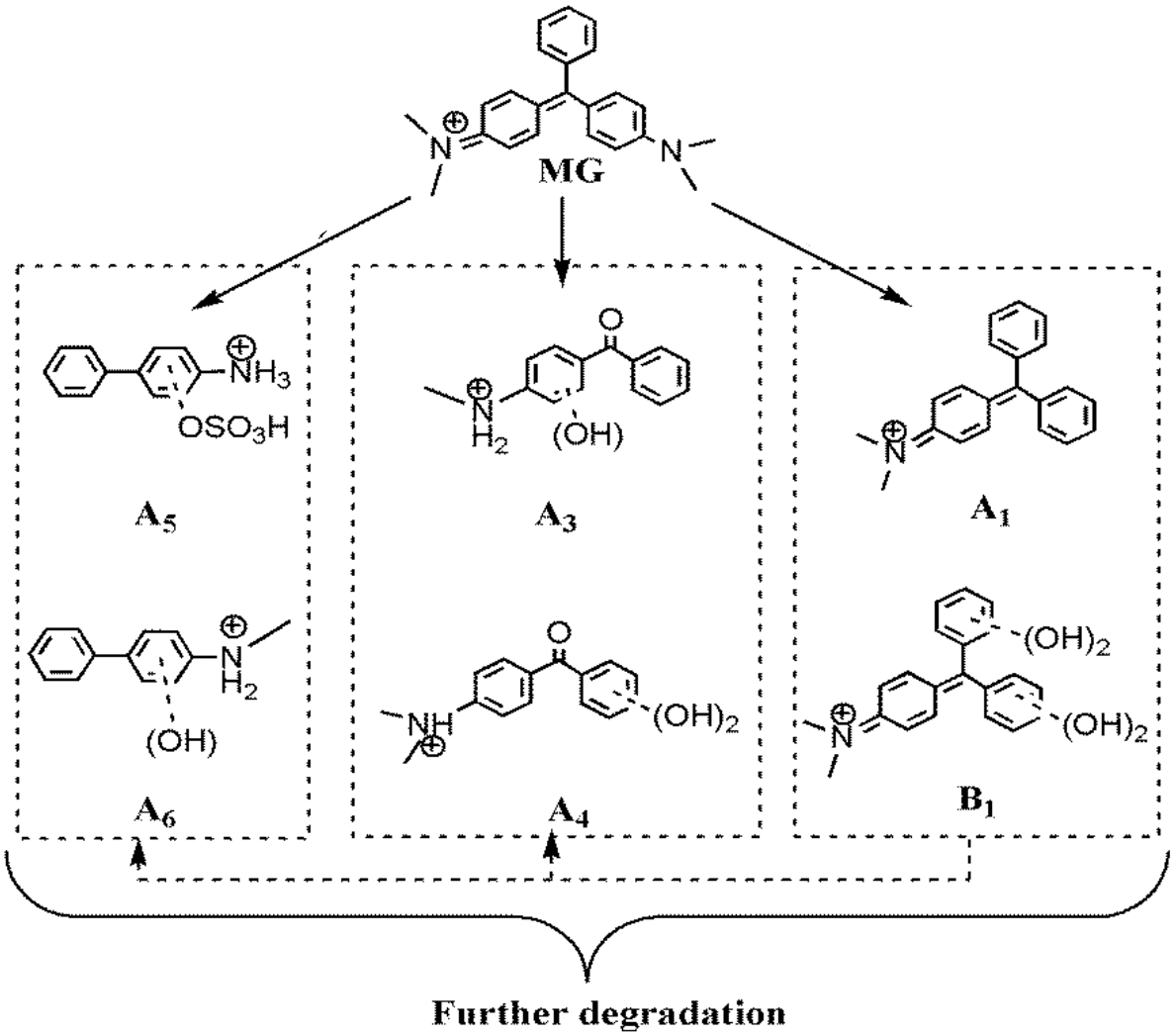

Figure 2.8 Possible reactions in degradation of MG by KPS in presence of C1.

122.5 (A6-C_6H_6), 144.25 (A6-CH_2-C-NH-CH_3) (Figure 2.7).

Earlier similar fragmentations were observed for aromatic amino derivatives.[20, 21] As mentioned above, reactive sulphate and hydroxyl radicals could generate a variety of intermediates, however, identification of all intermediates by mass spectrometry was not possible. It is important to note that, several factors such as concentration of intermediates present in analysis solution and the amount obtained after separation in the solid phase column, HPLC separation protocols, type of molecules and stability of charged ions, mass spectrometer used, presence of a variety of compounds and alkali metal ions in sample, complexity due to fragmentations in ESI source, and others could affect the analysis by mass spectrometer.[4, 13] Based on above discussion and available literature, important possible reactions for degradation of MG by KPS and C1 are proposed (Figure 2.8). Proposed degradation mechanism includes major reactions such as N-demethylation, hydroxyl adduct formation and removal of benzene ring, as reported earlier. [4, 13, 22]

2.3.2 Degradation of Ciprofloxacin (Cpf)

2.3.2 (a) Degradation of Cpf by KPS and activated KPS:

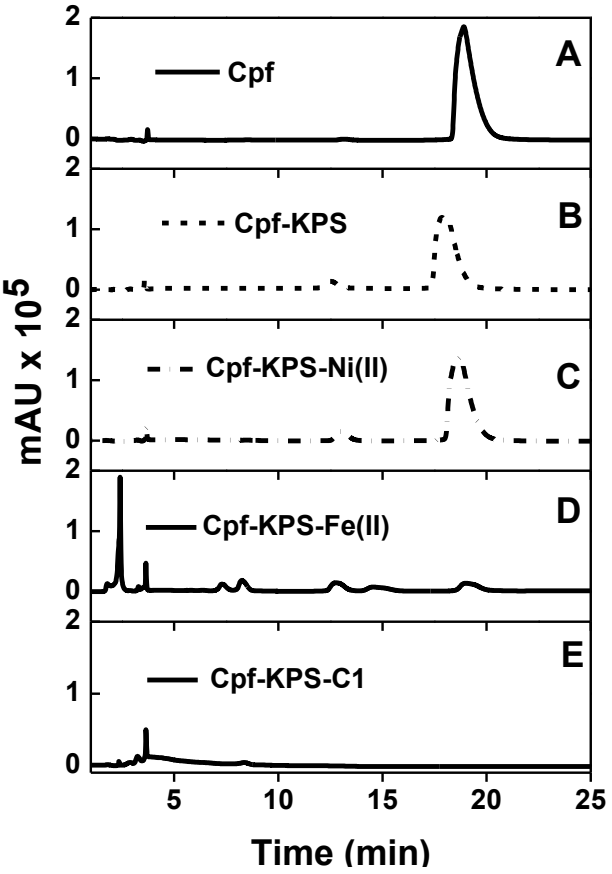

Figure 2.9 HPLC chromatogram of Cpf (A) Cpf degraded by KPS (B) Cpf degraded by KPS in presence of Ni(II) ions (C) Cpf degraded by KPS in presence of Fe(II) ions (D) Cpf degraded by KPS in presence of C1(E). [Cpf] = 15 mg/L; [C1] = [Fe(II)] = [Ni(II)]= 100 µM; [KPS]= 1 g/L. Treatment time = 180 min

HPLC chromatogram of undegraded Cpf solution monitored at 275 nm showed a distinct peak at RT ~18 min (Figure 2.9 A). HPLC chromatogram of Cpf solution treated with KPS alone showed a slight decrease in the Cpf peak and formation of a new peak at RT 13 min (Figure 2.9 B). On the other hand, Cpf treated with KPS in presence of C1 showed no Cpf peak and only one weak peak at RT 3 min (Figure 2.9 E). It should be noted that Ni(II) ions had no significant effect of the degradation of Cpf by KPS (Figure 2.10 C) whereas Fe(II) ions showed a marked decrease in the Cpf peak. However, Fe(II) ions activated Cpf caused incomplete degradation of Cpf with formation of several degradation products at RT 2,3,7,8,13 and 15 min (Figure 2.9 D).

Moreover, about 50% Cpf was degraded by KPS alone at pH 3, 7 and 9 (Figure 2.11 A). On the other hand, C1 activated KPS caused almost complete degradation of Cpf (> 98 %)

in pH 7 & 9, while at pH 3 degradation of Cpf was about 90% (Figure 2.10 A). It should be noted that Fe(II)ions activated KPS caused about 87%, 95%, and 65 % Cpf degradation at pH 3,7 and 9, respectively (Figure 2.10 B).

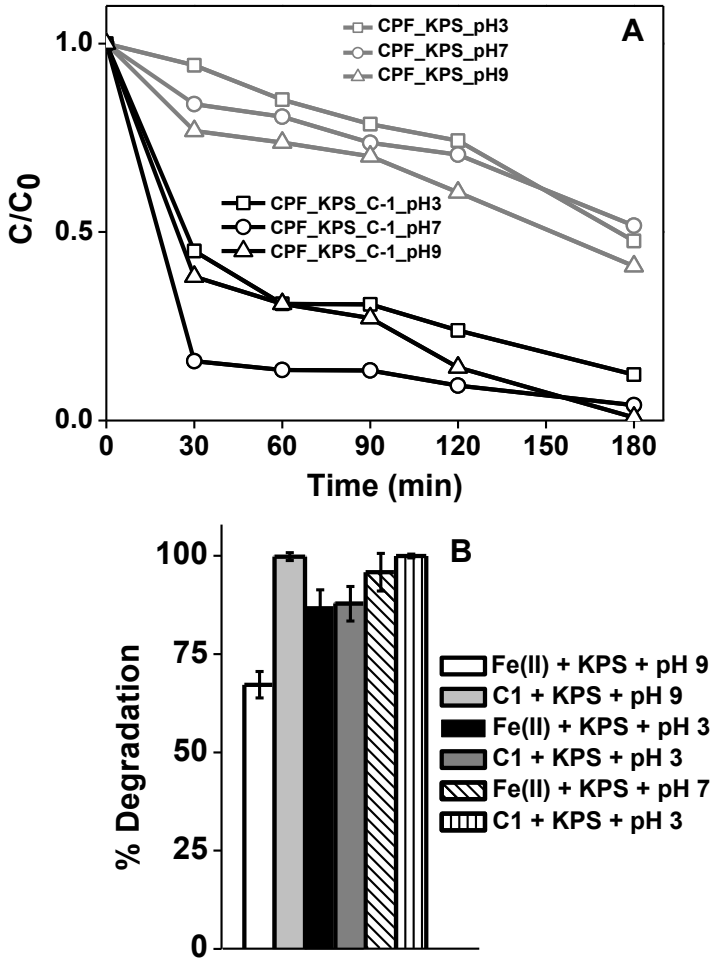

Figure 2.10 (A) Effect of pH of degradation of Cpf by KPS and KPS activated by C1. (B) Effect of pH of degradation of Cpf by KPS activated C1 and Fe(II) ions. Treatment time = 180 min.

Importantly, degradation of Cpf by C1 activated KPS is not significantly influenced by the initial pH of the reaction medium unlike degradation of Cpf by Fe(II) ions activated KPS (Figure 2.10). These results clearly revealed that degradation of Cpf by KPS in the presence C1 is much effective than by KPS alone, and by KPS in the presence Ni(II) or Fe(II) ions.

2.3.2 (b) Identification of degradation products:

The mass spectrum of Cpf showed a peak at m/z 332.1 that corresponds to Cpf (Figure 2.11A). Interestingly, this Cpf peak is completely absent after the degradation of Cpf by C1 activated KPS (Figure 2.11B). The presence of hydroxylated degradation intermediate m/z

366.7 indicated the generation of hydroxyl radicals upon activation of KPS by C1 in aqueous medium. Other low molecular weight degradation intermediates with m/z 230.8 and m/z 192.9 were also detected (Figure 2.11B).

These degradation intermediates were similar to those observed for the degradation of Cpf by peroxone and ozonation processes.[23, 24,25,26]

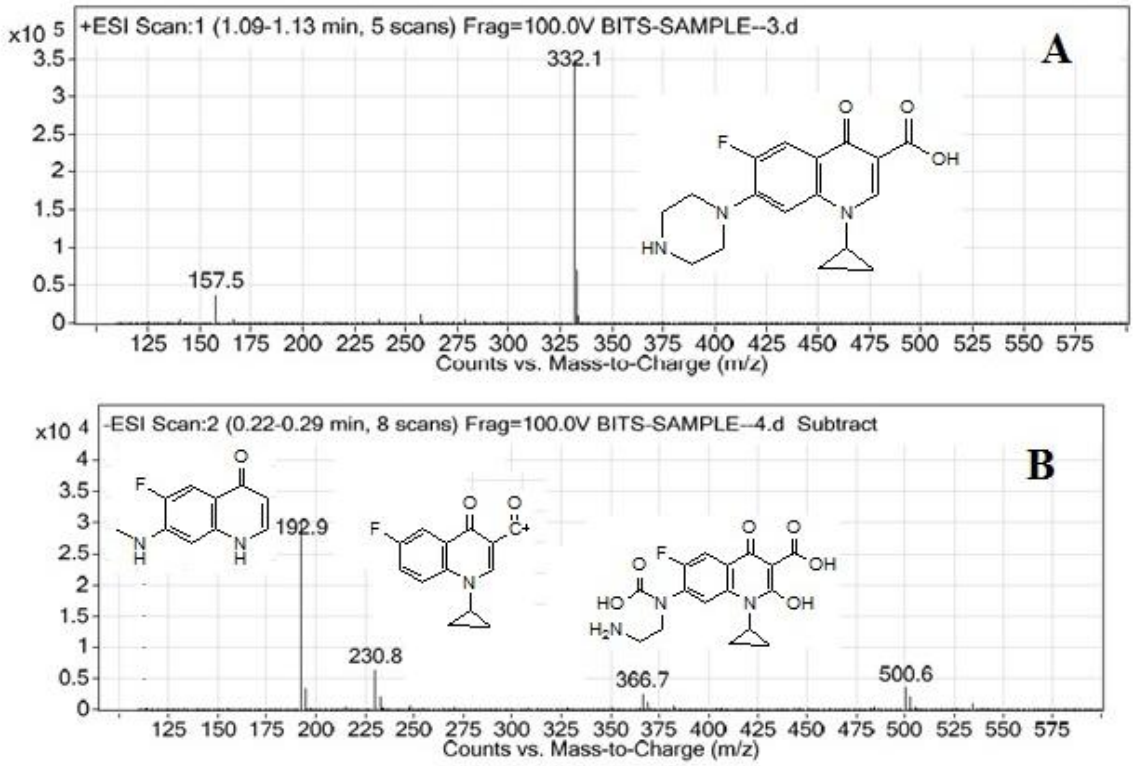

Figure 2.11 Mass Spectrum of Cpf (A) and (B) degraded Cpf solution.

Presence of low molecular weight compounds in the degraded Cpf solution indicate that degradation of Cpf by C1 activated KPS could reduce the total organic carbon content. TOC analysis revealed that, C1 activated KPS caused ~55% reduction in TOC whereas KPS alone caused ~20% reduction in TOC.

It is important to note that Cpf is a broad spectrum antibiotic and its antibacterial activity is due to the inhibition of bacterial DNA gyrase enzyme (topoisomerase II and topoisomerase IV) that are essential for bacterial replication.[27] Mass spectral results of Cpf degraded by C1 activated KPS revealed the complete loss of Cpf structure and the formation of structurally different degradation intermediates. The loss of structure of Cpf could affect its enzyme inhibition activity, thereby losing its toxicity towards bacteria that is favourable for conventional biological treatment. These results indicate that degradation of Cpf by C1 activated KPS could affect the antibacterial activity of Cpf.

2.3.2 (c) Antimicrobial activity of Cpf before and after degradation:

Incubation of *E. coli* cells for 60 min overnight in undegraded Cpf solution caused complete loss of *E. coli* cell viability (100%) (Figure 2.12, Plate A). Incubation of *E. coli* cells in Cpf solution treated with KPS caused about 50 % reduction in *E. coli* cell viability (Figure 2.12, Plate B). Interestingly, Cpf degraded by C1 activated KPS caused only negligible (about 2 %) reduction in cell viability revealing almost complete removal of antibacterial activity of Cpf after treatment (Figure 2.12, Plate C). It is known that the continuous exposure of bacteria to even small concentrations of antibiotic such as Cpf could lead to the emergence or persistence of antibacterial resistance.[28] Moreover, the presence of antibiotics in waste water can disrupt the wastewater treatment process and the microbial ecology in surface waters.[29] The significant removal of antibiotic activity of Cpf by C1 activated KPS imply that C1 activated KPS is an effective AOP for degradation of non-biodegradable compounds such as Cpf. Oxidative degradation leading to the removal of toxicity of compounds such as Cpf towards microbes has potential biotechnological significance in biological waste water treatment.

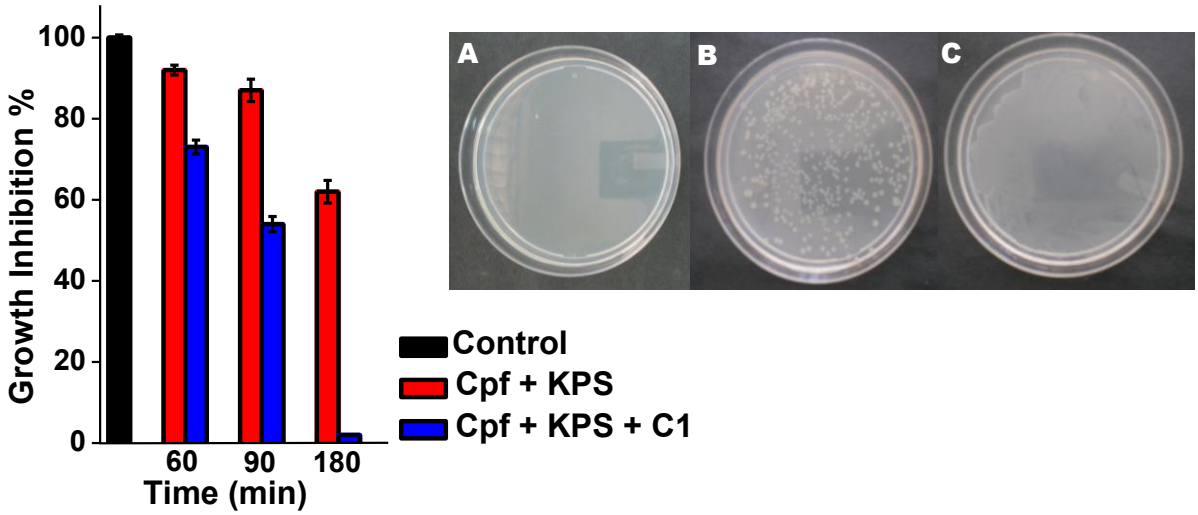

Figure 2.12 Cell viability of *E. coli* in Cpf solution (Plate A) and Cpf solution degraded by KPS (Plate B) and C1 activated KPS (Plate C).

2.3.3 Degradation of Methyl Orange (MO), Methylene Blue (MB) and Rhodamine B (RhB)

2.3.3 (a) Degradation of MO, MB and RhB by KPS and C1 activated KPS:

Treatment of different dye solutions MB, MO and RhB (Figure 2.13 A, B and C) with KPS (1g/L) for 1 hour resulted in ~25%, ~35% and ~65% degradation of MB, MO and RhB respectively (Figure 2.13 D).

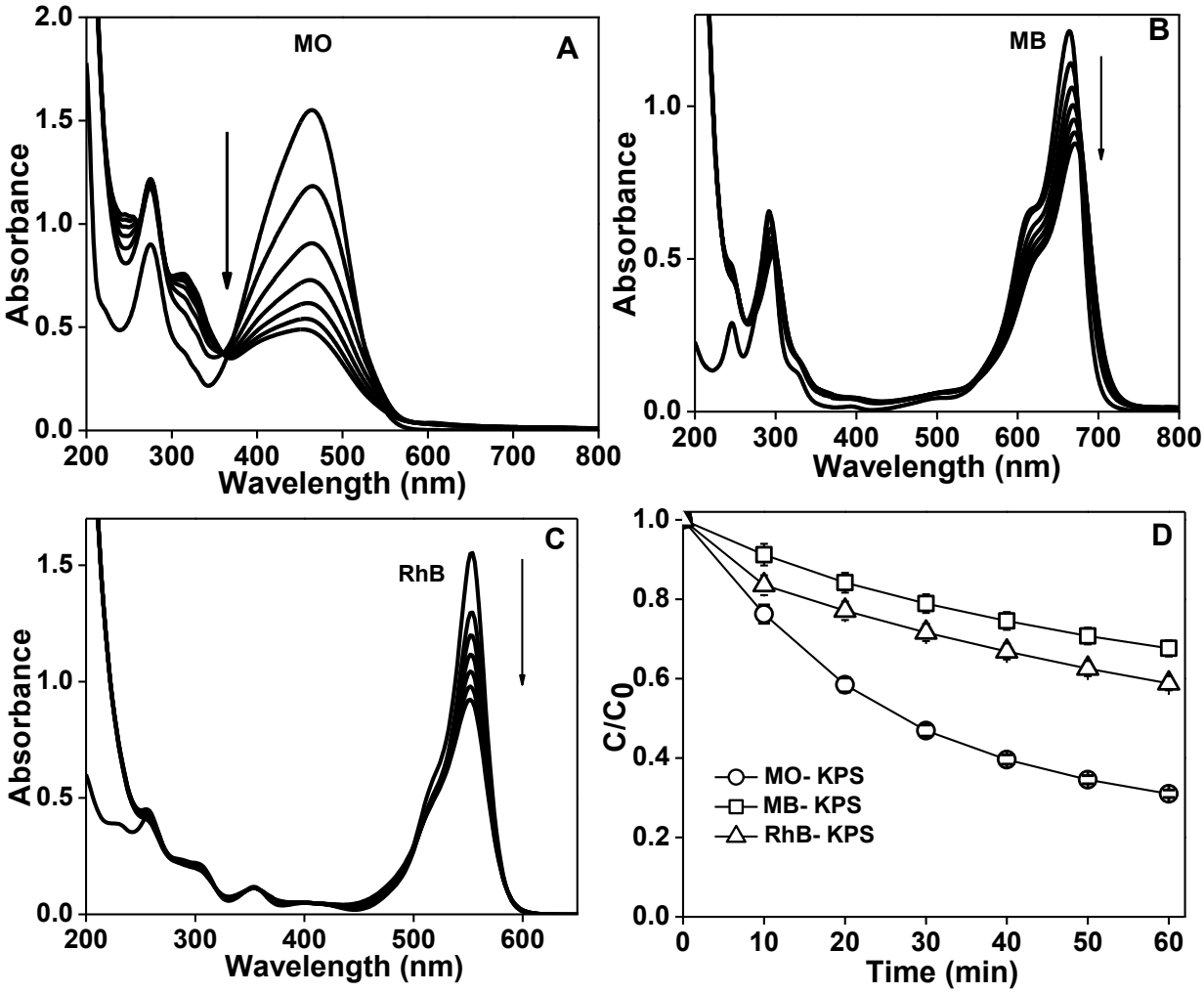

Figure 2.13 Change in absorption spectrum of (A) MO, (B) MB and (C) RhB at different time intervals after addition of KPS (1 g/L) in water. (D) C/C_0 Vs time plot showing the degradation of MO, MB and RhB by KPS.

The above results indicate that KPS alone has the ability to degrade dyes, and the degradation efficiency depends on the structure of the dyes. Interestingly, addition of micromolar amount of C1 to KPS (1 g/L), caused significant enhancement in the degradation of the dyes (Figure 2.14). MO, MB and RhB were found to be completely degraded within 10 min, 60 min and 20 min, respectively by activation of KPS using C1(Figure 2.14 A-D).Moreover, KPS caused ~15%, ~13% & ~12% TOC reduction of MO, MB and RhB, respectively whereas C1 activated PS caused ~74%, ~68% & ~72% TOC reduction of MO, MB and RhB, respectively (Figure 2.15). These results revealed the ability of C1 activated KPS to bring about effective degradation leading to the mineralisation of these dye pollutants.

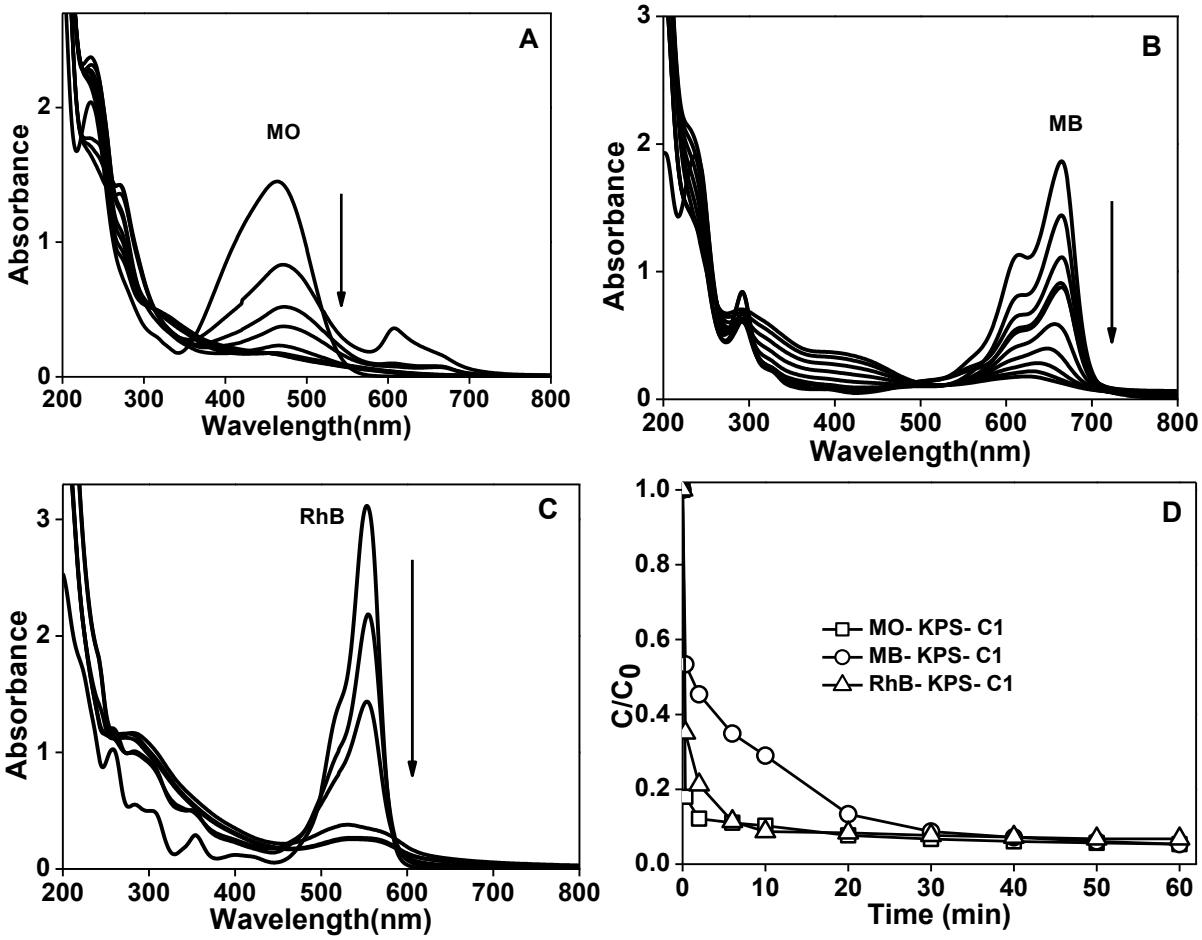

Figure 2.14 Change in absorption spectrum of (A) MO, (B) MB and (C) RhB at different time intervals after addition of KPS (1 g/L) in presence of C1 in water. (D) C/C_0 Vs time plot showing the degradation of MO, MB and RhB by KPS in presence of C1.

The dyes MO and RhB were completely degraded by C1 activated PS at three different pH 3, 7 and 9. In case of MB, complete degradation was observed at pH 3 & 7 whereas ~70% degradation was observed at pH 9 (Figure 2.16). It is important to note dye effluents highly vary in their pH.[30, 31]

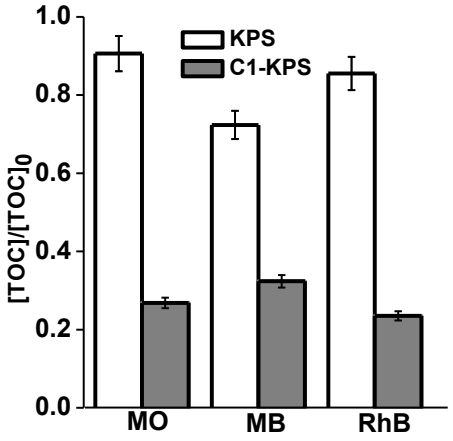

Figure 2.15 TOC reduction of MO, MB and RhB after the treatment with KPS (1 g/L) and C1 activated KPS.

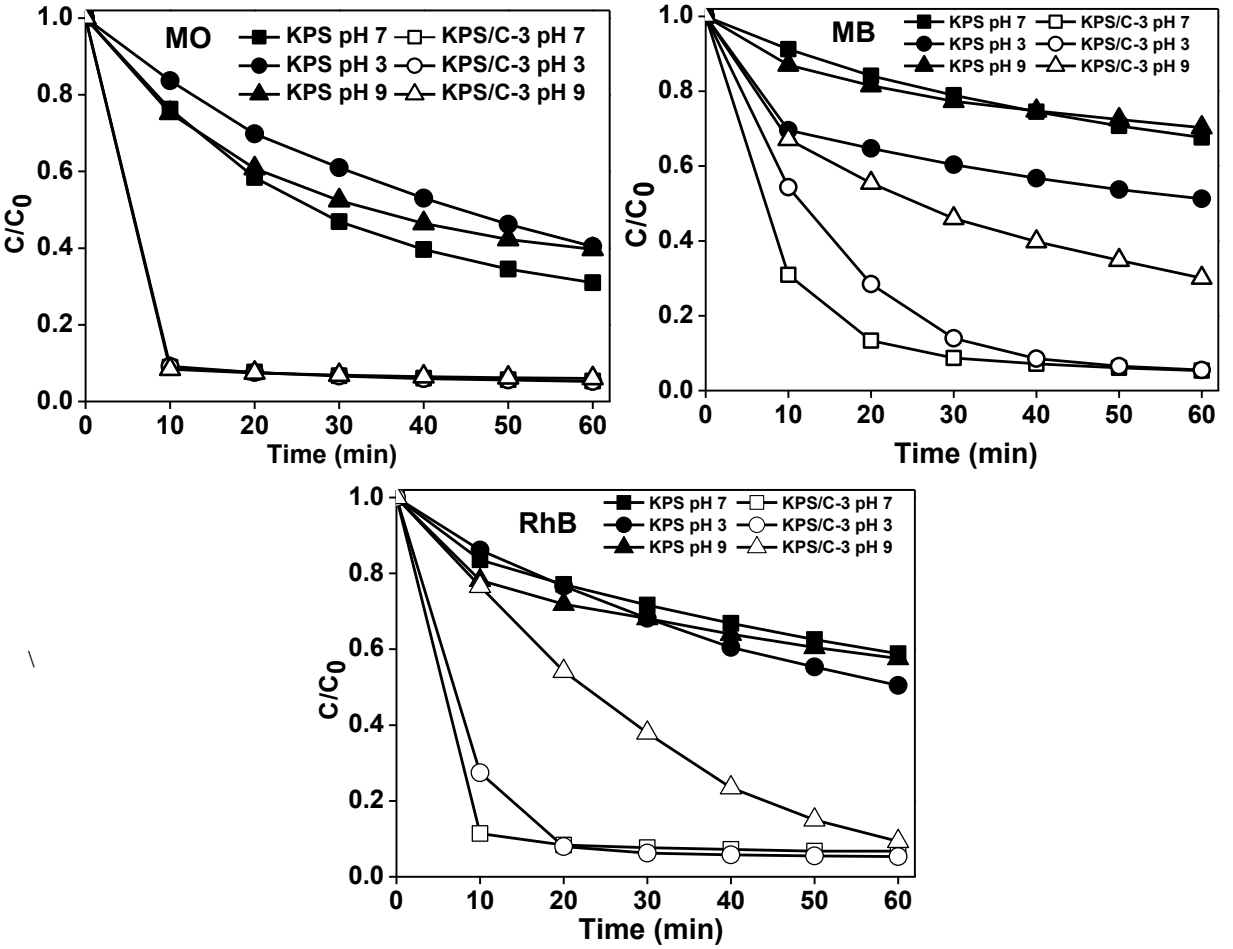

Figure 2.16 Effect of pH on degradation of MO, MB and RhB by C1 activated KPS.

The degradation of MO, RhB and MB were performed in simulated natural water containing a variety of inorganic ions and organic compound. The C/C_0 Vs time plot showed that the dyes MO, MB and RhB were almost completely degraded in simulated natural water containing a variety of inorganic ions and organic compounds (Figure 2.17A). These results revealed that the presence of common inorganic ions and organic compound had negligible effect on the degradation of these dyes by C1 activated KPS. Furthermore, C1 activated KPS effectively degraded a synthetic mixture of dyes (as model effluent) prepared by mixing MO, MB and RhB dyes in simulated natural water (Figure 2.17B). Notably, this synthetic dye effluent has wide absorption in the visible light region (350-710 nm) and almost black in colour. The effective degradation of this synthetic dye effluent further support the ability of C1 activated KPS based AOP for the treatment of textile dye effluents containing highly coloured dyes such as MO, RhB and MB. Water contaminated with such coloured effluents severely impede photosynthesis and thereby adversely affect the entire aquatic ecosystem.[30]

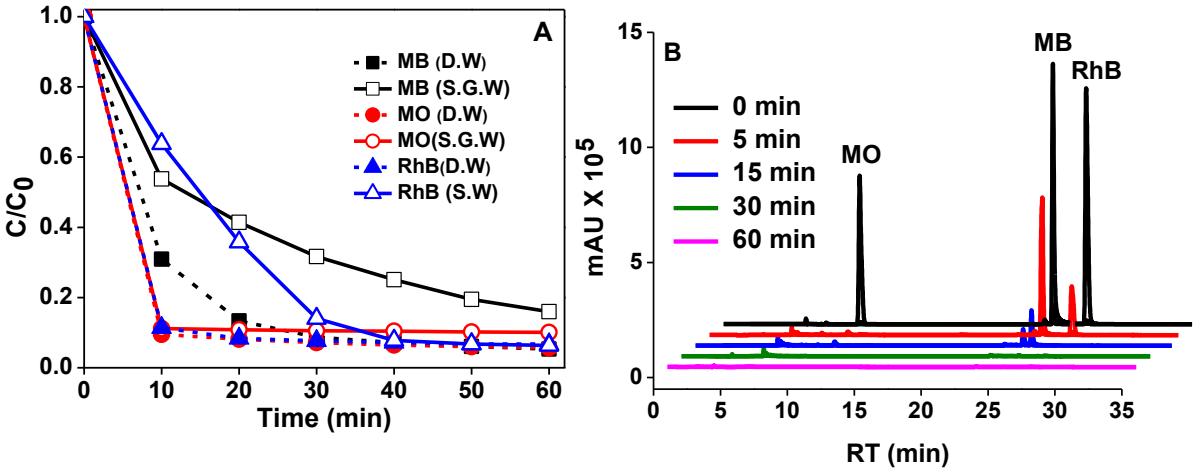

Figure 2.17 (A) C1 activated KPS degradation of MO, MB and RhB in simulated groundwater. (B) Degradation of synthetic dye effluent by C1 activated KPS.

Earlier, it has been shown that the inorganic ions such as carbonates and chlorides influence the degradation of organic contaminants by activated persulphate.[32, 33, 34] For example, Liang et al., showed that the degradation of trichloroethylene by activated persulphate reduced on increasing the concentration of bicarbonate ions from 0 mM to 9.2 mM in the reaction medium. [34] In case of chloride ions, it was shown that the concentration of chloride ions up to 200 mM had no effect on the degradation of trichloroethylene by activated persulphate.[32,34] Though C1 activated KPS degraded MO, RhB and MB in simulated natural water containing trace amounts of inorganic ions such as chlorides and bicarbonates, it is important to study the effect of these ions at higher concentration. Experiments were performed to examine the effect of chlorides and bicarbonates at relatively high concentration. In case of degradation of MO and MB by C1 activated KPS, NaCl had negligible effect whereas $NaHCO_3$ reduced the degradation (~65%) (Figure 2.18). In case of degradation of RhB by C1 activated KPS, both NaCl and $NaHCO_3$ reduced the degradation to ~65% and ~25%, respectively. Sulphate radicals generate hydroxyl radicals in aqueous solutions.[7,8] It is known that bicarbonate ions are scavengers of hydroxyl radicals and therefore, the concentration of hydroxyl radicals required for the effective degradation of MO was reduced in presence of HCO_3^- ions, resulting in the incomplete degradation.[32, 33, 34]

The observed results are consistent with earlier studies on degradation of trichloroethylene and p-nitrosodimethylaniline and further confirm the negative influence of HCO_3^- on activated persulphate based degradation (Figure 2.18). [32, 33, 34]

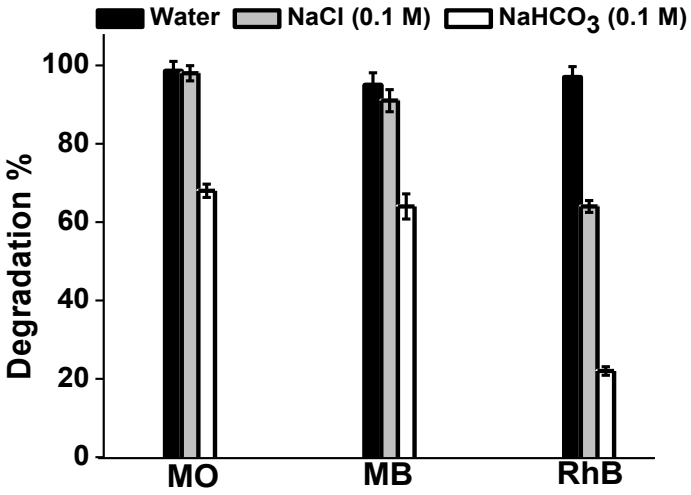

Figure 2.18 Degradation of MO, MB and RhB by C1 activated KPS in presence of high concentration of NaCl and $NaHCO_3$.

2.3.3 (b) Degradation of dye pollutants by silver tetra azamacrocyclic complex:

MO, MB and RhB were used as model dyes to study the effect of silver tetra azamacrocyclic complex (C2, Figure 1.5B) and KPS on the degradation of these dyes. Micromolar amount of C2 and KPS (1 g/L), caused significant enhancement in the degradation of the dyes. MO was found to be rapidly degraded within 10 min, where as the degradation of MB and RhB was incomplete after even after 60 min by activation of KPS using C2 (Figure 2.19). Earlier, it has been shown that Ag(I) activated persulphate and degraded contaminants such as 2,4 –DCP and Triclosan.[35, 36] The electrochemical oxidation of silver(II)tetra azamacrocyclic complex to silver(III)tetra azamacrocyclic complex has been reported.[37] However activation of persulphate using a silver(II)tetra azamacrocyclic complex has not been carried out. Importantly, the estimation of KPS by iodometric titration shows that C2 activated 8% and 11% of KPS after 2 min and 60 min, respectively. On the other hand, C1 activated about 19 % of KPS within 2 min (Appendix I S.I Figure 2.3). It should be noted that C1 activated KPS caused complete degradation of all the three dyes. These results indicate that activation of KPS depends on the structure of the complexes, and C1 is better for the activation of KPS when compared with C2.

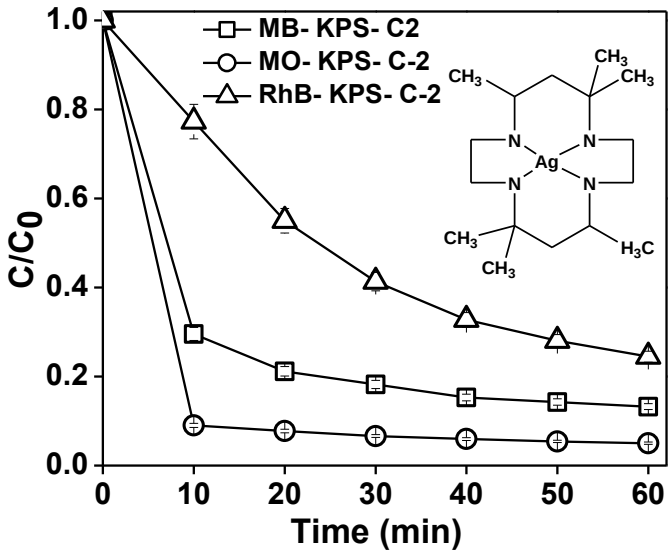

Figure 2.19 C/C_0 Vs time plot showing the degradation of MO, MB and RhB by KPS in presence of C2.

2.4 Conclusions:

MG and Cpf were completely degraded by C1 activated KPS. Interestingly, degradation of these contaminants by C1 activated KPS was found to occur in wide pH range (3‑9) with enhanced rate as compared to KPS alone. Degradation of MG and Cpf by Fe(II) ions activated KPS was incomplete while Ni(II) ions had no significant effect on degradation of MG and Cpf by KPS. Hydroxyl adducts and other low molecular weight compounds were identified as the degradation intermediates of MG and Cpf after their degradation by C1 activated KPS. Importantly, microbial assays revealed the complete removal of antibacterial activity of biocidal compounds MG and Cpf after treatment of these contaminants with C1 activated KPS. These results indicate that C1 activated KPS based AOP could aid the widely used biological oxidation for the treatment of recalcitrant organic contaminants.

Moreover, C1 activated KPS effectively degraded three highly coloured visible light absorbing dyes in a wide pH range. Importantly, C1 activated KPS had the ability to efficiently degrade a model dye effluent in a simulated natural water that contained a variety of ions. These results indicated the applicability of C1 activated KPS as a suitable AOP for treatment of dye pollutants in textile and related industries.

All the above results highlight C1 as potential persulphate activator for the degradation of non-biodegradable organic contaminants. Earlier studies on the redox reactivity of Ni(II) azamacrocyclic complexes in solid immobilised form imply that C1 could be immobilised onto solid supports.[38, 39] Immobilised C1 could be used as a heterogeneous persulphate activator that is easy to recover and reuse.

2.5 References:

1. Barefield, E. K.; Mocella, M. T., Complexes of silver (II) and silver (III) with macrocyclic tetraaza ligands. *Inorganic Chemistry* **1973,** *12* (12), 2829-2832.

2. Suh, M. P.; Kang, S. G., Synthesis and properties of nickel(II) and copper(II) complexes of 14-membered hexaaza macrocycles, 1,8-dimethyl- and 1,8-diethyl-1,3,6,8,10,13-hexaazacyclotetradecane. *Inorganic Chemistry* **1988,** *27* (14), 2544-2546.

3. Hameed, B.; Lee, T., Degradation of malachite green in aqueous solution by Fenton process. *Journal of Hazardous Materials* **2009,** *164* (2), 468-472.

4. Ju, Y.; Yang, S.; Ding, Y.; Sun, C.; Zhang, A.; Wang, L., Microwave-assisted rapid photocatalytic degradation of malachite green in TiO_2 suspensions: mechanism and pathways. *The Journal of Physical Chemistry A* **2008,** *112* (44), 11172-11177.

5. Modirshahla, N.; Behnajady, M. A., Photooxidative degradation of Malachite Green (MG) by UV/H_2O_2: Influence of operational parameters and kinetic modeling. *Dyes and Pigments* **2006,** *70* (1), 54-59.

6. Haines, R.; Rowley, J., Structure and Kinetics of Oxidation of Amphiphilic Nickel(II) Pentaazamacrocycles by Peroxodisulfate and by a Nickel(III) Pendant-Arm Macrocycle. *Journal of inclusion phenomena and macrocyclic chemistry* **2003,** *47* (1-2), 25-32.

7. Kolthoff, I.; Miller, I., The Chemistry of Persulfate. I. The Kinetics and Mechanism of the Decomposition of the Persulfate Ion in Aqueous Medium1. *Journal of the American Chemical Society* **1951,** *73* (7), 3055-3059.

8. Furman, O. S.; Teel, A. L.; Watts, R. J., Mechanism of Base Activation of Persulfate. *Environmental Science & Technology* **2010,** *44* (16), 6423-6428.

9. Zilbermann, I.; Maimon, E.; Cohen, H.; Meyerstein, D., Redox Chemistry of Nickel Complexes in Aqueous Solutions. *Chemical Reviews* **2005,** *105* (6), 2609-2626.

10. Zeigerson, E.; Bar, I.; Bernstein, J.; Kirschenbaum, L. J.; Meyerstein, D., Stabilization of the tervalent nickel complex with meso-5,7,7,12,14,14-hexamethyl-1,4,8,11-tetraazacyclotetradecane by axial coordination of anions in aqueous solution. *Inorganic Chemistry* **1982,** *21* (1), 73-80.

11. Kusvuran, E.; Gulnaz, O.; Samil, A.; Yildirim, O., Decolorization of malachite green, decolorization kinetics and stoichiometry of ozone-malachite green and removal of antibacterial activity with ozonation processes. *Journal of Hazardous Materials* **2011,** *186* (1), 133-143.

12. Chen, C. H.; Chang, C. F.; Liu, S. M., Partial degradation mechanisms of malachite green and methyl violet B by Shewanella decolorationis NTOU1 under anaerobic conditions. *Journal of Hazardous Materials 177* (1-3), 281-289.

13. Pérez Estrada, L. A.; Agüera, A.; Hernando, M. D.; Malato, S.; Fernández-Alba, A. R., Photo-degradation of malachite green under natural sunlight irradiation: Kinetic and toxicity of the transformation products. *Chemosphere* **2008,** *70* (11), 2068-2075.

14. Negreira, N.; Rodriguez, I.; Ramil, M.; Ruba, E.; Cela, R., Solid-phase extraction followed by liquid chromatography-"tandem mass spectrometry for the determination of hydroxylated benzophenone UV absorbers in environmental water samples. *Analytica chimica acta* **2009,** *654* (2), 162-170.

15. Neta, P.; Fessenden, R. W., Hydroxyl radical reactions with phenols and anilines as studied by electron spin resonance. *The Journal of Physical Chemistry* **1974,** *78* (5), 523-529.

16. Tripathi, G.; Sun, Q., Time-Resolved Raman Study of the Oxidation Mechanism of Aromatic Diamines by OH Radical in Water. *The Journal of Physical Chemistry A* **1999,** *103* (45), 9055-9060.

17. Mushinga, T.; Jonnalagadda, S., A kinetic approach for the mechanism of malachite green-peroxydisulphate reaction in aqueous solution. *International journal of chemical kinetics* **1992,** *24* (1), 41-49.

18. Behrman, E., The ortho-para ratio and the intermediate in the persulfate oxidation of aromatic amines (the Boyland-Sims Oxidation). *The Journal of Organic Chemistry* **1992,** *57* (8), 2266-2270.

19. Behrman, E. J., Studies on the reaction between peroxydisulfate ions and aromatic amines. Boyland-Sims oxidation. *Journal of the American Chemical Society* **1967,** *89* (10), 2424-2428.

20. Turesky, R. J.; Freeman, J. P.; Holland, R. D.; Nestorick, D. M.; Miller, D. W.; Ratnasinghe, D. L.; Kadlubar, F. F., Identification of aminobiphenyl derivatives in commercial hair dyes. *Chemical research in toxicology* **2003,** *16* (9), 1162-1173.

21. Wu, S. T.; Cao, K.; Bonacorsi, S. J.; Zhang, H.; Jemal, M., Distinguishing a phosphate ester prodrug from its isobaric sulfate metabolite by mass spectrometry without the metabolite standard. *Rapid Communications in Mass Spectrometry* **2009,** *23* (19), 3107-3113.

22. Ju, Y.; Yang, S.; Ding, Y.; Sun, C.; Gu, C.; He, Z.; Qin, C.; He, H.; Xu, B., Microwave-enhanced H 2 O 2-based process for treating aqueous malachite green solutions: intermediates and degradation mechanism. *Journal of Hazardous Materials* **2009,** *171* (1), 123-132.

23. Dewitte, B.; Dewulf, J.; Demeestere, K.; Van De Vyvere, V.; De Wispelaere, P.; Van Langenhove, H., Ozonation of ciprofloxacin in water: HRMS identification of reaction products and pathways. *Environmental Science & Technology* **2008,** *42* (13), 4889-4895.

24. De Witte, B.; Dewulf, J.; Demeestere, K.; Van Langenhove, H., Ozonation and advanced oxidation by the peroxone process of ciprofloxacin in water. *Journal of Hazardous Materials* **2009,** *161* (2), 701-708.

25. Sun, S. P.; Guo, H.Q.; Ke, Q.; Sun, J.H.; Shi, S. H.; Zhang, M. L.; Zhou, Q., Degradation of Antibiotic Ciprofloxacin Hydrochloride by Photo-Fenton Oxidation Process. *Environmental Engineering Science* **2008,** *26* (4), 753-759.

26.Tantis, I., Bousiakou, L., Karikas, G. A., & Lianos, P. Photocatalytic and photoelectrocatalytic degradation of the antibacterial agent ciprofloxacin. *Photochemical &*

Photobiological Sciences, **2015**, *14*(3), 603-607.

27. Giri, A. S., & Golder, A. K. . Decomposition of drug mixture in Fenton and photo-Fenton processes: Comparison to singly treatment, evolution of inorganic ions and toxicity assay. *Chemosphere*, **2015**,*127*, 254-261.

28. Kammerer, K.; Henninger, A., Promoting resistance by the emission of antibiotics from hospitals and households into effluent. *Clinical Microbiology and Infection* **2003,** *9* (12), 1203-1214.

29. Al Ahmad, A.; Daschner, F.; Kammerer, K., Biodegradability of cefotiam, ciprofloxacin, meropenem, penicillin G, and sulfamethoxazole and inhibition of waste water bacteria. *Archives of Environmental Contamination and toxicology* **1999,** *37* (2), 158-163.

30. Anjaneyulu, Y.; Sreedhara Chary, N.; Samuel Suman Raj, D., Decolourization of Industrial Effluents -" Available Methods and Emerging Technologies -" A Review. *Reviews in Environmental Science and Bio/Technology* **2005,** *4* (4), 245-273.

31. Lefebvre, O.; Moletta, R., Treatment of organic pollution in industrial saline wastewater: A literature review. *Water Research* **2006,** *40* (20), 3671-3682.

32.Ahmed, S., Rasul, M. G., Martens, W. N., Brown, R., & Hashib, M. A. Advances in heterogeneous photocatalytic degradation of phenols and dyes in wastewater: a review. **2011***Water, Air, & Soil Pollution*, *215*(1-4), 3-29.

33. Bennedsen, L. R.; Muff, J.; Sagaard, E. G., Influence of chloride and carbonates on the reactivity of activated persulfate. *Chemosphere* **2012,** *86* (11), 1092-1097.

34. Liang, C.; Wang, Z.S.; Mohanty, N., Influences of carbonate and chloride ions on persulfate oxidation of trichloroethylene at 20 C. *Science of the total environment* **2006,** *370* (2), 271-277.

35. Nfodzo, P.; Choi, H., Triclosan decomposition by sulfate radicals: effects of oxidant and metal doses. *Chemical Engineering Journal* **2011,** *174* (2), 629-634.

36. Anipsitakis, G. P.; Dionysiou, D. D., Transition metal/UV-based advanced oxidation technologies for water decontamination. *Applied Catalysis B: Environmental* **2004,** *54* (3), 155-163.

37. Barefield, E. K.; Mocella, M. T., Complexes of silver (II) and silver (III) with macrocyclic tetraaza ligands. *Inorganic Chemistry* **1973,** *12* (12), 2829-2832.

38. Gobi, K. V.; Ohsaka, T., Anion recognition and electrochemical characteristics of the self-assembled monolayer of nickel(II) azamacrocyclic complex. *Journal of Electroanalytical Chemistry* **2000,** *485* (1), 61-70.

39. Suh, M. P.; Moon, H. R.; Lee, E. Y.; Jang, S. Y., A Redox-Active Two-Dimensional Coordination Polymer: Preparation of Silver and Gold Nanoparticles and Crystal Dynamics on Guest Removal. *Journal of the American Chemical Society* **2006,** *128* (14), 4710-4718.

Nickel(II) hexaazamacrocyclic complex activated persulphate based AOP with adsorptive recovery and reuse of complex

3.1 Abstract:

Homogeneous metal ions/complexes are promising for activation of persulphate in advanced oxidation process (AOP) for oxidative degradation/mineralization of toxic organic pollutants in water. Nevertheless, these transition metal ions/metal complexes are leftover in the water after the degradation of organic pollutants. Adsorption of an effective persulphate activator such as nickel(II) azamacrocyclic complex, C1, onto adsorbents activated carbon (AC) and amberlite (Am) (that are used in water remediation) may allow easy separation and recyclability of the activator, thereby enhancing the overall efficiency of persulphate based AOP. Using Methyl Orange (MO), as model pollutant, the present chapter is focused on the investigation on the mechanism of MO degradation by C1 activated KPS, adsorption of C1 on to adsorbents AC & Am, the ability of C1 adsorbed onto AC and Am for activated persulphate based AOP. This chapter addresses the gap in literature discussed under the section 1.5 (b) of chapter 1.

Graphical Abstract:

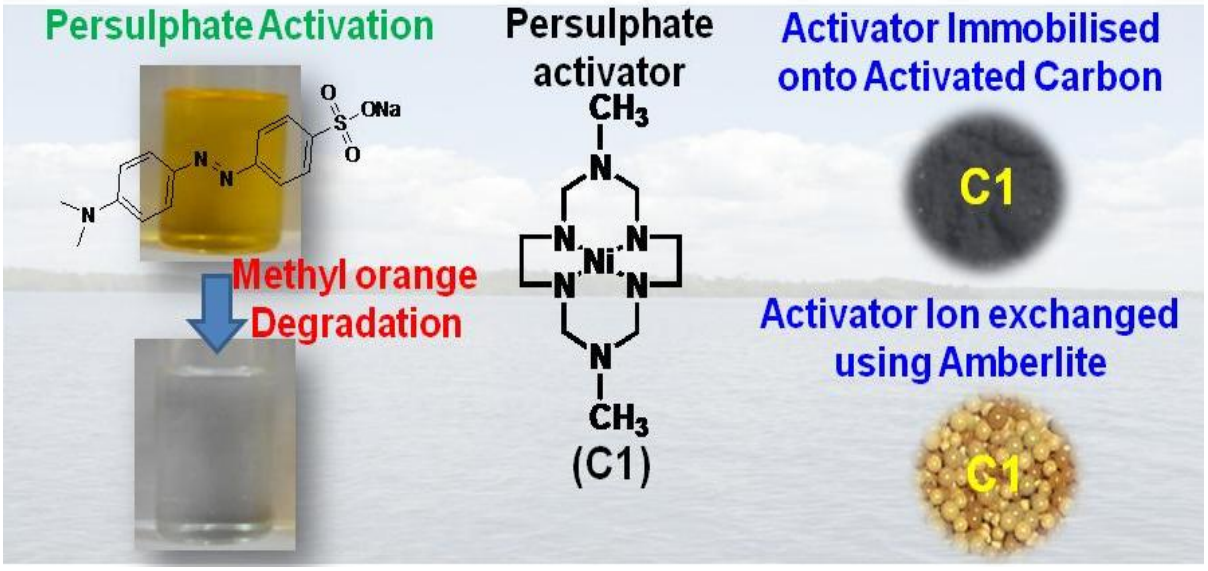

3.2 Experimental procedures and analysis:

3.2. (a) Materials and reagents:

Nickel chloride hexahydrate ($NiCl_2.6H_2O$), Potassium persulphate (KPS, $K_2S_2O_8$), Sulphuric acid (H_2SO_4), Sodium hydroxide (NaOH), Methyl orange, Potassium iodide (KI), Starch, Sodium chloride (NaCl), Acetic acid (CH_3COOH), Formic acid (HCOOH), Hydrochloric acid (HCl), Sodium thiosulphate ($Na_2S_2O_3$), Potassium dichromate ($K_2Cr_2O_7$),

Amberlite^{R} IR-120, Activated Carbon, Ethyl acetate, Tertiary butyl alcohol and Ethanol used were of guaranteed analytical grade, from SD fine chemicals, India. C1 was prepared as reported earlier.[1] Briefly, to a methanolic solution (50 mL) of $NiCI_2.6H_2O$ (1.5 g), Ethylenediamine 99% (6.8 mL), Formaldehyde 36% (20 mL) and Methylamine (8.6 mL) were added and stirred at reflux conditions for 24 hour. The resulting orange solution was cooled and filtered. The desired complex was precipitated after adding excess perchloric acid to the filtrate.[1]

For HPLC analysis, acetonitrile (HPLC grade) and Millipore water were used. Stock solutions of MO, complex C1, and KPS were prepared using double distilled water. Simulated ground or natural water was prepared by addition of following components to distilled water as reported earlier: $FeNO_3$ (0.24 µm), $NaHCO_3$ (1.2 mM), Na_2SO_4 (0.34 mM), Na_2HPO_4 (0.28 mM), NaCl (0.86 mM) and resorcinol (1 ppm). Freshly prepared KPS solution was used for all experiments.

3.2 (b) Degradation of MO by KPS using C1:

For degradation of Methyl orange (MO), appropriate amount of aqueous MO (20-30 ppm) solution was taken with and without C1 (C1 in the range 12-49 ppm), and the reaction was initiated by addition of required amount of KPS (5 g/L -0.5 g/L). Reaction volume was maintained at 5 ml, unless otherwise mentioned. The reaction was carried out at room temperature. Initial pH of the solution was ~7. Degradation of MO was studied by following the decrease in absorption maximum at 464 nm of MO, with respect to time, using JASCO V-570 UV/VIS/NIR spectrophotometer. Degradation of MO by (i) KPS alone (ii) KPS and $NiCl_2.6H_2O$ were performed as control experiments. Pseudo-first order rate constant (k) for the degradation of MO was determined from the C/C_0 Vs. time plot. Initial concentrations of C1, KPS and MO were varied and k values for the degradation of MO were determined. The optimised condition for MO degradation was determined to be [MO] = 20 ppm, [C1] = 48.3 ppm, and [KPS] = 1 g/L, based on rate constant (k) analysis.

Shimadzu UFLC prominence system with SPDM 20A Prominence diode array detector, equipped with phenomenex C18 HPLC column (250 mm × 4.5 mm, 5 µm) was used for high pressure liquid chromatography (HPLC) analysis. A 70:30 (v/v) mixture of ammonium acetate buffer (pH 4.5)/acetonitrile was used as the mobile phase, in isocratic mode with flow rate of 1 mL/min. For each analysis, 100 µL of sample taken from appropriate reaction mixture was injected and degradation of MO was monitored at 464 nm.

Shimadzu IR-Affinity-1 FT-IR spectrophotometer was used for Fourier transform

infrared (FT-IR) analysis of MO degradation. After treatment of MO with KPS and C1, the reaction mixture was completely evaporated using a rotary evaporator. Degraded intermediates present in this dry residue were extracted with ethanol and ethyl acetate and then evaporated to solid residues for FTIR analysis. In the liquid chromatography mass spectrometry (LCMS) analysis, Vantage TSQ triple stage quadrupole mass spectrometer (Thermo Fisher Scientific, San Jose, CA, USA) equipped with heated electro spray ionization (HESI) was used. The mass spectrometer is coupled with an Agilent 1290 infinity UHPLC system (Agilent Technologies India Pvt. Ltd., India). The UHPLC was provided with column oven (set at 40 ºC), auto-sampler and a thermo-controller (set at 4 °C). A flow through injection mode equipped with a needle wash system was used (with acetonitrile, 0.1% formic acid) before injection to ensure zero percent carry over problems. UHPLC system was equipped with Luna C-18(2) column (4.6 mm × 150 mm, 5 μm, Phenomenex, Inc). Mobile phase: Solvent A was 10 mM ammonium acetate containing 0.1% formic acid; and Solvent B was acetonitrile containing 0.1% formic acid. Binary gradient was optimized to get maximum separation (Gradient: 5% B at 0 min, 5% B at 3 min, 90% B at 15 min, 0% B at 15-17 min) at flow rate of 300 μL/min. Operating conditions were as follows: spray voltage -4000V; ion transfer capillary temperature-270 °C; source temperature- 300 °C; sheath gas-20, auxiliary gas-10 (arbitrary units) and ion polarity negative, full scan analysis- 50 to 400 m/z with the scan time of 500 millisecond. 10 μL of sample from appropriate reaction mixture of MO, KPS and C1 was injected after specific time interval.

Sievers 900 TOC analyser was used for Total Organic Carbon (TOC) analysis during degradation. An aliquot of 20 mL reaction solution was taken at specific time intervals from reaction mixture (100 mL) containing MO (20 mg/L), KPS (1 g/L) and C1 (100 μM) and injected into TOC analyser.

Redox reaction between C1 (100 μM) and KPS (1 g/L) leading to formation of trivalent nickel 290 nm species was monitored at its absorption maximum at 290 nm, similar to the reaction of tetraazamacrocyclic nickel complex with ammonium persulphate as reported by Haines *et al*.,[2, 3] C1 existing predominantly as trivalent nickel 290 nm species was prepared by incubating the reaction mixture containing KPS and C1.[2, 3] Reactivity of trivalent nickel 290 nm species with MO was also monitored by following the absorption changes of MO at 464 nm. Concentration of KPS during MO degradation in presence and absence of C1 was determined by iodometric titration as reported earlier.[4, 5] Tertiary butyl alcohol and Ethanol were used as scavengers for sulphate and hydroxyl radicals as reported earlier.[6, 7]

3.2 (c) Adsorption of C1 onto activated carbon (AC) and amberlite (Am):

Langmuir and Freundlich adsorption equations were used to determine the adsorptivity (K_F and q_m values) of C1 onto AC and Am.[8, 9]

$$\text{Langmuir isotherm: } q_e = \frac{q_m K_a C_e}{1 + K_a C_e}$$

$$\text{Freundlich Isotherm: } q_e = K_F C_e^{1/n}$$

q_e = amount of adsorbate adsorbed on to adsorbent (mg/g) at equlibrium; C_e = equilibrium concentration of adsorbate in the solution (mg/L); q_m(L) = Langmuir maximum adsorption capacity (mg/g); K_a = Langmuir constant (L/mg); K_F = Freundlich constant indicative of relative adsorption capacity of the adsorbent ($[mg^{1-(1/n)}.L^{1/n}]/g$); 1/n = Freundlich constant indicative of intensity of adsorption. Freundlich maximum adsorption capacity was determined from the equation $K_F = qm/ C_0^{1/n}$ where, q_m is Freundlich maximum adsorption capacity (mg/g), and C_0 is the initial concentration of adsorbate in the bulk solution (mg/L).[8, 9]

The equilibrium concentration of C1 during adsorption was determined by following the absorption of C1. In the absence of KPS, the concentration of C1 in the divalent state was followed by monitoring the d-d absorption maximum at 446 nm. In the presence of KPS, the concentration of C1 in the trivalent state was followed by monitoring the absorption band maximum around 290 nm.[2,3]

C1-AC was prepared by adding AC (1 g) to 100 ml of C1 (4.25 mM). This suspension was stirred overnight. Supernatant obtained after removing AC was filtered using 0.45 μM Polytetrafluoroethylene (PTFE**)** membrane filter and the absorption spectrum of the filtrate was recorded to determine the adsorption. Then the C1 immobilized onto AC (C1-AC) was removed by filtration and washed thrice with distilled water, and finally dried in a desiccator. The loading of C1 in C1-AC was determined to be 160.6 mg of C1 per gram of AC (16.0 %). Similarly for preparation of C1-Am, Am (1 g) was added to 50 ml of C1 (4.25 mM). The loading of C1 in C1-Am was determined to be 96.4 mg of C1 per gram of Am (9.64 %). X-ray photoelectron spectroscopy (XPS) measurements were carried out using a Thermo Fisher Scientific (East Grinstead, UK) θ probe spectrometer and monochromatic Al-Kα radiation (photon energy 1486.6 eV). The adsorption of MO onto AC was studied by following the absorbance of MO at 464 nm.

3.2 (d) Degradation of MO by KPS using C1 adsorbed onto AC (C1-AC) and Am (C1-Am):

Degradation of MO (30 ppm) by KPS (1 g/L) using C1-AC (0.3 g/L, 16.0 % C1 loading)/C1-Am (0.5 g/L, 9.64 % C1 loading) was studied spectrophotometrically, as mentioned above for homogeneous degradation of MO. Suspension of 0.3 g/L of C1-AC with

16.0 % C1 loading, or 0.5 g/L of C1-Am with 9.64 % C1 loading in reaction mixture (5 ml) corresponds to an effective concentration of 48.3 ppm of C1, similar to the amount of C1 used in homogeneous condition. Control experiments (i) bare AC/Am (without C1) and MO in presence of KPS (ii) C1-AC/C1-Am and MO in absence of KPS were performed. Reuse of C1-AC for MO degradation was studied by performing cyclic degradation experiment in presence and absence of KPS. After each cycle, C1-AC was removed by centrifugation and reused for the subsequent cycle. Degraded MO solution obtained from each cycle was analysed for the presence of C1 (as nickel) by AAS. Similarly, the reuse of C1-AC for MO degradation in simulated natural water was also performed. The concentration of C1 in the MO degraded solution was monitored by determination of the nickel content using atomic absorption spectrometer (AAS) (Perkin Elmer, AAS 400), as well as by following the change in the absorption of C1. Ion exchange (extraction) of C1 that was adsorbed onto Am was performed by eluting with 0.17 M NaCl solution. Degradation of MO by using the C1 that was extracted from C1-Am was performed similar to the protocol mentioned above.

3.3. Results and Discussion:

3.3 (a) Mechanism of MO degradation by C1 activated KPS:

Rate of degradation of MO by KPS and C1 with radical scavengers such as tertiary butyl alcohol and ethanol was found to be retarded (Figure 3.1, Table 3.1), indicating that both sulphate and hydroxyl radicals are involved in the degradation of MO by C1 activated KPS (Reactions 1-6). Similar results were reported for activation of persulphate using metal ions (Fe^{2+}, Fe^{3+}, Ag^{+}) for degradation of halocarbon.[6] Redox reaction between C1 (100 μM) and KPS (1 g/L) leads to formation of trivalent nickel 290 nm species with absorption maximum at 290 nm, similar to the reaction of tetraazamacrocyclic nickel complex with ammonium persulphate as reported by Haines *et al*., (Figure 3.2A).[2, 3]

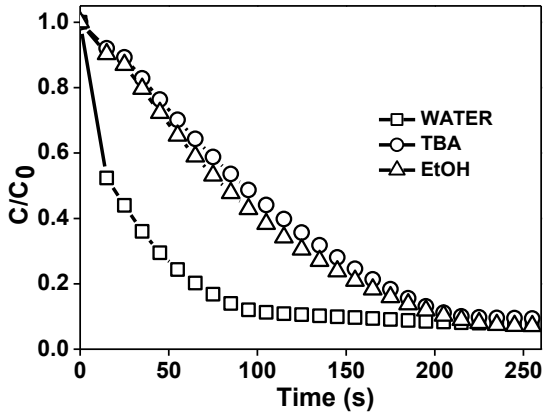

Figure 3.1 Effect of radical scavengers on the rate of degradation of MO by KPS and C1. [C1] = 48.3 mg/L; [KPS] = 1 g/L; [MO] = 50 mg/L; [TBA] = 0.5 M; [Ethanol] = 0.5 M.

Table 3.1 Pseudo-first order rate constants determined for degradation of MO by KPS in presence of radical scavengers

Scavenger	Pseudo-first order rate constant, k (s^{-1})
TBA (0.5 M)	0.38 ± 0.02
Ethanol (0.5M)	0.47 ± 0.01
None	1.96 ± 0.07

[C1] = 48.3 mg/L; [KPS] = 1g/L; [MO] = 50 mg/L.

Importantly, this trivalent nickel 290 nm species also caused rapid degradation of MO in presence of KPS. Moreover, it was determined by iodometric titration that about 21 % (0.21 g/L) of KPS was consumed for degradation of MO (20 ppm) by KPS (1 g/L) in presence of C1 (48.3 ppm) (with in 10 min), whereas only 4% (0.04 g/L) of KPS was consumed for the reaction between MO (20 ppm) and KPS (1 g/L) without C1 (after 60 min of reaction).

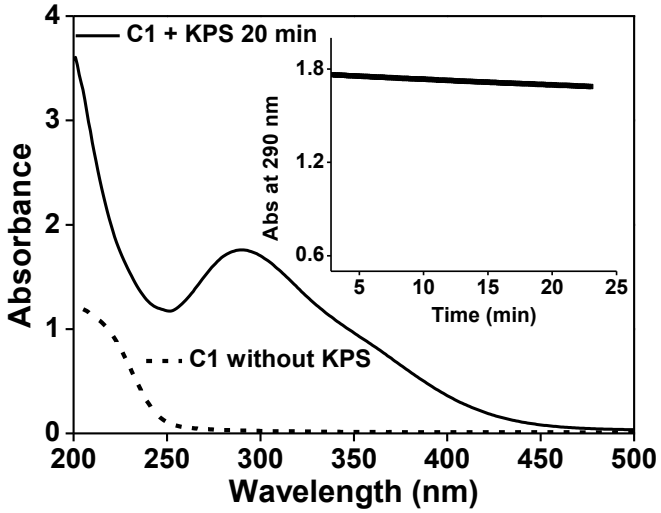

Figure 3.2 (A) Absorption spectral changes showing formation of 290 nm trivalent nickel species on addition of KPS (1 g/L) to C1 (300 µM); Inset shows saturation of Ni(III) species monitored at 290 nm. (B) Absorption spectral changes showing the degradation of MO by trivalent nickel 290 nm species [C1] = 100 µM; [KPS] = 1 g/L; [MO] = 20 ppm; [C1 in trivalent Nickel form (290 nm Ni(III) species)] = 100 µM.

Earlier it has been shown that trivalent nickel complexes could oxidise organic substrates (reaction 7).[10, 11] These results indicate that the trivalent nickel 290 nm species oxidise MO (reaction 7) and reduce to the divalent state. The resulting divalent C1 could be oxidised by KPS (reaction 1-3), leading to higher consumption of KPS (more than the stoichiometric amount of C1), as revealed by titration experiments. Based on these results the mechanism of degradation of MO by C1 activated KPS is proposed (Figure 3.3).

$$[Ni(II)L]^{2+} + S_2O_8^{2-} \underset{\text{ion-pair}}{\leftrightarrow} \{Ni(II)L^{2+}+, S_2O_8^{2-}\} \quad (1)$$

$$\{Ni(II)L^{2+}+, S_2O_8^{2-}\} \rightarrow [Ni(III)L(SO_4)]^{+} + SO_4^{\bullet -} \quad (2)$$

$$[Ni(II)]^{2+} + SO_4^{\bullet -} \rightarrow [Ni(III)L(SO_4)]^{+} \quad (3)$$

$$SO_4^{\bullet -} + \text{Organic Pollutant} \rightarrow \text{Oxidative degradation} \quad (4)$$

$$SO_4^{\bullet -} + H_2O \leftrightarrow OH^{\bullet} + H^{+} + SO_4^{2-} \quad (5)$$

$$OH^{\bullet} + \text{Organic Pollutant} \rightarrow \text{Oxidative degradation} \quad (6)$$

$$[Ni(III)L(SO_4)]^{+} + \text{Organic Pollutant} \rightarrow [Ni(II)L]^{2+} + SO_4^{2-} + \text{Oxidative degradation} \quad (7)$$

Where, $L = 1,8-\text{dimethyl}-1,3,6,8,10,13$ hexaazacyclotetradecane

$[Ni(III)L(SO_4)]^{+} = C1$ in trivalent form with absorption maximum at 290 nm

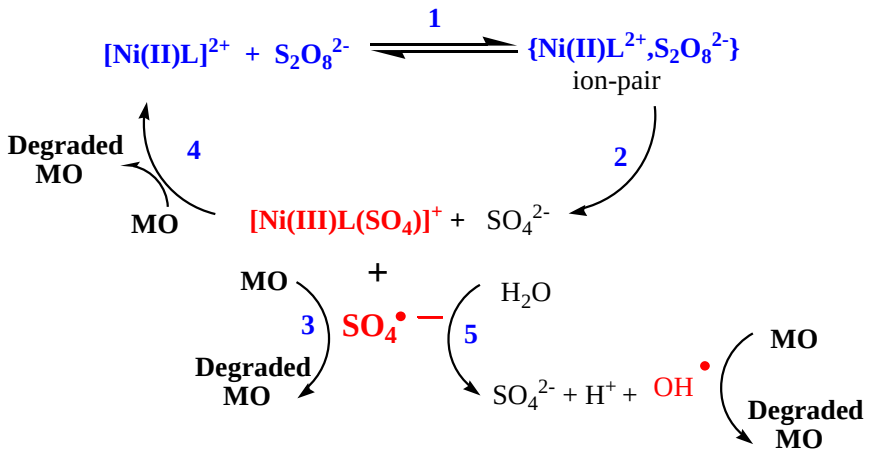

Figure 3.3 Proposed mechanism for the degradation of MO by C1 activated KPS.

3.3 (b) Identification of degradation intermediates:

The N=N- stretching peak at 1608 cm^{-1} of azo group was absent in FT-IR spectra of ethanol and ethyl acetate extract residues of MO degraded by KPS in presence of C1(Figure 3.4). Moreover, IR spectra of degraded MO showed peaks at 3000 cm^{-1} and 2785 cm^{-1} due to C-H stretching; 1223 cm^{-1} because of C-N-stretching; 858 cm^{-1} and 1051 cm^{-1} corresponding to aromatic ring vibrations, and 587 cm^{-1} and 692 cm^{-1} due to –C-S- and S=O stretching, respectively (Figure 3.4).[12-14] These IR results indicated the loss of characteristic azo group of MO, and transformation to aromatic amine and sulphonated intermediates during degradation.

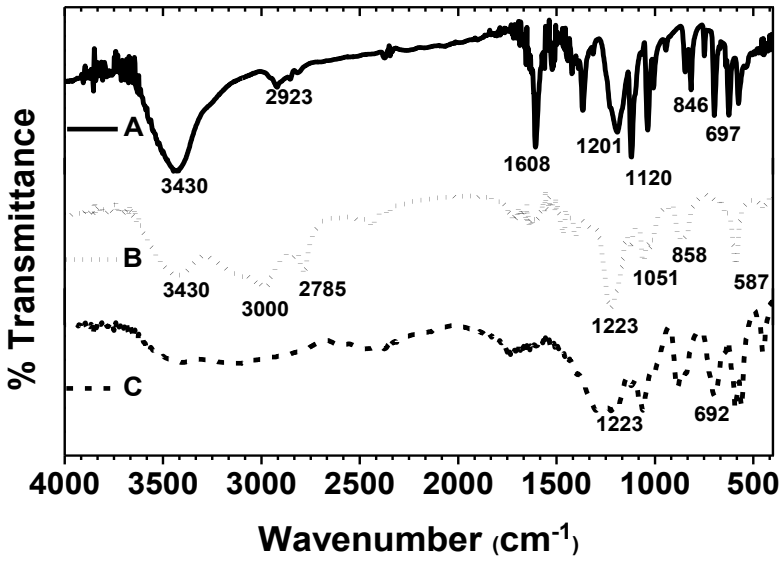

Figure 3.4 FT-IR spectra of (A) undegraded MO, (B) Ethanol and (C) Ethyl acetate extract residue of MO degraded by KPS in presence of C1. [MO] = 100 ppm; [KPS] = 1 g/L; [C1] = 100µM.

Total ion chromatogram (TIC) of MO showed a single peak at RT 14.4 min (Figure 3.5A) corresponding to 304 m/z of MO (Appendix I Figure 3.1).This MO peak was completely absent in TIC of MO degraded by KPS in presence of C1 (Figure 3.5D), whereas a prominent MO peak was observed in TIC of MO degraded by KPS alone (Figure 3.5B). Some of the degradation intermediates (Appendix I Figure 3.1, Figure 3.6) of MO observed during the reaction are similar to those reported earlier.[15-19] Degradation intermediates 200 m/z (RT 12.5 min) and 290 m/z (RT 13.7 min) disappeared in TIC of MO degraded by KPS in presence of C1, within 30 min (Figure Appendix I Figure 3.1), whereas these peaks were clearly observed in TIC of MO degraded by KPS alone even after 60 min (Figure Appendix I Figure 3.1). Although homogeneous C1 activated KPS and degraded MO, it is important to recover the C1 from the solution and reuse. The results on the adsorptive recovery and reuse of C1 using adsorbents for water remediation such as AC and Am[20, 21] are presented below.

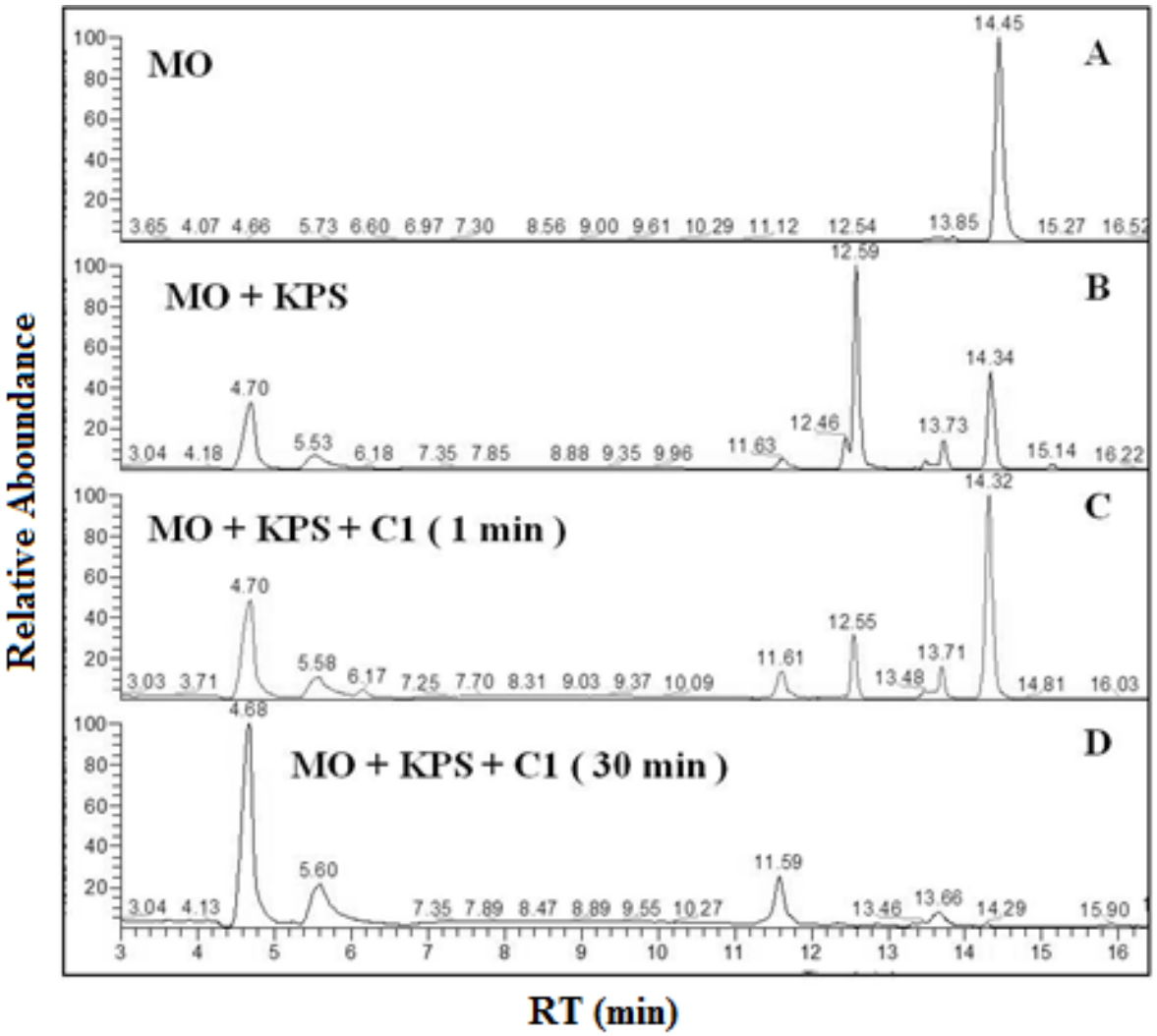

Figure 3.5 Total ion chromatogram (TIC) of (A) MO, (B) MO degraded for 30 min by KPS, (C) MO degraded by KPS in presence of C1 for 1 min, and (D) 30 min. [MO] = 100 mg/L; [KPS] = 1 g/L; [C1] = 100 µM.

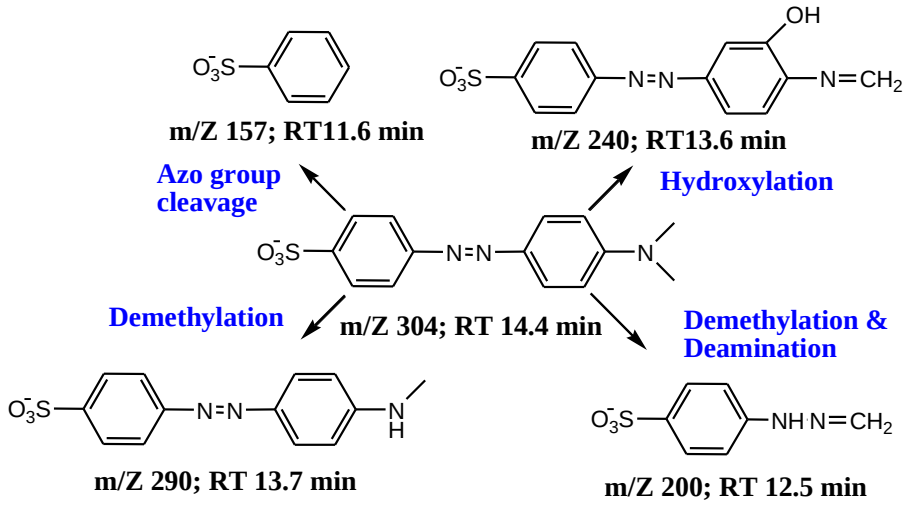

Figure 3.6 Proposed degradation intermediates of MO.

3.3 (c) Recovery and reuse of C1 using adsorbents:

Adsorption of C1 onto AC and Am adsorbents was determined to follow Freundlich adsorption isotherm model (Figure 3.7 and 3.8), and their adsorptivity parameters are tabulated (Table 2 & Appendix I Table 3.1). AAS results revealed the absence of C1 in water (not detectable, and less than 1 ppm) after the recovery of C1 using adsorbents. Thus, AC and Am are useful for adsorptive recovery of C1 in presence of persulphate, where C1 existed as trivalent nickel 290 nm species (Figure 3.1A), as well as for the recovery of C1 with nickel in divalent state in the absence of persulphate.

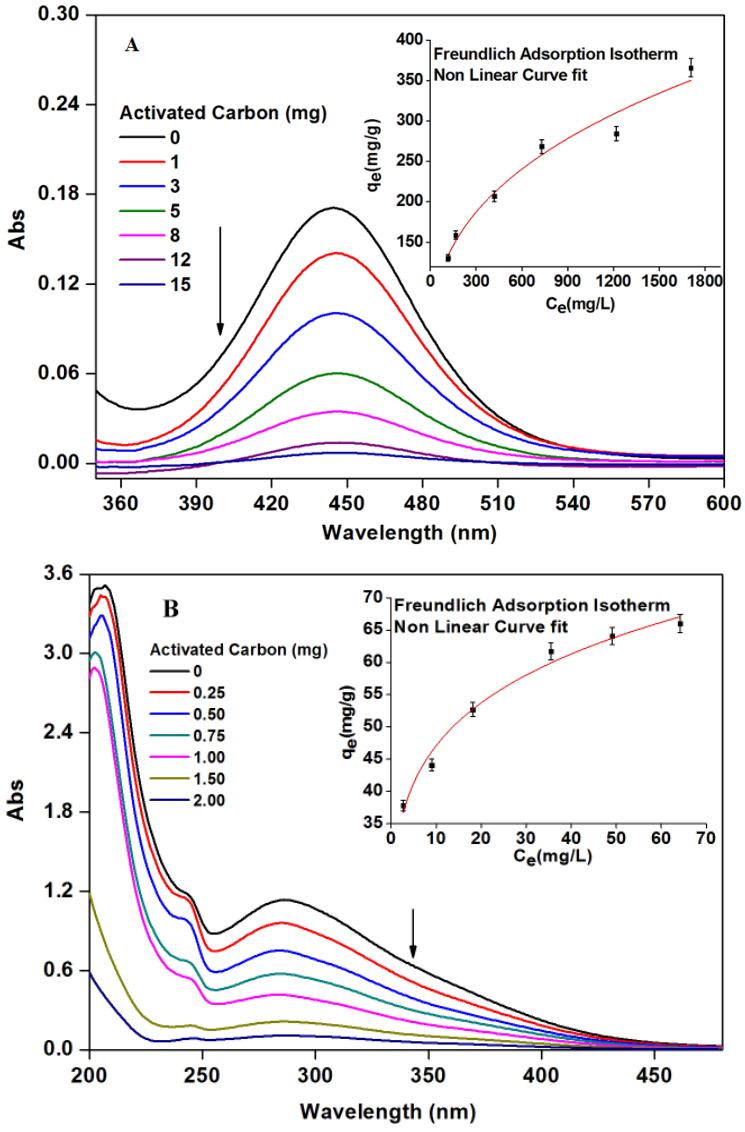

Figure 3.7 Adsorption of C1 onto activated carbon without KPS (A) and with KPS (B). Inset shows the non-linear fitting for Freundlich adsorption isotherm.

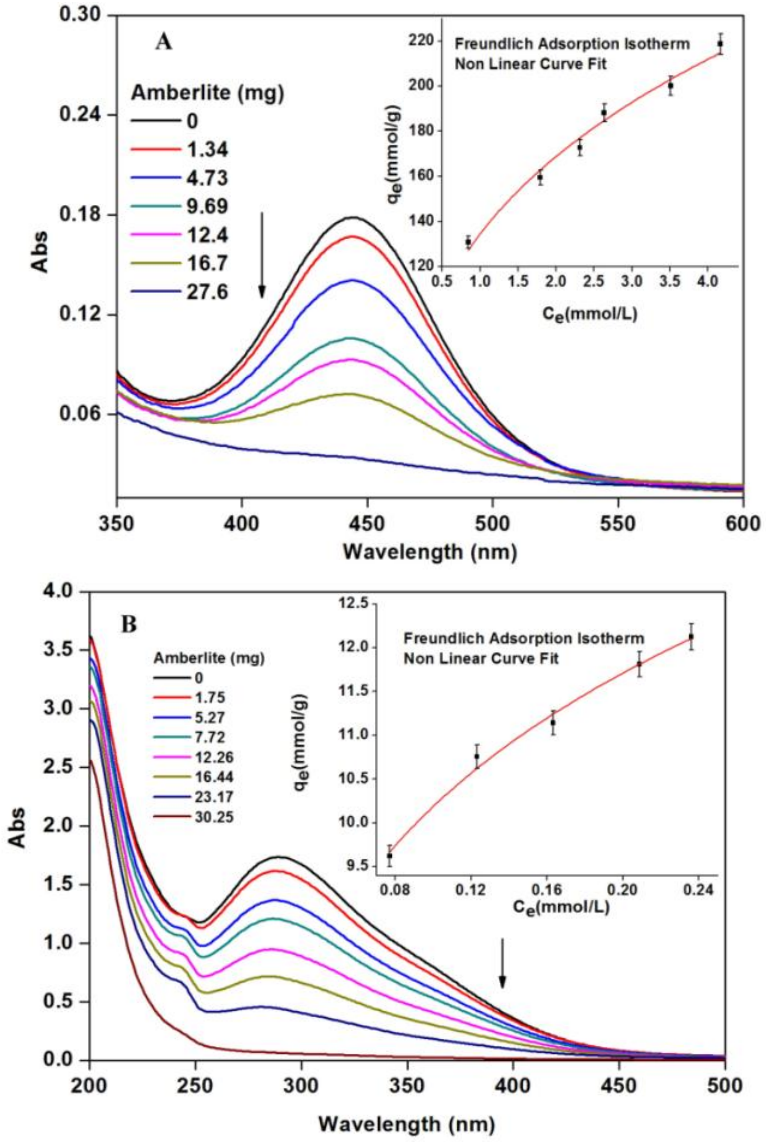

Figure 3.8 Adsorption of C1 on to amberlite without KPS (A), and with KPS (B), Inset shows the non-linear fitting for Freundlich adsorption isotherm, [C1] = 300 μM

Table 3.2 Freundlich adsorption isotherm parameters for adsorption of C1 onto Amberlite and Activated carbon in presence and absence of KPS.

Freundlich Adsorption Isotherm					
Adsorbent	Adsorbate	K_F	1/n	q_m	R^2
Am	C1[a]	2.27	0.20	6.1	0.989
AC	C1[a]	30.37	0.20	75.8	0.981
Am	C1[b]	8.61	0.33	106.9	0.979
AC	C1[b]	24.06	0.36	375.6	0.964

a = C1 in presence of KPS, b = C1, in absence of KPS; $[C1]_0$ = 2.06 g/L for Am and AC. K_F = Freundlich constant indicative of equilibrium adsorption capacity of the adsorbent ($[mg^{1-(1/n)}.L^{1/n}]/g$); 1/n = Freundlich constant indicative of intensity of adsorption; q_m = Freundlich maximum adsorption capacity (mg/g). R^2 = Correlation coefficient.

X-ray photoelectron spectrum of C1 adsorbed onto AC (C1-AC) showed peaks at 400.3 eV and 855.9 eV that correspond to binding energy of nitrogen, (N1s), and divalent nickel of C1 ($Ni2p_{3/2,}$), respectively (Figure 3.9).[22-29] C1 adsorbed onto Am (C1-Am) also showed similar peaks (Appendix I Figure 3.2).

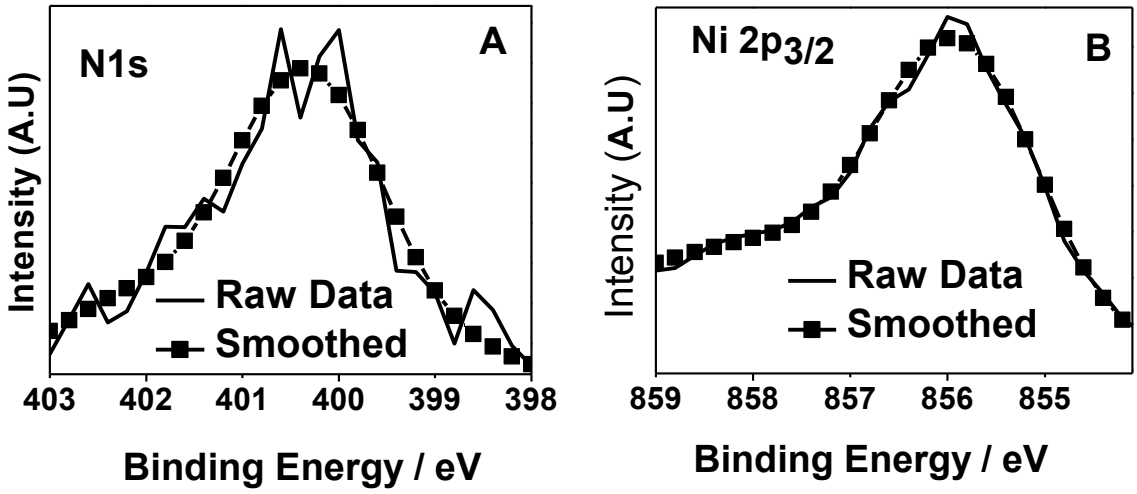

Figure 3.9 XPS of C1-AC showing (A) N1s and (B) $Ni2p_{3/2}$ peaks.[A.U – Arbitrary Unit]

The ability of solid C1-AC and C1-Am to activate persulphate and degrade MO was investigated, and the results are presented below. MO (30 ppm) was rapidly degraded by KPS (1 g/L) in presence of C1-AC (0.3 g/L, 16 % loaded C1) within 10 min, (Figure 3.10A). On the other hand, degradation of MO (30 ppm) by KPS (1 g/L) in presence of AC (0.3 g/L of bare AC without C1) was incomplete even after 60 min of treatment, (Figure 3.10A). Further, the adsorption of MO (30 ppm) onto C1-AC, and AC were determined to be ~ 9 ppm and 12 ppm, respectively (Figure 3.10A, Appendix I Table 3.2), revealing that the adsorptive removal of MO by C1-AC and AC was incomplete. It was observed that XPS of C1-AC treated with persulphate showed additional peaks at 401.6 eV and 854.8 eV that correspond to nitrogen (N1s), and trivalent nickel of C1 ($Ni2p_{3/2,}$) (Figure 3.11), respectively.[22-29]

Moreover, the iodometric titration results, as discussed earlier, also revealed higher consumption of persulphate (than the stochiometric amount of C1) during the degradation of MO. All the above results i.e. both the XPS and iodometric titration results reveal the redox reaction between C1 in solid form and KPS. C1-AC was reused for five times to activate persulphate and degrade MO, in which almost complete degradation of MO was observed for the first three reuse runs without significant loss of C1 from C1-AC (less than ~1 ppm in each reuse run, Figure 3.10B). At fourth and fifth reuse runs, MO degradation was determined to be ~80% and 60%, respectively. Moreover, AAS analysis revealed that there was about 10%

(5.52 ppm), and 20% (9.7 ppm) of leaching of nickel from C1-AC into water at the fourth and fifth reuse runs, respectively (Figure 3.10B, Appendix I Figure 3.3).

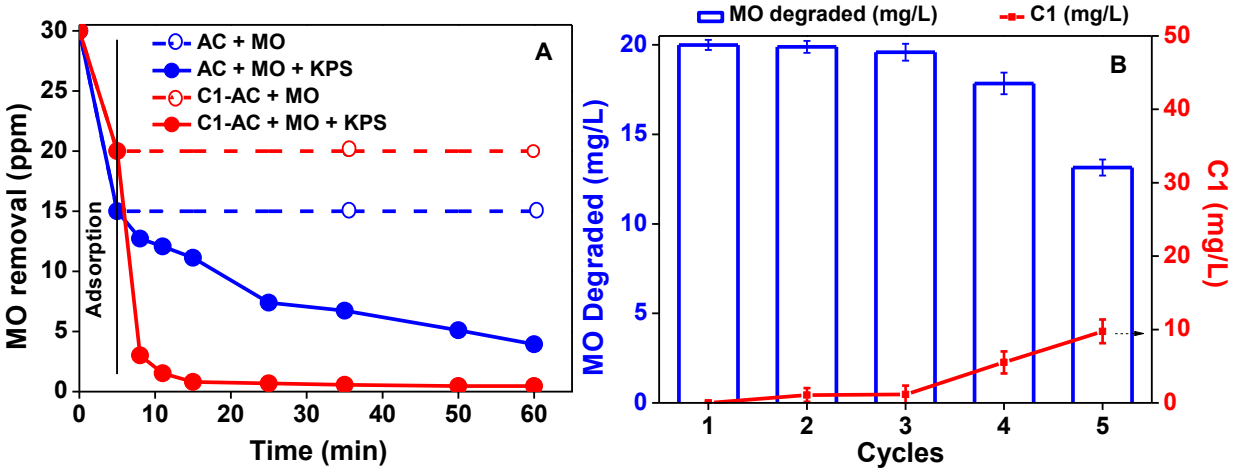

Figure 3.10 (A) Plot showing MO degradation by KPS in the presence of AC and C1-AC. [AC] = 0.3 g/L; [C1-AC] = 0.3 g/L (16% loading; effective concentration of C1 is 48.3 ppm); [KPS] = 1 g/L. The dotted lines represent the adsorptive removal of MO by AC and C1-AC in absence of KPS. (B) Reuse of C1-AC. Reuse runs (cycles) for degradation of MO by C1-AC in the presence of KPS, and the corresponding concentration of C1 (in ppm) at the end of each cycle in the treated solution. Initial concentration of MO at each cycle is 20 ppm

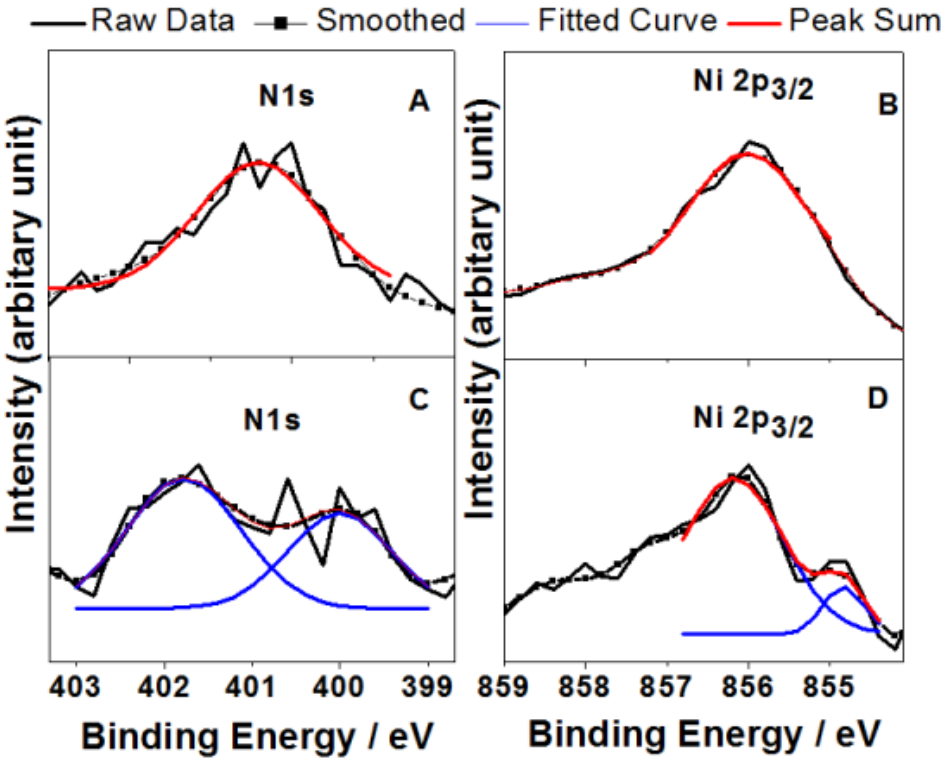

Figure 3.11 XPS of C1-AC (A & B), and C1-AC treated with KPS (C & D) with respect to the N1s and Ni2$p_{3/2}$ peaks

The reusability of C1-AC was also observed for the degradation of MO carried in simulated natural water (Appendix I Figure 3.4). All the above results reveal that AC is useful to recover C1 and reuse C1 as solid C1-AC.

Although, C1 was effectively adsorbed onto Am, the solid C1-Am was not effective to activate persulphate and degrade MO, unlike the solid C1-AC discussed above. It is proposed that the electrostatic repulsion between the negatively charged Am and persulphate anion is not favourable for their interaction to activate the persulphate anion by the C1 adsorbed onto Am. However, the adsorption of C1 onto Am was useful to completely recover the homogeneous C1 from the degraded MO solution, as revealed by absorption and AAS results (Figure 3.12, Black and Magenta).

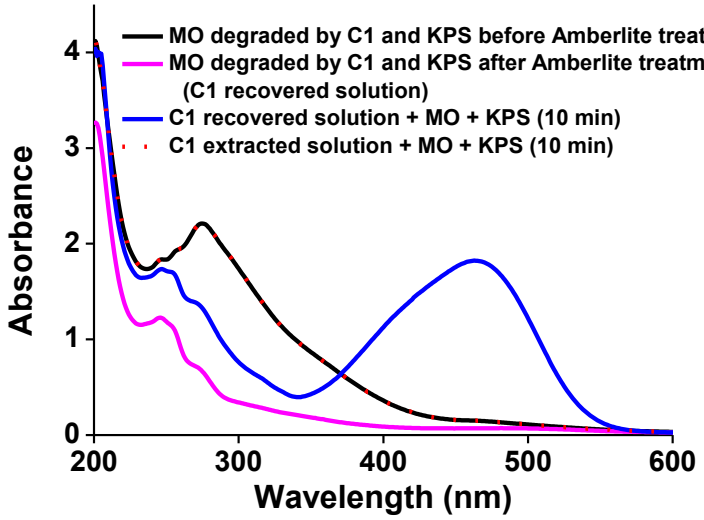

Figure 3.12 Reusability of C1 using amberlite. [MO] = 20 mg/L; [KPS] = 1g/L; [C1] = 48.3 ppm; [Am] = 15mg/L.

Further, the recovered C1-Am was ion exchanged using sodium chloride to obtain C1 (> 85% (extracted) as determined from AAS) that was reused for MO degradation. (Figure 3.12, Red dotted line). Almost similar results were also observed for the degradation of MO carried in simulated natural water (Appendix I Figure 3.5). Thus, Am was useful in a metal complex activated persulphate based AOP for adsorptive recovery of the complex, and for the reuse of complex in homogeneous form after ion exchange process.

3.4 Conclusions:

Nickel complex based persulphate activator C1 caused effective degradation of MO in presence of KPS. The propensity of C1 to adsorb on to Am and AC was beneficial in the recovery and reuse of C1 in the homogeneous and heterogeneous form, respectively. Thus, the study highlights the potential of C1 as a recoverable and a reusable persulphate activator,

in the homogeneous and heterogeneous form, for the degradation of MO in presence of KPS.

Recoverable and reusable metal based persulphate activators are profitable, and environment friendly as they prevent or control the entry of persulphate activator into water bodies. The study exemplifies for the first time, that a redox active metal complex based homogenous persulphate activator that could be recovered using an adsorbent, could be reused either in homogenous form after extraction from the adsorbent, or in the hetergeonous form, where the persulphate activator is bound to an adsorbent The study draws attention to the application of adsorbents in metal complexes activated persulphate based AOP for the removal of metal based persulphate activators from water after the treatment that would prevent the entry of metal ions into water bodies. Moreover, the study highlights the recyclability of an effective metal complex based persulphate activator using versatile adsorbents.

3.5 References:

1. Suh, M. P.; Kang, S. G., Synthesis and properties of nickel(II) and copper(II) complexes of 14-membered hexaaza macrocycles, 1,8-dimethyl- and 1,8-diethyl-1,3,6,8,10,13-hexaazacyclotetradecane. *Inorganic Chemistry* **1988,** *27* (14), 2544-2546.

2. Haines, R.; Rowley, J., Structure and kinetics of oxidation of amphiphilic Nickel(II) pentaazamacrocycles by peroxodisulfate and by a Nickel(III) pendant-arm macrocycle. *Journal of inclusion phenomena and macrocyclic chemistry* **2003,** *47* (1-2), 25-32.

3. Haines, R. I.; Northcott, S. J., Kinetics and mechanism of oxidation of nickel(II) tetraazamacrocycles by the peroxydisulphate anion in aqueous and binary aqueous mixtures. *Canadian Journal of Chemistry* **1992,** *70* (11), 2785-2791.

4. Wahba, N.; El Asmar, M. F.; El Sadr, M. M., Iodometric method for determination of persulfates. *Analytical Chemistry* **1959,** *31* (11), 1870-1871.

5. Rastogi, A.; Al-Abed, S. R.; Dionysiou, D. D., Sulfate radical-based ferrous-peroxymonosulfate oxidative system for PCBs degradation in aqueous and sediment systems. *Applied Catalysis B: Environmental* **2009,** *85* (3-4), 171-179.

6. Anipsitakis, G. P.; Dionysiou, D. D., Radical generation by the interaction of transition metals with common oxidants. *Environmental Science & Technology* **2004,** *38* (13), 3705-3712.

7. Yuan, S.; Liao, P.; Alshawabkeh, A. N., Electrolytic manipulation of persulfate reactivity by iron electrodes for trichloroethylene degradation in groundwater. *Environmental Science & Technology* **2013,** *48* (1), 656-663.

8. Halsey, G. D., The role of surface heterogeneity in adsorption. *Advances in Catalysis* **1952,** *4*, 259-269.

9. Hamdaoui, O.; Naffrechoux, E., Modeling of adsorption isotherms of phenol and chlorophenols onto granular activated carbon: Part I. Two-parameter models and equations allowing determination of thermodynamic parameters. *Journal of Hazardous Materials* **2007,** *147* (1-2), 381-394.

10. Zilbermann, I.; Meshulam, A.; Cohen, H.; Meyerstein, D., Stabilization of nickel(III)-1,8-dimethyl-1,3,6,8,10,13-hexaazacyclotetradecane by axial binding of anions in neutral aqueous solutions. *Inorganica Chimica Acta* **1993,** *206* (2), 127-130.

11. Lepentsiotis, V.; Domagala, J.; Grgic, I.; van Eldik, R.; Muller, J. G.; Burrows, C. J., Mechanistic information on the redox cycling of Nickel(II/III) complexes in the presence of sulfur oxides and oxygen. Correlation with DNA damage experiments. *Inorganic Chemistry* **1999,** *38* (15), 3500-3505.

12. Kalyani, D.; Phugare, S.; Shedbalkar, U.; Jadhav, J., Purification and characterization of a bacterial peroxidase from the isolated strain *Pseudomonas sp*. SUK1 and its application for textile dye decolorization. *Annals of Microbiology* **2011,** *61* (3), 483-491.

13. Chen, Y. P.; Liu, S. Y.; Yu, H. Q.; Yin, H.; Li, Q. R., Radiation-induced degradation of methyl orange in aqueous solutions. *Chemosphere* **2008,** *72* (4), 532-536.

14. Parshetti, G. K.; Telke, A. A.; Kalyani, D. C.; Govindwar, S. P., Decolorization and detoxification of sulfonated azo dye methyl orange by *Kocuria rosea* MTCC 1532. *Journal of Hazardous Materials* **2010,** *176* (1-3), 503-509.

15. Li, W.; Li, D.; Xian, J.; Chen, W.; Hu, Y.; Shao, Y.; Fu, X., Specific analyses of the active species on Zn0.28Cd0.72S and TiO_2 photocatalysts in the degradation of methyl orange. *The Journal of Physical Chemistry C* **2010,** *114* (49), 21482-21492.

16. Li, W.; Li, D.; Lin, Y.; Wang, P.; Chen, W.; Fu, X.; Shao, Y., Evidence for the active species involved in the photo-degradation process of methyl orange on TiO_2. *The Journal of Physical Chemistry C* **2012,** *116* (5), 3552-3560.

17. Dai, K.; Chen, H.; Peng, T.; Ke, D.; Yi, H., Photocatalytic degradation of methyl orange in aqueous suspension of mesoporous titania nanoparticles. *Chemosphere* **2007,** *69* (9), 1361-1367.

18. Wakimoto, R., Kitamura, T., Ito, F., Usami, H., & Moriwaki, H. (2015). Decomposition of methyl orange using C 60 fullerene adsorbed on silica gel as a photocatalyst via visible-light induced electron transfer. *Applied Catalysis B: Environmental*, *166*, 544-550.

19. Cai, M. Q., Wei, X. Q., Du, C. H., Ma, X. M., & Jin, M. C. (2014). Novel amphiphilic polymeric ionic liquid-solid phase micro-extraction membrane for the preconcentration of aniline as degradation product of azo dye Orange G under sonication by liquid chromatography–tandem mass spectrometry. *Journal of Chromatography A*, *1349*, 24-29.

20. Dabioch, M.; Skorek, R.; Kita, A.; Janoska, P.; Pytlakowska, K.; Zerzucha, P.; Sitko, R., A study on adsorption of metals by activated carbon in a large-scale (municipal) process of surface water purification. *Central European Journal of Chemistry* **2013,** *11* (5), 742-753.

21. Franco, P. E.; Veit, M. T.; Borba, C. E.; Gonsalves, G. d. C.; Fagundes Klen, M. R.; Bergamasco, R.; da Silva, E. A.; Suzaki, P. Y. R., Nickel(II) and zinc(II) removal using Amberlite IR-120 resin: Ion exchange equilibrium and kinetics. *Chemical Engineering Journal* **2013,** *221* (0), 426-435.

22. Matienzo, J.; Yin, L. I.; Grim, S. O.; Swartz, W. E., X-ray photoelectron spectroscopy of nickel compounds. *Inorganic Chemistry* **1973,** *12* (12), 2762-2769.

23. Roe, S.; Hill, J.; Liesegang, J., An x-ray photoelectron spectroscopic study of some nickel(II) tetraaza macrocyclic complexes. *Transition Metal Chemistry* **1985,** *10* (3), 100-106.

24. Solans Monfort, X.; Fierro, J. L. G.; Hermosilla, L.; Sieiro, C.; Sodupe, M.; Mas Balleste, R., O-O Bond activation in H_2O_2 and $(CH_3)_3COOH$ mediated by $[Ni(cyclam)(CH_3CN)_2](ClO_4)_2$: Different mechanisms to form the same Ni(III) product? *Dalton Transactions* **2011,** *40* (26), 6868-6876.

25. Suh, M. P.; Moon, H. R.; Lee, E. Y.; Jang, S. Y., A Redox-Active Two-dimensional coordination polymer: Preparation of silver and gold nanoparticles and crystal dynamics on guest removal. *Journal of the American Chemical Society* **2006,** *128* (14), 4710-4718.

26. Zhang, Q.; Ma, J. P.; Wang, P.; Shi, Z. Q.; Dong, Y.-B.; Huang, R. Q., Unusual Ni-Ag mixed-metal, mixed-valence, and cluster-containing coordination polymers generated from Nickel-Macrocyclic Ligand and Silver Ion by Metal-Exchange. *Crystal Growth & Design* **2008,** *8* (7), 2581-2587.

27. Etacheri, V.; Seery, M. K.; Hinder, S. J.; Pillai, S. C., Nanostructured heterojunctions for efficient visible-light-induced photocatalysis. *Inorganic Chemistry* **2012,** *51* (13), 7164-7173.

28. Periyat, P.; McCormack, D. E.; Hinder, S. J.; Pillai, S. C., One-Pot Synthesis of anionic (Nitrogen) and cationic (Sulfur) codoped high-temperature stable, visible light active, Anatase Photocatalysts. *The Journal of Physical Chemistry C* **2009,** *113* (8), 3246-3253.

29. Yang, Z.; Miao, Y.; Wang, T.; Liang, X.; Xiao, M.; Li, W.; Yang, Y., The self-adsorption of Ni ultrathin layer on glassy carbon surface and their electrocatalysis toward glucose. *Journal of The Electrochemical Society* **2014,** *161* (6), H375-H378.

Photochemical activation of persulphate using tris(2,2′-bipyridyl) ruthenium(II) complex for photodegradation of methyl orange and photoinactivation of bacteria in visible light

4.1 Abstract:

Visible light photolysis of persulphate in presence of $[Ru(bpy)_3]^{2+}$ complex in aqueous solutions results in cleavage of peroxo bond of persulphate, and generates oxidants such as sulphate radical, hydroxyl radical and $[Ru(bpy)_3]^{3+}$ that could degrade organic and bacterial pollutants (chapter 1, reactions 10-12). However, the effect of photochemical activation of persulphate using $[Ru(bpy)_3]^{2+}$ on recalcitrant pollutants and bacteria in aqueous media has not been studied. The present study is focused on the photochemical activation of persulphate using tris(2,2′-bipyridyl)ruthenium(II) bypyridine, (denoted as Complex1) under visible light irradiation (400-700 nm) and its effect on a model azo dye (Methyl orange, MO), and Gram negative and Gram positive bacteria. This chapter addresses the gap in literature discussed under the section 1.5 (c) and 1.7 (a) of chapter 1.

Graphical Abstract:

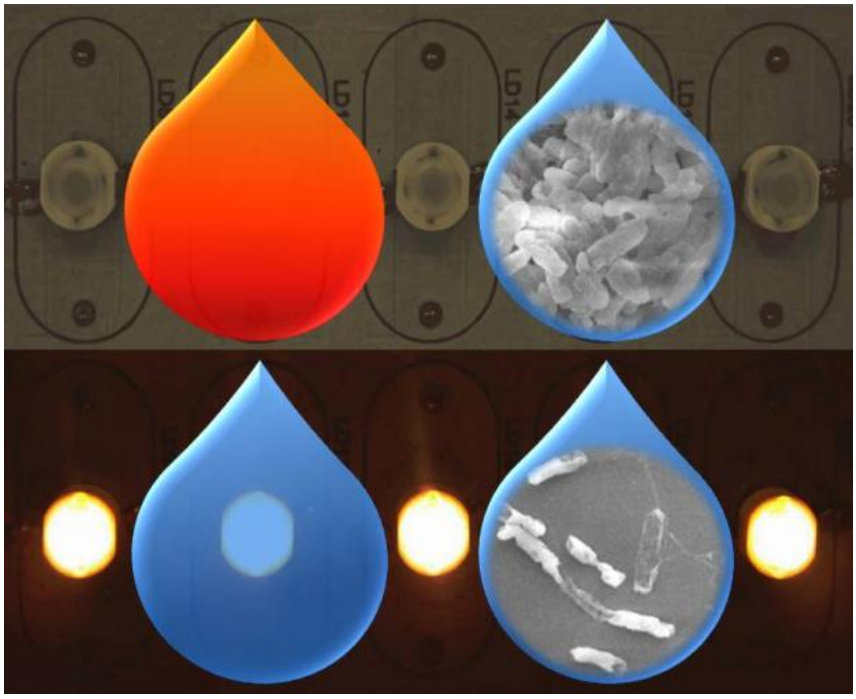

4. 2 Experimental procedures and analysis:

4.2 (a) Materials:

Ruthenium(III) chloride hydrate ($RuCl_3.H_2O$), 2,2'- Bipyridine, Potassium persulphate ($K_2S_2O_8$), Resorcinol, Methyl orange (MO), Sodium nitrite ($NaNO_2$), Disodium hydrogen phosphate (Na_2HPO_4), Sodium hydrogen phosphate (NaH_2PO_4), Sodium sulphate (Na_2SO_4),

and Sodium hydrogen carbonate ($NaHCO_3$) used, were of guaranteed analytical grade, purchased from SD fine chemicals, India. $[Ru(bpy)_3]$ $(PF_6)_2$ (Complex1) was prepared according to earlier report. [1] For HPLC analysis, methanol (HPLC grade) and millipore water were used.

4.2 (b) Photolytic experimental setup:

Visible light LED array containing warm white LED bulbs (400 - 700 nm, with peak maxima around 450 and 600 nm) manufactured by Kwality Photonics Pvt. Ltd, India was used as light source. Details of LED array and photograph of photolysis experimental setup are provided in supporting information (Appendix Figure 4.1). Fluence rate was measured by Ophir PD100 Nova II power meter.

4.2 (c) Photo-degradation of MO:

2 mL of aqueous solution (double distilled water) of MO (12 mg L^{-1}) with appropriate concentration of Complex1 and persulphate was taken in a quartz cuvette and photolysed at the fluence rate of 0.095 Wcm^{-2} (Appendix I Figure 4.1). Photo-degradation of MO was spectrophotometrically followed (JASCO V-570 UV/VIS/NIR) by monitoring decrease in absorbance at 464 nm. Quartz cuvettes containing reaction mixture were wrapped completely with aluminium foil and used for dark controls. All experiments were carried at neutral pH and at 37 ºC. Radical scavenging experiments were performed by addition of sulphate and hydroxyl radical scavengers such as methanol (0.1 M) and sodium nitrite (0.02 M) to reaction mixture containing MO (12 mg L^{-1}), Complex1 (1 µM) and persulphate (2 mM) followed by irradiation.[2] Similarly, effect of inorganic ions on photo-degradation was investigated by addition of salts such as 0.1 M of Na_2HPO_4, Na_2SO_4 and $NaHCO_3$ to reaction mixture. Addition of Na_2SO_4 (0.1 M) to double distilled water (neutral pH) did not change the pH of the solution. The change in pH after addition of 0.1 M of NaH_2PO_4 or $NaHCO_3$ to double distilled water was adjusted to neutral pH by adding few drops of 0.05 N HCl. Total organic carbon (TOC) measurements were performed using Sievers 900 TOC analyser by injection of appropriate volume of sample at different time intervals during irradiation. The results are expressed as TOC/ TOC_0 where TOC is Total organic carbon at time t, and TOC_0 is the initial Total organic carbon of MO (12 mg L^{-1}).

4.2 (d) Photo-inactivation of bacteria:

Bacterial strains *Escherichia coli* (NCIM 2345), *Pseudomonas aeruginosa* (NCIM 2581), *Staphylococcus aureus* (NCIM 2127) and *Bacillus subtilis* (NCIM 2545) were cultured

in nutrient broth (NB) medium using orbital shaker set at 100 rpm, 37 °C for 12 h. Cells (at log phase) were harvested by centrifugation at 1000 g for 15 min and washed twice with 10 mM phosphate buffer saline (PBS). Composition of 10 mM PBS (pH 7.2): Na_2HPO_4 (6.1 mM), NaH_2PO_4 (2 .05 mM), NaCl (154 mM). Bacterial stock solution was prepared by suspending cell pellet in appropriate volume of PBS, and concentration was found to be ~10^9 colony forming units (CFU) mL^{-1}. Cell concentration was determined by counting colonies after serial dilution and spread plating 0.1 mL of sample on NB agar plates, followed by overnight incubation.

It has been shown that irradiation of bacteria in visible light region caused reduction in its cell viability.[3] Considering this fact, in the present study, control experiments were performed to optimize the light intensities such that only irradiation of light (400-700 nm) had no effect on the viability of bacterial strains. Irradiation of *B. subtilis* at light intensity of 0.048 Wcm^{-2}, irradiation of *S. aureus* at light intensity of 0.060 Wcm^{-2}, and irradiation of *E. coli* and *P. aeruginosa* at light intensity 0.095 Wcm^{-2} had no effect on their cell viability at least for three hours of irradiation period, at the specified conditions. Irradiation of the bacterial strains more than specified light intensity caused slight reduction in the cell viability. Therefore, photo-inactivation experiments of the respective bacterial strains were carried out at above mentioned light intensities. Light dosage in Jcm^{-2} was determined by multiplying irradiance in Wcm^{-2} with time in seconds (Table 1).[4] Photolysis reactions were performed in sterilized quartz cuvettes (Appendix I Figure. 4.1) and reaction mixture (2 ml) contained ~10^7 CFU mL^{-1} of bacterial cells with appropriate concentration of Complex1 and persulphate in PBS (10 mM). Quartz cuvettes containing reaction mixture were wrapped completely with aluminium foil and used for dark controls. All experiments were carried at pH 7.2 and at 37 ^oC. Cell viability after irradiation was examined by spread plate technique as mentioned above. Two independent experiments in triplicates were performed for each bacterial species. One-way ANOVA was used to assess the significance of difference in photo-inactivation among the bacterial strains, and also for significance of difference in photo-inactivation of *E. coli* at different Complex1: persulphate ratios. Data was assessed for normal distribution and homogeneity of variances using Kolmogorov-Smirnov test and Levene test respectively. A value of $p < 0.05$ was considered as statistically significant.[5] All the statistical analysis was performed using OriginPro 8.0.

Radical scavenging experiments were performed by addition of sulphate and hydroxyl radical scavengers such as methanol (0.1 M) and sodium nitrite (0.02 M)[2] to reaction mixture containing *E. coli* cells (~10^7 CFU mL^{-1}), Complex1 (1μM) and persulphate (2 mM) in PBS

(10 mM) followed by irradiation.

4.2 (e) Cell membrane integrity assay:

Integrity of *E. coli* cell membrane was examined using Invitrogen Molecular Probes® LIVE/DEAD® BacLight™ Bacterial Viability Kit (L7012).[6] This assay is based on competitive binding of two different fluorescent nucleic acid stains SYTO® 9 and Propidium Iodide (PI). SYTO® 9 can easily diffuse in to cell membrane and gives a green fluorescence (500 nm) on binding to DNA whereas, PI can enter only cells with damaged membrane and gives a red fluorescence (635 nm) on binding to DNA.[6] *E. coli* cells treated with Complex1 and persulphate in absence and presence of light for 90 min were harvested by centrifugation, and cell pellet resuspended in 50 µL saline were stained with 1:1 mixture of two dyes, SYTO® 9 and PI according to manufacturer's instructions. These stained samples were fixed on glass slide and examined at magnification of 150 X using a Nikon Eclipse Ti-U microscope (Nikon, Japan) with excitation wavelength of 480 nm (SYTO® 9) and 490 nm (PI).

4.2 (f) Scanning electron microscopy:

Structural change in bacterial cell wall caused by photodamage was examined using Scanning Electron Microscopy (SEM).[7-9] *E. coli* cells treated with Complex1 and persulphate in absence and presence of light for 90 min were harvested by centrifugation. Obtained cell pellet was resuspended in 100 µL of PBS and fixed with 2% glutaraldehyde solution for 1 h. Cells were then washed thrice with PBS, gradually dehydrated using graded ethanol/H_2O mixture of 10, 25, 50, 75, 90 (v/v %) and finally with 100% ethanol followed by air drying.[7] Dried cells were then coated with platinum by JEOL JFC-1600 Autobine sputter and images were taken with a JEOL JSM-6360 LV Scanning Electron Microscope at a voltage of around 10 kV.

4.2 (g) Chromosomal DNA extraction:

E. coli chromosomal DNA was extracted using SRL BioLit™ Bacterial Genomic DNA extraction kit (BTK007). *E. coli* cells treated with Complex1 and persulphate in absence and presence of light for 90 min were harvested by centrifugation and genomic DNA was extracted immediately from cell pellet according to manufacturer's instruction. Extracted chromosomal DNA was mixed with 3 µL of 6X gel loading buffer (SRL BioLit™ BTK007). DNA samples were loaded to 1% agarose gel and electrophoresis was carried out for 3 hour at 60 V. After electrophoresis, DNA was stained by immersing gel in Ethidium bromide solution

(1 mg mL^{-1}) for 15 min and was photographed using Biorad Gel Doc™ XR.

4.2 (h) Photo-inactivation of bacteria in presence of organic compound:

Simultaneous degradation of resorcinol and photo-inactivation of *E. coli* were investigated by High pressure liquid chromatography (HPLC) analysis and antimicrobial assays, respectively.[10] Typically, reaction mixture containing 5/10 mg L^{-1} of resorcinol, *E. coli* cells (~10^7 CFU mL^{-1}), Complex1 (1 µM) and persulphate (2 mM) were photolysed for 120 min. For HPLC analysis, 1 mL of sample from this reaction mix was withdrawn, filtered using 0.45 µM Polytetrafluoroethylene (PTFE) filter to remove bacteria. 0.1 mL of this filtered solution was injected in to Shimadzu UFLC, equipped with a phenomenex C18 HPLC column (250 mm × 4.5 mm, 5 µm) and SPDM 20A Prominence diode array detector. HPLC was performed with 30/70 (v/v) methanol-water as mobile phase in isocratic mode with flow rate of 1 mL min^{-1} and chromatogram was monitored at 280 nm.[10] For microbial assays, 0.1 mL of sample from reaction mix was withdrawn at appropriate time intervals during irradiation and viable cells were determined by spread plate technique, as mentioned above.

4.2 (i) Effect of inorganic ions:

Effect of inorganic ions on photo-inactivation was investigated by addition of salts such as 0.1 M of Na_2HPO_4, Na_2SO_4 and $NaHCO_3$ [11, 12] to reaction mixture containing *E. coli* cells (~10^7 CFU mL^{-1}), Complex1 (1 µM) and persulphate (2 mM) in PBS (10 mM) followed by irradiation. Addition of Na_2SO_4 (0.1 M) to 10 mM PBS (pH 7.2) did not change the pH of the solution. The change in pH after addition of 0.1 M of NaH_2PO_4 or $NaHCO_3$ to 10 mM PBS was adjusted to pH 7.2 by adding few drops of 0.05 N HCl. Control experiments with only 0.1 M of methanol, sodium nitrite (0.02 M), Na_2HPO_4, Na_2SO_4, and $NaHCO_3$ either in dark or light had no effect on cell viability.[11]

4.2 (j) Effect in simulated ground water:

Photo-degradation of azodye (MO 12 mg L^{-1}) and photo-inactivation of bacteria (*E. coli* and *S. aureus*) by activation of persulphate (2 mM) using Complex1 (1 µM) was studied in simulated ground water that contained a defined composition of inorganic and organic matter. Simulated ground water was prepared by addition of following components to distilled water: $Fe(NO_3)_3.9H_2O$ (0.24 µm), $NaHCO_3$ (1.2 mM), Na_2SO_4 (0.34 mM), Na_2HPO_4 (0.28 mM), NaCl (0.86 mM) and resorcinol (9.0 µm).[13]

4.3. Results and Discussion:

4.3 (a) Photo-degradation of MO:

Irradiation (420-700 nm) of MO in presence of Complex1 and persulphate caused almost complete degradation (~ 98%) rapidly within 12 min (Figure.4.1A).

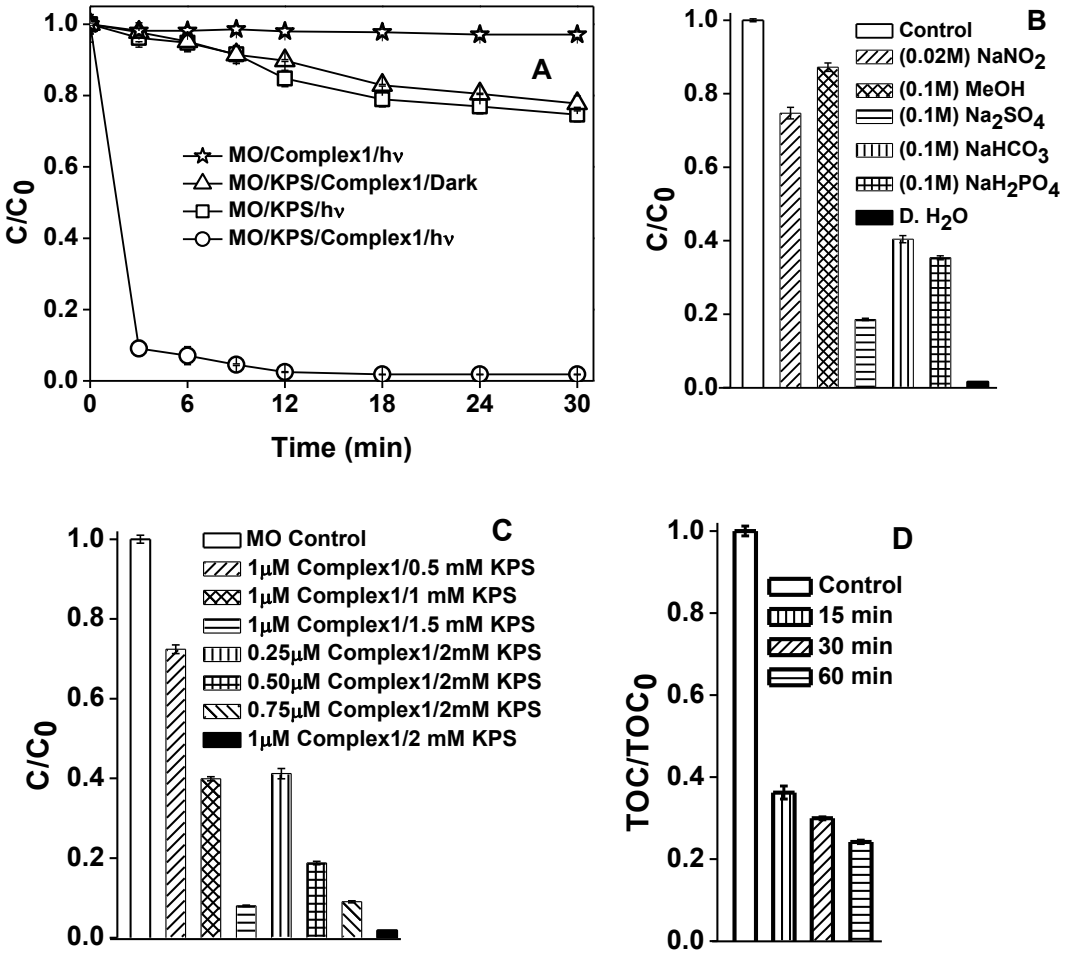

Figure 4.1 Photo-degradation of MO by activation of persulphate (KPS) using Complex1 in neat and simulated ground water. [MO] = 12 mg L^{-1}, [KPS] = 2 mM, [Complex1] =1 μM and Fluence rate = 0.095 Wcm^{-2}. (A) Photo-degradation of MO at different time intervals. C = concentration of MO at time t, C_0 = initial concentration of MO (B) Effect of radical scavengers and inorganic ions, Control – Concentration of MO after 15 min irradiation, Light dosage = 85.5 J cm^{-2}. (C) Photo-degradation of MO at different [Complex1]: [persulphate] ratio after 15 min irradiation, Light dosage = 85.5 J cm^{-2} (D) Reduction in Total organic carbon before (control) and after different time intervals during irradiation. Control – Total organic carbon of MO (12 mg L^{-1}).

It is known that photolysis of $[Ru(bpy)_3]^{2+}$ (Complex1) and persulphate results in formation of $[Ru(bpy)_3]^{3+}$, sulphate radicals and sulphate ions [reactions 1 and 2].[14]

In aqueous solutions, sulphate radicals react with water to produce hydroxyl radicals [reaction 3].[15]

$$[Ru(bpy)_3]^{2+} + h\nu + [S_2O_8]^{2-} \longrightarrow [Ru(bpy)_3]^{3+} + SO_4^{2-} + SO_4^{\bullet -} \quad ....(1)$$

$$[Ru(bpy)_3]^{2+} + SO_4^{\bullet -} \longrightarrow [Ru(bpy)_3]^{3+} + SO_4^{2-} \quad .....(2)$$

$$SO_4^{\bullet -} + H_2O \rightleftharpoons HO^{\bullet} + H^+ + SO_4^{2-} \quad .....(3)$$

The reactive species such as sulphate and hydroxyl radicals are very strong oxidants, capable of degrading organic compounds effectively. Activation of persulphate in aqueous medium effectively generates sulphate radicals and secondary hydroxyl radicals, and enhances the efficiency of degradation.[16-18] Thus, rapid and efficient degradation of MO observed on irradiation of MO in presence of Complex1 and persulphate is attributed to the photochemical activation of persulphate by Complex1 (reactions 1-3). Importantly, irradiation of MO in presence of persulphate for 30 min caused only about 20% degradation of MO (Figure 4.1 A). Similar result was also observed for treatment of MO with Complex1 and persulphate without irradiation (dark control) (Figure 4.1A). Moreover, irradiation of MO in presence of Complex1 and persulphate in simulated ground water also resulted in significant degradation of MO (~80%) (Figure 4.1A). The slight decrease in percentage of photo-degradation of MO when compared with double distilled water could be accounted to the presence of a variety of inorganic salts and organic matter in simulated ground water. Persulphate is an oxidant (E^o = 2.01 V) and has the ability to degrade organic compounds due to slow decomposition and generation of sulphate radicals.[17] The slight degradation (~20%) of MO observed on irradiation in presence of persulphate, and in dark control is due to slow decomposition of persulphate (Figure 4.1A).

Irradiation of MO in presence of Complex1 and persulphate containing sodium nitrite (20 mM) and methanol (0.1 M) for 15 min caused only ~25% and ~15% degradation of MO, respectively (Figure 4.1B). This significant inhibition in photo-degradation is due to the effective scavenging of hydroxyl and sulphate radicals by methanol and sodium nitrite.[2, 16] The above result indicates that sulphate and secondary hydroxyl radicals produced during photoactivation of persulphate by Complex1 play a major role in photo-degradation of MO.

Percentage of degradation of MO decreased on decreasing the concentration of either Complex1 or persulphate (Figure 4.1C). Decreasing the concentration of Complex1 may not be favourable to produce sufficient amount of excited state Complex1 to cause effective photochemical activation of persulphate for degradation. At lower concentration of

persulphate, relatively lower amount of radicals are generated on activation, which may not be sufficient for efficient degradation. Earlier studies on degradation of dyes by persulphate reported that increasing the concentration of persulphate increased the percentage of degradation of dyes.[20] These results reveal that photo-degradation of MO is dependent on concentration of both persulphate and Complex1, and an optimal concentration of persulphate (2 mM) and Complex1 (1 μM) was required to cause complete degradation of MO (12 mgL^{-1}) (Figure 4.1C).

4.3 (b) Reduction of total organic carbon:

Irradiation of MO in presence of Complex1 and persulphate caused about 65 %, 71% and 76 % reduction of TOC in 15, 30 and 60 min respectively (Figure 4.1D). TOC reduction obtained in the present study is comparable with TOC reduction obtained on degradation of phenol (0.5 mM) by activation of persulphate (84 mM) by UV photolysis.[17] Thus, the above results indicate that visible light activation of persulphate by Complex1 caused not only rapid degradation of MO, but also its significant reduction of TOC indicating mineralization.

4.3 (c) Effect of inorganic ions:

Irradiation of MO in presence of Complex1 and persulphate containing salts (0.1 M) such as NaH_2PO_4, $NaHCO_3$ and Na_2SO_4 retarded the photo-degradation of MO (Figure 4.1B). Earlier, it has been shown that the presence of inorganic ions such as sodium bicarbonate and sodium chloride retarded the degradation of organic contaminants such as acetic acid and chlorinated ethenes by persulphate.[15,16] In addition, it is known that at higher ionic strength, ion pair Complexation between Complex1 and persulphate is reduced, which is not favourable for photoinduced electron transfer between Complex1 and persulphate.[14] Therefore, photo-degradation of MO was retarded at relatively higher ionic strength of the medium. The above facts indicate that degradation of MO by photochemical activation of persulphate using Complex1 is dependent on the composition of ions and ionic strength of medium.

4.3 (d) Photo-inactivation of bacteria:

Visible light irradiation of Gram negative bacteria (*E. coli* and *P. aeruginosa*) in presence of Complex1 and persulphate caused complete photo-inactivation, within 90 and 120 min, respectively (Table 4.1, Figure 4.2A). Gram positive bacteria (*S. aureus* and *B. subtilis*) were also photo-inactivated within 60 min, with relatively lower light dosage than required for Gram negative bacteria (Table 4.1, Figure 4.2B).

The pattern of decrease in cell viability during the irradiation period varied within

Gram negative strains (*E. coli* and *P. aeruginosa*) (Figure 4.2A) (ANOVA, $p < 0.05$). In case of Gram positive strains (*S. aureus* and *B. subtilis*), the pattern of decrease in cell viability during irradiation period was similar (Figure 4.2B), (ANOVA, $p > 0.05$). The results show that the differences in photo-inactivation of Gram positive and Gram negative strains were statistically significant (ANOVA, $p < 0.05$). Among the bacterial strains examined *P. aeruginosa* was found to be the most resistant to photo-inactivation. Control experiments, (i) 5 µm of Complex1 alone in absence and presence of light (ii) 2 mM of persulphate alone in absence and presence of light (iii) mixture of 1 µm of Complex1 and 2 mM of persulphate without irradiation, had no effect on cell viability (Figure 4.2).

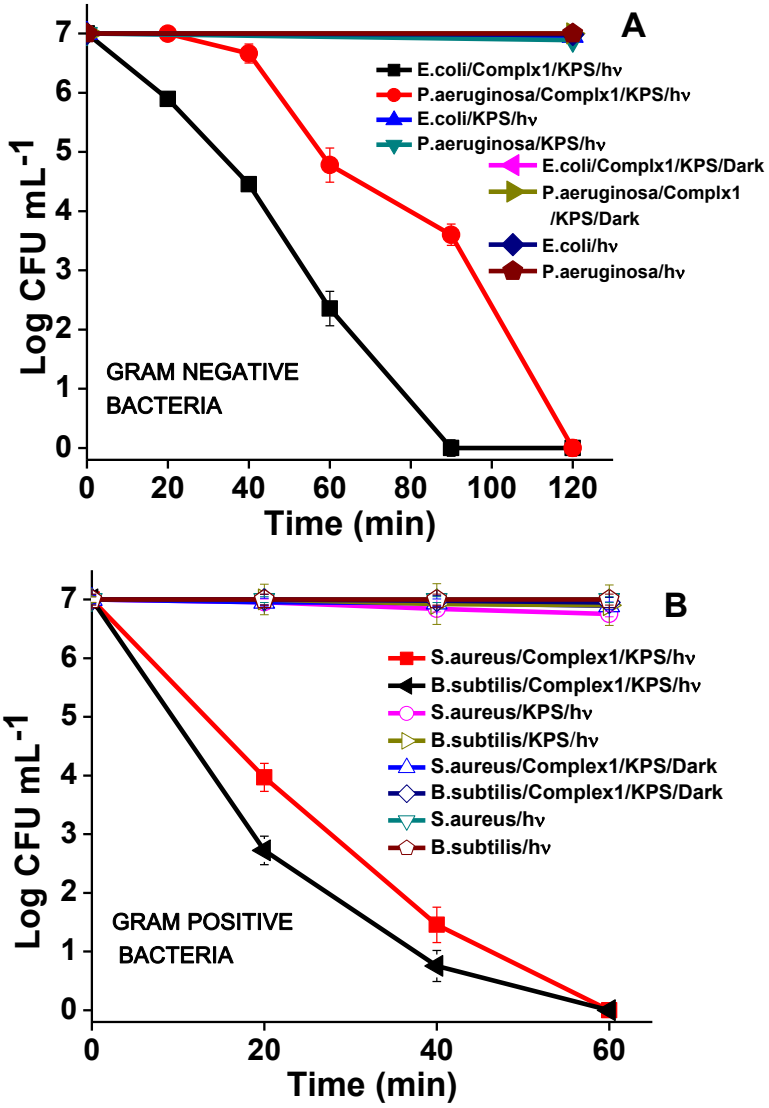

Figure 4.2 Cell viability Vs Time plot for photo-inactivation of (A) Gram negative bacteria (B) Gram positive bacteria. Cell concentration = ~10^7 CFU mL^{-1}, [KPS] = 2 mM, [Complex1] = 1 µM, Fluence rate = 0.095 Wcm^{-2} for *E. coli* and *P. aeruginosa*, 0.060 Wcm^{-2} for *S. aureus* and 0.048 Wcm^{-2} for *B. subtilis*.

Earlier, D.D. Dionysiou et al., had shown degradation (~ 50%) of microcystin by thermal activation of persulphate at 30 °C.[21] However, in the present study, degradation of MO by persulphate alone at 37 °C was not significant (Figure 4.1), and also the cell viability of the bacteria was not affected by persulphate alone at 37 °C (Figure 4.2). As discussed above, photolysis of Complex1 in presence of persulphate activates persulphate and generates reactive species such as, sulphate radicals, secondary hydroxyl radicals and $[Ru(bpy)_3]^{3+}$ [reactions 1-3].[14, 15]

Table 4.1 Conditions for complete inactivation of bacteria

Bacterial Strains	Irradiation Time (min)	Fluence Rate (Wcm^{-2})	Light Dosage (Jcm^{-2})
E. coli †	90	0.095	513
P.aeruginosa†	120	0.095	684
S. aureus‡	60	0.060	216
B. subtilis‡	60	0.048	173

†Gram negative bacteria [Complex1] = 1 µM
‡Gram positive bacteria [persulphate] = 2 mM

Importantly, sulphate and hydroxyl radicals are strong oxidants and cause damage to biomolecules such as protein, DNA and membrane.[22, 23] Earlier, it has been shown that photolysis of $[Ru(bpy)_3]^{2+}$ and persulphate induced *in vitro* DNA damage.[24] However, no study has been carried out to investigate the effect of $[Ru(bpy)_3]^{2+}$ activated persulphate on bacteria in aqueous media. Present results show that photochemical activation of persulphate by Complex1 caused complete inactivation of both Gram positive and Gram negative bacteria (Figure 4.2, Table 4.1). In addition, irradiation of bacteria (*E. coli* and *S. aureus*) in presence of Complex1 and persulphate in simulated ground water also caused complete inactivation of bacteria. The relatively less ionic strength of simulated ground water than PBS medium (10 mM) favored complete inactivation (Figure 4.3).

Moreover, irradiation of *E. coli* with persulphate and Complex1 in presence of either methanol (0.1 M) or sodium nitrite (20 mM) for 120 min caused only ~1 log reduction of *E. coli* (Appendix I Figure 4.2). This significant inhibition in photo-inactivation of *E. coli* is due to the effective scavenging of hydroxyl and sulphate radicals by methanol and sodium nitrite.[10,29] It is important to note that photo-degradation of MO was also inhibited in presence of sulphate and hydroxyl radical scavengers (Figure 4.1B). The above results emphasise that sulphate and hydroxyl radicals produced during photoactivation of persulphate by Complex1 play a major role in inactivation of *E. coli*.

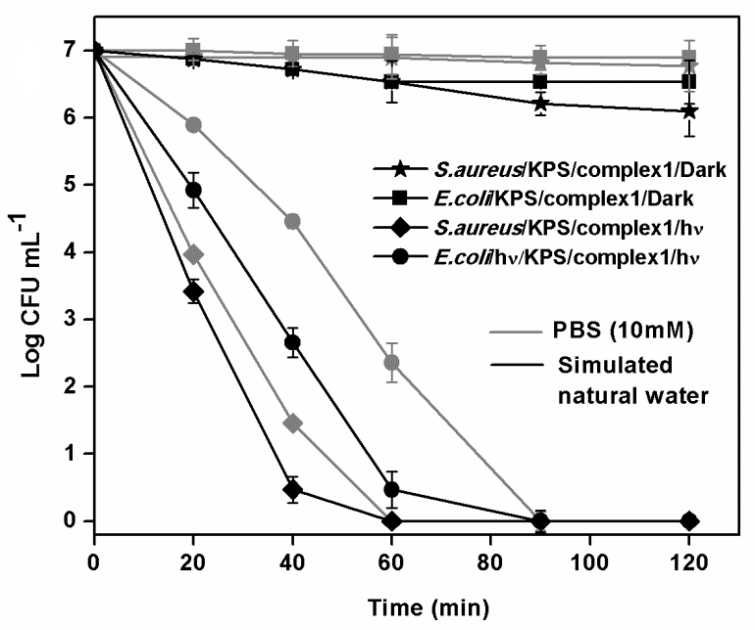

Figure 4.3 Cell viability Vs Time plot for photo-inactivation of *E. coli* and *S. aureus* (~10^7 CFU mL^{-1}) in simulated ground water, Fluence rate = 0.095 Wcm^{-2} for *E. coli* and 0.060 Wcm^{-2} for *S. aureus* inactivation. [KPS] = 2 mM, [Complex1] =1 µM.

Photo-inactivation of Gram positive strains was faster than Gram negative strains (Table 1, Figure 4.2). Cell wall of Gram positive bacteria is relatively simple with two layers namely cytoplasmic membrane and peptidoglycan layer, whereas cell wall of Gram negative bacteria is complex and has an outer lipopolysaccharide membrane in addition to cytoplasmic membrane and peptidoglycan layer.[4, 25-27] This additional layer offers resistance against reactive species generated during irradiation and therefore Gram negative bacteria are less susceptible to photo-inactivation than Gram positive bacteria. Earlier reports on photo-inactivation of bacteria have also shown that Gram negative bacteria are relatively less susceptible.[4, 5, 25-29]

The change in cell viability on changing concentration of Complex1: persulphate ratio was studied using *E. coli* as model organism. Decreasing either concentration of Complex1 or persulphate was not favorable for complete photo-inactivation of *E. coli* (Figure 4.4). It was found that the difference in the photo-inactivation of *E. coli* at different Complex1: persulphate ratios were statistically significant (ANOVA, $p < 0.05$). As discussed above, relatively lower amount of Complex1 was not sufficient for effective photochemical activation of persulphate to cause inactivation. Activation of lower concentration of persulphate could generate relatively lower amount of radicals, which may not be sufficient for complete inactivation.

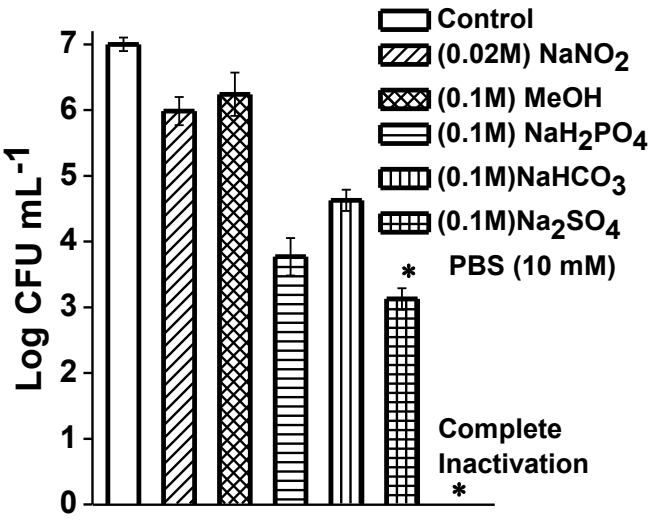

Figure 4.4 Photo-inactivation of *E. coli* at different [Complex1]: [persulphate] ratio. Cell concentration = ~10^7 CFU mL^{-1}, [KPS] = 2 mM, [Complex1] = 1 µM, Light dosage = 513 Jcm^{-2}.

Thus, these results indicate that complete photo-inactivation of *E. coli* depends on concentration of both Complex1 and persulphate (Figure 4.4). The optimised concentrations of persulphate and Complex1 for the complete photo inactivation of bacteria under present experimental conditions are [KPS] = 2 mM, and [Complex1] = 1 µM.

Persulphate is a promising oxidant in advanced oxidation processes, and has been shown to degrade organic contaminants effectively on activation in aqueous medium.[15-19, 30, 31] However, the effect of activated persulphate on bacteria in aqueous media is not known. The present study shows the ability of activated persulphate to cause complete inactivation of bacteria in aqueous medium besides the degradation of azo dye MO. Importantly, both photo-degradation of MO and photo-inactivation of bacteria were achieved using LED as the visible light source.

4.3 (e) Effect of photo-inactivation on cell membrane integrity:

In order to study the effect of photolysis of Complex1 and persulphate on cell membrane integrity, Baclight Live/Dead assay was performed using *E. coli*.[6] Fluorescent microscopic image of *E. coli* cells treated with Complex1 and persulphate without irradiation, showed only green fluorescence (Figure 4.5A) indicating that cells had intact membrane and allowed only diffusion of green fluorescent SYTO® 9.[6] On irradiation of *E. coli* cells in presence of Complex1 and persulphate, red fluorescence was observed indicating the cell membrane damage (Figure 4.5B). The loss of cell membrane integrity facilitated entry of PI and competitive binding of red fluorescent PI to DNA than SYTO® 9.

SEM images of *E. coli* cells treated with Complex1 and persulphate without irradiation showed that cells were intact (Figure 4.5C). However, irradiation of *E. coli* cells with Complex1 and persulphate resulted in severe deformation of cells with ruptured surfaces and craters (Figure 4.5D). Strong oxidizing agents such as hydroxyl and sulphate radicals are known to cause biomolecular damage.[22, 23, 32]

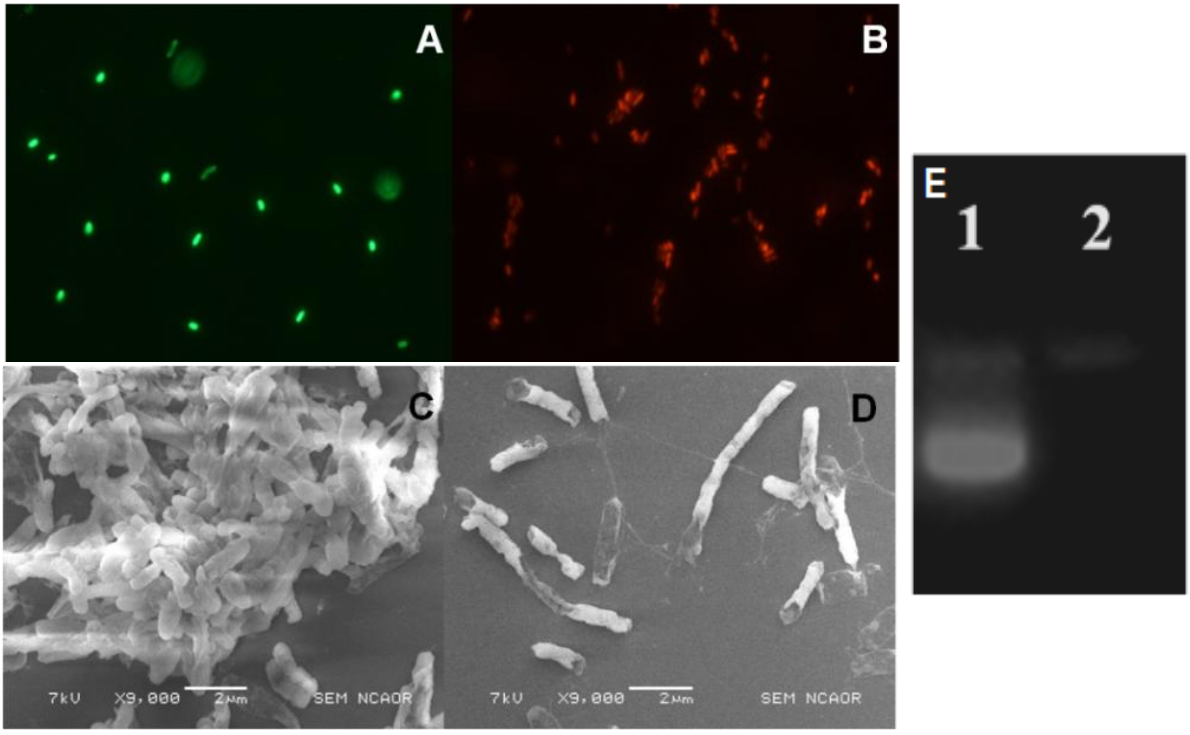

Figure 4.5 Fluorescence microscopic image of *E. coli* treated with Complex1 and persulphate (A) in absence of light (control) (B) in presence of light. SEM images of *E. coli* treated with Complex1 and persulphate (C) in absence of light (control) (D) in presence of light. *E. coli* concentration = ~10^7 CFU mL^{-1}, [KPS] = 2 mM, [Complex1] = 1 µM, Light dosage = 513 Jcm^{-2}. (E) Photograph of agarose gel showing the extracted chromosomal DNA of *E. coli* treated with Complex1 and persulphate in dark (control, Lane1), and in presence of light (Lane 2). *E. coli* concentration = ~10^7 CFU mL^{-1}, [Complex1] = 1 µM, [persulphate] = 2 mM, Light dosage = 513 Jcm^{-2}.

Thus, both Baclight Live/Dead assay, as well as SEM image results clearly revealed cell membrane damage, which indicates oxidative stress caused to *E. coli*. Previous studies on photocatalytic disinfection involving reactive oxidizing species had also shown such membrane damage leading to cell death.[8, 33] In addition, agarose gel electrophoresis showed a clear chromosomal DNA band for cells treated with Complex1 and persulphate in absence of light (Figure 4.5E). On the other hand, chromosomal DNA band was not clear for cells treated with Complex1 and persulphate in presence of light. This result indicates that there is

significant reduction of chromosomal DNA from photolysed cells. Similar reduction in chromosomal DNA has been observed in case of photodynamic inactivation of *E. coli* by 5,10,15,20-tetrakis(1-methylpyridinium-4-yl)porphyrin, due to damage of cell membrane leading to discharge of cell constituents including DNA.[8] The above results further emphasize loss of cell membrane integrity. To the best of our knowledge, present study is the first report showing complete inactivation of bacteria due to bacterial membrane damage and loss of chromosomal DNA on photochemical activation of persulphate in aqueous medium.

4.3 (f) Simultaneous degradation of organic and bacterial contaminants:

Treatment of *E. coli* in presence of resorcinol 10 mg L^{-1} with or without irradiation,[10] and treatment of *E. coli* with Complex1 (1 µM) and KPS (2 mM) in presence of resorcinol 10 mg L^{-1} without irradiation did not affect the cell viability. HPLC chromatogram of resorcinol showed a clear peak at retention time (RT) 6 min (Figure 4.6A). HPLC profile of resorcinol after irradiation in presence of Complex1 and persulphate showed significant decrease in resorcinol peak and formation of new peak at RT 3 min revealing the degradation of resorcinol (Figure 4.6A). Irradiation of resorcinol (5 mg L^{-1}) in presence of Complex1 and persulphate in PBS (10 mM) caused ~95 % degradation of resorcinol (Figure 4.6A, Inset-A). Under same conditions, in presence of *E. coli* (10^7 CFU/ml), ~90 % degradation of resorcinol (Figure 4.6A, Inset-B) and ~5 log reduction in cell viability was observed (Figure.4.6B). This result reveals that photoactivation of persulphate by Complex1 has the ability to cause simultaneous degradation of resorcinol and inactivation of *E. coli*. On increasing the concentration of resorcinol to 10 mg L^{-1}, simultaneous photo-degradation of resorcinol and photo-inactivation of *E. coli* was retarded (Figure 4.6 A, Inset-D and Figure 4.6B). Reactive species such as sulphate and hydroxyl radicals are diffusible and have non specific reactivity.[10, 15, 34] These radicals can degrade organic compound, and can also oxidize biomolecule such as membrane leading to cell death, involving a competitive reaction between organic compounds and microbes.[10, 35] Thus, at higher concentration of organic matter (resorcinol), simultaneous photo-degradation of resorcinol and photo-inactivation of *E. coli* was retarded. It has been shown that photo-inactivation of bacteria by advanced oxidation processes such as TiO_2 photocatalysis and photo-Fenton process was affected by the presence of organic matter.[10, 35]

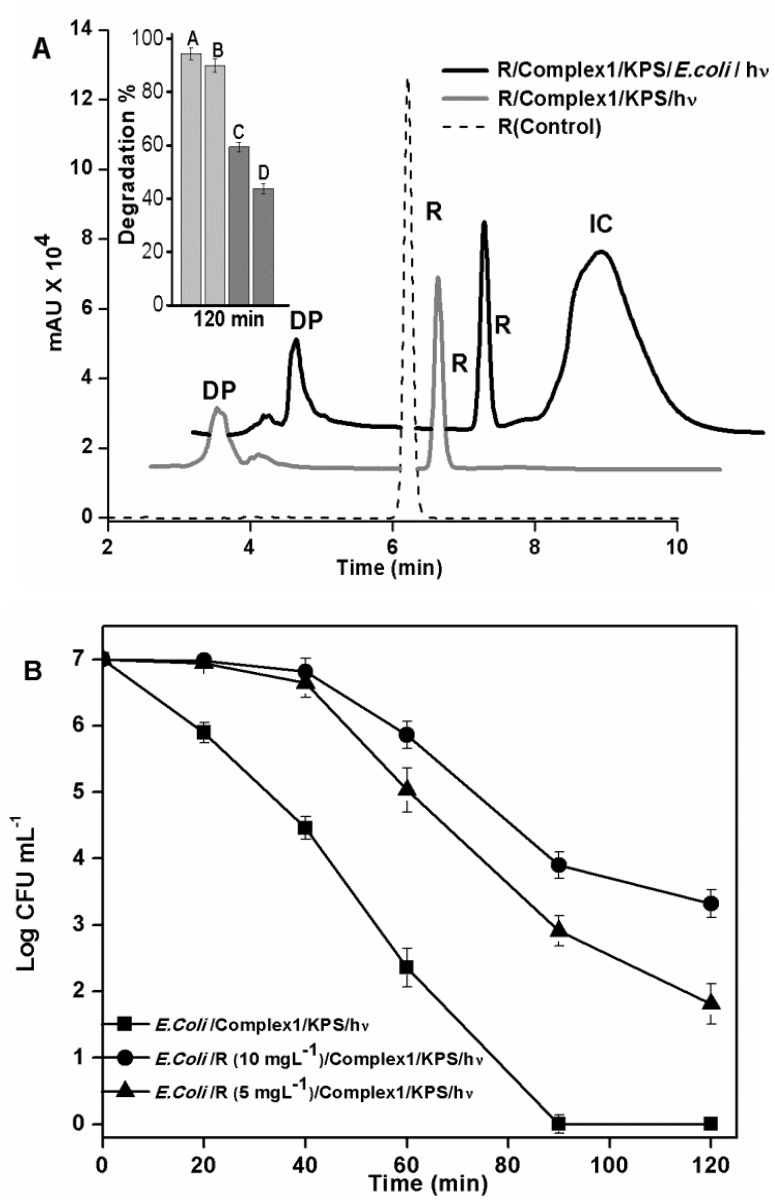

Figure 4.6 (A) HPLC chromatogram showing degradation of resorcinol (10 mg L^{-1}) in absence and presence of *E. coli*. R- Resorcinol, DP- Degraded products and IC- Intracellular components. Inset – A and B, degradation percentage of resorcinol (5 mg L^{-1}) in absence and presence of *E. coli*, respectively. C and D, degradation percentage of resorcinol (10 mg L^{-1}) in absence and presence of *E. coli*, respectively. (B) Cell viability Vs Time plot for photo-inactivation of *E. coli* in absence, and presence of resorcinol (5 & 10 mg L^{-1}). *E. coli* concentration = ~10^7 CFU mL^{-1}, [Complex1] = 1 µM, [persulphate] = 2 mM

Interestingly, HPLC profile of resorcinol after irradiation in presence of Complex1 and persulphate containing *E. coli*, showed a wide peak at RT 7-8 min, in addition to resorcinol peak (RT 6 min), and its degradation product peak (RT 3 min) (Figure 4.6B). The absorption spectrum of this new peak had a maximum around 260-280 nm, characteristic of DNA and proteins (Appendix I Figure 4.3). Earlier, it has been shown that loss of membrane

integrity results in leakage of cellular components such as proteins and DNA that have absorption in 260-280 nm range.[36, 37] These facts indicate that wide peak at RT 7-8 min corresponds to intracellular components leaching out of cell due to photodamage of cell membrane. The above observation further emphasizes loss of cell membrane integrity.

4.3 (g) Photo-inactivation of bacteria in presence of inorganic salts:

Photo-inactivation of *E. coli* was retarded in presence of salts such as 0.1M of NaH_2PO_4, $NaHCO_3$ and Na_2SO_4 (Appendix I Figure 4.2). As discussed above, ion pair complexation between Complex1 and persulphate is reduced at higher ionic strength which is not favorable for photoinduced electron transfer between Complex1 and persulphate.[14] Thus, these results indicate that the complete photo-inactivation of *E. coli* depends on composition of ions and ionic strength of the medium, as observed in photo-degradation of MO.

Importantly, the above results reveal that photoactivation of persulphate by Complexl has the propensity to degrade MO and completely inactivate bacteria in simulated ground water that contained a variety of inorganic ions, and organic matter. As discussed above, both the photo-degradation of MO and photo-inactivation of *E. coli* were affected in a medium with relatively higher ionic strength and organic content. Therefore, both the photo-degradation of MO and photo-inactivation of bacteria could be affected in a more complex media than the simulated ground water used in the present study. Inorganic and organic composition of the medium has been shown to affect photolytic water treatment processes such as UV-TiO_2, and photo-Fenton process.[10, 38]

4.4 Conclusions:

Photolytic process that has potential to degrade organic contaminants as well as inactivate bacteria in aqueous media has great environmental significance. Activation of persulphate is a promising strategy in advanced oxidation process for degradation of organic contaminants. Oxidation using persulphate is effective, easy to handle and no toxic byproducts are produced. The present study shows that visible light activation of persulphate using tris(2,2'-bipyridyl)ruthenium(II) caused rapid degradation (98%) of model azo dye methyl orange with significant mineralization, and also complete inactivation of both Gram negative and Gram positive bacteria. BacLight LIVE/DEAD assay, scanning electron microscopy and genomic DNA analysis revealed cell membrane damage and loss of chromosomal DNA, indicating oxidative stress caused to *E. coli* during photo-inactivation. Significant degradation of MO and complete inactivation of bacteria were observed in simulated ground water containing a variety of common ions and organic compound. The

present study is the first to reveal that activation of persulphate using a visible light absorbing metal complex in aqueous media has the ability for simultaneous degradation of organic contaminants and bacteria in water.

4.5 References:

1. Gao, F. G.; Bard, A. J., Solid-state organic light-emitting diodes based on Tris(2,2-bipyridine)ruthenium(II) complexes. *Journal of the American Chemical Society* **2000,** *122* (30), 7426-7427.

2. Anipsitakis, G. P.; Dionysiou, D. D., Degradation of organic contaminants in water with sulfate radicals generated by the conjunction of peroxymonosulfate with Cobalt. *Environmental Science & Technology* **2003,** *37* (20), 4790-4797.

3. Enwemeka, C. S.; Williams, D.; Enwemeka, S. K.; Hollosi, S.; Yens, D., Blue 470-nm light kills methicillin-resistant staphylococcus aureus (mrsa) in vitro. *Photomedicine and Laser Surgery* **2009,** *27* (2), 221-226.

4. Maclean, M.; MacGregor, S. J.; Anderson, J. G.; Woolsey, G., Inactivation of bacterial pathogens following exposure to light from a 405-nanometer light-emitting diode array. *Applied and Environmental Microbiology* **2009,** *75* (7), 1932-1937.

5. Arrojado, C.; Pereira, C.; Tome, J. P. C.; Faustino, M. A. F.; Neves, M. G. P. M. S.; Tome, A. C.; Cavaleiro, J. A. S.; Cunha, A.; Calado, R.; Gomes, N. C. M.; Almeida, A., Applicability of photodynamic antimicrobial chemotherapy as an alternative to inactivate fish pathogenic bacteria in aquaculture systems. *Photochemical & Photobiological Sciences* **2011,** *10* (10), 1691-1700.

6. Zhang, L. S.; Wong, K. H.; Yip, H. Y.; Hu, C.; Yu, J. C.; Chan, C. Y.; Wong, P. K., effective photocatalytic disinfection of *E. coli* k-12 using Ag-AgBr nanojunction system irradiated by visible light: The Role of Diffusing Hydroxyl Radicals. *Environmental Science & Technology* **2010,** *44* (4), 1392-1398.

7. Hartmann, M.; Berditsch, M.; Hawecker, J.; Ardakani, M. F.; Gerthsen, D.; Ulrich, A. S., Damage of the bacterial cell envelope by antimicrobial peptides gramicidin s and pgla as revealed by transmission and scanning electron microscopy. *Antimicrobial Agents and Chemotherapy* **2010,** *54* (8), 3132-3142.

8. Salmon-Divon, M.; Nitzan, Y.; Malik, Z., Mechanistic aspects of *Escherichia coli* photodynamic inactivation by cationic tetra-meso(N-methylpyridyl)porphine. *Photochemical & Photobiological Sciences* **2004,** *3* (5), 423-429.

9. Kang, S.; Herzberg, M.; Rodrigues, D. F.; Elimelech, M., Antibacterial effects of carbon nanotubes: size does matter! *Langmuir* **2008,** *24* (13), 6409-6413.

10. Moncayo-Lasso, A.; Mora-Arismendi, L. E.; Rengifo-Herrera, J. A.; Sanabria, J.; Benitez, N.; Pulgarin, C., The detrimental influence of bacteria on the degradation of organic compounds in TiO_2 photocatalysis and near-neutral photo-Fenton processes under simulated solar light. *Photochemical & Photobiological Sciences* **2012,** *11* (5), 821-827.

11. Hu, C.; Hu, X.; Guo, J.; Qu, J., Efficient Destruction of Pathogenic Bacteria with $NiO/SrBi_2O_4$ under Visible Light Irradiation. *Environmental Science & Technology* **2006,** *40* (17), 5508-5513.

12. Hu, X.; Hu, C.; Peng, T.; Zhou, X.; Qu, J., Plasmon-Induced Inactivation of Enteric Pathogenic Microorganisms with $Ag\text{-}AgI/Al_2O_3$ under Visible-Light Irradiation. *Environmental Science & Technology* **2010,** *44* (18), 7058-7062.

13. Dash, B. P.; Chaudhari, S., Electrochemical denitrificaton of simulated ground water. *Water Research* **2005,** *39* (17), 4065-4072.

14. Kaledin, A. L.; Huang, Z.; Geletii, Y. V.; Lian, T.; Hill, C. L.; Musaev, D. G., Insights into photoinduced electron transfer between $[Ru(bpy)_3]^{2+}$ and $[S_2O_8]^{2-}$ in Water: Computational and Experimental Studies. *The Journal of Physical Chemistry A* **2009,** *114* (1), 73-80.

15. Waldemer, R. H.; Tratnyek, P. G.; Johnson, R. L.; Nurmi, J. T., Oxidation of chlorinated ethenes by heat-activated persulfate:- kinetics and products. *Environmental Science & Technology* **2006,** *41* (3), 1010-1015.

16. He, X. X.; de la Cruz, A. A.; Dionysiou, D. D., Destruction of cyanobacterial toxin cylindrospermopsin by hydroxyl radicals and sulfate radicals using UV-254 nm activation of hydrogen peroxide, persulfate and peroxymonosulfate. Journal of Photochemistry and Photobiology a-Chemistry **2013**, 251, 160-166.

17. He, X. X.; de la Cruz, A. A.; O'Shea, K. E.; Dionysiou, D. D., Kinetics and mechanisms of cylindrospermopsin destruction by sulfate radical-based advanced oxidation processes. Water Research **2014**, 63, 168-178.

18. Liu, H. Z.; Bruton, T. A.; Doyle, F. M.; Sedlak, D. L., In Situ Chemical Oxidation of Contaminated Groundwater by Persulfate: Decomposition by Fe(III)- and Mn(IV)-Containing Oxides and Aquifer Materials. Environmental Science & Technology **2014**, 48 (17), 10330-10336.

19. Xu, M.; Gu, X.; Lu, S.; Qiu, Z.; Sui, Q., Role of Reactive Oxygen Species for 1,1,1-Trichloroethane Degradation in a Thermally Activated Persulfate System. Industrial & Engineering Chemistry Research **2014**, 53, 1056−1063.

20. Yang, S.; Yang, X.; Shao, X.; Niu, R.; Wang, L., Activated carbon catalyzed persulfate oxidation of Azo dye acid orange 7 at ambient temperature. *Journal of Hazardous Materials* **2011,** *186* (1), 659-666.

21. Antoniou, M. G.; de la Cruz, A. A.; Dionysiou, D. D., Degradation of microcystin-LR using sulfate radicals generated through photolysis, thermolysis and transfer mechanisms. *Applied Catalysis B: Environmental* **2010,** *96* (3-4), 290-298.

22. Lepentsiotis, V.; Domagala, J.; Grgic, I.; van Eldik, R.; Muller, J. G.; Burrows, C. J., Mechanistic information on the redox cycling of nickel(II/III) complexes in the presence of sulfur oxides and oxygen. correlation with dna damage experiments. *Inorganic Chemistry* **1999,** *38* (15), 3500-3505.

23. Gogniat, G. T.; Dukan, S., TiO_2 Photocatalysis Causes DNA Damage via Fenton Reaction-Generated Hydroxyl Radicals during the Recovery Period. *Applied and Environmental Microbiology* **2007,** *73* (23), 7740-7743.

24. Aboul-Enein, A.; ScHulte-Frohlinde, D., Biological deactivation and single-strand breakage of plasmid dna by photosensitization using tris(2,2′- bipyridyl)ruthenium(II) and peroxydisulfate. *Photochemistry and Photobiology* **1988,** *48* (1), 27-34.

25. Bourre, L.; Giuntini, F.; Eggleston, I. M.; Mosse, C. A.; MacRobert, A. J.; Wilson, M., Effective photo-inactivation of Gram-positive and Gram-negative bacterial strains using an HIV-1 Tat peptide-porphyrin conjugate. *Photochemical & Photobiological Sciences* **2010,** *9* (12), 1613-1620.

26. Jori, G.; Brown, S. B., Photosensitized inactivation of microorganisms. *Photochemical & Photobiological Sciences* **2004,** *3* (5), 403-405.

27. George, S.; Hamblin, M. R.; Kishen, A., Uptake pathways of anionic and cationic photosensitizers into bacteria. *Photochemical & Photobiological Sciences* **2009,** *8* (6), 788-795.

28. Minnock, A.; Vernon, D. I.; Schofield, J.; Griffiths, J.; Howard Parish, J.; Brown, S. B., Photo-inactivation of bacteria. Use of a cationic water-soluble zinc phthalocyanine to photoinactivate both Gram-negative and Gram-positive bacteria. *Journal of Photochemistry and Photobiology B: Biology* **1996,** *32* (3), 159-164.

29. Szpakowska, M.; Lasocki, K.; Grzybowski, J.; Graczyk, A., Photodynamic activity of the haematoporphyrin derivative with rutin and arginine substituents (HpD-Rut2- Arg2) against staphylococcus aureus and pseudomonas aeruginosa. *Pharmacological Research* **2001,** *44* (3), 243-246.

30. Gao, Y. Q.; Gao, N. Y.; Deng, Y.; Yang, Y. Q.; Ma, Y., Ultraviolet (UV) light-activated persulfate oxidation of sulfamethazine in water. *Chemical Engineering Journal* **2012,** *195-196* (0), 248-253.

31. Criquet, J.; Leitner, N. K. V., Degradation of acetic acid with sulfate radical generated by persulfate ions photolysis. *Chemosphere* **2009,** *77* (2), 194-200.

32. Muller, J. G.; Hickerson, R. P.; Perez, R. J.; Burrows, C. J., DNA Damage from sulfite autoxidation catalyzed by a Nickel(II) peptide. *Journal of the American Chemical Society* **1997,** *119* (7), 1501-1506.

33. Hou, Y.; Li, X.; Zhao, Q.; Chen, G.; Raston, C. L., Role of hydroxyl radicals and mechanism of escherichia coli inactivation on Ag/Agbr/TiO_2 nanotube array electrode under visible light irradiation. *Environmental Science & Technology* **2012,** *46* (7), 4042-4050.

34. Cho, M.; Lee, Y.; Chung, H.; Yoon, J., Inactivation of *Escherichia coli* by photochemical reaction of ferrioxalate at slightly acidic and near-neutral pHs. *Applied and Environmental Microbiology* **2004,** *70* (2), 1129-1134.

35. Chen, F.; Yang, X.; Xu, F.; Wu, Q.; Zhang, Y., Correlation of photocatalytic bactericidal effect and organic matter degradation of TiO_2 Part I: Observation of phenomena. *Environmental Science & Technology* **2009,** *43* (4), 1180-1184.

36. Chen, C. Z.; Cooper, S. L., Interactions between dendrimer biocides and bacterial membranes. *Biomaterials* **2002,** *23* (16), 3359-3368.

37. Caminos, D. A.; Spesia, M. B.; Pons, P.; Durantini, E. N., Mechanisms of *Escherichia coli* photodynamic inactivation by an amphiphilic tricationic porphyrin and 5,10,15,20-tetra(4-N,N,N-trimethylammoniumphenyl) porphyrin. *Photochemical & Photobiological Sciences* **2008,** *7* (9), 1071-1078.

38. Marugan, J.; Van Grieken, R.; Pablos, C.; Sordo, C., Analogies and differences between photocatalytic oxidation of chemicals and photocatalytic inactivation of microorganisms. *Water Research* **2010,** *44* (3), 789-796.

Activation of hydrogen peroxide by Copper based photo Fenton-like process for disinfection of bacteria in water

5.1 Abstract:

Natural sunlight or monochromatic near UV light irradiation of Cu(II) complexes of amino acids are known to cause photoreduction of Cu(II) to Cu(I) state.[1, 2] On the other hand, Cu(I) complexes could rapidly react with H_2O_2 to generate hydroxyl radical that is commonly known as Copper based Fenton-like process, implying the activation of hydrogen peroxide.[1-6] Moreover, it is important to note that Cu(II) ions are known to bind to bacteria via complexation with bacterial cell components such as proteins and other biomolecules.[7-9] Herein, for the first time. a Copper based photo-Fenton like process to inactivate bacteria in water using concentration of Cu(II)ions less than the permissible limit in water is presented. In addition, the ability of a new Cu(II) polypyridyl complex to act as a photosensitiser for inactivation of bacteria in water is also presented.This chapter addresses the gaps in literature discussed under the section 1.6 (a), 1.7 and 1.7 (a) of chapter 1.

Graphical Abstract:

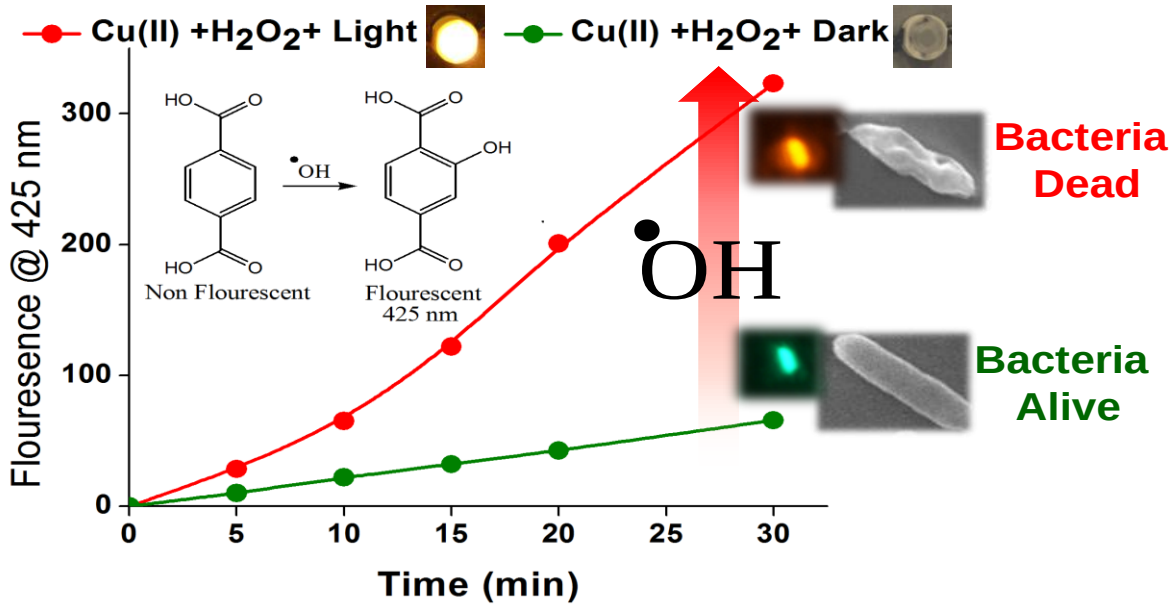

5. 2. Experimental procedures and analysis:

5.2 (a) Materials:

Copper (II) chloride pentahydrate ($CuCl_2.5H_2O$), 1, 10 phenanthroline (phen), 5-amino 1,10 phenanthroline (5-NH_2-Phen), Hydrogen peroxide (30%), Tertiary butyl alcohol (t-

BuOH), Humic acid, Sodium teraphthalate ($C_8H_4Na_2O_4$), Calcium carbonate ($CaCO_3$), Sodium nitrate ($NaNO_3$), Disodium hydrogen phosphate (Na_2HPO_4), Sodium hydrogen phosphate (NaH_2PO_4), Sodium sulphate (Na_2SO_4), and Sodium hydrogen carbonate ($NaHCO_3$) used, were of guaranteed analytical grade, purchased from SD fine chemicals, India. Bovine serum albumin (BSA) was purchased from Molychem. The complexes $[Cu(Phen)_2]Cl$ and $[Cu(5\text{-}NH_2\text{-}Phen)_2]Cl$ (where Phen = 1,10 phenenthroline and 5-NH_2-Phen = 1,10-Phenanthrolin-5-amine) were prepared according to a general synthetic method in which an aqueous solution of $CuCl_2.5H_2O$ (1.0 mmol) was reacted with a methanolic solution of Phen or 5-NH_2-Phen (2.0 mmol) stirred at 35-38 °C for 2 h and filtered. The solid was isolated, washed with cold aqueous methanol (1:1 v/v), and dried in dessicator.[4] For HPLC analysis, Acetonitrile (HPLC grade) and millipore water were used. The aqueous solution of these complexes showed a huge absorption at 200-300 nm that corresponds to charge π-π* transitions and a broad peak at around 650-720 nm corresponding to d-d transitions[10, 11] (Appendix I Figure 5.1). ESI-MS of C1 showed two major peaks at m/z 459 and 489 corresponding to the mass of $[Cu(Phen)_2]Cl$ and $[Cu(5\text{-}NH_2\text{-}Phen)_2]Cl$, respectively (Appendix I Figure 5.2).

5.2 (b) Photolytic experimental setup:

Visible light LED array containing warm white LED bulbs (400 - 700 nm, with peak maxima around 450 and 600 nm) manufactured by Kwality Photonics Pvt. Ltd, India was used as light source. Details of LED array and photograph of photolysis experimental setup are provided in supporting information (Appendix I Figure 4.1). Fluence rate was measured by Ophir PD100 Nova II power meter.

5.2 (c) Photo-inactivation of bacteria:

Photoantimicrobial assays were performed as described in Chapter 4, Section 4.2.4, except that the reaction mixture (0.2 ml) contained ~10^7 CFU mL^{-1} of bacterial cells with appropriate concentration of Cu(II)ions or $[Cu(Phen)_2]^{2+}$ or $[Cu(5\text{-}NH_2\text{-}Phen)_2]^{2+}$ in PBS (10 mM) was irradiated in 96 well plates. For experiments in dark, the LED array was switched off. Radical scavenging experiments were performed by addition of t-butyl alcohol (0.1 M) to reaction mixture. Photo-inactivation of bacteria (*E. coli*) was studied in simulated tap water that contained a defined composition of inorganic and organic matter. For scavenging hydroxyl radicals, t-BuOH was used as reported earlier.[12] Composition of simulated tap water: $[CO_3^{2-}]$ = 300 mgL^{-1}, $[Cl^-]$ = 250 mgL^{-1}, $[SO_4^{2-}]$ = 200 mgL^{-1}, $[NO_3^-]$ = 45 mgL^{-1}; Natural organic matter (Humic acid) = 1 mgL^{-1}. Two independent experiments in triplicates

were performed for each bacterial species. All the statistical analysis was performed using OriginPro 8.0.

Integrity of *E. coli* cell membrane and structural change in bacterial cell wall of *E. coli* cells treated with Cu(II)ions and H_2O_2 in absence and presence of light for 20 min were examined by Invitrogen Molecular Probes® LIVE/DEAD® BacLight™ assay and Scanning Electron Microscopy (SEM) analysis, respectively as described in Chapter 4, Section 4.2.(e) and 4.2.(f).

The membrane binding ability of $[Cu(Phen)_2]Cl$ or $[Cu(5\text{-}NH_2\text{-}Phen)_2]Cl$ to *E. coli* cell membrane was investigated by the following the absorption spectral changes before and after incubation of *E. coli* cells with these complexes as reported earlier.[18] In brief, suspensions of *E. coli* in phosphate-buffered saline (PBS, 10 mM, pH 7.0) were incubated with 100 µM Cu(II) complexes at 37 ◦C for 30 min in dark. Then the cultures were ultrafiltered through a 0.22 µm Millipore membrane to remove *E. coli* cells and the Cu(II) complexes bound on them. The absorption spectra of the filtrates were recorded to determine the free Cu(II) complexes.

5.2 (d) Detection of hydroxyl radical:

Sodium teraphthalate was used as a hydroxyl radical detection probe as described earlier.[13, 14] Reaction mixture (2 ml) containing sodium teraphthalate (200 µM), Cu(II)ions (1 µM) with and without H_2O_2 (2 mM) in PBS (10 mM) was irradiated in 24 well plates. For experiments in dark, the LED array was switched off. The fluorescence emission spectrum of these solutions was measured using Jasco Fluorescence spectrophotometer.

5.3 Results and Discussion:

5.3 (a) Photo-inactivation of bacteria:

Irradiation (above 400 nm) of *E. coli* in presence of Cu(II) ions and H_2O_2 caused rapid and complete loss of cell viability within 20 min (Figure 5.1). On the other hand, in the absence of irradiation, exposure of *E. coli* to Cu(II) ions in presence of H_2O_2 caused no significant reduction (< 1 log decrease in CFU/ml) of *E. coli* cell viability (Figure 5.1). Moreover, exposure of *E. coli* to Cu(II) ions or H_2O_2 with and without irradiation, caused negligible *E. coli* inactivation (Figure 5.1). Similar results were also observed for *S. aureus* (Figure 5.1B), and *P. aureginosa* (Figure 5.1C). Moreover, a model fungus *C. albicans*, was also inactivated upon irradiation in presence of Cu(II) and H_2O_2 (Figure 5.2).

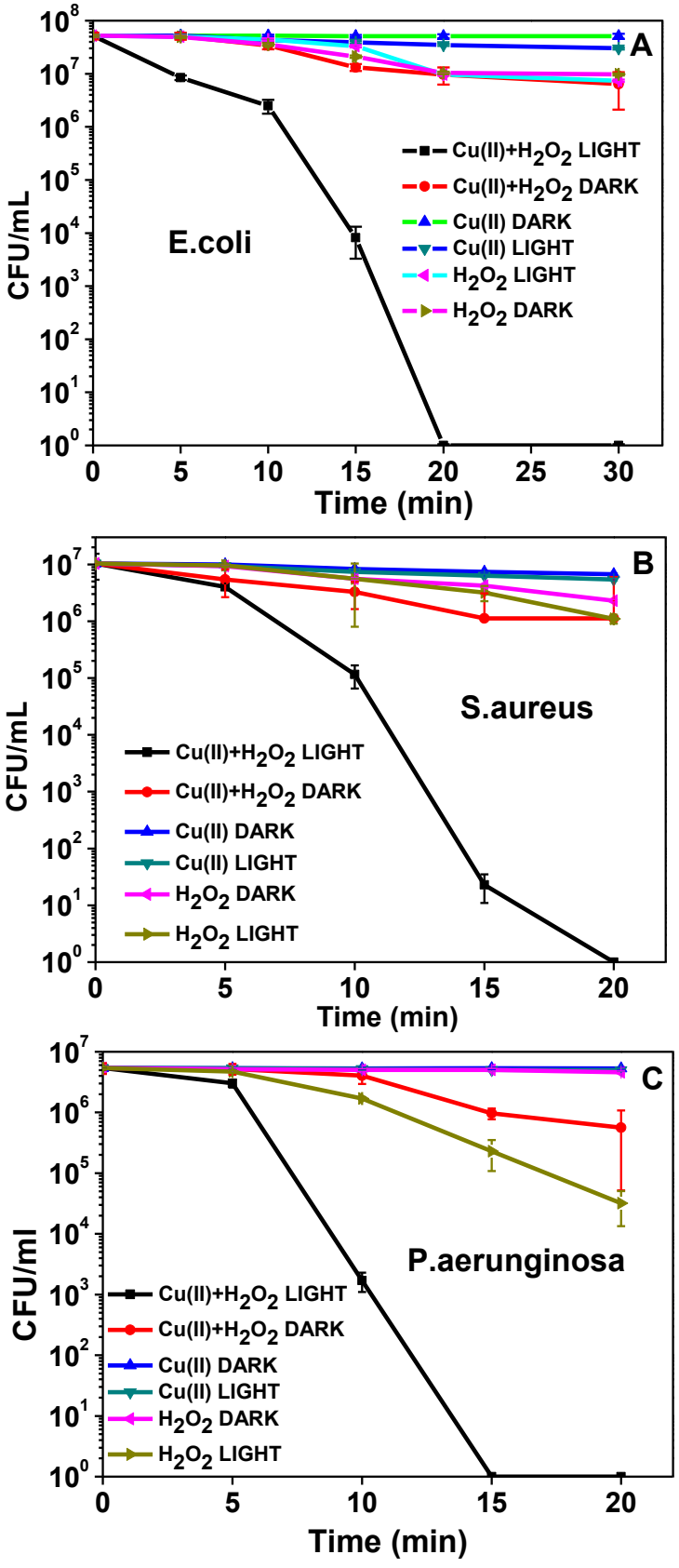

Figure 5.1 Cell viability Vs Time plot for photo-inactivation of (A) *E. coli*, (B) *S. aureus* and (C) *P. aeruginosa.* Cell concentration = ~10^7 CFU mL^{-1}, [H_2O_2] = 2 mM, [Cu(II) ions] = 1 µM, Fluence rate = 0.163 Wcm^{-2}.

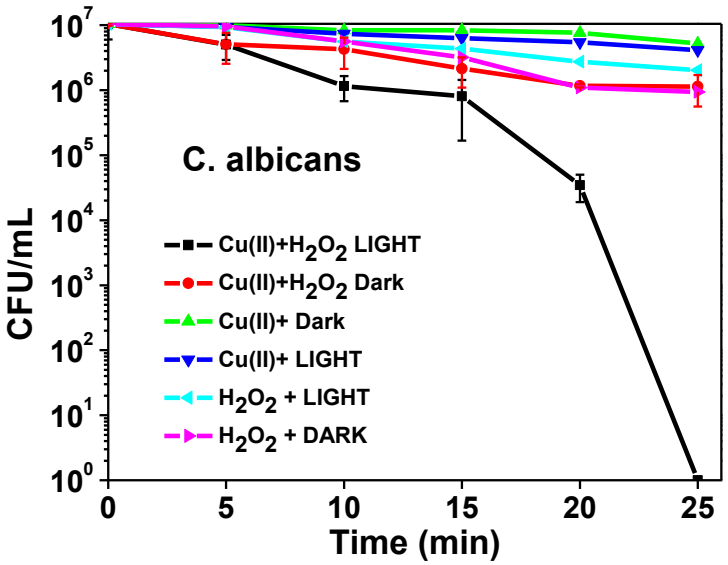

Figure 5.2 Cell viability Vs Time plot for photo-inactivation of *C .albicans*. Cell concentration = ~10^7 CFU mL^{-1}, [H_2O_2] = 2 mM, [Cu(II) ions] = 1 µM, Fluence rate = 0.163 Wcm^{-2}.

Both Gram negative and Gram positive bacteria are inactivated (Table 5.1) revealing a broad spectrum of bactericidal activity. It is important to note that the permissible level of copper in drinking water as per regulatory bodies are US – EPA - 1.3 mg/L or 20.45 µM, WHO - 1 mg/L or 15.73 µM, CPCB (India) – 1.5 mg/L or 23.6 µM.[15] Favourably, in the present study, the complete photoinactivation of bacteria was achieved at very low concentration of Cu(II)ions, 0.06 mg/L or 1 µM i.e., ~20 times less than the permissible level of copper in in drinking water. Furthermore, complete photo-inactivation of *E. coli* by Cu(II) ions and H_2O_2 was unaffected in the presence of a variety of common ions and natural organic matter (Appendix I Figure 5.3) indicating the potential of the proposed process for water disinfection.

Table 5.1 Conditions for complete inactivation of microbes

Microbe	Irradiation Time (min)	Light Dosage (Jcm^{-2})
E. coli †	20	195.6
P. aeruginosa†	15	146.7
S. aureus‡	20	195.6
*C. albicans**	25	244.5
†Gram negative bacteria	*Fungus	[Cu(II)] = 1 µM
‡Gram positive bacteria		[H_2O_2] = 2 mM

Decreasing the concentration of Cu(II) ions (from 1 µM to 0.25 µM) or H_2O_2 (from 2 mM to 0.5 mM) under visible light irradiation decreased the reduction in the cell viability of *E. coli* (Figure 5.3) revealing that photoinactivation of *E. coli* by Cu(II) ions in presence of

H_2O_2 is dependent on the dosage of Cu(II) ions and H_2O_2. The optimised concentrations of Cu(II)ions and H_2O_2 required for the complete photo-inactivation of bacteria under the present experimental conditions are 1 μM and 2 mM, respectively.

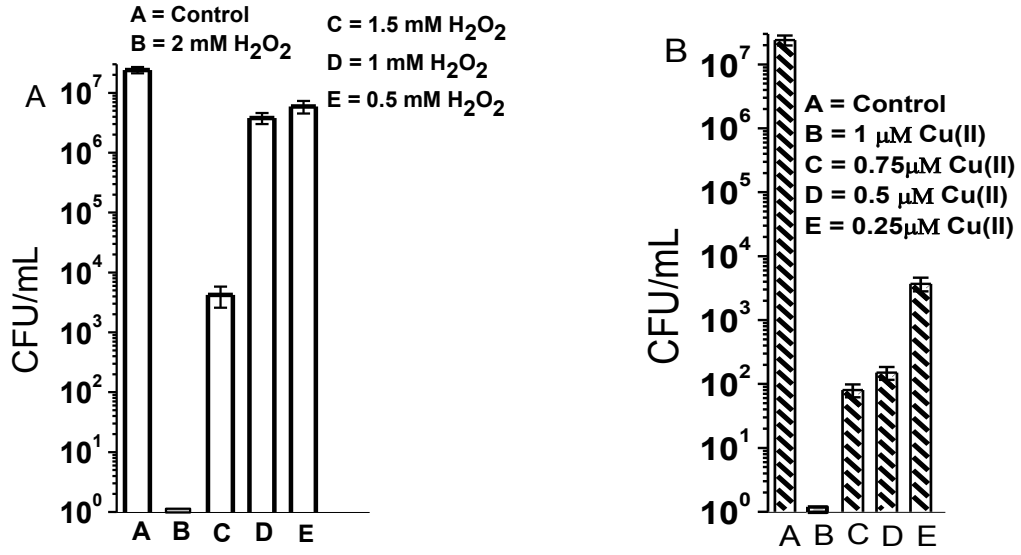

Figure 5.3 Effect of Cu(II) ions and H_2O_2 concentration on photoinactivation of *E. coli.* cell concentration = ~ 10^7 CFU mL^{-1}, [H_2O_2] = 2 mM, [Cu(II) ions] = 1 μM, Light dosage = 195.6 J/cm^2.

Moreover, in BacLight Live/Dead assay, green fluorescence was observed for the control *E. coli* cells (Figure 5.4A), as well as for *E. coli* cells exposed to Cu(II) ions in presence of H_2O_2 under dark condition (Figure 5.4B). These results reveal that *E. coli* cells subjected to Cu(II) ions and H_2O_2 under dark condition had intact cell membranes and live cells. On the other hand, *E. coli* cells irradiated under visible light in presence of Cu(II) ions and H_2O_2 showed red fluorescence (Figure 5.4C). Furthermore, SEM images showed that the membrane surfaces of control *E. coli* cells (Figure 5.4D) and *E. coli* exposed to Cu(II)ions in presence of H_2O_2 under dark condition were smooth and rod shaped (Figure 5.4E), whereas membrane surfaces of *E. coli* cells irradiated under visible light with Cu(II)ions in presence of H_2O_2 were deformed and showed craters indicating severe cell membrane damage (Figure 5.4F).

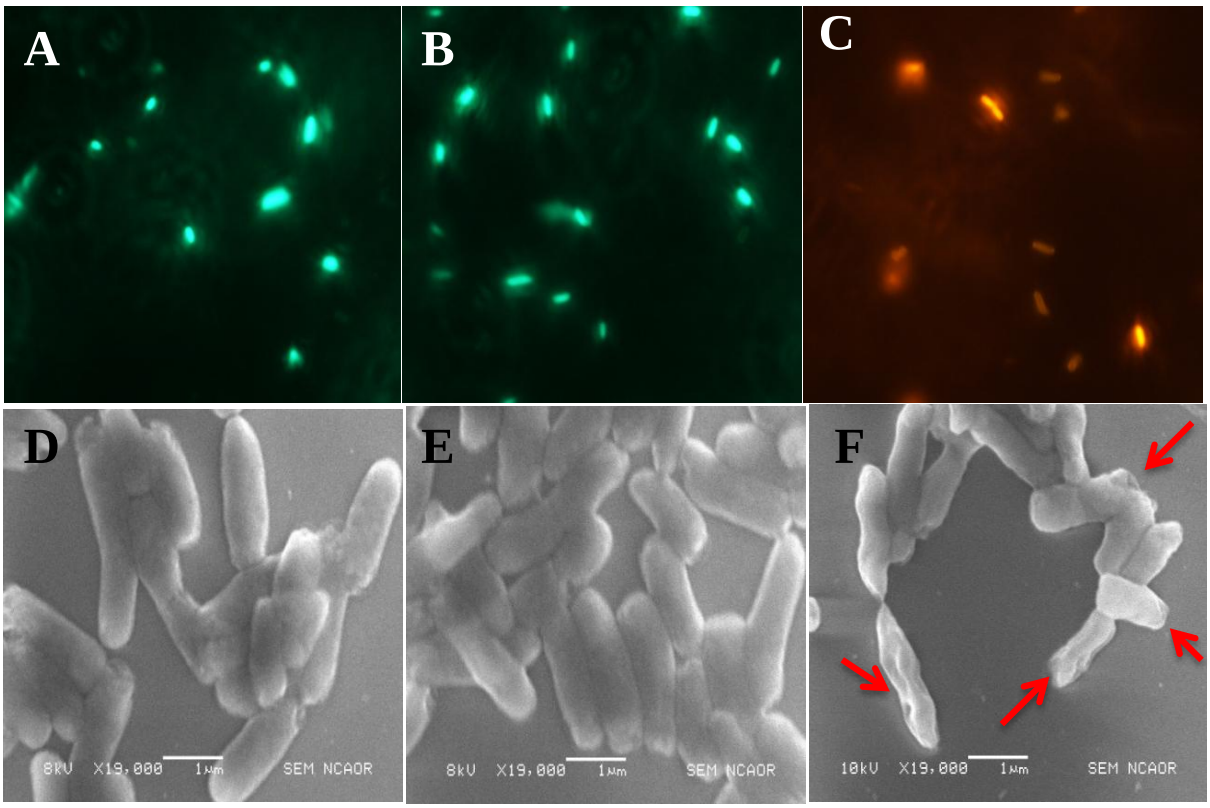

Figure 5.4 Fluorescence microscopic image of *E. coli* (A), *E. coli* treated with Cu(II) ions and H_2O_2 in absence of light (control) (B) in presence of light (C). SEM images of *E. coli* (D), *E. coli* treated with Cu(II) ions and H_2O_2 in absence of light (control) (E) in presence of light (F). Red arrows point damaged cell membranes. *E. coli* concentration = ~10^7 CFU mL^{-1}, [H_2O_2] = 2 mM, [Cu(II) ions] = 1 µM, Light dosage = 195.6 J/cm^2.

The bacterial cell membrane damage indicated the severe oxidative stress probably caused due to hydroxyl radicals generated by activation of hydrogen peroxide.

5.3 (b) Effect of visible light irradiation on hydroxyl radical generation:

Terephthalic acid (TA) has been recognised as an excellent probe for the detection of hydroxyl radicals generated due to activation of hydrogen peroxide by Fenton reaction in aqueous solutions.[13, 14] TA reacts with hydroxyl radical to from a fluorescent compound, hydroxy terephthalic acid (HTA) according to the reaction 1.[13, 14] Importantly, the reaction between TA and hydroxyl radical is highly specific and not affected by the presence of other reactive oxygen species such as $HO_2^{\bullet}$, O_2^{-}, H_2O_2.[13]

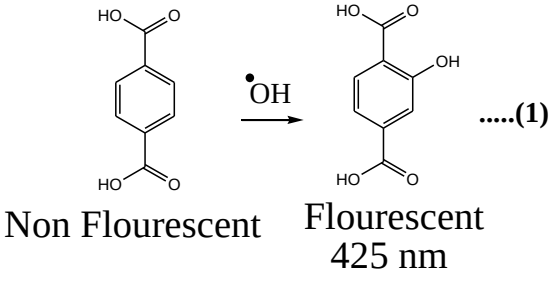

.....(1)

It was determined that photolysis of TA in presence of Cu(II) ions and H_2O_2 showed fluorescence. This result revealed that visible light irradiation of Cu(II) ions in presence of H_2O_2 generated hydroxyl radicals that could cause oxidative stress to bacteria. The generation of hydroxyl radical is proposed to occur by photo Fenton-like reaction that involves the photoreduction of Cu(II) to Cu(I) state and activation of H_2O_2 by Cu(I) to generate hydroxyl radical (reaction 2).

$$\text{L-Cu(I)} + H_2O_2 \longrightarrow \text{L-Cu(II)} + OH^- + OH^{\bullet} \quad .....(2)$$

Moreover, reaction of TA with Cu(II) ions and H_2O_2, under dark condition showed slight flouresence i.e., ~5 times lower than that produced by Cu(II) ions and H_2O_2 under visible light irradiation (Figure 5.5A and B, Appendix I Figure 5.4). The effective microbicidal activity (Figure 5.1 and 5.2) is attributed to the hydroxyl radicals generated by the proposed Copper based photo Fenton like process. It should be noted that photolysis of TA in presence of Cu(II) ions alone or H_2O_2 alone (control experiments) showed no fluorescence (Figure 5.5A).

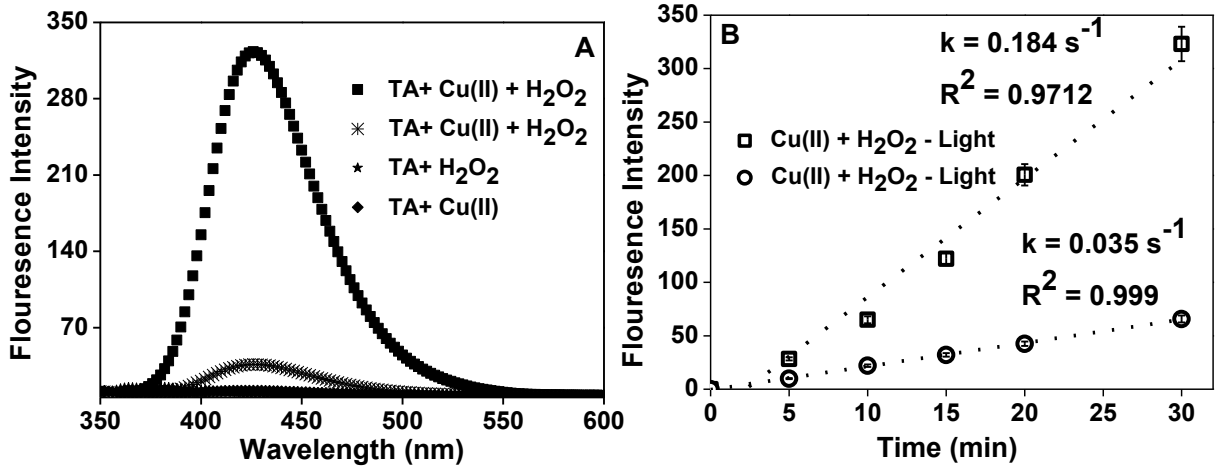

Figure 5.5 (A) Fluorescence spectra showing the formation of HTA on reaction of TA with Cu(II) ions and H_2O_2 under different experimental conditions. Light dosage = 293.4 J/cm^2 (B) Comparison of formation of HTA on reaction of TA with Cu(II) ions and H_2O_2 in presence and absence of irradiation. [TA] = 200 µM, [H_2O_2] = 2 mM, [Cu(II) ions] = 1 µM, Fluence rate = 0.163 Wcm^{-2}.

Earlier, it was reported that bovine serum albumin (BSA) was oxidatively degraded in presence of Cu(II) ions and H_2O_2. A mechanism involving a slow reduction of Cu(II) to Cu(I) in presence H_2O_2 and reaction of Cu(I) with H_2O_2 (copper based Fenton like reaction, reaction 3) was proposed for the degradation of BSA.[3] Importantly, in the present study, irradiation of BSA bound to Cu(II) ions in presence of H_2O_2 resulted in significant degradation of BSA

(Figure 5.6), revealing that Copper species bound BSA activates H_2O_2 upon irradiation. On the other hand, no significant degradation of BSA bound to Cu(II) ions in presence of H_2O_2 was observed under dark condition (Figure 5.6).

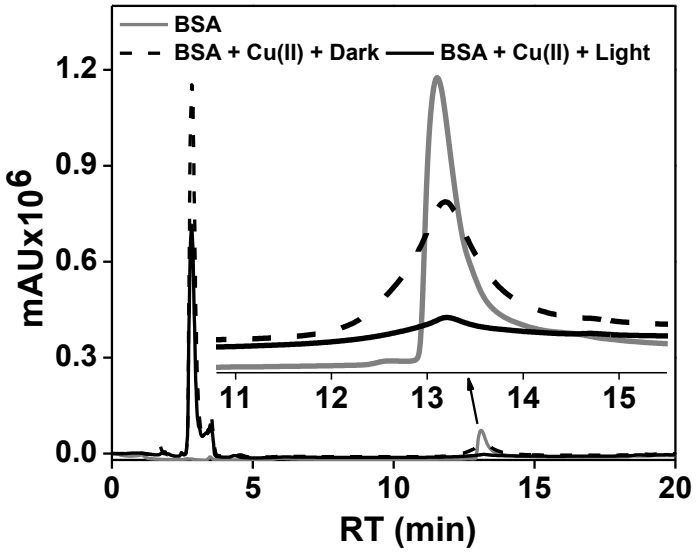

Figure 5.6 Degradation of BSA by Cu(II) ions and H_2O_2 in presence and absence of irradiation. [H_2O_2] = 200 mM, [Cu(II) ions] = 100 µM, [BSA] = 25 µM; Light dosage = 1,760.4 J/cm^2.

Irradiation (above 400 nm) of BSA in presence Cu(II) ion and H_2O_2 along with hydroxyl radical scavenger terephthalic acid (TA), showed formation of fluorescent hydroxylated terephathalic acid (HTA) (Figure. 5.7). Moreover, it should be noted that the HTA formed on irradiation of TA, Cu(II) ion and H_2O_2, in presence of BSA is relatively less (Figure. 5.7) than in the absence of BSA (Figure. 5.7). This decrease in the formation of HTA is attributed to the competitive scavenging of hydroxyl radicals by BSA and TA. Moreover, in absence of irradiation, under the same experimental conditions, the reaction of BSA in presence Cu(II) ion and H_2O_2 along with hydroxyl radical scavenger terephthalic acid (TA) showed minimum flouresence. These results revealed the in-situ generation of hydroxyl radicals by irradiation of Cu(II) ions bound to BSA in presence of H_2O_2 via Copper based photo Fenton-like mechanism as discussed above. Similar results were observed for the reaction of *E.coli* in presence Cu(II) ion and H_2O_2 along with hydroxyl radical scavenger TA (Figure. 5.7).

These results reveal the effective generation of hydroxyl radical by the activation of H_2O_2 under visible light irradiation mediated by Cu(II) ions bound to BSA or bacteria in presence of H_2O_2.

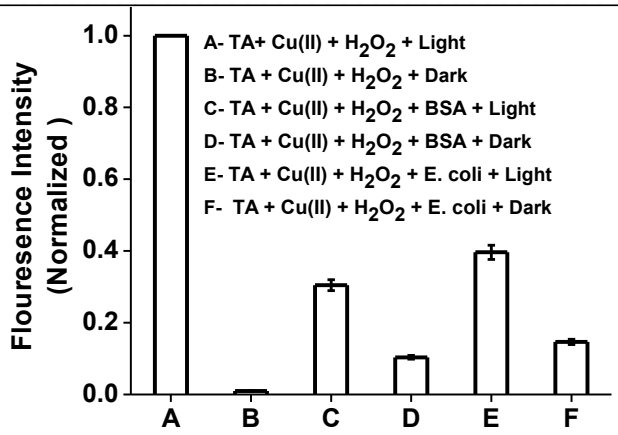

Figure 5.7 Normalized Fluorescence intensity showing the formation of HTA on reaction of TA with Cu(II) ions and H_2O_2 in absence and presence of BSA and *E.coli*. Light dosage = 195.6 J/cm^2; [TA] = 200 µM, [H_2O_2] = 2 mM, [Cu(II) ions] = 1 µM, *E. coli* concentration = ~10^7 CFU mL^{-1}; [BSA] = 25 µM; Fluence rate = 0.163 Wcm^{-2}.

Thus, the present findings highlight that the proposed Copper based photo Fenton-like process is promising for photo-inactivation of bacteria in water.

5.4 Photoinactivation of *E. coli* using Copper(II) complexes:

Metal complexes having the ability to photo-inactivate bacteria in the visible light region has potential applications in the Photoantimicrobial Chemotherapy (PACT).[18] It is important to note that Cu(II) polypyridyl complexes are known to generate reactive oxygen species such as singlet oxygen, hydroxyl radical and superoxide anion etc upon irradiation of visible light.[10, 11] Earlier studies have shown that copper polypyridyl complexes induce DNA damage upon visible light irradiation,[10, 11] however, to the best of our knowledge no report is available on the investigation of copper polypyridyl complexes for bacterial photo-inactivation in water under visible light irradiation. Herein, visible light photobactericidal activity of a new Cu(II) polypyridyl complex Cu(5-NH_2 -Phen)$_2$]$^{2+}$ is investigated. The absorption spectral features and the mass spectral data of Cu(5-NH_2 -Phen)$_2$]$^{2+}$ is provided in (Appendix 1, Figure 5.1 and 5.2)

Absorption of Cu(5-NH_2 -Phen)$_2$]$^{2+}$ (around 250-500 nm) was decreased on treatment with *E.coli* cells indicating the binding capacity of [Cu(5-NH_2 -Phen)$_2$]$^{2+}$ to *E. coli* cells (Figure. 5.8). Earlier, it was reported that the decrease in the absorption spectrum of the Ruthenium photosensitizer after the incubation with *E. coli* in dark indicate the membrane binding capacity of photosensitizer. On the other hand, [Cu(Phen)$_2$]$^{2+}$ had no membrane binding capacity as revealed by absorption spectroscopic results (Figure. 5.8). These results revealed that Cu(5-NH_2 -Phen)$_2$]$^{2+}$ has the ability to bind with bacterial membrane unlike [Cu(Phen)$_2$]$^{2+}$. Earlier, it was shown that the membrane biniding capacity of photosensitizers

such as such as Ru(II) polypyridyl complexes and cationic porphyrins was dependent on the nature of the ligands and the compounds with membrane binding capacity caused effective photoinactivation of bacteria.[18,19]

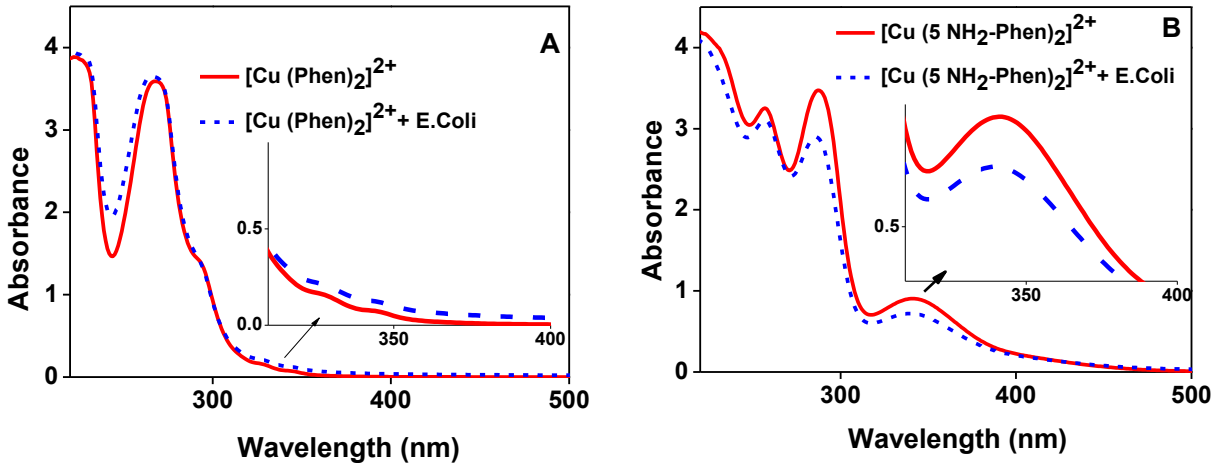

Figure 5.8 Absorption spectra of (A) $[Cu(Phen)_2]^{2+}$ and (B) $[Cu(5\text{-}NH_2\text{-}Phen)_2]^{2+}$ before and after treatment with *E. coli*. $[Cu(Phen)_2]^{2+}$ = $[Cu(5\text{-}NH_2\text{-}Phen)_2]^{2+}$ = 100 µM; [*E. coli*] = ~10^7 CFU mL^{-1}.

Exposure of *E. coli* to $[Cu(Phen)_2]^{2+}$ or Cu(II) ions with and without irradiation, and exposure of *E. coli* to $[Cu(5\text{-}NH_2\text{-}Phen)_2]^{2+}$ without irradiation caused no significant reduction of *E. coli* cell viability (~1.5 log decrease in CFU/ml) (Figure. 5.9). On the other hand, irradiation of *E. coli* with $[Cu(5\text{-}NH_2\text{-}Phen)_2]^{2+}$ caused rapid and complete loss of cell viability within 20 min (Figure. 5.9). These results reveal that $[Cu(5\text{-}NH_2\text{-}Phen)_2]^{2+}$ is a potential photo-antibacterial agent that could effectively inactivate bacteria upon irradiation in the concentration range of 10µM upon visible light irradiation.

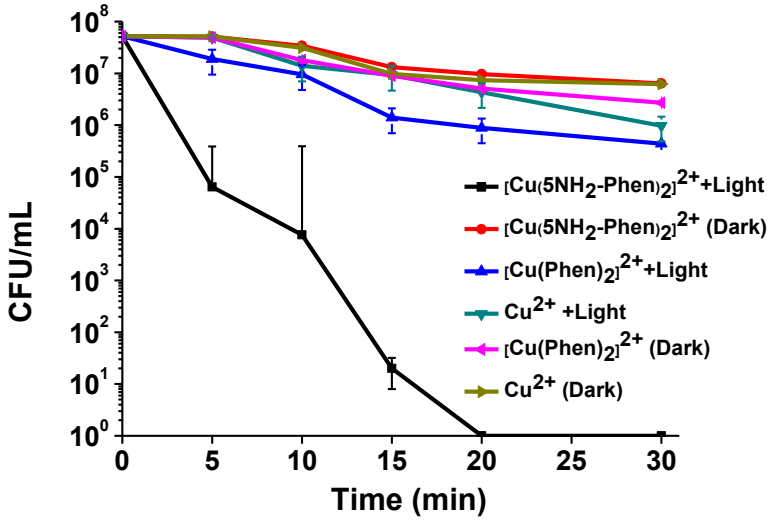

Figure 5.9 (A)Photo-inactivation of *E. coli* by $[Cu(Phen)_2]^{2+}$ and $[Cu(5\text{-}NH_2\text{-}Phen)_2]^{2+}$ $[Cu(Phen)_2]^{2+}$ =$[Cu(5\text{-}NH_2\text{-}Phen)_2]^{2+}$ = 10µM; [*E. coli*] = 10^7 CFU/mL; Fluence rate 0.163 W/cm^2; pH 7.2 (PBS 10 mM);Room temperature 25-30 °C.

Earlier, it was shown that the binding of photosensitizers such as Ru(II) polypyridyl complexes and cationic porphyrins to the bacterial membrane was favourable for photoinactivation of bacteria.[18,19] The present results demonstrated the potential of a novel Cu(II) polypyridyl complex that has the ability to bacterial cell membrane and cause effective photo-inactivation of bacteria upon visible light irradiation.

Earlier, photosensitizers such as Rose Bengal, and PACT agents such as Ru(II) polypyridyl complexes were used for water disinfection.[20] Moreover, it has been demonstrated that PACT agents are an effective alternate for water disinfection in fisheries.[21] It is important to note that $[Cu(5\text{-}NH_2\text{-}Phen)_2]^{2+}$ caused complete photo-inactivation of bacteria without the requirement of oxidant such as H_2O_2, implying the applicability of $[Cu(5\text{-}NH_2\text{-}Phen)_2]^{2+}$ as a photobactericidal agent in PACT as well as in water disinfection.

5.5 Conclusions:

The present study demonstrates the inactivation of bacteria upon visible light irradiation using low concentration of Cu(II)ions in presence of hydrogen peroxide. Importantly, the photo-inactivation of bacteria by Cu(II)ions and hydrogen peroxide was unaffected by the presence of common ions and natural organic matter. These results implied that the combination of visible light, Cu(II)ions and hydrogen peroxide has potential for water disinfection.

The present findings also demonstrate photo-inactivation of *E. coli* by new Cu(II) polypyridyl complex $[Cu(5\text{-}NH_2\text{-}Phen)_2]^{2+}$. $[Cu(5\text{-}NH_2\text{-}Phen)_2]^{2+}$ had cell membrane binding ability and caused effective photoinactivation. The present findings demonstrate for the first time the potential of photoactive Cu(II) polypyridyl complexes as promising PACT agents. The availability of a variety of polypyridyl ligands with different functional groups provide opportunity to tune the photophysical properties of Cu(II) polypyridyl complexes to bring about desired effects in PACT.

References:

1. Hayase, K.; Zepp, R. G., Photolysis of copper(II)-amino acid complexes in water. *Environmental Science & Technology* **1991,** *25* (7), 1273-1279.

2. Sakora, J. n., Photochemistry of copper complexes and their environmental aspects. *Coordination Chemistry Reviews* **1997,** *159* (0), 95-108.

3. Kocha, T.; Yamaguchi, M.; Ohtaki, H.; Fukuda, T.; Aoyagi, T., Hydrogen peroxide-mediated degradation of protein: different oxidation modes of copper- and iron-dependent hydroxyl radicals on the degradation of albumin. *Biochimica et Biophysica Acta (BBA) - Protein Structure and Molecular Enzymology* **1997,** *1337* (2), 319-326.

4. Pham, A. N.; Xing, G.; Miller, C. J.; Waite, T. D., Fenton-like copper redox chemistry revisited: Hydrogen peroxide and superoxide mediation of copper-catalyzed oxidant production. *Journal of Catalysis* **2013,** *301* (0), 54-64.

5. Lin, T. Y.; Wu, C.-H., Activation of hydrogen peroxide in copper(II)/amino acid/H_2O_2 systems: effects of pH and copper speciation. *Journal of Catalysis* **2005,** *232* (1), 117-126.

6. Robbins, M. H.; Drago, R. S., Activation of hydrogen peroxide for oxidation by copper (II) complexes. *Journal of Catalysis* **1997,** *170* (2), 295-303.

7. Moehl, W.; Motschi, H.; Schweiger, A., Magnetic resonance studies of copper(II) adsorbed on the surface of the bacterium klebsiella pneumoniae. *Langmuir* **1988,** *4* (3), 580-583.

8. Patikarnmonthon, N.; Nawapan, S.; Buranajitpakorn, S.; Charoenlap, N.; Mongkolsuk, S.; Vattanaviboon, P., Copper ions potentiate organic hydroperoxide and hydrogen peroxide toxicity through different mechanisms in Xanthomonas campestris pv. campestris. *FEMS microbiology letters* **2010,** *313* (1), 75-80.

9. Cooksey, D. A., Copper uptake and resistance in bacteria. *Molecular microbiology* **1993,** *7* (1), 1-5.

10. Patra, A. K.; Bhowmick, T.; Ramakumar, S.; Nethaji, M.; Chakravarty, A. R., DNA cleavage in red light promoted by copper(ii) complexes of α-amino acids and photoactive phenanthroline bases. *Dalton Transactions* **2008,** (48), 6966-6976.

11. Patra, A. K.; Bhowmick, T.; Roy, S.; Ramakumar, S.; Chakravarty, A. R., Copper(II) Complexes of l-Arginine as Netropsin Mimics Showing DNA Cleavage Activity in Red Light. *Inorganic Chemistry* **2009,** *48* (7), 2932-2943.

12. Anipsitakis, G. P.; Dionysiou, D. D., Radical Generation by the Interaction of Transition Metals with Common Oxidants. *Environmental Science & Technology* **2004,** *38* (13), 3705-3712.

13. Sahni, M.; Locke, B. R., Quantification of Hydroxyl Radicals Produced in Aqueous Phase Pulsed Electrical Discharge Reactors. *Industrial & Engineering Chemistry Research* **2006,** *45* (17), 5819-5825.

14. Linxiang, L.; Abe, Y.; Nagasawa, Y.; Kudo, R.; Usui, N.; Imai, K.; Mashino, T.; Mochizuki, M.; Miyata, N., An HPLC assay of hydroxyl radicals by the hydroxylation reaction of terephthalic acid. *Biomedical Chromatography* **2004,** *18* (7), 470-474.

15. Kumar, M.; Puri, A., A review of permissible limits of drinking water. *Indian journal of occupational and environmental medicine* **2012,** *16* (1), 40-47.

16. Nguyen, T. T. M.; Park, H. J.; Kim, J. Y.; Kim, H. E.; Lee, H.; Yoon, J.; Lee, C., Microbial Inactivation by Cupric Ion in Combination with H_2O_2: Role of Reactive Oxidants. *Environmental Science & Technology* **2013,** *47* (23), 13661-13667.

17. Nieto-Juarez, J. I.; Pierzcha, K.; Sienkiewicz, A.; Kohn, T., Inactivation of MS2 coliphage in Fenton and Fenton-like systems: role of transition metals, hydrogen peroxide and sunlight. *Environmental Science & Technology* **2010,** *44* (9), 3351-3356.

18. Lei, W.; Zhou, Q.; Jiang, G.; Zhang, B.; Wang, X., Photodynamic inactivation of Escherichia coli by Ru(II) complexes. *Photochemical & Photobiological Sciences* **2011,** *10* (6), 887-890.

19. Reddi, E.; Ceccon, M.; Valduga. G.; Jori .G.; Bommer. J. C.; Elisei. F.; Latterini. L.; and Mazzucato. U.; Photophysical properties and antibacterial activity of meso-substituted cationic porphyrins, *Photochemistry and Photobiology* **2002**, (75), 462-469.

20. Rengifo-Herrera, J. N. A.; Sanabria, J.; Machuca, F.; Dierolf, C. F.; Pulgarin, C.; Orellana, G., A comparison of solar photocatalytic inactivation of waterborne E. coli using Tris (2, 2-bipyridine) ruthenium (II), Rose Bengal, and TiO2. *Journal of Solar Energy Engineering* **2007,** *129* (1), 135-140.

21. 1. Arrojado, C. T.; Pereira, C.; Tome, J. O. P.; Faustino, M. A.; Neves, M. G.; Tome, A. C.; Cavaleiro, J. A.; Cunha, A. N.; Calado, R.; Gomes, N. C., Applicability of photodynamic antimicrobial chemotherapy as an alternative to inactivate fish pathogenic bacteria in aquaculture systems. *Photochemical & Photobiological Sciences* **2011**, (10), 1691-1700.

Conclusions

Activation of peroxo compounds such as persulphate and hydrogen peroxide to generate reactive sulphate and hydroxyl radicals for the degradation of recalcitrant organic and bacterial contaminants is a subject of great environmental importance. In the present work, the ability of a redox active Ni(II) hexaazamacrocyclic complex and a photoredox active Ru(II) polypyridyl complex to activate persulphate and its effect on recalcitrant organic and bacterial contaminants in water are presented. Moreover, the results revealed the potential of Cu(II) species in presence of hydrogen peroxide to inactivate bacteria under visible light irradiation.

An introduction on the current research and existing gaps on the metal ion and metal complex based activation of peroxo compounds is presented (chapter 1). Ni(II) hexaaza macrocyclic complex activated persulphate and degraded a variety of recalcitrant organic compounds such as malachite green (MG), ciprofloxacin (Cpf), methyl orange (MO), rhodamine B (RhB) and methylene blue (MB) (chapter 2). It is important to note that the widely used Fe(II) ions activated persulphate is effective only at acidic pH whereas, Ni(II) hexaaza macrocyclic complex activated persulphate caused the degradation of organic contaminants in a wide pH (3-9) that is advantageous. Moreover, toxicity of MG and Cpf towards model bacteria *E. coli* was removed on treatment with persulphate in presence of Ni(II) hexaaza macrocyclic complex, indicating that Ni(II) hexaaza macrocyclic complex activated persulphate, could aid conventional microbiological oxidation in treatment of non biodegradable pollutants such as MG and Cpf. In addition, Ni(II) hexaaza macrocyclic complex adsorbed effectively on to activated carbon and amberlite and provided the possibility for recovery and reuse of the complex (chapter 3). The use of adsorbents to recover and reuse a metal complex based persulphate activator is demonstrated for the first time. Importantly, Ni(II) hexaaza macrocyclic complex adsorbed on to activated carbon acted as a reusable heterogeneous persulphate activator and degraded MO for five cyclic runs without significant loss of activity.

In an effort to activate persulphate under visible light irradiation, a photo-redox active Ru(II) trisbipyridyl complex was used (chapter 4). Very low concentration (1µM) Ru(II) trisbipyridyl complex effectively activated persulphate upon irradiation in visible light region (400-700 nm) with the use of LED array as light source. Ru(II) trisbipyridyl complex activated persulphate not only degraded organic contaminant methyl orange but also caused the complete photoinactivation of four different bacterial species in water. Sulphate radical,

hydroxyl radical and Ru(III) trisbipyridyl complex produced upon activation of persulphate by Ru(II) trisbipyridyl complex caused severe oxidative stress leading to the damage of vital biomolecules such as membrane and DNA. Importantly, the potential of activated persulphate to simultaneously degrade organic and bacterial contaminants in water was revealed for the first time.

The combination of visible light irradiation, very low concentration of Cu(II) ions and hydrogen peroxide had propensity to rapidly photoinactivate bacteria in water (chapter 5). The enhancement of inactivation of bacteria and generation of hydroxyl radical upon visible light irradiation by copper based photo Fenton-like reaction was demonstrated for the first time. The photoinactivation of bacteria was also observed in simulated tap water that contained a variety of common ions and natural organic matter. The permissible level of copper in drinking water as per regulatory bodies are US–EPA - 1.3 mg/L or 20.45 µM, WHO - 1 mg/L or 15.73 µM, CPCB – 1.5 mg/L or 23.6 µM. It is important to note that in the present study, complete photoinactivation of bacteria was achieved using concentration of Cu(II) ions as low as 0.06 mg/L or 1 µM, indicating the potential of the proposed system for water disinfection.

The main findings of the present thesis are (i) identification of Ni(II) hexaaza macrocyclic complex as a promising persulphate activator for the degradation of a variety of recalcitrant organic chemicals (ii) transformation of homogeneous metal complex based persulphate activators into heterogeneous form by simple adsorption (iii) identification of Ru(II) trisbipyridyl complex as the potential photochemical activator of persulphate for simultaneous degradation of organic and microbial contaminants and (iv) photoenhanced hydroxyl radical generation and rapid photoinactivation of bacteria upon visible light irradiation of Cu(II) ions in presence of hydrogen peroxide in water.

The potential of unexplored transition metal complexes (Ni, Cu and Ru) to activate peroxo compounds for degradation recalcitrant organic and bacterial contaminants in water is demonstrated.

Future Scope

The results presented in this thesis have revealed the potential of metal complexes to activate peroxo compounds for the degradation of recalcitrant organic and microbial contaminants in water. One major finding of the present work is that Ni(II) hexaazamacrocyclic complex activated persulphate based degradation occurred at a wide pH range that is particularly advantageous over the widely used Fe(II) ions activated persulphate. The versatility of the reaction between Ni(II) hexaaza macrocyclic complex and persulphate to degrade other contaminants such as pesticides, halogenated solvents and natural toxins shall be carried out in future. It is important to note that apart from Ni(II) hexaazamacrocyclic complex, other structurally related redox active azamacrocyclic complexes of transition metal ions are available that could activate persulphate to degrade organic contaminants. The study draws attention to explore other redox active metal complexes for activation of persulphate.

Additionally, chapter 3 revealed the beneficial role of adsorbents in metal complex activated persulphate based degradation. The availability of versatile adsorbents provide a scope for transforming the effective homogeneous metal complex based persulphate activators into heterogeneous activators that are easy to separate from the treated waters and reuse. However, the variable factors such as nature of water matrix, adsorptivity of adsorbents, type of pollutants, and others need to be optimised for obtaining desired results.

Ruthenium complexes have received interest as potential visible light photosensitizers in environmental studies. Photochemical activation of persulphate in the visible light region has a huge potential in solar based degradation of organic and microbial contaminants in water. Chapter 4 revealed Ru(II) trisbipyridyl complex as a promising photochemical activator of persulphate. Favourably, the transition metal ions and their complexes including $[Ru(bpy)_3]^{2+}$ that are cationic in nature are known to be adsorbed on common adsorbents such as silica and activated charcoal. Thus, these complexes and degraded products could be removed from aqueous media. Future studies on immobilization of Ru(II) trisbipyridyl complex onto solid supports is beneficial for easy separation and reuse of the activator.

Chapter 5 revealed the significant role of visible light irradiation on enhanced hydroxyl radical generation and microbial inactivation by Cu(II) ions in presence of hydrogen peroxide. Additional research shall be carried out by preparing redox active Cu(II) complexes with different ligands in order to futher enhance the photobactericidal efficiency. Chapters 4 and 5 implied the use of LED arrays as light source for photodegradation of organic contaminants and photoinactivation of microbes. These results highlight the potential for

future research on the design and development of LED based photo reactors with desired compactness (surface to volume ratio) that may have applications in small scale point-of-use water purifiers, and PACT.

Appendix I: Supplementary Information

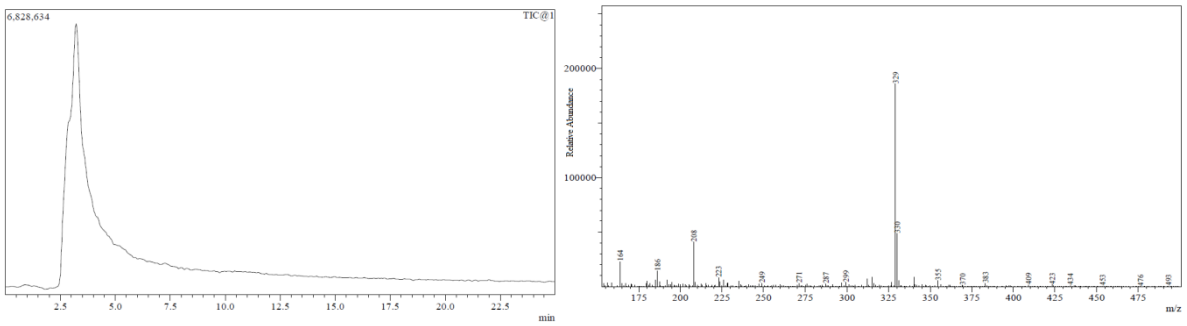

Supplementary Figure 2.1 TIC plot and LC-ESI-MS of MG.

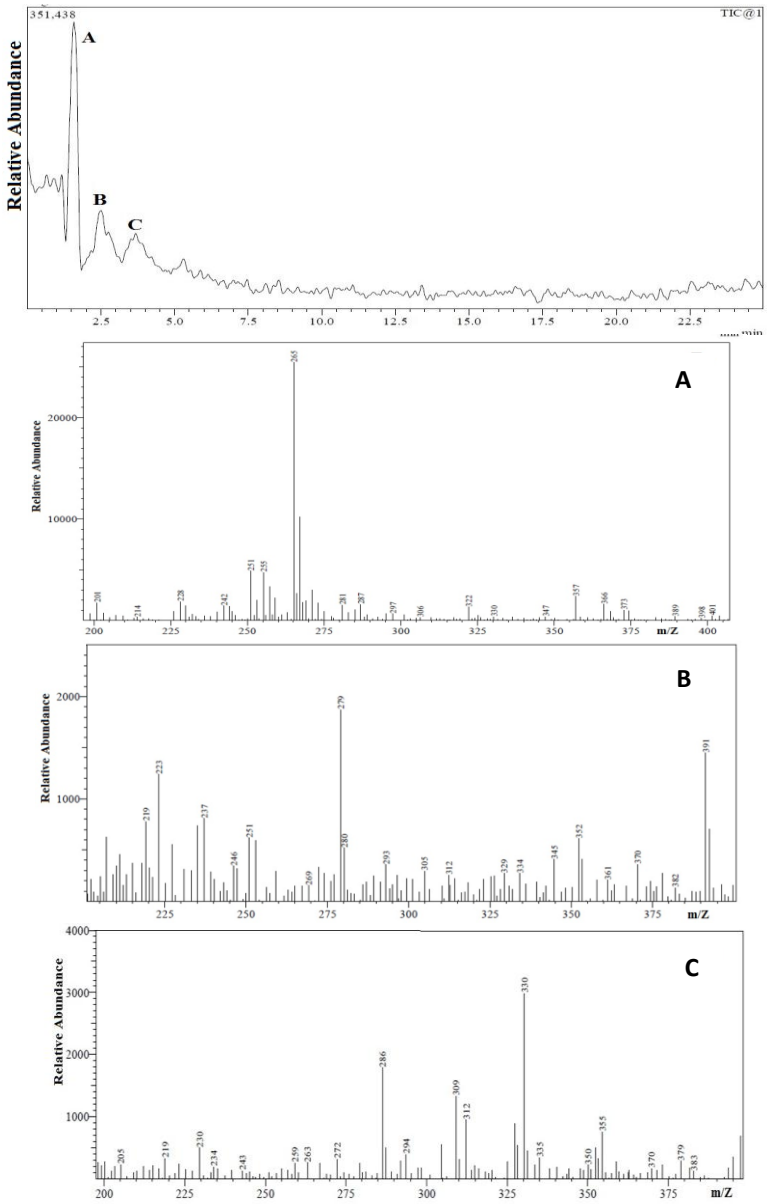

Supplementary Figure 2.2 TIC plot and LC-ESI-MS of MG after 1hr treatment with KPS in presence of C1 and the mass spectra of the peaks A, B and C, respectively in the TIC plot.

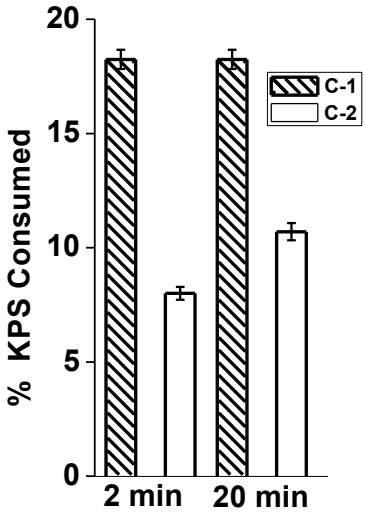

Supplementary Figure 2.3 Persulphate consumed (%) on reaction with C1 and C2.

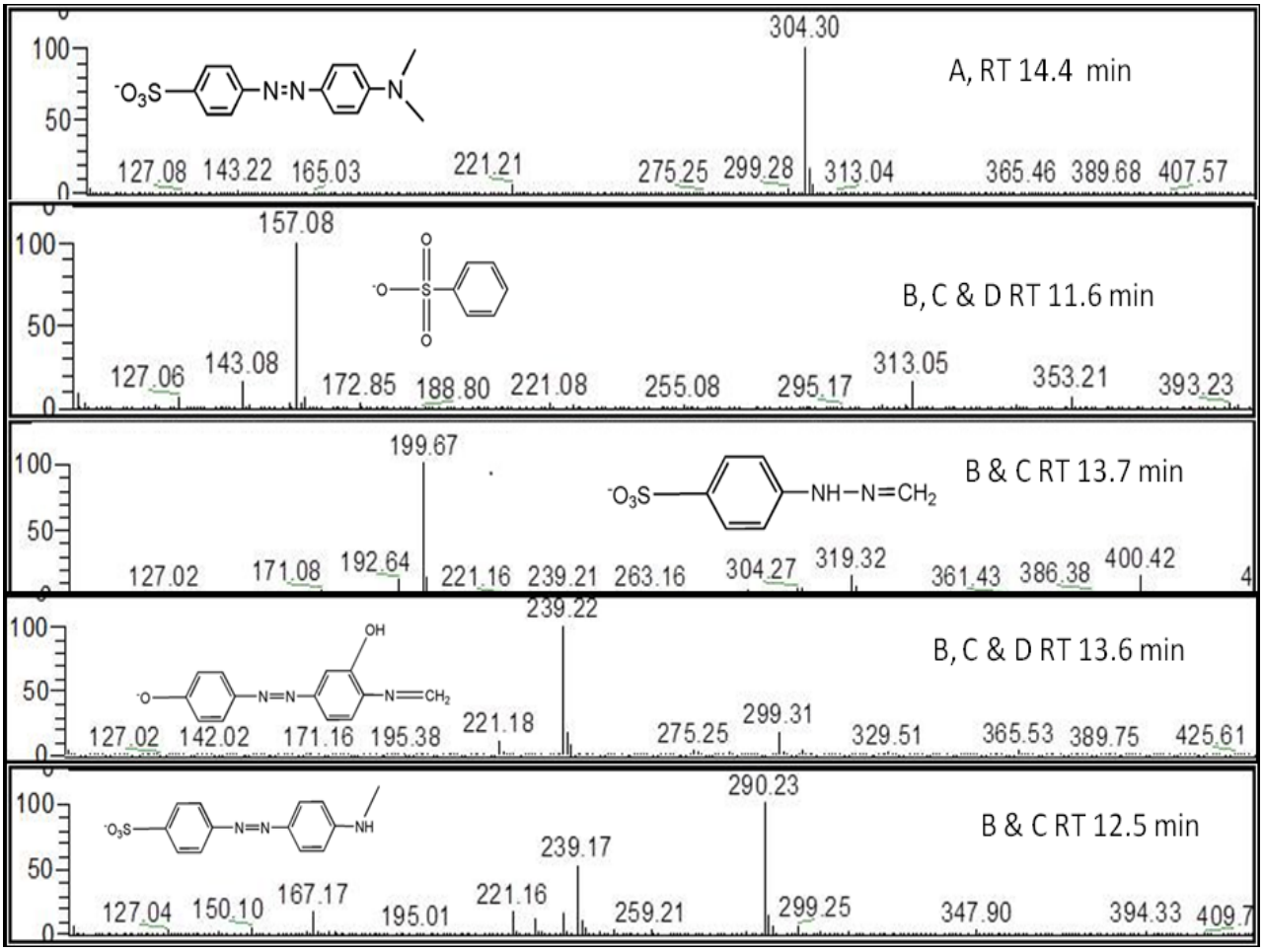

Supplementary Figure 3.1 Mass spectra of some stable intermediates presented in Figure 3.6. A, B, C & D correspond to the TIC of Figure 3.5.

Supplementary Table 3.1 Langmuir adsorption isotherm parameters for adsorption of C1 onto Amberlite and Activated carbon in presence and absence of KPS.

Langmuir Adsorption Isotherm				
Adsorbent	**Adsorbate**	**q_m**	**Ka**	**R^2**
Am	C1 + KPS	6.642	0.062	0.976
Am	C1	123.82	0.002	0.908
AC	C1	380.99	0.003	0.892
AC	C1 + KPS	65.54	0.0363	0.8174

Adsorption Capacity (q_m) = mg/g dry adsorbent; Langmuir constant = 1/n; Correlation coefficient = R^2.

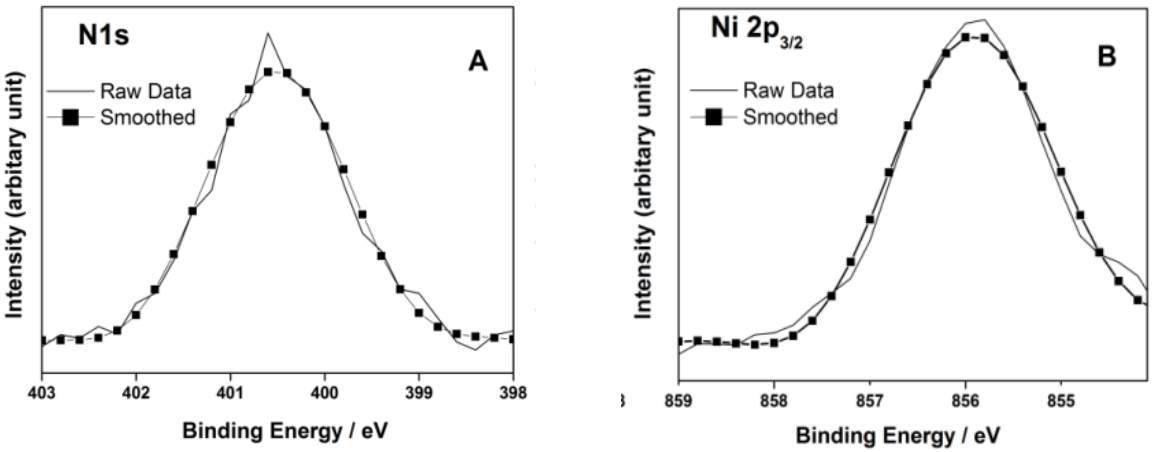

Supplementary Figure 3.2 XPS of C1-Am showing (A) N1s and (B) $Ni2p_{3/2}$ peaks.

Supplementary Table 3.2 Freundlich isotherm parameters for adsorption of MO on to AC and C1-AC.

Freundlich Adsorption Isotherm				
Adsorbent	**Adsorbate**	**K_F**	**n**	**R^2**
Activated Carbon	MO	777.07	2.95	0.985
C1-AC	MO	296.89	3.43	0.986

K_F = Freundlich constant indicative of equilibrium adsorption capacity of the adsorbent ($[mg^{1-(1/n)}.L^{1/n}]/g$); n = Freundlich constant indicative of intensity of adsorption; R^2 = Correlation coefficient.

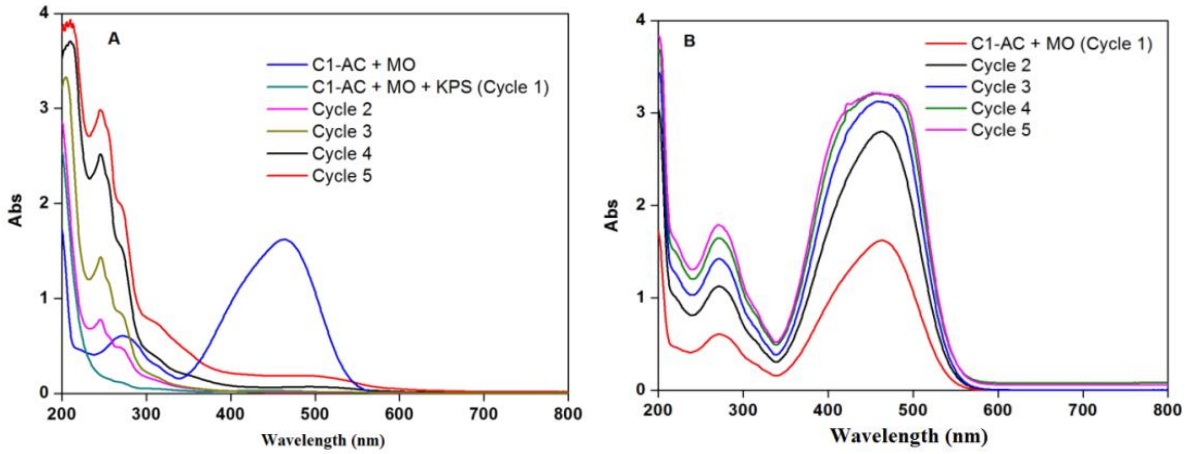

Supplementary Figure 3.3 Absorption spectral changes for the experiment on the cyclic degradation of MO using C1-AC with KPS (A) and without KPS (B).

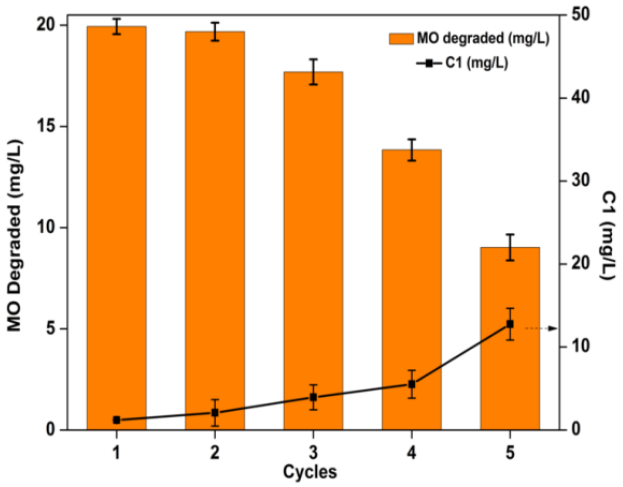

Supplementary Figure 3.4 Cyclic degradation of MO using C1-AC with KPS in simulated natural water. All the other experimental conditions are similar to that of Figure 3.10 B.

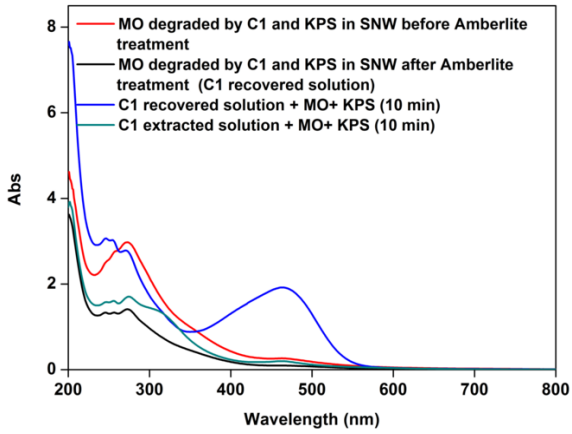

Supplementary Figure 3.5 Recovery and reuse of C1 using Amberlite in SNW (simulated natural water). [MO] = 20 mg/L; [KPS] = 1 g/L; [C1] = 48.3 mg/L; [Amberlite] = 15mg/L.

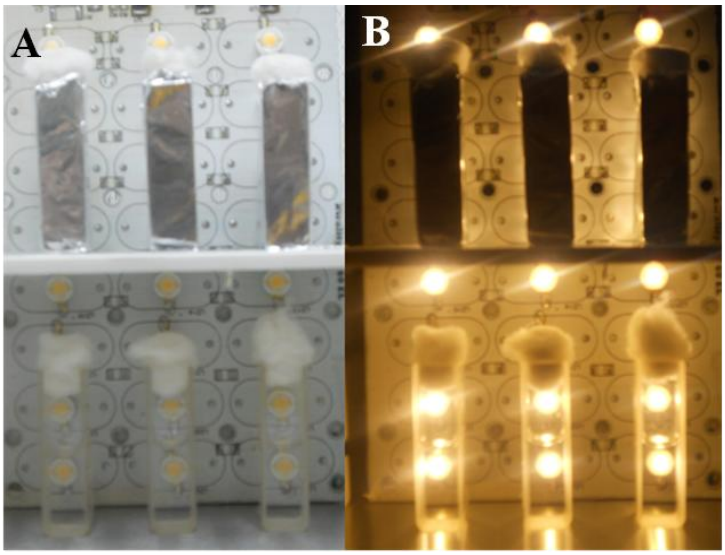

Supplementary Figure 4.1 Photograph of experimental set up of photolysis. Quartz cuvettes containing the reaction mixture are placed at appropriate distance from the array. For dark controls, the reaction vessels are covered with aluminium foil. (A) LED bulbs are switched off (B) LED bulbs are switched on.

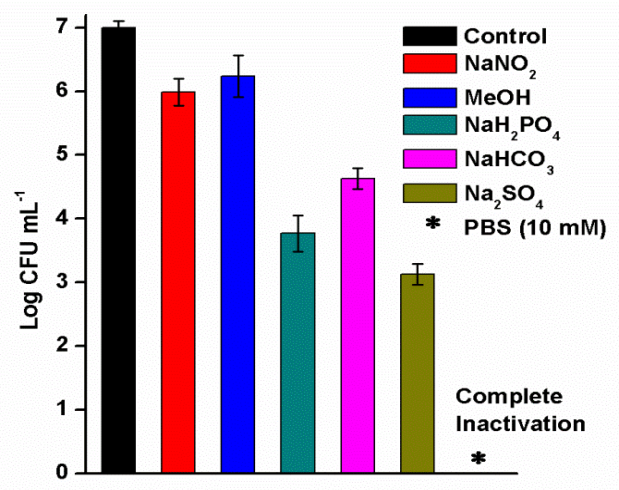

Supplementary Figure 4.2 Cell viability of *E. coli* in the presence of radical scavengers and inorganic salts. Methanol (0.1 M), Sodium nitrite (0.02 M), Na_2HPO_4 (0.1 M), Na_2SO_4 (0.1 M) and $NaHCO_3$ (0.1 M); *E. coli* concentration = ~10^7 CFU mL^{-1}, [persulphate] = 2 mM, [complex1] = 1 µM, Light dosage = 513 Jcm^{-2}.

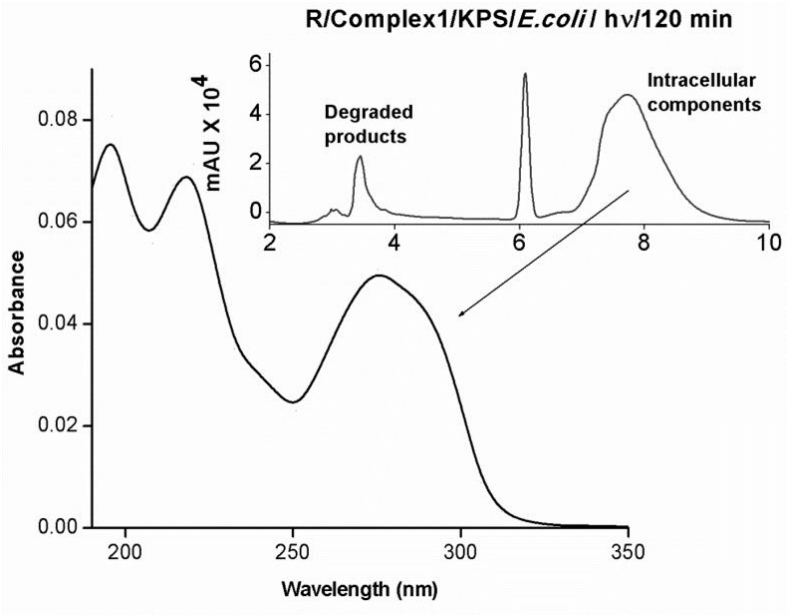

Supplementary Figure 4.3 Absorption spectrum of the peak at RT 7-8 min corresponding to the chromatogram of *E. coli* cells photolysed with complex1 and persulphate in the presence of resorcinol. Inset shows the HPLC profile. *E. coli* concentration = ~10^7 CFU mL^{-1}, [complex1] = 1 µM, [persulphate] = 2 mM, Resorcinol = 10 mgL^{-1} .Light dosage = 684 Jcm^{-2}.

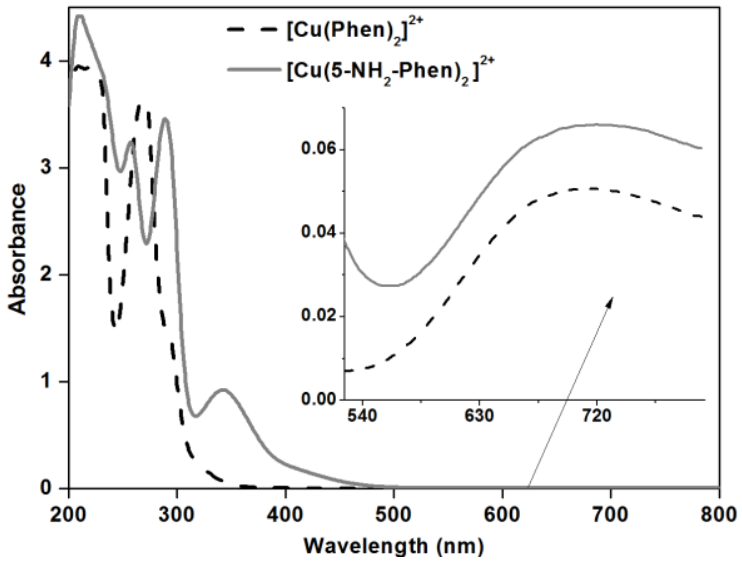

Supplementary Figure 5.1 Absorption spectra of $[Cu(Phen)_2]^{2+}$ and $[Cu(5\text{-}NH_2\text{-}Phen)_2]^{2+}$ in water. Inset shows the absorption spectra of $[Cu(Phen)_2]^{2+}$ and $[Cu(5\text{-}NH_2\text{-}Phen)_2]^{2+}$ due to d-d trasitions.

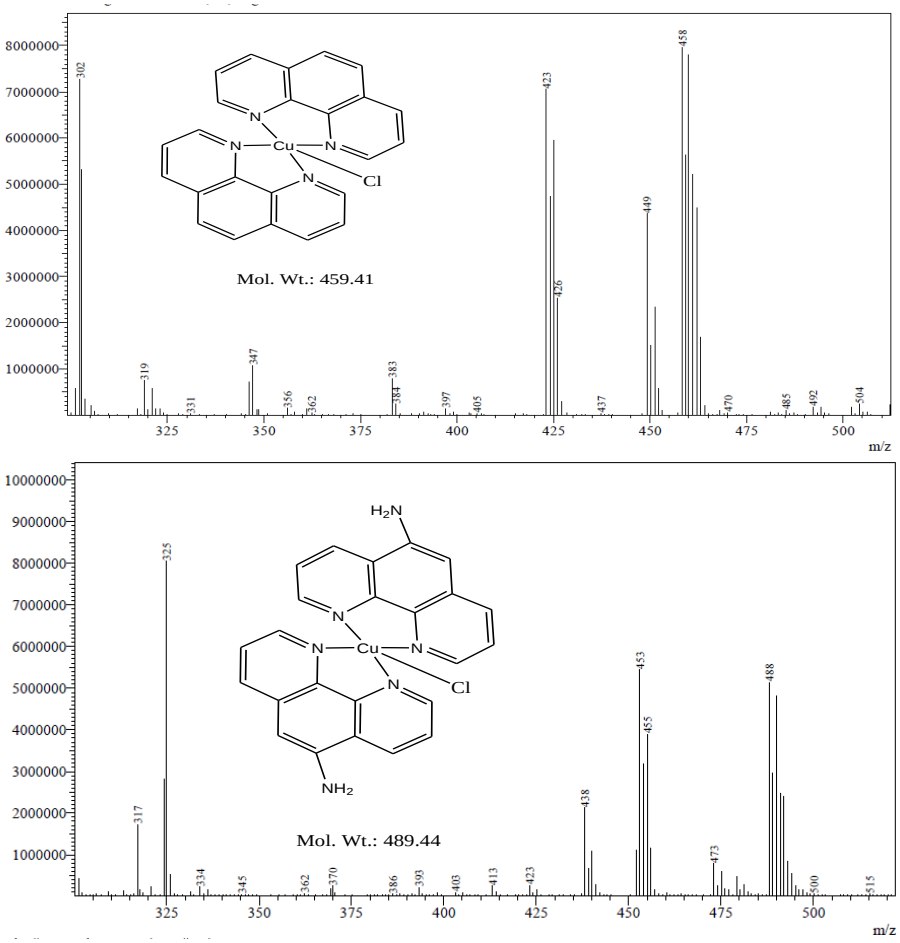

Supplementary Figure 5.2 Mass spectra of $[Cu(Phen)_2]^{2+}$ and $[Cu(5\text{-}NH_2\text{-}Phen)_2]^{2+}$.

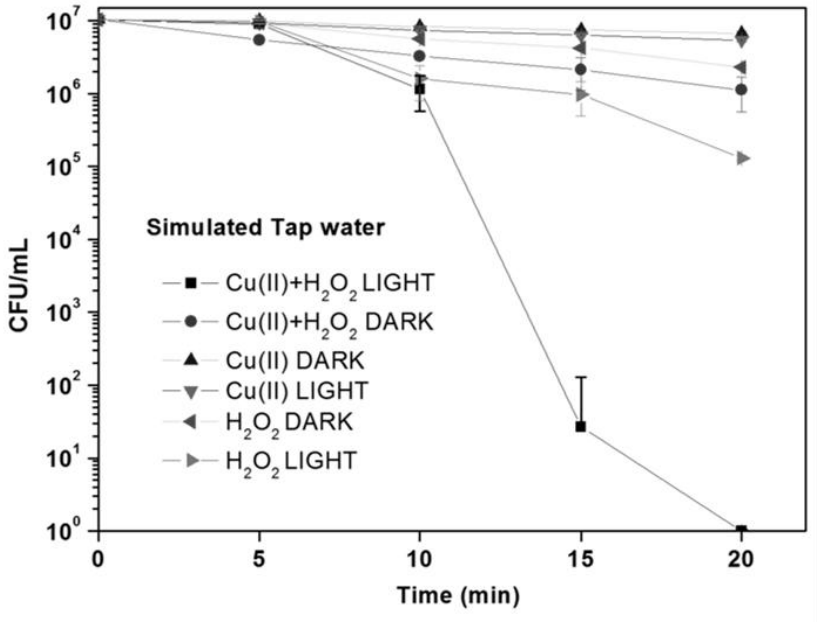

Supplementary Figure 5.3 Cell viability Vs Time plot for photo-inactivation of *E. coli* in simulated tap water. Cell concentration = ~10^7 CFU mL^{-1}, $[H_2O_2]$ = 2 mM, [Cu(II) ions] = 1 µM, Fluence rate = 0.163 Wcm^{-2}. Composition of simulated tap water $[CO_3^{2-}]$= 300 mgL^{-1}, $[Cl^-]$= 250 mgL^{-1}, $[SO_4^{2-}]$= 200 mgL^{-1}, $[NO_3^-]$= 45 mgL^{-1}, Natural organic matter, Humic acid = 1 mgL^{-1}.

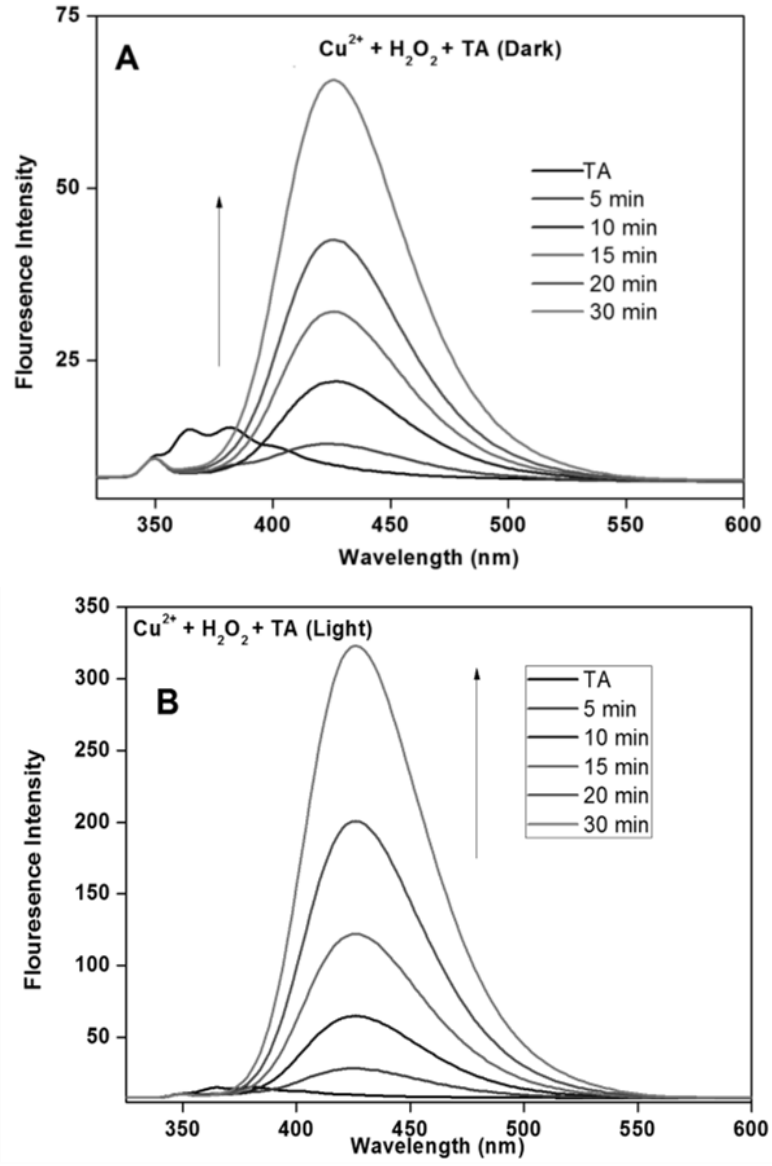

Supplementary Figure 5.4 Fluorescence spectra showing the formation of HTA on reaction of TA with Cu(II) ions and H_2O_2 (A)in absence of irradiation and (B) upon irradiation. [TA] = [200 µM] [H_2O_2] = 2 mM, [Cu(II) ions] = 1 µM, Fluence rate = 0.163 Wcm^{-2}

List of Publications

1. Gokulakrishnan Subramanian, Priyadarshini Parakh, Halan Prakash, Degradation of Malachite green by potassium persulphate, its enhancement by 1,8-dimethyl-1,3,6,8,10,13-hexaazacyclotetradecane nickel(II) perchlorate complex, and removal of antibacterial activity, *Journal of Hazardous Materials,* 2012, 213–214, 19–27. No. of citations = 15.

2. Gokulakrishnan Subramanian, Priyadarshini Parakh, Halan Prakash, Photodegradation of Methyl orange and photoinactivation of bacteria by visible light activation of persulphate using a tris(2,2'bipyridyl)Ru(II) complex, *Photochemistry& Photobiological Sciences,* 2013, 12, 456–466, *Work is featured as cover page article (March issue, 2013).* No. of citations = 7.

3. Priyadarshini Parakh, Gokulakrishnan Subramanian, Halan Prakash,Visible light water disinfection using$[Ru(bpy)_2(phendione)](PF_6)_2.2H_2O$ and $[Ru(phendione)_3]Cl_2.2H_2O$ complexes and their effective adsorption on activated carbon, *Separation and Purification Technology*, 2013, 109, 9–17. No. of citations = 7.

4. Gokulakrishnan Subramanian, Pranav Nalwade, Steven J. Hinder, Suresh C. Pillai, Halan Prakash "Nickel azamacrocyclic complex activated persulphate based oxidative degradation of methyl orange: Recovery and reuse of complex using adsorbents" *RSC Advances*, 2015, 5, 31716-31724. No. of citations = 1.

Conferences attended:

1. Participated, presented and received best poster award in "International Conference on Advanced Oxidation Process – AOP 2014", Munnar, India.

2. Participated and presented poster in International Workshop "Indo-UK Perspective on Water Quality" – by Royal Society of Chemistry, 2013, IISc, Bangalore, India.

3. Participated and presented poster in "International Conference on Advanced Oxidation Process – AOP 2012, Kottayam, India.

4. Participated, presented and received best poster award in National Conference "Recent Advances in Inorganic Chemistry – RAIC 2012, Trichy, India.

Brief Biography of the Candidate

Gokulakrishnan Subramanian
2010PHXF017G
Department of Chemistry, BITS-Pilani K K Birla Goa Campus
NH-17B, Zuarinagar, Goa, India.
E-mail: krisgokul86@gmail.com; p2010017@goa.bits-pilani.ac.in
Phone: 91-9561276122

Education:

Ph. D. (2010-Current) BITS-Pilani K K Birla Goa Campus**,** Goa.

M. Sc. Molecular Biosciences (2007-2009), 1st rank holder (82.4 %), Bishop Heber College, Bharathidasan University, Trichy, Tamil Nadu.

B. Sc. (Hons.) Biosciences, (2004-2007), First class distinction (80 %), Sathya Sai University, Puttaparthi, Andhra Pradesh.

Completed an online course on "Introduction to Water Treatment" conducted by Delft University of Technology, The Netherlands, (2013).

Qualified as Council of Scientific and Industrial Research (CSIR) – Senior Research Fellow (SRF) (2013).

Cleared Council of Scientific and Industrial Research (CSIR) – National Eligibility Test (NET) for Lectureship (2009).

Research Experience:

PhD Student (2010-current), Department of Chemistry, BITS-Pilani K K Birla Goa Campus, Goa. PhD Supervisor: Prof. Halan Prakash, Department of Chemistry.

Junior Research Fellow (2010-2013) in Department of Biotechnology funded project,
Project Title: "Chemical modification of some metal ion binding peptides with photoactive molecules, and investigation on their photoinduced DNA damage and photoenhanced antimicrobial activity",
Project P.I: Prof. Halan Prakash.

Publications and Awards:

Four manuscripts published in peer reviewed journals. Received best poster award in a national and an international conference.

Brief Biography of Ph. D Supervisor

Name: Prof. Halan Prakash
Associate Professor,
Department of Chemistry, BITS-Pilani K K Birla Goa Campus
NH-17B, Zuarinagar, Goa, India.
E-mail: halanprakash@goa.bits-pilani.ac.in.
Phone: +91-832-2580344

Education:
Master's degree (M.Sc, Chemistry) in 1997 from Bharathiar University. India.
Ph.D. (Chemistry) in 2003, Department of Inorganic Chemistry and National Center for Ultrafast Processes at the University of Madras.

Postdoctoral Experience:
2003-2005 - Tata Institute of Fundamental Research (TIFR), India.
2006 Kyoto Pharmaceutical University and NAIST, Japan (JSPS fellowship).

No. of Sponsored Research Projects:
Completed: RGYI DBT (Department of Biotechnology), India.
On-going: ABG (Aditya Birla Group), India, project.

Honours and Awards:
NAIST young scientist visiting fellowship
JSPS fellowship

Publications:
20 research papers, and presented work in more than 30 conferences (international and national level). Received more than 200 citations, and published work as cover article in prestigious Photochemical and Photo-biological Sciences, Royal Society of Chemistry.

Membership:
Member of Royal Society of Chemistry, UK, and Executive member of Society for Environmental Chemistry and Allied Sciences (SECAS), India.

Reviewer for International Journals:
Reviewer for over 10 reputed journals, and received appreciation as an active reviewer from Royal Society of Chemistry, UK.

No. of PhD Students:
Guided one as co-supervisor, and guiding two students as supervisor at BITS-Pilani K K Birla Goa Campus.

Journal of Hazardous Materials 213–214 (2012) 19–27

Contents lists available at SciVerse ScienceDirect

Journal of Hazardous Materials

journal homepage: www.elsevier.com/locate/jhazmat

Degradation of Malachite green by Potassium persulphate, its enhancement by 1,8-dimethyl-1,3,6,8,10,13-hexaazacyclotetradecane nickel(II) perchlorate complex, and removal of antibacterial activity

Subramanian Gokulakrishnan, Priyadarshini Parakh, Halan Prakash *

Department of Chemistry, Birla Institute of Technology and Science, Pilani, K.K. Birla Goa Campus, NH17B, Zuarinagar, Goa 403 726, India

ARTICLE INFO

Article history:
Received 23 April 2011
Received in revised form
31 December 2011
Accepted 10 January 2012
Available online 25 January 2012

Keywords:
Advanced oxidation process
Persulphate activation
Malachite green
Nickel(II) azamacrocyclic complex
Antibacterial activity

ABSTRACT

In this study, degradation of Malachite green (MG) (10 mg/L) by Potassium persulphate (KPS) (1 g/L), and KPS in presence of (1,8-dimethyl-1,3,6,8,10,13-hexaazacyclotetradecane) nickel(II) perchlorate (complex1), (200 μM), was investigated by spectrophotometric and HPLC methods. KPS alone had ability to degrade MG. Interestingly, rate of degradation of MG was enhanced upon addition of complex1. Degradation was effective at pH range of 3–9 and was found to be dependent on initial concentration of KPS, complex1, MG, and pH. Degradation of MG by KPS was not significantly affected in presence of Ni(II) ions whereas in presence of Fe(II) ions degradation was incomplete. Ability of KPS to reduce TOC increased in presence of complex1. Transformation products were analysed by LC–ESI–MS. Finally, treatment of MG with complex1 and KPS resulted in removal of antibacterial activity of MG under *in vitro* conditions.

1. Introduction

Malachite green (MG) is extensively used as a biocide in aquaculture, as colouring agent and additive in food industry, as disinfectant and antihelminthic in medical field, and also as dye in textile, paper and acrylic industries [1]. Despite its wide applications, use of MG has been banned in several countries and it is not approved by the US Food and Drug Administration [2] due to its harmful effects on immune system, reproductive system as well as its genotoxic and carcinogenic properties [3,4]. However, it is still being used in many parts of the world due to its low cost, ready availability and efficacy.

Moreover, MG is also environmentally persistent and poses potential environmental problems. MG has a strong absorption band in visible light region and when released in to water bodies could reduce transmission of solar light thereby affecting aquatic biota of the habitat. Thus, effective removal of MG from water bodies is environmentally very significant.

Conventional biological treatment processes [5,6], as well as biological decolourization of MG and related dyes using a batch and continuous system have been reported [7]. Microorganisms such as *Kocuria rosea*, *Cyathus bulleri* have been shown to degrade MG with efficiency more than 90%. However, these strategies were found to be time consuming, and require proper care for maintenance of microorganisms.

On the other hand, advanced oxidation processes (AOP's) are promising in development of treatment of wastewater, which are based on use of reactive oxidizing radicals that could rapidly degrade a variety of organic contaminants [8–12]. AOP's are not only less time consuming for effective degradation, they have added advantages like cost effectiveness, easy to treat, and usually do not produce toxic compounds during oxidation. Common oxidants used for AOP's include Permanganate, H_2O_2 (Fenton-like reactions), and Ozone [8].

Persulphate oxidation chemistry is an emerging technology in the field of AOP's to degrade organic contaminants [8,13,14]. Persulphate is relatively stable like permanganate. Moreover, it could be activated to generate reactive sulphate radicals and secondary radicals like OH•, similar to activation of H_2O_2 to produce radicals for degradation of a wide range of contaminants [13]. Thus, persulphate remains impressive because it offers advantages of both permanganate and H_2O_2 [13].

Thermal activation [14,15], UV-irradiation [14,15], base activation [16] and activation by transition metal catalysis [17] have been used to activate persulphate to generate reactive $SO_4^{\bullet -}$ radicals. Activation of persulphate by metal ion catalysis occurs by an

* Corresponding author. Tel.: +91 832 2580344; fax: +91 832 2557033.
E-mail addresses: halanprakash@bits-goa.ac.in, halanprakash@gmail.com (H. Prakash).
URL: http://universe.bits-pilani.ac.in/goa/halanprakash/Profile (H. Prakash).

0304-3894/$ – see front matter © 2012 Elsevier B.V. All rights reserved.
doi:10.1016/j.jhazmat.2012.01.031

oxidation – reduction reaction in which low valent metal ions M^{n+} act as electron donors (Reaction (1)) [14,15].

$$S_2O_8^{2-} + M^{n+} \rightarrow SO_4^{\bullet -} + SO_4^{2-} + M^{n+1} \quad (1)$$

Sulphate radicals produced during activation of persulphate initiates a cascade of reactions leading to formation of intermediate oxidants (H_2O_2, HSO_5^-) and reactive hydroxyl radicals, as shown in reactions (2)–(4), [18] which could effectively degrade a variety of organic contaminants.

$$SO_4^{\bullet -} + H_2O \rightleftharpoons HO^{\bullet} H^+ + SO_4^{2-} \quad (2)$$

$$SO_4^{\bullet -} + HO^{\bullet} \rightarrow HSO_5^- \quad (3)$$

$$2HO^{\bullet} \rightarrow H_2O_2 \quad (4)$$

Moreover, macrocyclic polyamine ligands such as tetra-, penta-, hexa-, azamacrocycles are extensively studied, and they generate continuous interest because of their biological properties and rich metal co-ordination chemistry [19,20]. A variety of azamacrocyclic complexes with nickel as metal ion are reported to exhibit different redox properties [21–24]. Earlier, Haines et al., has reported that persulphate could oxidize nickel tetra and penta azamacrocyclic complexes and this oxidation reaction occurs through an ion-pair mechanism leading to generation of reactive sulphate radicals and stable trivalent nickel species (reactions (5) and (6)) [25]. Moreover, trivalent nickel species are also known to act as strong oxidants [26].

$$[Ni(II)L]^{2+} + S_2O_8^{2-} \underset{\text{ion-pair}}{\{Ni(II)L^{2+}, \quad S_2O_8^{2-}\}} \quad (5)$$

$$\{Ni(II)L^{2+}, S_2O_8^{2-}\} \rightarrow [Ni(II)L]^{3+} + SO_4^{\bullet -} + SO_4^{2-} \quad (6)$$

L, Azamacrocyclic ligand.

Based on above facts, we envisaged that persulphate, and persulphate in presence of nickel azamacrocyclic complex could be useful for degradation of MG. AOP's such as Ozonation [27], Photocatalyst assisted degradation [28,29] Fenton processes [30], Photodegradation by UV/H_2O_2 [31] and Microwave assisted photocatalytic degradation [32] have been explored for degradation of MG, emphasizing the need of alternative methods for degradation of MG. However, activation of persulphate by nickel azamacrocyclic complex and its effect on MG has not been studied.

Present report is focused on study of effect of (i) Potassium persulphate (KPS) oxidation, (ii) (1,8-dimethyl-1,3,6,8,10,13-hexaazacyclotetradecane) nickel(II) perchlorate (complex1), (Fig. 1) and KPS oxidation system and (iii) Transition metal ions [Ni(II)/Fe(II)] and KPS oxidation system on degradation of MG by spectrophotometric as well as high pressure liquid chromatographic (HPLC) methods. The effect of various parameters such as initial oxidant concentration, catalyst concentration, dye concentration and pH was studied. We also examined antibacterial activity of MG after its degradation by KPS and complex1 oxidation system. Change in total organic carbon (TOC) was analysed. Degradation intermediates were identified by liquid chromatography electrospray ionization mass spectrometry (LC–ESI–MS), and possible degradation pathway was proposed.

2. Materials and methods

2.1. Reagents

$NiCl_2{\cdot}6H_2O$, $FeSO_4{\cdot}7H_2O$, $K_2S_2O_8$, H_2SO_4, NaOH of guaranteed analytical grade from SD fine chemicals, India were used. Malachite green (MG) was obtained from Hi media, India. Complex1 was prepared and purified according to earlier report [33]. Care must be taken as large amount of perchlorate salts could be explosive [33]. For HPLC analysis, acetonitrile (HPLC grade) and Millipore water

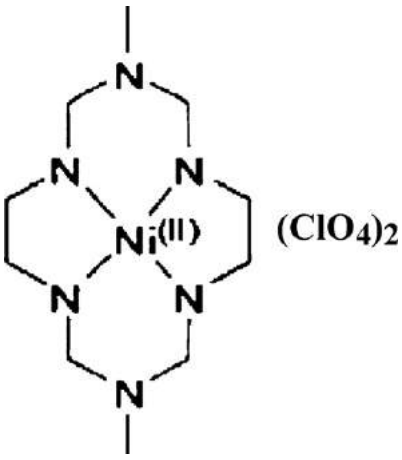

Fig. 1. Complex1 (1,8-dimethyl-1,3,6,8,10,13-hexaazacyclotetradecane), nickel(II) perchlorate.

were used. Ammonium acetate buffer (pH 4.5) was prepared as reported earlier [32].

2.2. Experimental procedure

Stock solutions of MG (0.97 g/L) and complex1 (8.3 mM) were prepared using double distilled water. Freshly prepared KPS solution was used for all experiments. These stock solutions were diluted to get solutions of desired concentrations. For all experiments, MG (10 mg/L), KPS (1 g/L) and complex1 (200 μM) were used unless otherwise specified. All reactions were carried out at $27 \pm 2\,^{\circ}C$ at pH 7 unless specified. pH was adjusted to desired value with help of pH meter (EU Tech) by adding 0.1N H_2SO_4 or NaOH.

Decolourization of MG was monitored spectrophotometrically using JASCO V-570 UV/VIS/NIR. A reaction mixture of 2 mL was prepared by adding appropriate volumes of stock solutions of MG and KPS. KPS stock solution was added to MG and mixed thoroughly using a micropipette for 25 s, and then change in absorption spectrum was recorded at different time intervals. Similarly, for measuring change in absorbance in presence of complex1, reaction mixture (2 mL) contained complex1 in addition to MG and KPS.

Kinetics of degradation of MG was studied by monitoring decrease in absorbance at 618 nm every 10 s, after an initial delay of 25 s (time taken to mix the reactants thoroughly) [34]. This initial delay was maintained uniformly in all experiments. Change in absorbance at 618 nm was fitted to first order equation (mono-exponential decay) to obtain rate constants of decolourization of MG. Origin lab 6.1 software was used for all kinetic analysis.

Kinetic experiments were carried out with different concentrations of KPS and complex1, to investigate effect of initial concentration of KPS and complex1, respectively. Effect of pH on degradation of MG by KPS and KPS in presence of complex1 was studied at different pH (3, 7 and 9). Effect of Ni(II) and Fe(II) metal ions on degradation of MG by KPS was also studied at pH (3, 7 and 9). Effect of initial concentration of MG (10 mg/L and 30 mg/L) by KPS and KPS in presence of complex1 was studied using HPLC. In all spectrophotometric measurements, concentration of MG was maintained at 10 mg/L because concentration more than 10 mg/L caused saturation of absorbance.

2.3. HPLC analysis

Degradation of MG was studied by high-performance liquid chromatography (HPLC), using Shimadzu UFLC, equipped with

a phenomenex C18 HPLC column (250 mm × 4.5 mm, 5 μm) and SPDM 20A Prominence diode array detector. The measurement was performed with 20:80 (v/v) ammonium acetate buffer (pH 4.5)/acetonitrile as mobile phase in isocratic mode with flow rate of 1 mL/min. For each analysis, 100 μL of sample was injected and chromatogram was monitored at 618 nm.

2.4. Microbial assays

Microbial assays were performed according to standard literature procedures [35,36]. Sterile distilled water was used. Reaction mixture (1 mL) containing MG (20 mg/L), KPS (2 g/L) and complex1 (400 μM) was prepared by adding appropriate volumes of respective stock solutions. This solution was mixed thoroughly and kept undisturbed for 60 min. After 60 min, 1 mL of 2X NB was added to the above solution followed by addition of *E. coli* cells (~10^6). The contents were mixed well and incubated in a shaking incubator for overnight at 37 °C. Similar procedure was followed for control experiment except that reaction mixture contained only 1 mL MG (20 mg/L). 0.1 mL of above culture suspensions were spread plated on nutrient agar plates followed by overnight incubation at 37 °C. Above microbial assay consisted of two replicates.

2.5. TOC analysis

TOC was measured using Shimadzu TOC-V_{CSH} analyser with a nondispersive infrared (NDIR) detector. For TOC analysis, an aliquot of 20 mL was taken at specific time intervals from reaction mixture (100 mL) containing appropriate concentration of MG, KPS and complex1 [27].

2.6. LC–ESI–MS analysis

LC–ESI–MS analysis was performed using Thermo Finnigan LCQ Deca LC/MS/MS Electrospray quadrupole ion trap mass spectrometer. Surveyor LC was equipped with a C-18 column (150 mm × 2 mm). The measurement was performed in acetonitrile/water = 60:40 (v/v) as mobile phase with flow rate of 0.3 mL/min and injection volume of 5 μL. MG solution and MG solution treated with KPS and complex1 for 1 h was injected for analysis. Nitrogen was used as sheath and auxiliary gas. Ion source conditions were; sheath gas flow rate ~7.5 L/min. Capillary temperature was maintained at 200 °C and capillary voltage was kept at 15 V. Ion-spray voltage and tube lens offset were maintained at +4.5 kV and −7 V respectively. Normalized collusion energy was varied from 30% to 60% for fragmentation profile, and other parameters were similar to earlier report [37].

3. Results and discussion

Absorption spectra of MG showed three main peaks with absorption maxima at 618, 425 and 315 nm (Fig. 2a). Absorbance of these bands decreased upon addition of KPS to MG with a significant decrease in absorbance at 618 nm, and became almost zero at ~60 min (Fig. 2a). At 60 min, a new weak peak with absorption maximum around 365 nm was observed. These spectral changes revealed the ability of KPS to degrade MG. Earlier, disappearance of absorption band (500–700 nm) with peak at 618 nm was monitored to study degradation of MG by various methods [30–32].

HPLC chromatogram of MG monitored at 618 nm showed a single sharp peak with retention time (RT) at 4 min, which corresponds to MG (Fig. 2b) [32]. A very weak peak was also detected at RT 3.5 min, which could be due to trace impurities. Addition of KPS to MG resulted in decrease of intensity of these peaks, and formation of new peak with RT at 1.8 min (Fig. 2b). MG

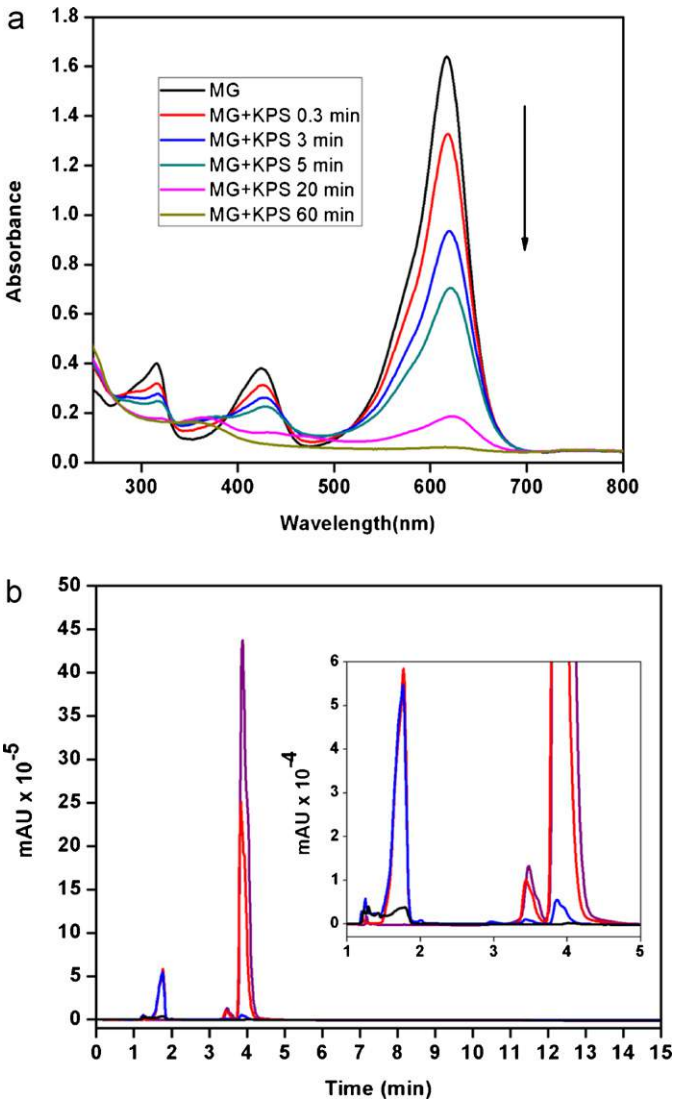

Fig. 2. (A) Absorption spectrum of MG (10 mg/L) after addition of KPS (1 g/L) at different time intervals. (B) HPLC chromatogram (618 nm) of MG (10 mg/L) after addition of KPS (1 g/L) at different time intervals. Colours: Violet – only MG, Red – 5 min, Blue – 20 min, Black – 60 min. (For interpretation of the references to colour in this figure legend, the reader is referred to the web version of this article.)

peak at 4 min completely disappeared after 60 min, while peak at RT 1.8 min was reduced to negligible level (Fig. 2b, inset). HPLC results clearly showed that KPS has ability to decompose MG to other species, leading to degradation. Earlier, it has been reported that peak at 1.8 min correspond to N-demethylated MG species, which are known to have absorbance around 594, 608 and 618 nm [32].

Absorption spectral changes of MG observed after addition of both KPS and complex1 showed a rapid decrease in absorption at 618 nm within 20 min (Fig. 3a). Moreover, after 60 min, a shoulder around 450 nm and also a peak around 290 nm were observed (Fig. 3b), which corresponds to trivalent nickel species formed due to reaction between KPS and complex1, as reported earlier [25]. The corresponding HPLC profiles monitored at 618 nm also revealed that MG, as well as, N-demethylated species with absorption around 618 nm were degraded within 20 min on addition of KPS with complex1 (Fig. 3b). Interestingly, rate of degradation of MG by KPS increased nine times higher in presence of complex1 than rate of degradation of MG by KPS alone (Table 1 and Fig. 4).

Table 1
Rate constants determined for degradation of MG by KPS under various conditions.

Reaction	KPS (g/L)	Complex1 (μM)	pH	Rate constants (min^{-1})
MG + KPS	1	–	7	0.11 ± 0.01
MG + KPS	1	–	3	0.20 ± 0.01
MG + KPS	1	–	9	0.23 ± 0.02
MG + KPS	1.5	–	7	0.14 ± 0.01
MG + KPS	2	–	7	0.19 ± 0.02
MG + KPS + complex1	1	200	7	0.93 ± 0.05
MG + KPS + complex1	1	200	3	0.59 ± 0.02
MG + KPS + complex1	1	200	9	0.63 ± 0.03
MG + KPS + complex1	1	50	7	0.71 ± 0.03
MG + KPS + complex1	1	10	7	0.25 ± 0.01
MG + KPS + Ni(II)[a]	1	–	7	0.12 ± 0.01
MG + KPS + Ni(II)[a]	1	–	3	0.14 ± 0.01
MG + KPS + Ni(II)[a]	1	–	9	0.11 ± 0.01
MG + KPS + Fe(II)[a]	1	–	3, 7, 9	Not determined[b]

Initial MG concentration for the above reactions is 10 mg/L.
[a] 200 μM.
[b] Reaction incomplete.

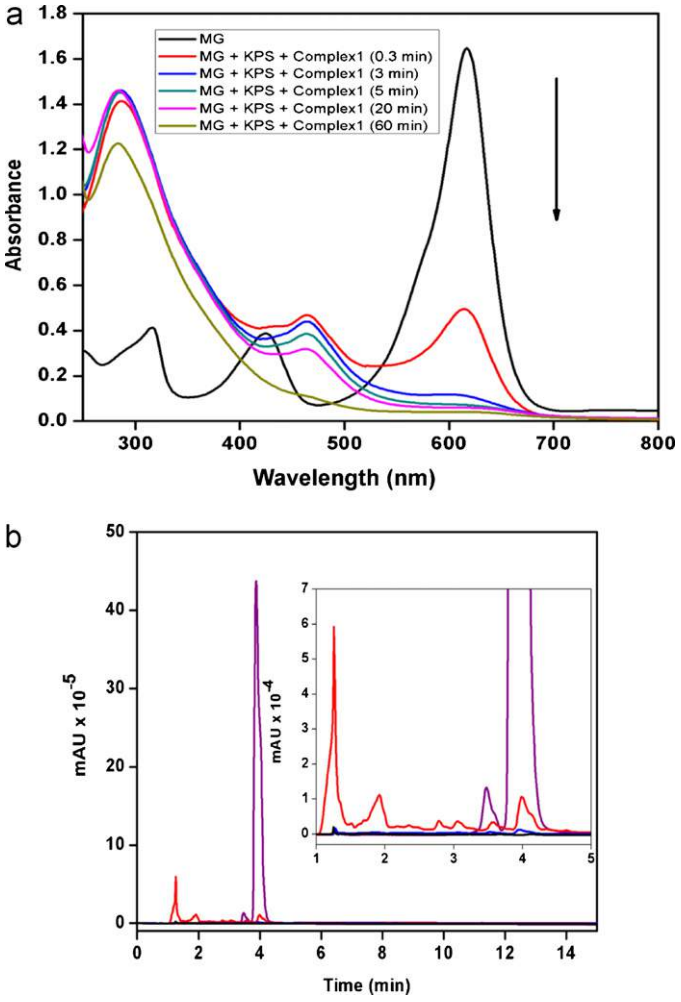

Fig. 3. (A) Absorption spectrum of MG (10 mg/L) after addition of KPS in presence of complex1 at different time intervals. (B) HPLC chromatogram (618 nm) of MG (10 mg/L) after addition of KPS in presence of complex1 (200 μM) at different time intervals. Colours: Violet – only MG, Red – 5 min, Blue – 20 min, Black – 60 min. (For interpretation of the references to colour in this figure legend, the reader is referred to the web version of this article.)

3.1. Effect of initial concentration of KPS and complex1

Rate of degradation of MG was found to increase on increasing concentration of KPS (Table 1 and Fig. 5a). On increasing the concentration of KPS, more reactive radicals could be generated and rate of MG degradation could become faster. Similar trend was observed for photochemical oxidation of Arsenic using persulphate [38].

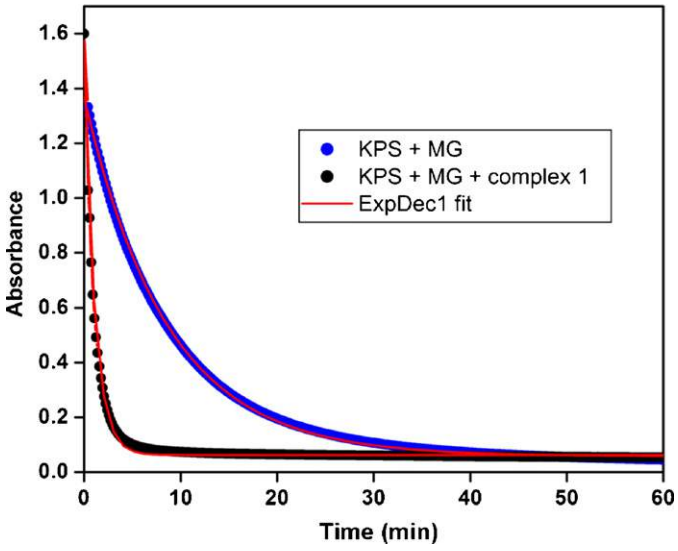

Fig. 4. Degradation of MG (10 mg/L) by KPS (1 g/L) in presence and absence of complex1 (200 μM) ExpDec1 fit (mono exponential decay).

Rate of degradation of MG by KPS in presence of complex1 (50–200 μM) was not significantly changed (Table 1 and Fig. 5b). However, on decreasing concentration of complex1 to as low as 10 μM, rate constant was decreased approximately four times. These results indicated that an optimum concentration of complex1 was required for effective decomposition of KPS and generation of reactive radicals for degradation of MG.

3.2. Effect of pH

Rates of degradation of MG at pH 3 and 9 were found to be almost similar, and slightly higher than at pH 7 (Table 1 and Fig. 6a). It is known that decomposition of KPS is enhanced by acid catalysis [39]. Moreover, base such as sodium hydroxide is also known to activate decomposition of persulphate [16]. Increase in rate of degradation of MG by KPS at pH 3 and 9 in present study was due to acid catalysis and base activation of KPS, respectively.

Rapid redox reaction between KPS and complex1 generates reactive sulphate radicals as well as trivalent nickel species, which

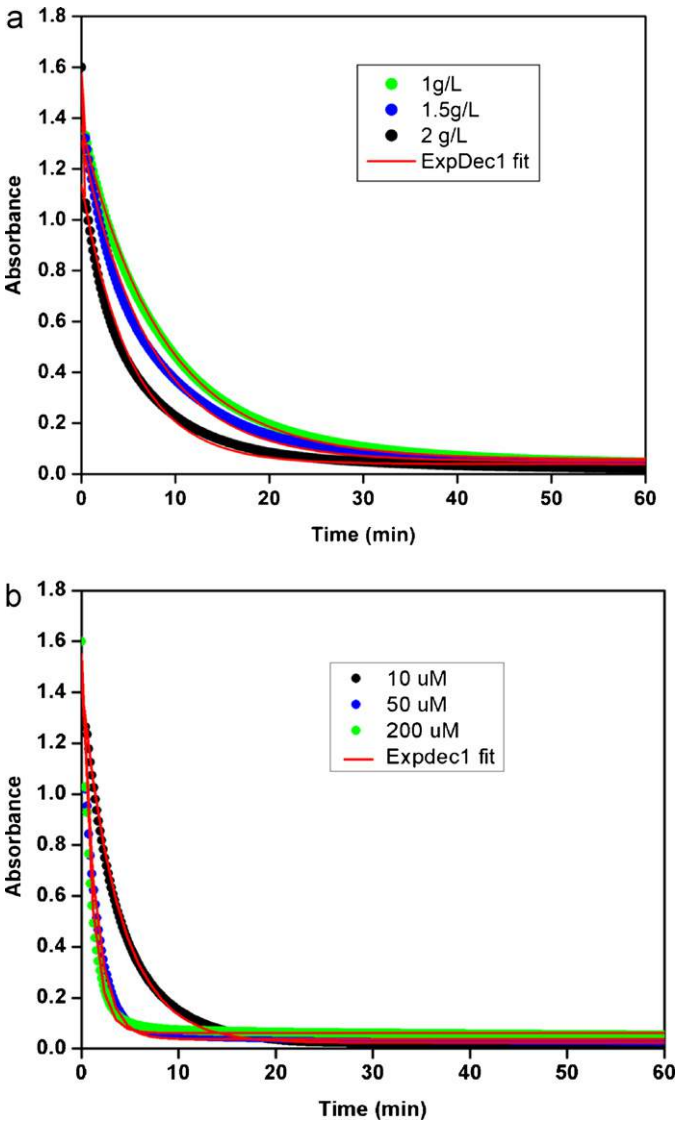

Fig. 5. (A) Degradation of MG (10 mg/L) with different concentrations of KPS. (B) Degradation of MG (10 mg/L) by KPS (1 g/L) in presence of different concentrations of complex1.

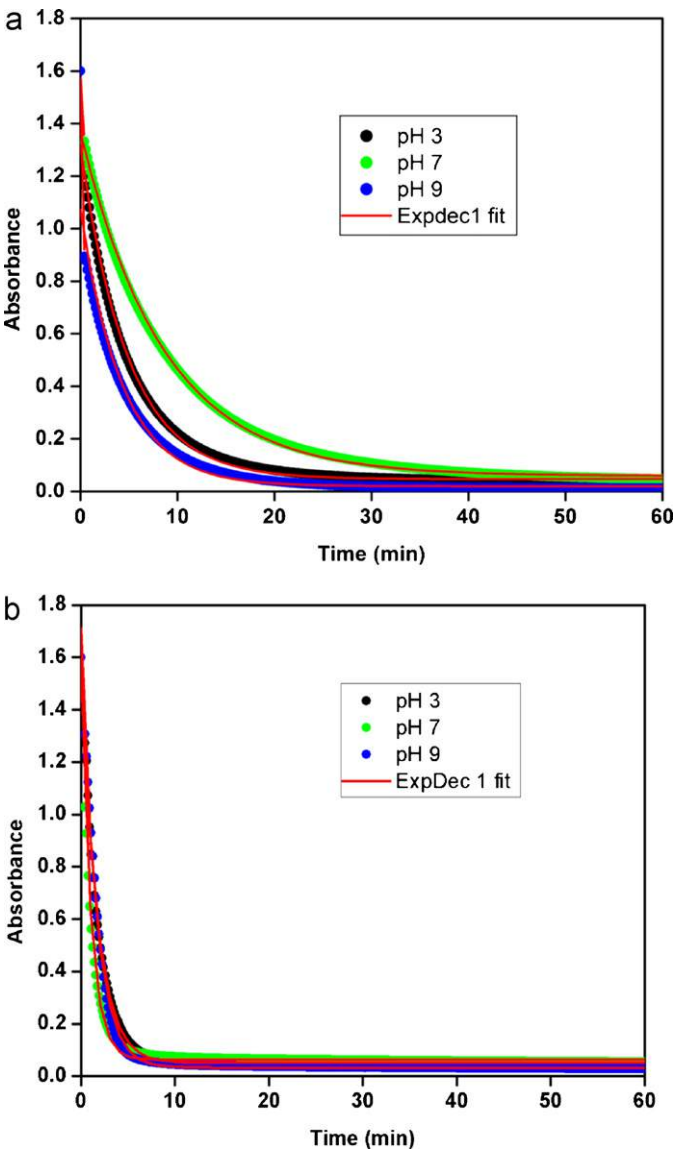

Fig. 6. (A) Degradation of MG (10 mg/L) by KPS (1 g/L) at various pH values. (B) Degradation of MG (10 mg/L) by KPS (1 g/L) in presence of complex1 (200 μM) at various pH values.

were reported to be strong oxidizing agents [25,26]. Therefore, degradation of MG by KPS became rapid in presence of complex1. Present results also show that degradation of MG by complex1-activated KPS was faster and more efficient than KPS activated by acid catalysis or base.

Rates of degradation of MG by KPS in presence of complex1 at pH 3 and 9 were found to be almost similar, and slightly lower at pH 7 (Table 1 and Fig. 6b). Earlier, it has been suggested that trivalent nickel species act as effective catalyst for oxidation process in aqueous neutral media and slightly alkaline media than under acidic condition, and the present results are in accordance with these reports [26]. Moreover, stability of trivalent nickel species is dependent on pH, nature of ligands and type of axial coordinating ions [26,39,40]. It is known that stability of trivalent species is highest in acidic, lowest in alkaline and intermediate in neutral conditions [26,40,41], indicating that trivalent nickel species are highly stabilized under acidic conditions and not favourable for oxidation reactions. It is important to note that, although there was a variation in rate of degradation of MG by KPS in presence of complex1 at pH range 3–9, advantage of KPS – complex1 mediated degradation of MG is that, MG is degraded effectively over a broad range of pH.

3.3. *Effect of initial concentration of MG*

HPLC chromatogram obtained for degradation of MG (30 mg/L) by KPS after 60 min of treatment showed peaks with RT at 1.8 and 4 min, which corresponds to N-demethylated species and MG, respectively (Fig. 7). However, HPLC chromatogram obtained for degradation of MG (10 mg/L) by KPS after 60 min of treatment showed that peak at RT 1.8 min was very weak and peak at RT 4 min almost disappeared. Thus, the results showed that as initial concentration of dye was increased, efficiency of degradation of MG, as well as N-demethylated species by KPS (1 g/L) was reduced. Similar trend was also observed for degradation of MG on increasing initial concentration of MG from 10 mg/L to 30 mg/L, by KPS in presence of complex1 (Fig. 7). Degradation of MG by KPS is associated with concentration of reactive radicals in solution. On increasing the initial dye concentration, degradation became incomplete due to less availability of reactive radicals in solution [38]. However, overall degradation of MG (10 mg/L and 30 mg/L) by KPS is more effective in presence of complex1 than by KPS alone.

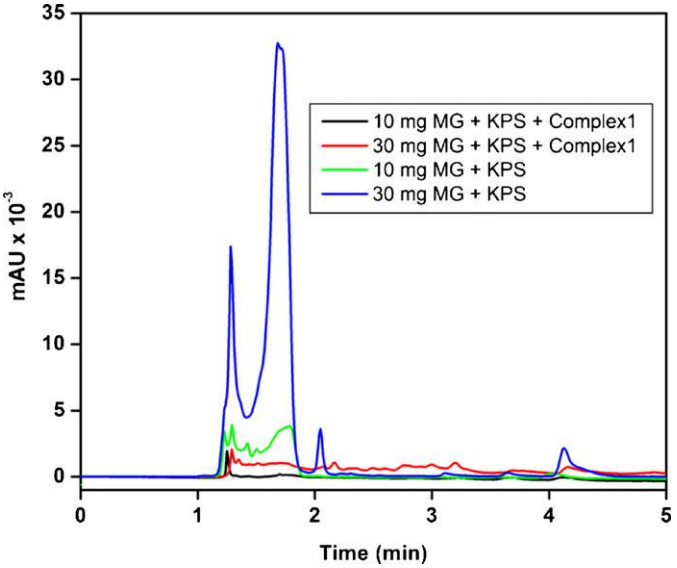

Fig. 7. HPLC chromatogram (618 nm) of MG (10 mg/L and 30 mg/L) after addition of KPS (1 g/L) in absence and presence of complex1 (200 μM).

3.4. Effect of nickel(II) and iron(II) ions

Rate of degradation of MG by KPS in presence of Ni(II) (200 μM) at pH 3–9 was similar to rate of degradation of MG by KPS alone (Table 1). On the other hand, degradation of MG by KPS in presence Fe(II) (200 μM) at pH 3–9 showed relatively higher absorbance at 618 nm (Fig. 8a), indicating that degradation was not efficient. Moreover, HPLC chromatogram showed a peak at 4 min corresponding to MG, and peaks at 1.8 min and 3.5 corresponding to N-demethylated species produced during degradation (Fig. 8b) [32]. These results clearly showed that, in presence of Fe(II), both MG and N-demethylated species are not effectively degraded compared to degradation of MG by KPS in presence of complex1.

On the basis of decrease in absorption at 618 nm and disappearance of MG peak with RT at 4 min in LC chromatogram, order of degradation of MG under mentioned experimental conditions is as follows:

KPS: ferrous sulphate < KPS: nickel chloride < KPS < KPS: complex1

Effect of various parameters observed for degradation of MG by KPS and by KPS in presence of complex1 followed a similar trend as observed for degradation of MG by Fenton processes [30] and Ozonation [27]. However, it is important to note that present results showed that degradation of MG by KPS and by KPS in presence of complex1 was effective over a wide pH range (3–9) while Fenton processes as well as Ozonation process were mainly effective under acidic conditions.

3.5. Total organic carbon analysis

TOC analysis results showed that treatment of MG (20 mg/L) with KPS (2 g/L) alone could reduce 7% of TOC whereas treatment of MG (20 mg/L) with KPS (2 g/L) along with complex1 (400 μM) could remove 11% of TOC within 3 h (Fig. 9). This shows that treatment of MG with KPS alone and KPS with complex1 not only results in degradation of MG but also in reduction of TOC.

3.6. Antimicrobial activity of MG before and after degradation

E. coli cells suspended in NB containing MG (untreated) were incubated overnight, and solution was found to be clear (Fig. 10a). This solution when spread plated on NB agar and incubated

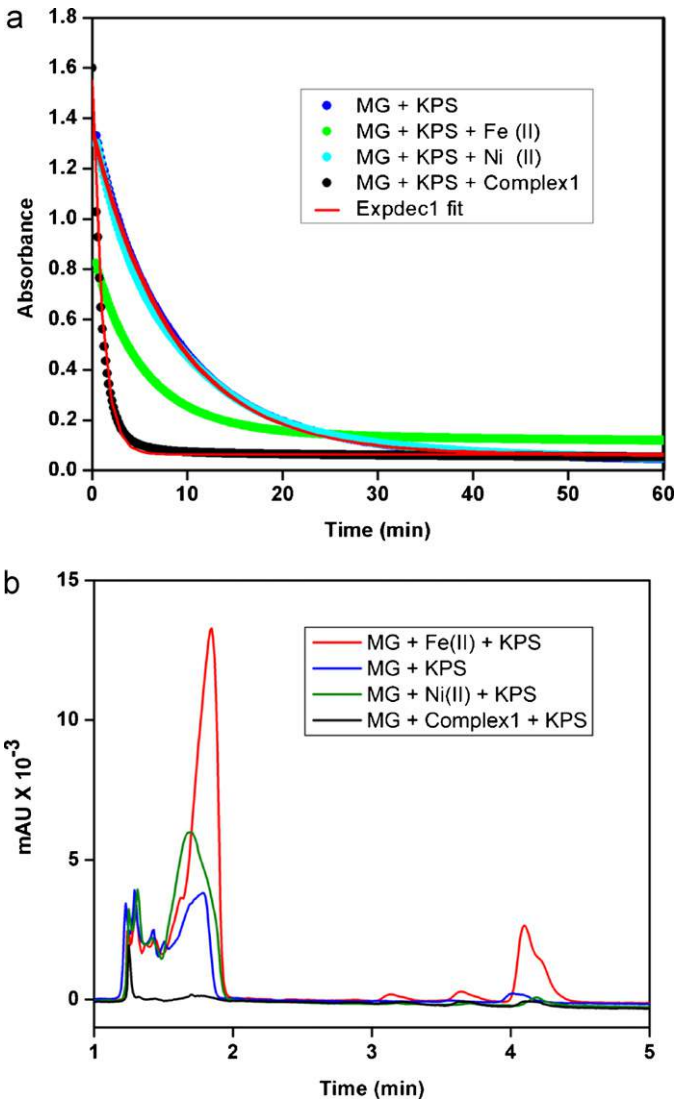

Fig. 8. (A) Degradation of MG (10 mg/L) by KPS (1 g/L) in absence and presence of complex1 (200 μM); Fe (II) (200 μM) and Ni(II) (200 μM). (B) HPLC chromatogram of MG (10 mg/L) after addition of KPS in absence and presence of complex1 (200 μM); Fe (II) (200 μM) and Ni(II) (200 μM) after 60 min.

overnight, did not show formation of any bacterial colonies (Fig. 10b), which clearly revealed that MG alone is toxic to bacteria. On the other hand, when *E. coli* cells were suspended in NB, containing degraded MG (after treatment with KPS in presence of complex1 for 60 min), solution was found to be turbid (Fig. 10c). This solution when spread plated and observed after overnight incubation, displayed formation of numerous bacterial colonies (matt growth) (Fig. 10d). Similarly, control experiments which were carried out in absence of MG also showed matt growth (Fig. 10e and f). Thus, above results indicated that KPS and complex1 system has propensity to reduce antibacterial activity of MG drastically under *in vitro* conditions. Earlier, it has been shown that degradation of MG by ozonation processes [27] and decolourization of MG by dye-decolourizing bacterium (*Shewanella decolorationis* NTOU1) [42] showed reduction in antibacterial activity.

3.7. Mass spectral analysis of MG and its degradation intermediates

MG solution showed a single peak in TIC plot, and its corresponding mass spectrum had a clear peak with 329 *m*/*z* (S.I. Fig. 1).

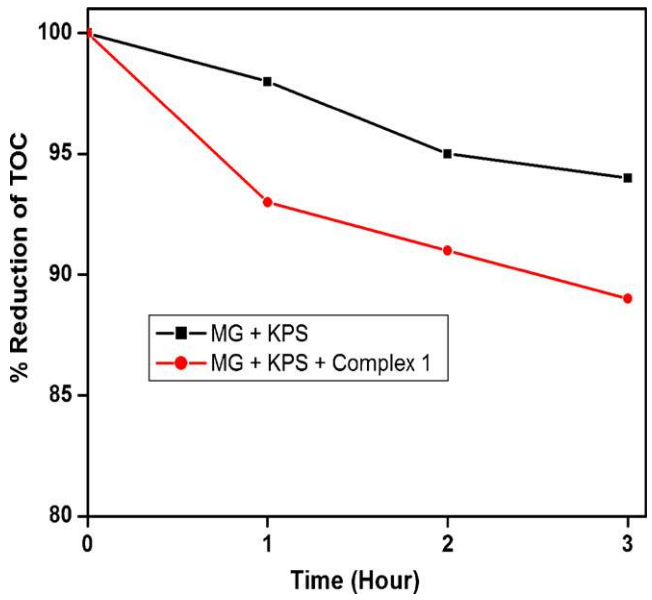

Fig. 9. TOC reduction (%) of MG (20 mg/L) after the treatment with KPS (2 g/L) in absence and presence of complex1 (400 μM).

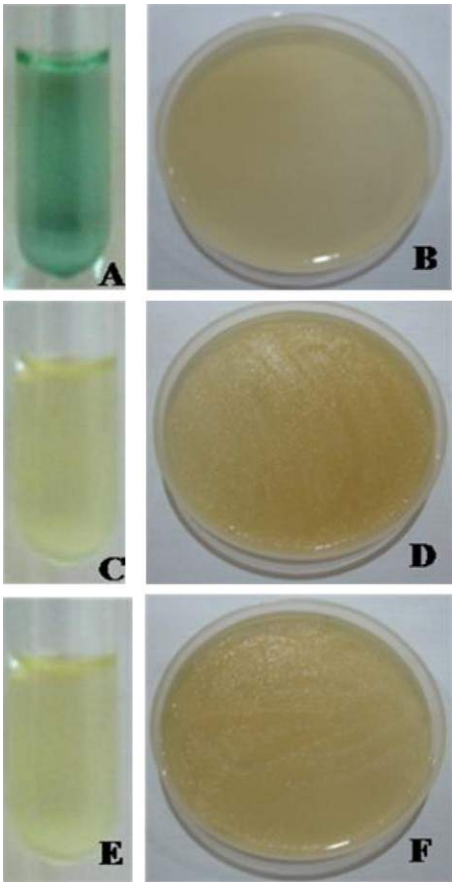

Fig. 10. Photograph showing effect of MG (10 mg/L) on growth of *E. coli* (~10^6 cells) before and after treatment by KPS (1 g/L) and complex1 (200 μM). A, C and E tubes containing *E. coli* with MG, *E. coli* with MG after treatment by KPS and complex1, and *E. coli*., respectively. B, D and F are the plates corresponding to the tubes A, C and E respectively after overnight incubation.

Table 2
m/*z* values of degradation intermediates and tentative structures.

TIC peak[a]	Tentative structure		*m*/*z*
A	MG–3CH_2	A_1	287.16
A	DLBP + OH	A_2	242.11
A	DLBP–CH_2 + OH	A_3	228.50
A	DLBP + 2OH	A_4	257.11
A	BPA + HSO_4^-	A_5	266.00
A	BPA + CH_3 + OH	A_6	200.10
A	MG–4CH_2–NH + 4OH	A_7	322.11
B	MG–2CH_2–NH + 4OH	B_1	352.15
B	MG–4CH_2 + 2OH	B_2	305.13
C	LMG	C_1	331.00
C	MG–4CH_2–2NH + 4OH	C_2	309.10
C	MG–2CH_2–NH	C_3	286.16

[a] Peaks and their corresponding RT: A (1.48–1.53 min), B (2.38–2.41 min) and C (3.61–3.65 min).

Degraded MG solution showed 3 peaks (A, B, C) in TIC plot (S.I. Fig. 2), and corresponding mass spectra of these peaks revealed the formation of a variety of degraded intermediates, and complexity of degradation.

Earlier studies on degradation of MG mediated by hydroxyl radicals reported the formation of complex reaction mixture with N-demethylated intermediates of MG, DLBP (dimethylaminobenzophenone) and their hydroxyl adducts along with many other possible intermediates [32,43,44]. Analysis of present mass spectral results clearly showed ions that could correspond to N-demethylated intermediates, hydroxyl adducts of N-demethylated intermediates and DLBP (Table 2). Interestingly, these results showed that persulphate mediated degradation of MG could form hydroxyl adducts.

It is known that in aqueous solution sulphate radicals react with water to produce hydroxyl radicals that could react with aromatic ring to form hydroxyl adducts [45,46]. Moreover, sulphate radicals could directly attack the aromatic ring and form hydroxyl adducts [46,47]. Thus, in the present study, formation of hydroxyl adducts of degradation intermediates could be attributed to both the sulphate radicals and secondary hydroxyl radicals generated upon activation of KPS by complex1.

ESI-MS/MS analysis of MG showed following ions, 329.17 (MG); 285.12 (MG–2CH_2–NH_2); 251.20 (MG–C_6H_6); 237.11 (MG–C_6H_6–CH_2) and 208.28 (MG–C_6H_6–CH_2), which was similar to earlier report (S.I. Fig. 3) [32]. Importantly, ESI-MS/MS of degradation intermediate A_3 (DLBP–CH_2 + OH) with 228.5 *m*/*z* value showed a fragment ion with 149.10 *m*/*z* (A_3–C_6H_6); (S.I. Fig. 3). Similar fragmentation has been reported for bezenophenone type molecule [48]. Thus, this result further supports the presence of degradation intermediate with hydroxyl adduct.

Hydroxyl radicals could cause deamination of aromatic amines [43,44,52,53]. Earlier, report on the oxidation of MG by persulphate suggested the formation of biphenyl amine (BPA) intermediates [34]. In addition, persulphate is known to react with aromatic amines to form aromatic amine sulphate adducts [49–51]. A peak with 266 *m*/*z* identified in the mass spectra could correspond to BPA sulphate adduct (A_5) (S.I. Fig. 2). ESI-MS/MS of this intermediate A_5 (BPA + HSO_4^-), showed a fragment ion with 169.2 *m*/*z* (A_5–H_2SO_4). (S.I. Fig. 3). In addition, intermediate A_6 (BPA + CH_3 + OH) with 200.19 *m*/*z* showed following fragment ions; 122.5 (A_6–C_6H_6), 144.25 (A_6–CH_2–C–NH–CH_3). Earlier similar fragmentations were observed for aromatic amino derivatives [54–56] (S.I. Fig. 3).

As mentioned above, reactive sulphate and hydroxyl radicals could generate a variety of intermediates, however, identification of all intermediates by mass spectrometry was not possible. It is important to note that, several factors such as concentration of intermediates present in analysis solution and the amount obtained after separation in the solid phase column, HPLC

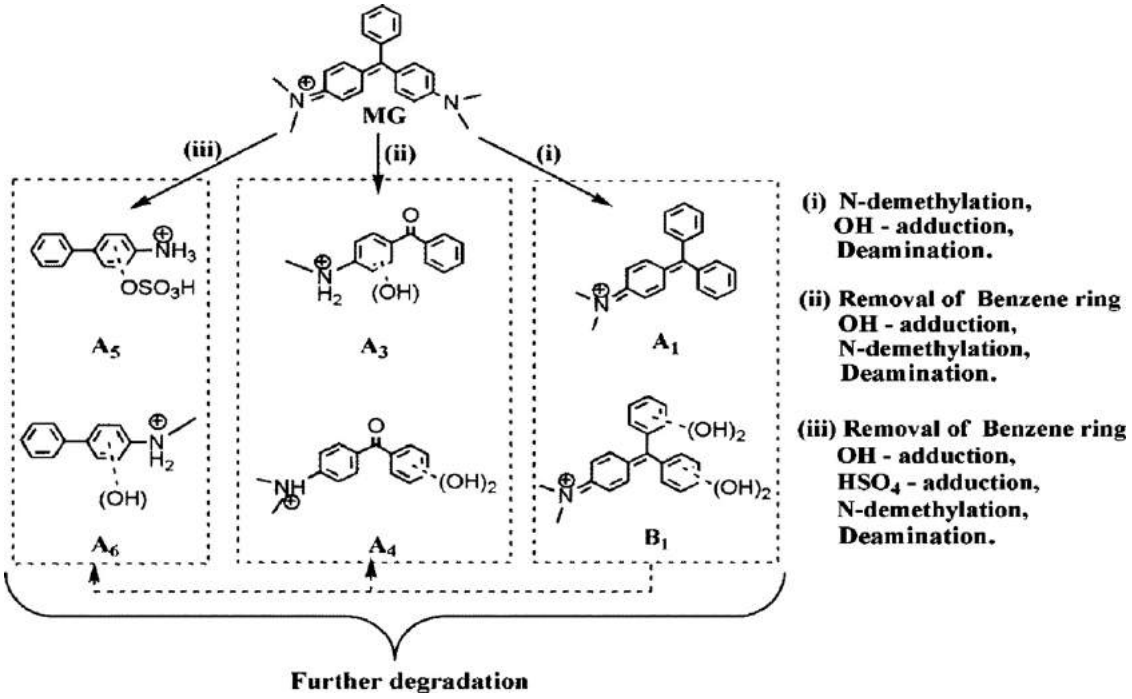

Scheme 1. Possible reactions in degradation of MG by KPS in presence of complex1.

separation protocols, type of molecules and stability of charged ions, mass spectrometer used, presence of a variety of compounds and alkali metal ions in sample, complexity due to fragmentations in ESI source, and others could affect the analysis by mass spectrometer [32,37,43,44].

Based on above discussion and available literature, important possible reactions for degradation of MG by KPS and complex1 are proposed (Scheme 1). Proposed degradation mechanism includes major reactions such as N-demethylation, hydroxyl adduct formation and removal of benzene ring, as reported earlier [32,43,44].

4. Conclusions

MG and its structurally related N-demethylated species were almost completely degraded by KPS alone. Interestingly, degradation of MG by KPS and complex1 oxidation system was found to occur in wide pH range (3–9) with enhanced rate as compared to KPS alone. Degradation of MG by KPS in trace amount of Fe(II) ions was incomplete whereas addition of trace amount of Ni(II) ions had no significant effect on degradation of MG by KPS. Degradation of MG by KPS was dependent on initial concentration of KPS, complex1, and MG. Microbial assay revealed removal of antibacterial activity of MG after treatment of MG by KPS in presence of complex1, indicating that this oxidation system has ability to decrease toxicity of MG significantly towards bacteria. Moreover, TOC analysis indicated the ability of KPS, and KPS in presence of complex1 to reduce TOC. Hydroxyl adducts of MG, DLBP and BPA intermediates were identified in degraded solution by LC–ESI–MS analysis. Thus, this study demonstrates that KPS and complex1 oxidation system could be a better choice for degradation of environmentally persistent and hazardous MG and possibly other related dyes that are released in to water bodies.

Acknowledgements

H.P. acknowledges research Grant No. BT/PR133316/GBP/27/251/2009 from Department of Biotechnology (DBT), Government of India. G.S. and P.P. acknowledge DBT and Council of Scientific and Industrial Research (CSIR) for fellowships, respectively. Authors are thankful to Dr. Meenal Kowshik, BITS, Pilani, Goa for providing bacterial culture, Prof. Shyamalava Mazumdar and Mr. Shibdas Banerjee, TIFR, Mumbai for ESI–MS, Director and Chairperson, Syngenta India Ltd., Goa for TOC analysis. IMA facility of BITS-Pilani, Goa, India, is acknowledged.

Appendix A. Supplementary data

Supplementary data associated with this article can be found, in the online version, at doi:10.1016/j.jhazmat.2012.01.031.

References

[1] S.J. Culp, F.A. Beland, Malachite green: a toxicological review, Int. J. Toxicol. 15 (1996) 219–238.
[2] C.F. Chang, C.H. Yang, Y.O. Shu, T.I. Chen, M.S. Shu, I.C. Liao, Effects of temperature, salinity and chemical drugs on the in vitro propagation of the Dinoflagellate parasite, *Amylodinium ocellatum*, Asian Fish Soc. P31 (2001).
[3] S. Srivastava, R. Sinha, D. Roy, Toxicological effects of Malachite green, Aquat. Toxicol. 66 (2004) 319–329.
[4] A. Stammati, C. Nebbia, I.D. Angelis, A.G. Albo, M. Carletti, C. Rebecchi, F. Zampaglioni, M. Dacasto, Effects of Malachite green (MG) and its major metabolite, leucomalachite green (LMG), in two human cell lines, Toxicol. In Vitro 19 (2005) 853–858.
[5] T. Sauer, G. Cesconeto Neto, H.J. José, R.F.P.M. Moreira, Kinetics of photocatalytic degradation of reactive dyes in a TiO_2 slurry reactor, J. Photochem. Photobiol. A 149 (2002) 147–154.
[6] N. Daneshvar, D. Salari, A.R. Khataee, Photocatalytic degradation of azo dye acid red 14 in water: investigation of the effect of operational parameters, J. Photochem. Photobiol. A 157 (2003) 111–116.
[7] C.-Y. Chen, J.-T. Kuo, C.-Y. Cheng, Y.-T. Huang, I.H. Ho, Y.-C. Chung, Biological decolorization of dye solution containing Malachite green by *Pandoraea pulmonicola* YC32 using a batch and continuous system, J. Hazard. Mater. 172 (2009) 1439–1445.
[8] A. Romero, A. Santos, F. Vicente, C. González, Diuron abatement using activated persulphate: Effect of pH, Fe(II) and oxidant dosage, Chem. Eng. J. 162 (2010) 257–265.
[9] M.I. Stephen, N.H. Ince, J.R. Bolton, UV/H_2O_2 degradation and toxicity reduction of textile azo dyes, J. Adv. Oxid. Technol. 2 (1997) 442–448.
[10] D.T. Gonenc, N.H. Ince, Treatability of a textile azo dye by UV/H_2O_2, Environ. Technol. 18 (1997) 179–185.
[11] M.P. Georgiou, D.A. Aivasidis, K. Gimouhopoulos, Degradation of azo-reactive dyes by ultraviolet radiation in the presence of hydrogen peroxide, Dyes Pigments 52 (2002) 69–78.

[12] A. Mohey El-Dein, J.A. Libra, U. Wiesmann, Mechanism and kinetic model for the decolorization of the azo dye Reactive Black 5 by hydrogen peroxide and UV radiation, Chemosphere 52 (2003) 1069–1077.
[13] R.J. Watts, A.L. Teel, Treatment of contaminated soils and groundwater using ISCO, Pract. Period. Hazard. Radioact. Toxicol. Waste Manage. 10 (2006) 2–9.
[14] C. Liang, C.J. Bruell, Thermally activated persulfate oxidation of trichloroethylene: experimental investigation of reaction orders, Ind. Eng. Chem. Res. 47 (2008) 2912–2918.
[15] W.K. Wilmarth, A. Haim, Mechanisms of oxidation by peroxydisulfate ion, in: J.O. Edwards (Ed.), Peroxide Reaction Mechanisms, Interscience, New York, 1962, pp. 175–225.
[16] O.S. Furman, A.L. Teel, R.J. Watts, Mechanism of base activation of persulfate, Environ. Sci. Technol. 44 (2010) 6423–6428.
[17] G.P. Anipsitakis, D.D. Dionysiou, Radical generation by the interaction of transition metals with common oxidants, Environ. Sci. Technol. 38 (2004) 3705–3712.
[18] R.H. Waldemer, P.G. Tratnyek, R.L. Johnson, J.T. Nurmi, Oxidation of chlorinated ethenes by heat-activated persulfate: kinetics and products, Environ. Sci. Technol. 41 (2007) 1010–1015.
[19] X. Liang, P.J. Sadler, Cyclam complexes and their applications in medicine, Chem. Soc. Rev. 33 (2004) 246–266.
[20] K.P. Wainwright, Synthetic and structural aspects of the chemistry of saturated polyaza macrocyclic ligands bearing pendant coordinating groups attached to nitrogen, Coord. Chem. Rev. 166 (1997) 35–90.
[21] A. McAuley, S. Subramanian, Synthesis, spectroscopy, and redox behavior of the binuclear complex cation $[Ni_2(6,6'\text{-spirobi(cyclam)})]^{4+}$ (cyclam = 1,4,8,11-tetraazacyclotetradecane): characteristics of a transient Ni(II)–Ni(III) species, Inorg. Chem. 36 (1997) 5376–5383.
[22] I. Zilbermann, E. Maimon, H. Cohen, D. Meyerstein, Redox chemistry of nickel complexes in aqueous solutions, Chem. Rev. 105 (2005) 2609–2626.
[23] K. Nag, A. Chakravorty, Monovalent, trivalent and tetravalent nickel, Coord. Chem. Rev. 33 (1980) 87.
[24] E. Zeigerson, I. Bar, J. Bernstein, L.J. Kirschenbaum, D. Meyerstein, Stabilization of the tervalent nickel complex with meso-5,7,7,12,14,14-hexamethyl-1,4,8,11-tetraazacyclotetradecane by axial coordination of anions in aqueous solution, Inorg. Chem. 21 (1982) 73–80.
[25] R.I. Haines, J.E. Rowley, Structure and kinetics of oxidation of amphiphilic nickel(II) pentaazamacrocycles by peroxodisulfate and by a nickel(III) pendant-arm macrocycle, J. Incl. Phenom. Macrocycl. 47 (2003) 25–32.
[26] I. Zilbermann, A. Meshulam, H. Cohen, D. Meyerstein, Stabilization of nickel(III)-1,8-dimethyl-1,3,6,8,10,13-hexaazacyclotetradecane by axial binding of anions in neutral aqueous solutions, Inorg. Chim. Acta 206 (1993) 127–130.
[27] E. Kusvuran, O. Gulnaz, A. Samil, Ö. Yildirim, Decolorization of malachite green, decolorization kinetics and stoichiometry of ozone-malachite green and removal of antibacterial activity with ozonation processes, J. Hazard. Mater. 186 (2011) 133–143.
[28] A.G.S. Prado, L.L. Costa, Photocatalytic decouloration of malachite green dye by application of TiO_2 nanotubes, J. Hazard. Mater. 169 (2009) 297–301.
[29] Y. Liu, Y. Ohko, R. Zhang, Y. Yang, Z. Zhang, Degradation of malachite green on Pd/WO_3 photocatalysts under simulated solar light, J. Hazard. Mater. 184 (2010) 386–391.
[30] B.H. Hameed, T.W. Lee, Degradation of malachite green in aqueous solution by Fenton process, J. Hazard. Mater. 164 (2009) 468–472.
[31] N. Modirshahla, M.A. Behnajady, Photooxidative degradation of Malachite Green (MG) by UV/H_2O_2: influence of operational parameters and kinetic modeling, Dyes Pigments 70 (2006) 54–59.
[32] Y. Ju, S. Yang, Y. Ding, C. Sun, A. Zhang, L. Wang, Microwave-assisted rapid photocatalytic degradation of Malachite green in TiO_2 suspensions: mechanism and pathways, J. Phys. Chem. A 112 (2008) 11172–11177.
[33] M.P. Suh, S.G. Kang, Synthesis and properties of nickel(I1) and copper(I1) complexes of 14-membered hexaaza macrocycles, 1,bdimethyl- and 1,8-diethyl-1,3,6,8,10,13-hexaazacyclotetradecane, Inorg. Chem. 27 (1988) 2544–2546.
[34] T. Mushinga, S.B. Jonnalagadda, A kinetic approach for the mechanism of malachite green-peroxydisulphate reaction in aqueous solution, Int. J. Chem. Kinet. 24 (1992) 41–49.
[35] V. Lorian, Antibiotics in Laboratory Medicine, 2005.
[36] S. Egger, R.P. Lehmann, M.J. Height, M.J. Loessner, M. Schuppler, Antimicrobial properties of a novel silver-silica nanocomposite material, Appl. Environ. Microbiol. 75 (2009) 2973–2976.
[37] S. Banerjee, H. Prakash, S. Mazumdar, Evidence of molecular fragmentation inside the charged droplets produced by electrospray process, J. Am. Soc. Mass Spectrom. 22 (2011) 1707–1717.
[38] B. Nepollian, E. Celik, H. Choi, Photochemical oxidation of arsenic(III) to arsenic(V) using peroxydisulfate ions as an oxidizing agent, Environ. Sci. Technol. 42 (2008) 6179–6184.
[39] I.M. Kolthoff, I.K. Millar, The chemistry of persulfate. I. The kinetics and mechanism of the decomposition of the persulfate ion in aqueous medium, J. Am. Chem. Soc. 73 (7) (1951) 3055–3059.
[40] E. Zeigerson, I. Bar, J. Bernstein, L.J. Kirschenbaum, D. Meyerstein, Stabilization of the tervalent nickel complex with *meso*-5,7,7,12,14,14-hexamethyl-1,4,8,11-tetraazacyclotetradecane by axial coordination of anions in aqueous solution, Inorg. Chem. 21 (1982) 73–80.
[41] I. Zilbermann, E. Maimon, H. Cohen, D. Meyerstein, Redox chemistry of nickel complexes in aqueous solutions, Chem. Rev. 105 (2005) 2609–2625.
[42] C.H. Chen, C.F. Chang, S.M. Liu, Partial degradation mechanisms of malachite green and methyl violet B by *Shewanella decolorationis* NTOU1 under anaerobic conditions, J. Hazard. Mater. 177 (2010) 281–289.
[43] Y. Ju, S. Yang, Y. Ding, C. Sun, C. Gu, Z. He, C. Qin, H. He, B. Xu, Microwave-enhanced H_2O_2-based process for treating aqueous malachite green solutions: intermediates and degradation mechanism, J. Hazard. Mater. 171 (2009) 123–132.
[44] L.A. Perez-Estrada, A. Aguera, M.D. Hernando, S. Malato, A.R. Fernandez-Alba, Photodegradation of malachite green under sunlight irradiation: kinetics and toxicity of the transformation products, Chemosphere 70 (2008) 2068–2075.
[45] H. Hori, A. Yamamoto, E. Hayakawa, S. Taniyasu, N. Yamashita, S. Kutsuna, Efficient decomposition of environmentally persistent trefluorocarcoxylic acids by use of persulfate as a photochemical oxidant, Environ. Sci. Technol. 39 (2005) 2383–2388.
[46] X.-Y. Yu, Z.C. Bao, J.R. Barker, Free radical reactions involving $Cl^{\bullet}$, $Cl_2^{\bullet-}$ and $SO_4^{\bullet-}$ in the 248 nm photolysis of aqueous solutions containing $S_2O_8^{2-}$ and Cl^-, J. Phys. Chem. A 108 (2004) 295–308.
[47] G.P. Anipsitakis, D.D. Dionysiou, M.A. Gonzalez, Cobalt-mediated activation of peroxomonosulfate and sulfate radical attack on phenolic compounds. implication of chloride ions, Environ. Sci. Technol. 40 (2006) 1000–1007.
[48] N. Negreira, I. Rodriguez, M. Ramil, E. Rubi, R. Cela, Solid-phase extraction followed by liquid chromatography–tandem mass spectrometry for the determination of hydroxylated benzophenone UV absorbers in environmental water samples, Anal. Chim. Acta 654 (2009) 162–170.
[49] E.J. Behrman, The ortho-para ratio and the intermediate in the persulfate oxidation of aromatic amines (the Boyland-Sims Oxidation), J. Org. Chem. 57 (1992) 2266–2270.
[50] E.J. Behrman, Studies on the reaction between peroxydisulfate ions and aromatic amines. The Boyland-Sims Oxidation, JACS 89 (1967) 2424–2428.
[51] E. Boyland, D. Manson, P. Sims, D.C. Willams, The resistance of some o-aminoaryl sulphates to hydrolysis by aryl sulphatases, Biochem. J. 62 (1956) 68–71.
[52] P. Neta, R.W. Fessenden, Hydroxyl radical reactions with phenols and anilines as studied by electron spin resonance, J. Phys. Chem. 78 (1974) 523–529.
[53] G.N.R. Tripathi, Q. Sun, Time-resolved Raman study of the oxidation mechanism of aromatic diamines by $^{\bullet}OH$ radical in water, J. Phys. Chem. A 103 (1999) 9055–9060.
[54] M. Villagrasa, M. Guillamon, A. Navarro, E. Eljarrat, D. Barcelo, Development of a pressurized liquid extraction solid-phase extraction followed by liquid chromatography–electrospray ionization tandem mass spectrometry method for the quantitative determination of benzoxazolinones and their degradation products in agricultural soil, J. Chromatogr. A 1179 (2008) 190–197.
[55] R.J. Turesky, J.P. Freeman, R.D. Holland, D.M. Nestorick, D.W. Miller, D.L. Ratnasinghe, F.F. Kadlubar, Identification of aminobiphenyl derivatives in commercial hair dyes, Chem. Res. Toxicol. 16 (2003) 1162–1173.
[56] S.T. Wu, K. Cao, S.J. Bonacorsi, H. Zang, M. Jemal, Distinguishing a phosphate ester prodrug from its isobaric sulphate metabolite by mass spectrometry with the metabolite standard, Rapid Commun. Mass Spectrom. 23 (2009) 3107–3113.

Photochemical & Photobiological Sciences

An international journal

www.rsc.org/pps

Volume 12 | Number 3 | March 2013 | Pages 409–584

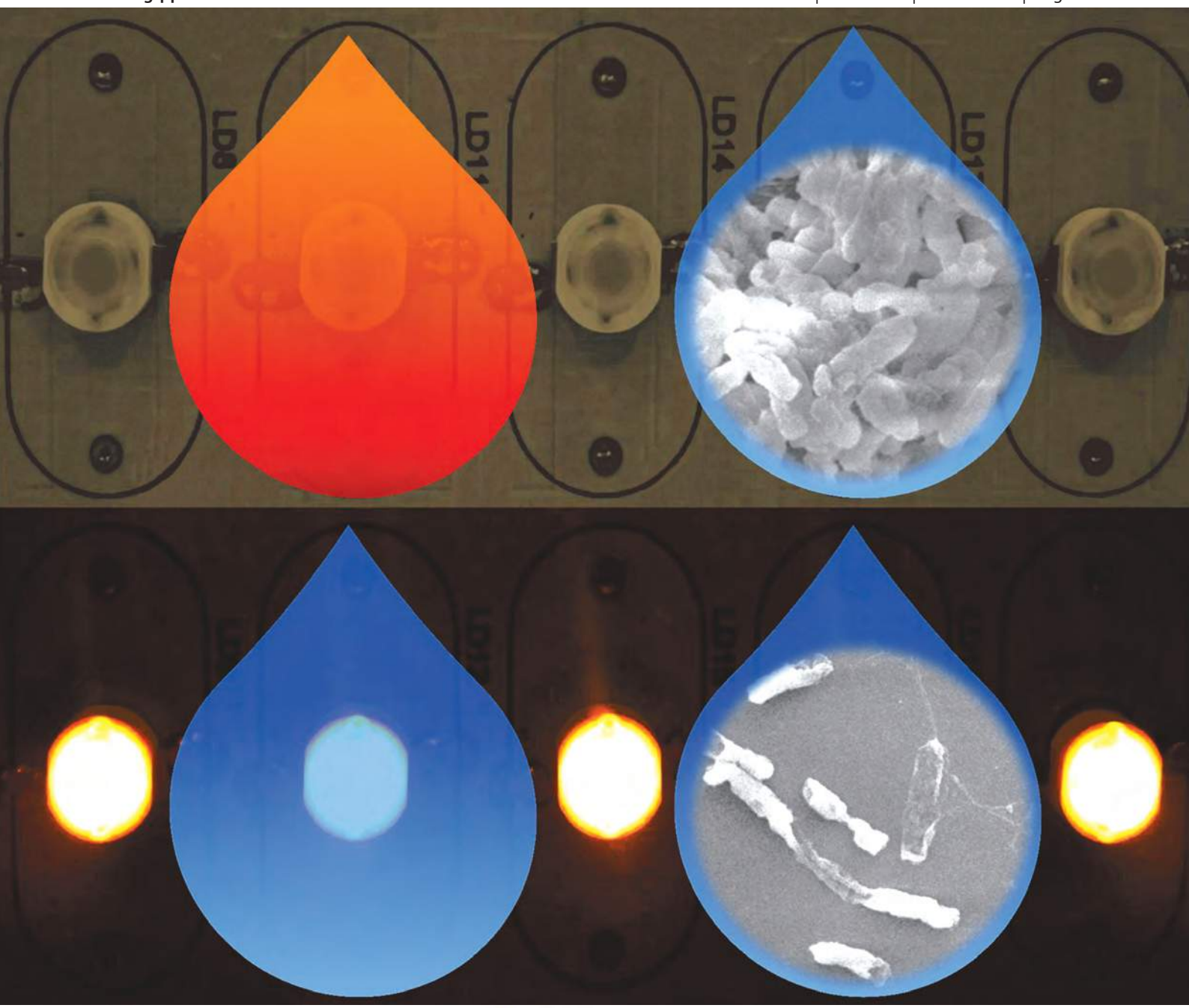

ISSN 1474-905X

RSC Publishing

1474-905X(2013)12:3;1-Y

Photochemical & Photobiological Sciences

RSC Publishing

PAPER

View Article Online
View Journal | View Issue

Cite this: *Photochem. Photobiol. Sci.*, 2013, **12**, 456

Photodegradation of methyl orange and photoinactivation of bacteria by visible light activation of persulphate using a tris(2,2′-bipyridyl)ruthenium(II) complex†

Gokulakrishnan Subramanian, Priyadarshini Parakh and Halan Prakash*

Persulphate is an emerging oxidant in the field of advanced oxidation processes for the degradation of environmentally persistent organic compounds. The present study shows that visible light activation of persulphate (2 mM) using tris(2,2′-bipyridyl)ruthenium(II) (complex **1**) (1 μM) caused rapid degradation (98%) of model azo dye methyl orange (MO) (12 mg L^{-1}) with significant mineralization (76%), and also complete inactivation of both Gram negative and positive bacteria (~10^7 CFU mL^{-1}). BacLight LIVE/DEAD assay, scanning electron microscopy and genomic DNA analysis revealed cell membrane damage and loss of chromosomal DNA, indicating oxidative stress caused to *E. coli* during photoinactivation. The effect of concentration of complex **1** : persulphate ratio and presence of inorganic ions (0.1 M), such as sodium hydrogen phosphate, sodium sulphate, and sodium hydrogen carbonate, on the photodegradation of MO and photoinactivation of *E. coli* were studied. In addition, the effect of the presence of the organic contaminant resorcinol on the photoinactivation of *E. coli* was also studied. Significant degradation of MO and complete inactivation of bacteria were observed in simulated ground water. The present study is the first to reveal that activation of persulphate using a visible light absorbing metal complex in aqueous media has the ability to cause degradation of organic contaminants as well as complete inactivation of bacteria.

Received 17th September 2012,
Accepted 13th November 2012

DOI: 10.1039/c2pp25316j

www.rsc.org/pps

1. Introduction

Depletion of water quality due to contamination of water bodies by recalcitrant compounds and microbial pathogens is a serious global problem. In efforts to improve water quality, active research is being pursued for degradation of organic contaminants and inactivation of microorganisms in aqueous media.[1–3] Advanced oxidation processes, such as Fenton, Photo-Fenton, UV-TiO_2 photocatalysis and ozonation, have been reported to be effective for the degradation of pollutants and inactivation of bacteria.[4–9] Persulphate is an emerging oxidant used in advanced oxidation processes for generating sulphate radicals that are very strong oxidants (E° = 2.6 V) capable of degrading a variety of organic contaminants. Moreover, studies on activation of persulphate are gaining attention because activation of persulphate effectively generates sulphate radicals and enhances the efficiency of degradation of organic contaminants.[10–18]

Additionally, persulphate has been studied as a sacrificial electron acceptor for the photo oxidation of tris(2,2′-bipyridyl)-ruthenium(II) bypyridine, ($[Ru(bpy)_3]^{2+}$) in the photolytic water splitting for hydrogen production.[19–22] In this context, it has been shown that visible light photolysis of persulphate in presence of the $[Ru(bpy)_3]^{2+}$ complex results in cleavage of the peroxo bond of persulphate, and generates sulphate radicals, sulphate ions and $[Ru(bpy)_3]^{3+}$ (reactions 1 and 2).[21]

$$[Ru(bpy)_3]^{2+} + h\nu + [S_2O_8]^{2-} \rightarrow [Ru(bpy)_3]^{3+} + SO_4^{2-} + SO_4^{\cdot -} \quad (1)$$

$$[Ru(bpy)_3]^{2+} + SO_4^{\cdot -} \rightarrow [Ru(bpy)_3]^{3+} + SO_4^{2-} \quad (2)$$

In aqueous solutions, at neutral and alkaline pH, sulphate radicals react with water to produce hydroxyl radicals.[16,23]

$$SO_4^{\cdot -} + H_2O \rightleftharpoons HO^{\cdot} + H^+ + SO_4^{2-} \quad (3)$$

Department of Chemistry, Birla Institute of Technology and Science, Pilani, K.K. Birla Goa Campus, NH17B, Zuarinagar, Goa 403 726, India. E-mail: halanprakash@goa.bits-pilani.ac.in, halanprakash@gmail.com; Fax: +0832-2557033; Tel: +0832-2580344; http://www.bits-goa.ac.in/Departments/Faculty/faculty%20pages/halan.htm, http://universe.bits-pilani.ac.in/goa/halanprakash/profile

†Electronic supplementary information (ESI) available: Details of the visible light photolysis setup, and additional figures and tables are provided. See DOI: 10.1039/c2pp25316j

Thus, these facts imply that visible light photolysis of persulphate in the presence of $[Ru(bpy)_3]^{2+}$ activates persulphate and produce reactive species, such as sulphate radicals, hydroxyl radicals and $[Ru(bpy)_3]^{3+}$. However, the effect of photochemical activation of persulphate using $[Ru(bpy)_3]^{2+}$ on recalcitrant pollutants has not been studied.

Persulphate is also used in *in situ chemical oxidation processes* (ISCO) for treatment of soil contaminated with organic compounds.[24,25] A few studies have shown that persulphate used in ISCO processes for the degradation of soil contaminants could retard the metabolic activity of indigenous soil microorganisms.[26,27] However, the direct effect of activated persulphate on bacteria in aqueous media has not been studied. It is important to note that the reactive radicals generated by activation of persulphate in aqueous media could have a detrimental effect on bacteria, in addition to their detrimental effect on organic contaminants. Based on the above facts, we envisaged that visible light activation of persulphate using a ruthenium complex could cause degradation of organic pollutants, as well as, inactivation of bacteria in aqueous medium.

In this study, we used tris(2,2′-bipyridyl)ruthenium(II) bypyridine, (complex **1**) for visible light activation of persulphate and studied its effect on a model azo dye (methyl orange, MO), Gram negative and positive bacteria. Azo dyes constitute one of the largest organic contaminants (70%) among textile dye pollutants.[17] Methyl orange is an azo dye, non biodegradable and toxic to living organisms and has been used as a model for studying the degradation of azo dyes.[17] Total organic carbon measurements were performed to determine the extent of mineralization of MO. Inactivation of bacteria was studied using *Escherichia coli* and *Pseudomonas aeruginosa* to represent Gram negative bacteria, and *Staphylococcus aureus* and *Bacillus subtilis* to represent Gram positive bacteria. BacLight LIVE/DEAD assay; scanning electron microscopy and genomic DNA analysis were performed to investigate the cell membrane integrity of *E. coli*. The effect of radical scavengers and inorganic salts on the photodegradation of MO and inactivation of *E. coli* were studied. The photoinactivation of *E. coli* in the presence of the organic compound resorcinol was also investigated. Additionally, the photodegradation of MO and photoinactivation of bacteria in simulated ground water was examined. A light emitting diode (LED) array was used as the visible light source for photolysis experiments.

2. Experimental

2.1. Materials

Ruthenium(III) chloride hydrate, 2,2′-bipyridine, potassium persulphate ($K_2S_2O_8$), resorcinol, methyl orange, sodium nitrite ($NaNO_2$), disodium hydrogen phosphate (Na_2HPO_4), sodium hydrogen phosphate (NaH_2PO_4), sodium sulphate (Na_2SO_4), and sodium hydrogen carbonate ($NaHCO_3$) used, were of guaranteed analytical grade, purchased from SD fine chemicals, India. $[Ru(bpy)_3]$ $(PF_6)_2$ (complex **1**) was prepared according to an earlier report.[28] For HPLC analysis, methanol (HPLC grade) and millipore water were used.

2.2. Photolytic experimental setup

A visible light LED array containing warm white LED bulbs (400–700 nm, with peak maxima around 450 and 600 nm) manufactured by Kwality photonics pvt Ltd, India was used as light source. Details of the LED array and a photograph of the photolysis experimental setup are provided in the ESI (Fig. SI 1 and 2†). Fluence rate was measured by an Ophir PD100 Nova II power meter.

2.3. Photodegradation of MO

2 mL of aqueous solution (double distilled water) of MO (12 mg L^{-1}) with an appropriate concentration of complex **1** and persulphate was taken in a quartz cuvette and photolysed at the fluence rate of 0.095 W cm^{-2} (Fig. SI 2†). The photodegradation of MO was spectrophotometrically followed (JASCO V-570 UV/VIS/NIR) by monitoring decrease in absorbance at 464 nm. Quartz cuvettes containing the reaction mixture were wrapped completely with aluminium foil and used for dark controls. All experiments were carried out at neutral pH and at 37 °C. Radical scavenging experiments were performed by addition of sulphate and hydroxyl radical scavengers, such as methanol (0.1 M) and sodium nitrite (0.02 M), to the reaction mixture containing MO (12 mg L^{-1}), complex **1** (1 μM) and persulphate (2 mM) followed by irradiation.[29] Similarly, the effect of inorganic ions on photodegradation was investigated by the addition of salts, such as 0.1 M of Na_2HPO_4, Na_2SO_4 and $NaHCO_3$, to the reaction mixture. The addition of Na_2SO_4 (0.1 M) to double distilled water (neutral pH) did not change the pH of the solution. The change in pH after addition of 0.1 M of NaH_2PO_4 or $NaHCO_3$ to double distilled water was adjusted to neutral pH by adding a few drops of 0.05 N HCl.[30,31] Total organic carbon (TOC) measurements were performed using a Sievers 900 TOC analyser by injection of appropriate volume of sample at different time intervals during irradiation. The results are expressed as TOC/TOC_0 where TOC is total organic carbon at time t, and TOC_0 = initial total organic carbon of MO (12 mg L^{-1}).

2.4. Photoinactivation of bacteria

Bacterial strains *Escherichia coli* (NCIM 2345), *Pseudomonas aeruginosa* (NCIM 2581), *Staphylococcus aureus* (NCIM 2127) and *Bacillus subtilis* (NCIM 2545) were cultured in nutrient broth (NB) medium using an orbital shaker set at 100 rpm, 37 °C for 12 h. Cells (at log phase) were harvested by centrifugation at 1000*g* for 15 min and washed twice with 10 mM phosphate buffer saline (PBS). Composition of 10 mM PBS (pH 7.2): Na_2HPO_4 (6.1 mM), NaH_2PO_4 (2.05 mM), NaCl (154 mM). A bacterial stock solution was prepared by suspending cell pellet in an appropriate volume of PBS, and the concentration was found to be $\sim 10^9$ colony forming units (CFU) mL^{-1}. Cell concentration was determined by counting colonies after serial dilution and spread plating 0.1 mL of sample on NB agar plates, followed by overnight incubation.

It has been shown that irradiation of bacteria in the visible light region caused reduction in its cell viability.[32,33] Considering this fact, in the present study, control experiments were performed to optimize the fluence rate such that irradiation of light (400–700 nm) had no effect on the viability of bacterial strains. Fluence rates were optimized by adjusting the distance between the light source and the quartz cuvette containing the bacterial suspension ($\sim 10^7$ CFU mL^{-1}). Irradiation of *B. subtilis* at a fluence rate of 0.048 W cm^{-2}, irradiation of *S. aureus* at a fluence rate of 0.060 W cm^{-2}, and irradiation of *E. coli* and *P. aeruginosa* at a fluence rate 0.095 W cm^{-2} had no effect on their cell viability. Irradiation of the bacterial strains at more than the specified fluence rate caused a slight reduction in the cell viability. Therefore, photoinactivation experiments of the respective bacterial strains were carried out at the above mentioned fluence rate. Light dosage in J cm^{-2} was determined by multiplying irradiance in W cm^{-2} with time in seconds (Table 1).[34] Photolysis reactions were performed in sterilized quartz cuvettes (Fig. SI 2†) and the reaction mixture (2 mL) contained $\sim 10^7$ CFU mL^{-1} of bacterial cells with an appropriate concentration of complex **1** and persulphate in PBS (10 mM). Quartz cuvettes containing the reaction mixture were wrapped completely with aluminium foil and used for dark controls. All experiments were carried out at pH 7.2 and at 37 °C. Cell viability after irradiation was examined by a spread plate technique, as mentioned above. Two independent experiments in triplicate were performed for each bacterial species. One-way analysis of variance (ANOVA) was performed to assess the significance of difference in photoinactivation among the bacterial strains, and also to assess the significance of difference in the photoinactivation of *E. coli* at different complex **1** : persulphate ratios. Data was assessed for normal distribution and homogeneity of variances using the Kolmogorov–Smirnov test and Levene test, respectively. A value of $p < 0.05$ was considered as statistically significant.[35] All the statistical analysis was performed using OriginPro 8.0.

Radical scavenging experiments were performed by addition of sulphate and hydroxyl radical scavengers, such as methanol (0.1 M) and sodium nitrite (0.02 M),[29,30] to a reaction mixture containing *E. coli* cells ($\sim 10^7$ CFU mL^{-1}), complex **1** (1 μM) and persulphate (2 mM) in PBS (10 mM) followed by irradiation.

2.5. Cell membrane integrity assay

The integrity of the *E. coli* cell membrane was examined using Invitrogen Molecular Probes® LIVE/DEAD® BacLight™ Bacterial Viability Kit (L7012).[36] This assay is based on competitive binding of two different fluorescent nucleic acid stains SYTO® 9 and propidium iodide (PI). SYTO® 9 can easily diffuse through a cell membrane and gives a green fluorescence (500 nm) on binding to DNA whereas, PI can only enter cells with a damaged membrane and gives a red fluorescence (635 nm) on binding to DNA.[36] *E. coli* cells treated with complex **1** and persulphate in the absence and presence of light for 90 min were harvested by centrifugation, and cell pellet resuspended in 50 μL saline was stained with a 1 : 1 mixture of the two dyes, SYTO® 9 and PI according to the manufacturer's instructions. These stained samples were fixed in glass slide and examined at a magnification of 150× using a Nikon Eclipse Ti-U microscope (Nikon, Japan) with an excitation wavelength of 480 nm (SYTO® 9) and 490 nm (PI).

Table 1 Conditions for complete inactivation of bacteria[a]

Bacterial strains	Irradiation time (min)	Fluence rate (W cm^{-2})	Light dosage (J cm^{-2})
E. coli[b]	90	0.095	513
P. aeruginosa[b]	120	0.095	684
S. aureus[c]	60	0.060	216
B. subtilis[c]	60	0.048	173

[a] [complex **1**] = 1 μM, [persulphate] = 2 mM. [b] Gram negative bacteria. [c] Gram positive bacteria.

2.6. Scanning electron microscopy

Structural changes in the bacterial cell wall caused by photodamage were examined using Scanning Electron Microscopy (SEM).[37–39] *E. coli* cells treated with complex **1** and persulphate in the absence and presence of light for 90 min were harvested by centrifugation. The obtained cell pellet was resuspended in 100 μL of PBS and fixed with 2% glutaraldehyde solution for 1 h. Cells were then washed thrice with PBS, gradually dehydrated using a graded ethanol–H_2O mixture of 10, 25, 50, 75, 90 (v/v %) and finally with 100% ethanol followed by air drying.[37–39] Dried cells were then coated with platinum by JEOL JFC-1600 Autobine sputter and images were taken with a JEOL JSM-6360 LV Scanning Electron Microscope at a voltage of around 10 kV.

2.7. Chromosomal DNA extraction

E. coli chromosomal DNA was extracted using a SRL BioLit™ Bacterial Genomic DNA extraction kit (BTK007). *E. coli* cells treated with complex **1** and persulphate in the absence and presence of light for 90 min were harvested by centrifugation and genomic DNA was extracted immediately from the cell pellet according to the manufacturer's instruction. Extracted chromosomal DNA was mixed with 3 μL of 6X gel loading buffer (SRL BioLit™ BTK007). DNA samples were loaded onto a 1% agarose gel and electrophoresis was carried out for 3 hour at 60 V. After electrophoresis, DNA was stained by immersing the gel in an ethidium bromide solution (1 mg mL^{-1}) for 15 min and was photographed using a Biorad Gel Doc™ XR.

2.8. Photoinactivation of bacteria in presence of organic compound

Simultaneous degradation of resorcinol and photoinactivation of *E. coli* were investigated by high pressure liquid chromatography (HPLC) analysis and antimicrobial assays, respectively.[6] Typically, reaction mixtures containing 5/10 mg L^{-1} of resorcinol, *E. coli* cells ($\sim 10^7$ CFU mL^{-1}), complex **1** (1 μM) and persulphate (2 mM) were photolysed for 120 min. For HPLC analysis, 1 mL of sample from this reaction mix was withdrawn, filtered using a 0.45 μm polytetrafluoroethylene (PTFE)

filter to remove bacteria. 0.1 mL of this filtered solution was injected into a Shimadzu UFLC, equipped with a Phenomenex C18 HPLC column (250 mm × 4.6 mm, 5 μm) and a SPDM 20A Prominence diode array detector. HPLC was performed with 30 : 70 (v/v) methanol–water as the mobile phase in isocratic mode with a flow rate of 1 mL min^{-1} and the chromatogram was monitored at 280 nm.[6] For microbial assays, 0.1 mL of sample from the reaction mix was withdrawn at appropriate time intervals during irradiation and viable cells were determined by a spread plate technique, as mentioned above.

2.9. Effect of inorganic ions

The effect of inorganic ions on photoinactivation was investigated by addition of salts, such as 0.1 M of Na_2HPO_4, Na_2SO_4 and $NaHCO_3$,[30,31] to a reaction mixture containing *E. coli* cells (~10^7 CFU mL^{-1}), complex **1** (1 μM) and persulphate (2 mM) in PBS (10 mM), followed by irradiation. Addition of Na_2SO_4 (0.1 M) to 10 mM PBS (pH 7.2) did not change the pH of the solution. The change in pH after addition of 0.1 M of NaH_2PO_4 or $NaHCO_3$ to 10 mM PBS was adjusted to pH 7.2 by adding a few drops of 0.05 N HCl.[30,31] Control experiments with only 0.1 M of methanol, sodium nitrite (0.02 M), Na_2HPO_4, Na_2SO_4, and $NaHCO_3$ either in the dark or light had no effect on cell viability.[30]

2.10. Effect in simulated ground water

The photodegradation of an azo dye (MO 12 mg L^{-1}) and photoinactivation of bacteria (*E. coli* and *S. aureus*) by activation of persulphate (2 mM) using complex **1** (1 μM) were studied in simulated ground water that contained a defined composition of inorganic and organic matter. Simulated ground water was prepared by addition of the following components to distilled water: $Fe(NO_3)_3{\cdot}9H_2O$ (0.24 μM), $NaHCO_3$ (1.2 mM), Na_2SO_4 (0.34 mM), Na_2HPO_4 (0.28 mM), NaCl (0.86 mM) and resorcinol (9.0 μM).[40,41]

3. Results and discussion

3.1. Photodegradation of MO

The irradiation (420–700 nm) of MO in the presence of complex **1** and persulphate caused almost complete degradation (~98%) rapidly within 12 min (Fig. 1A). Photolysis of $[Ru(bpy)_3]^{2+}$ (complex **1**) and persulphate results in the formation of $[Ru(bpy)_3]^{3+}$, sulphate radicals and sulphate ions (reactions 1 and 2), indicating the activation of persulphate.[21] In aqueous solutions, sulphate radicals react with water to produce hydroxyl radicals (reaction 3).[16] The reactive species, such as sulphate and hydroxyl radicals, are very strong oxidants, capable of degrading organic compounds effectively. The activation of persulphate in an aqueous medium effectively generates sulphate radicals and secondary hydroxyl radicals, and enhances the efficiency of degradation.[10–16] Thus, rapid and efficient degradation of MO observed on irradiation of MO in the presence of complex **1** and persulphate is attributed to the photochemical activation of persulphate by complex

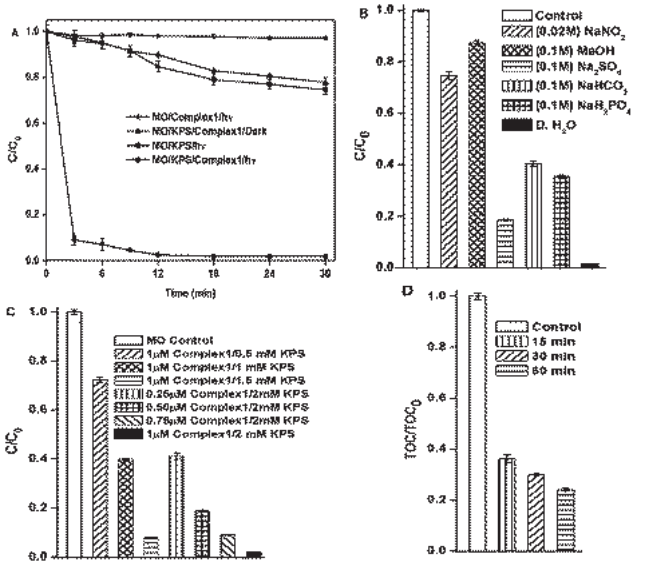

Fig. 1 Photodegradation of MO by the activation of persulphate (KPS) using complex **1**. [MO] = 12 mg L^{-1}, [KPS] = 2 mM, [complex **1**] = 1 μM and fluence rate = 0.095 W cm^{-2}. (A) Photodegradation of MO at different time intervals, C = concentration of MO at time t, C_0 = initial concentration of MO. (B) Effect of radical scavengers and inorganic ions, Control – concentration of MO after 15 min irradiation, light dosage = 85.5 J cm^{-2}. (C) Photodegradation of MO at different [complex **1**] : [persulphate] ratio after 15 min irradiation, Light dosage = 85.5 J cm^{-2}. (D) Reduction in total organic carbon before (control) and after different time intervals during irradiation. Control – total organic carbon of MO (12 mg L^{-1}).

1. Importantly, irradiation of MO in the presence of persulphate for 30 min caused only about 20% degradation of MO (Fig. 1A). A similar result was also observed for treatment of MO with complex **1** and persulphate without irradiation (dark control) (Fig. 1A). Persulphate is an oxidant (E° = 2.01 V) and has the ability to degrade organic compounds due to slow decomposition and generation of sulphate radicals.[11,13] The slight degradation (~20%) of MO observed on irradiation in the presence of persulphate, and in the dark control is due to the slow decomposition of persulphate.

Irradiation of MO in the presence of complex **1** and persulphate containing sodium nitrite (20 mM) and methanol (0.1 M) for 15 min caused only ~25% and ~15% degradation of MO, respectively (Fig. 1B). This significant inhibition in photodegradation is due to the effective scavenging of hydroxyl and sulphate radicals by methanol and sodium nitrite.[10,29,30] The above result indicates that sulphate and secondary hydroxyl radicals produced during photoactivation of persulphate by complex **1** play a major role in photodegradation of MO.

Percentage of degradation of MO decreased on decreasing the concentration of either complex **1** or persulphate (Fig. 1C). Decreasing the concentration of complex **1** may not be favourable to produce sufficient amount of excited state complex **1** to cause effective photochemical activation of persulphate for degradation. At lower concentrations of persulphate, relatively lower amounts of radicals are generated on activation, which may not be sufficient for efficient degradation. Earlier studies

on the degradation of dyes by persulphate reported that increasing the concentration of persulphate increased the percentage of degradation of dyes.[11,17] These results reveal that photodegradation of MO is dependent on concentration of both persulphate and complex **1**, and an optimal concentration of persulphate (2 mM) and complex **1** (1 μM) was required to cause complete degradation of MO (12 mg L^{-1}) (Fig. 1C).

It has been shown that activation of persulphate by UV photolysis enhanced the degradation of sulphamethazine[12] and 2,4-dichlorophenol.[18] Recently, we have shown that chemical activation of persulphate by Ni(II)azamacrocyclic complex enhanced the degradation of Malachite green (carcinogenic dye) by about ten fold.[11] Here, we show for the first time that visible light activation of persulphate using complex **1** has the ability to cause rapid and efficient degradation of MO.

3.2. Reduction of total organic carbon

Irradiation of MO in presence of complex **1** and persulphate caused about 65%, 71% and 76% reduction of TOC in 15, 30 and 60 min, respectively (Fig. 1D). TOC reduction obtained in the present study is comparable with TOC reduction obtained on degradation of phenol (0.5 mM) by activation of persulphate (84 mM) on UV photolysis.[13] Thus, the above results indicate that visible light activation of persulphate by complex **1** caused not only rapid degradation of MO, but also its significant reduction of TOC, indicating mineralization.

3.3. Effect of inorganic ions

Irradiation of MO in the presence of complex **1** and persulphate, containing salts (0.1 M) such as NaH_2PO_4, $NaHCO_3$ and Na_2SO_4 retarded the photodegradation of MO (Fig. 1B). Earlier, it has been shown that the presence of inorganic ions, such as sodium bicarbonate and sodium chloride, retarded the degradation of organic contaminants, such as acetic acid and chlorinated ethenes, by persulphate.[15,16] In addition, it is known that at higher ionic strength, ion pair complexation between complex **1** and persulphate is reduced, which is not favourable for photoinduced electron transfer between complex **1** and persulphate.[21] Therefore, photodegradation of MO was retarded at relatively higher ionic strength of the medium. The above facts indicate that degradation of MO by photochemical activation of persulphate using complex **1** is dependent on the composition of ions and ionic strength of the medium.

3.4. Photoinactivation of bacteria

Visible light irradiation of Gram negative bacteria (*E. coli* and *P. aeruginosa*) in the presence of complex **1** and persulphate caused complete photoinactivation, within 90 and 120 min, respectively (Table 1, Fig. 2A). Gram positive bacteria (*S. aureus* and *B. subtilis*) were also photoinactivated within 60 min, with relatively lower light dosage than that required for Gram negative bacteria (Table 1, Fig. 2B). The difference in photoinactivation of Gram positive and negative strains was found to be statistically significant (ANOVA, $p < 0.05$). The results also showed that the pattern of decrease in cell viability during the irradiation period varied within Gram negative strains (*E. coli* and *P. aeruginosa*) (Fig. 2A) (ANOVA, $p < 0.05$). In the case of Gram positive strains (*S. aureus* and *B. subtilis*), the pattern of decrease in cell viability during the irradiation period was similar (Fig. 2B), (ANOVA, $p > 0.05$). Among the bacterial strains examined, *P. aeruginosa* required the highest light dosage for complete inactivation (Table 1). Control experiments, (i) 5 μM of complex **1** alone in the absence and presence of light (ii) 2 mM of persulphate alone in the absence and presence of light (iii) a mixture of 1 μM of complex **1** and 2 mM of persulphate without irradiation, had no effect on cell viability (Fig. 2). Earlier, Antoniou *et al.*, had shown degradation (~50%) of microcystin-LR by thermal activation of persulphate at 30 °C.[42] However, in the present study, degradation of MO by persulphate alone at 37 °C was not significant

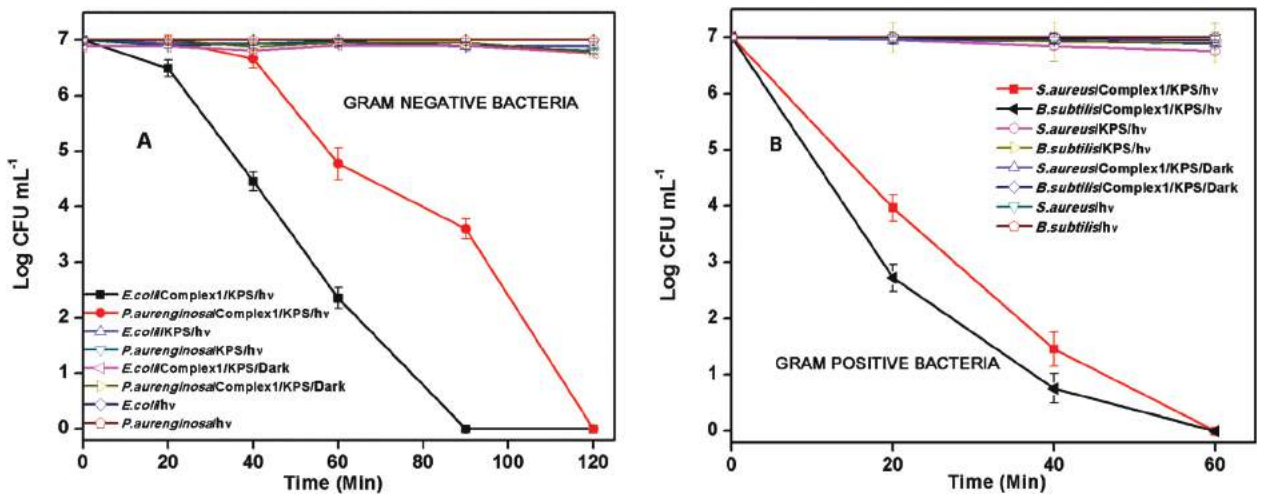

Fig. 2 Cell viability *vs.* time plot for the photoinactivation of (A) Gram negative bacteria (B) Gram positive bacteria. Cell concentration = ~10^7 CFU mL^{-1}, [KPS] = 2 mM, [complex **1**] = 1 μM, fluence rate = 0.095 W cm^{-2} for *E. coli* and *P. aeruginosa*, 0.060 W cm^{-2} for *S. aureus* and 0.048 W cm^{-2} for *B. subtilis*.

(Fig. 1A), and also the cell viability of the bacteria was not affected by persulphate alone at 37 °C (Fig. 2).

As discussed above, the photolysis of complex **1** in the presence of persulphate activates persulphate and generates reactive species, such as sulphate radicals, hydroxyl radicals (formed by reaction of sulphate radicals with water) and $[Ru(bpy)_3]^{3+}$ (reactions 1–3).[16,21] Importantly, sulphate and hydroxyl radicals are strong oxidants and cause damage to biomolecules, such as protein, DNA and membrane.[5,43–45] Earlier, it has been shown that photolysis of $[Ru(bpy)_3]^{2+}$ and persulphate induced *in vitro* DNA damage.[46] However, no study has been carried out to investigate the effect of activated persulphate on bacteria in aqueous media. The present results show that photochemical activation of persulphate by complex **1** caused complete inactivation of both Gram positive and negative bacteria (Fig. 2, Table 1).

Irradiation of *E. coli* with persulphate and complex **1** in the presence of either methanol (0.1 M) or sodium nitrite (20 mM) for 120 min caused only ~1 log reduction of *E. coli* (Fig. SI 3†). This significant inhibition in photoinactivation of *E. coli* is due to the effective scavenging of hydroxyl and sulphate radicals by methanol and sodium nitrite.[10,29] It is important to note that photodegradation of MO was also inhibited in the presence of sulphate and hydroxyl radical scavengers (Fig. 1B). The above results emphasise that sulphate and hydroxyl radicals produced during photoactivation of persulphate by complex **1** play a major role in the inactivation of *E. coli*.

Photoinactivation of Gram positive strains were faster than Gram negative strains (Table 1, Fig. 2). The cell wall of Gram positive bacteria is relatively simple with two layers, namely the cytoplasmic membrane and peptidoglycan layer, whereas the cell wall of Gram negative bacteria is complex and has an outer lipopolysaccharide membrane in addition to the cytoplasmic membrane and peptidoglycan layer.[34,47–49] This additional layer offers resistance against reactive species generated during irradiation and therefore Gram negative bacteria are less susceptible to photoinactivation than Gram positive bacteria. Earlier reports on photoinactivation of bacteria have also shown that Gram negative bacteria are relatively less susceptible.[34,35,47–51]

The change in cell viability on changing the complex **1** : persulphate ratio was studied using *E. coli* as a model organism. Decreasing either the concentration of complex **1** or persulphate was not favorable for complete photoinactivation of *E. coli* (Fig. 3). It was found that the difference in the photoinactivation of *E. coli* at different complex **1** : persulphate ratios were statistically significant (ANOVA, $p < 0.05$). As discussed above, a relatively lower amount of complex **1** was not sufficient for effective photochemical activation of persulphate to cause inactivation. Activation of a lower concentration of persulphate could generate a relatively lower amount of radicals, which may not be sufficient for complete inactivation. Thus, these results indicate that complete photoinactivation of *E. coli* depends on the concentrations of both complex **1** and persulphate (Fig. 3).

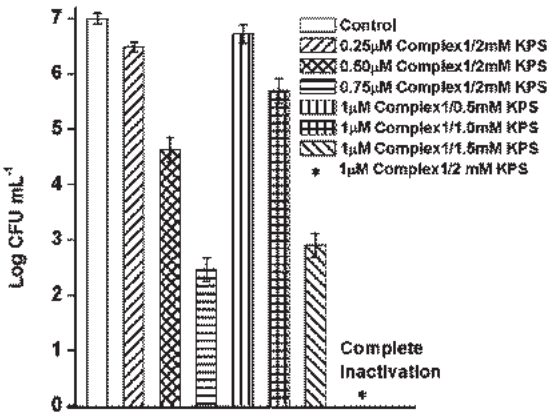

Fig. 3 Photoinactivation of *E. coli* at different [complex **1**] : [persulphate] ratio. Cell concentration = ~10^7 CFU mL^{-1}, [KPS] = 2 mM, [complex **1**] = 1 μM, Light dosage = 513 J cm^{-2}.

Persulphate is a promising oxidant in advanced oxidation processes, and has been shown to degrade organic contaminants effectively on activation in aqueous medium.[10–17] However, the effect of activated persulphate on bacteria in aqueous media is not known. The present study shows the ability of activated persulphate to cause complete inactivation of bacteria in aqueous medium besides the degradation of azo dye MO. Importantly, both photodegradation of MO and photoinactivation of bacteria were achieved using energy efficient LEDs as the visible light source (Fig. SI 2†).[52,53]

3.5. Effect of photoinactivation on cell membrane integrity

In order to study the effect of photolysis of complex **1** and persulphate on cell membrane integrity, BacLight LIVE/DEAD assay was performed using *E. coli*.[36] The fluorescent microscopic image of *E. coli* cells treated with complex **1** and persulphate without irradiation showed only green fluorescence (Fig. 4A), indicating that the cells had intact membranes and allowed only diffusion of green fluorescent SYTO® 9.[36] On irradiation of *E. coli* cells in the presence of complex **1** and persulphate, red fluorescence was observed, indicating the cell membrane damage (Fig. 4B). The loss of cell membrane integrity facilitated entry of PI and competitive binding of red fluorescent PI to DNA with SYTO® 9.

SEM images of *E. coli* cells treated with complex **1** and persulphate without irradiation showed that cells were intact (Fig. 4C). However, irradiation of *E. coli* cells with complex **1** and persulphate resulted in severe deformation of cells with ruptured surfaces and craters (Fig. 4D). Strong oxidizing agents, such as hydroxyl and sulphate radicals, are known to cause biomolecular damage.[43–45] Previous studies on photocatalytic disinfection involving reactive oxidizing species had also shown such membrane damage, leading to cell death.[38,54] Thus, both BacLight LIVE/DEAD assay, as well as SEM image results, clearly revealed cell membrane damage, which indicates oxidative stress caused to *E. coli*.

In addition, agarose gel electrophoresis showed a clear chromosomal DNA band for cells treated with complex **1** and

persulphate in the absence of light. On the other hand, the chromosomal DNA band was not clear for cells treated with complex **1** and persulphate in presence of light. This result indicates that there is significant reduction of chromosomal DNA from photolysed cells (Fig. SI 4†). Similar reduction in chromosomal DNA has been observed in the case of photodynamic inactivation of *E. coli* by 5,10,15,20-tetrakis(1-methylpyridinium-4-yl)porphyrin, due to damage of cell membranes, leading to discharge of cell constituents including DNA.[38] The above results further emphasize loss of cell membrane integrity. To the best of our knowledge, the present study is the first report showing complete inactivation of bacteria due to bacterial membrane damage and loss of chromosomal DNA on the photochemical activation of persulphate in aqueous medium.

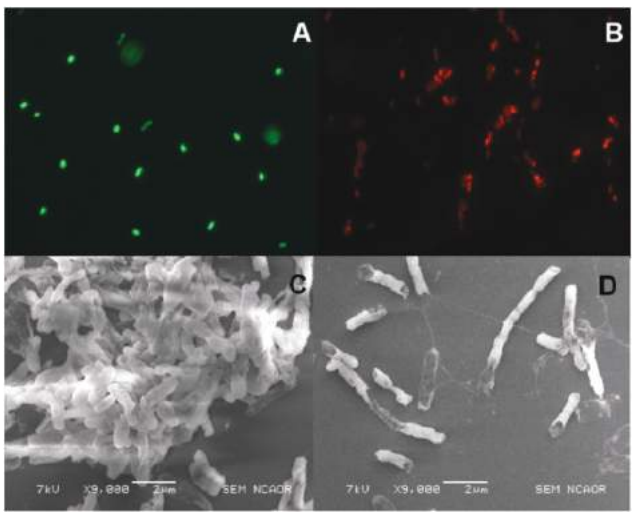

Fig. 4 Fluorescence microscopic images of *E. coli* treated with complex **1** and persulphate (A) in the absence of light (control) (B) in the presence of light. SEM images of *E. coli* treated with complex **1** and persulphate (C) in the absence of light (control) (D) in the presence of light. *E. coli* concentration = $\sim 10^7$ CFU mL^{-1}, [KPS] = 2 mM, [complex **1**] = 1 μM, light dosage = 513 J cm^{-2}.

3.6. Photoinactivation of bacteria in presence of organic compound

Methyl orange is toxic to living organisms[17] whereas resorcinol is a model phenolic pollutant and has been shown to be non toxic to microorganisms (at least up to 10 mg L^{-1}) hence, resorcinol was used to study the effect of organic compounds on the photoinactivation of *E. coli*.[6] Treatment of *E. coli* in the presence of resorcinol 10 mg L^{-1} with or without irradiation, and treatment of *E. coli* with complex **1** (1 μM) and KPS (2 mM) in the presence of resorcinol 10 mg L^{-1} without irradiation did not affect the cell viability (Fig. SI 5†).

The HPLC chromatogram of resorcinol showed a clear peak at retention time (RT) 6 min (Fig. 5A). The HPLC profile of resorcinol after irradiation in the presence of complex **1** and persulphate showed a significant decrease in the resorcinol peak and formation of a new peak at RT 3 min, revealing the degradation of resorcinol (Fig. 5A). Irradiation of resorcinol (5 mg L^{-1}) in the presence of complex **1** and persulphate in PBS (10 mM) caused ~95% degradation of resorcinol (Fig. 5A, Inset-A). Under the same conditions, in the presence of *E. coli* ($\sim 10^7$ CFU mL^{-1}), ~90% degradation of resorcinol (Fig. 5A, Inset-B) and ~5 log reduction in cell viability were observed (Fig. 5B). This result reveals that photoactivation of persulphate by complex **1** has the ability to cause simultaneous degradation of resorcinol and inactivation of *E. coli*. On increasing the concentration of resorcinol to 10 mg L^{-1}, simultaneous photodegradation of resorcinol and photoinactivation of *E. coli* was retarded (Fig. 5A, Inset-D and 5B). Reactive species, such as sulphate and hydroxyl radicals, are diffusible and have non specific reactivity.[5,6,11,16] These radicals can

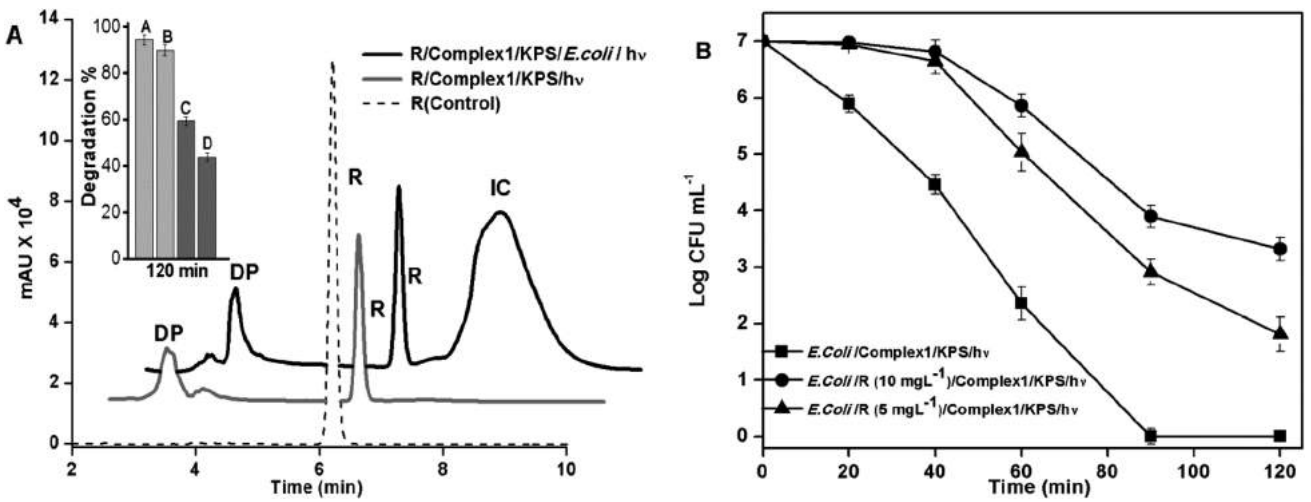

Fig. 5 (A) A HPLC chromatogram showing degradation of resorcinol (10 mg L^{-1}) in the absence and presence of *E. coli*. R – resorcinol, DP – degraded products and IC – intracellular components. Inset – A and B, degradation percentage of resorcinol (5 mg L^{-1}) in the absence and presence of *E. coli*, respectively. C and D, degradation percentage of resorcinol (10 mg L^{-1}) in the absence and presence of *E. coli*, respectively. (B) Cell viability *vs.* time plot for photoinactivation of *E. coli* in the absence and presence of resorcinol (5 and 10 mg L^{-1}). *E. coli* concentration = $\sim 10^7$ CFU mL^{-1}, [complex **1**] = 1 μM, [persulphate] = 2 mM, light dosage = 684 J cm^{-2}.

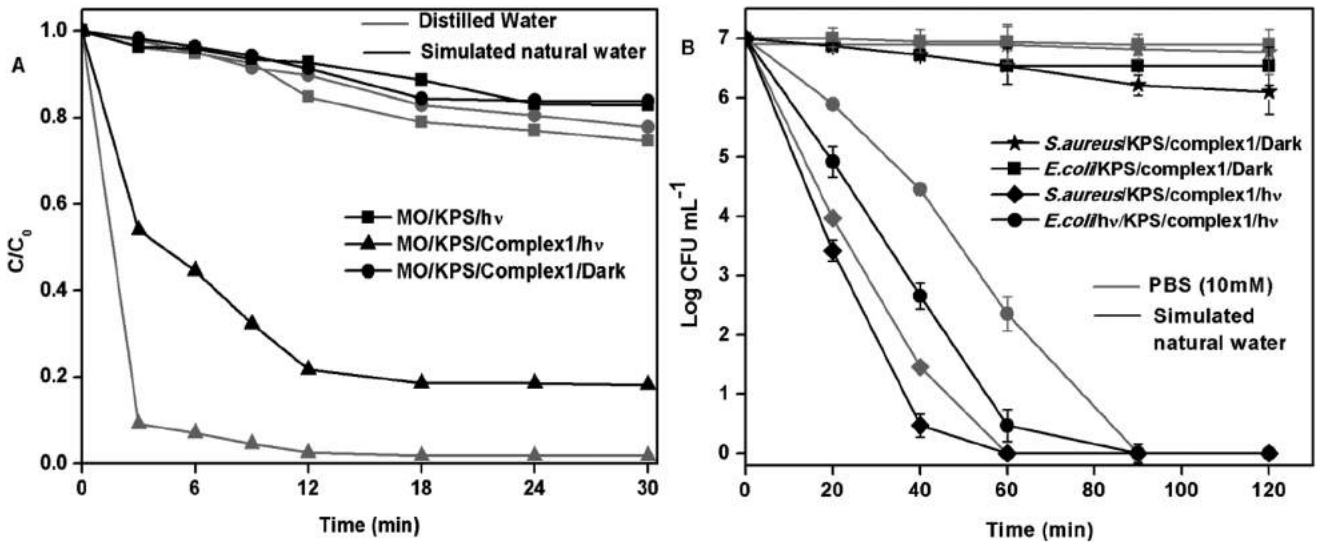

Fig. 6 (A) Photodegradation of MO (12 mg L^{-1}) in simulated ground water, fluence rate = 0.095 W cm^{-2}. (B) Cell viability *vs.* time plot for photo inactivation of *E. coli* and *S. aureus* (~10^7 CFU mL^{-1}) in simulated ground water, fluence rate = 0.095 W cm^{-2} for *E. coli* and 0.060 W cm^{-2} for *S. aureus*. [KPS] = 2 mM, [complex **1**] = 1 μM.

degrade organic compounds, and can also oxidize biomolecules, such as membranes, leading to cell death, thus there is a competitive reaction between organic compounds and microbes.[6,55,56] Thus, at a higher concentration of organic matter (rescorcinol), simultaneous photodegradation of resorcinol and photoinactivation of *E. coli* was retarded. It has been shown that photoinactivation of bacteria by advanced oxidation processes, such as TiO_2 photocatalysis and photo-Fenton process, was affected by the presence of organic matter.[6,55]

Interestingly, the HPLC profile of resorcinol after irradiation in the presence of complex **1** and persulphate containing *E. coli*, showed a wide peak at RT 7–8 min, in addition to the resorcinol peak (RT 6 min), and its degradation product peak (RT 3 min) (Fig. 5B). The absorption spectrum of this new peak had a maximum around 260–280 nm, characteristic of DNA and proteins (Fig. SI 6†). Earlier, it has been shown that loss of membrane integrity results in leakage of cellular components, such as proteins and DNA, that have absorptions in the 260–280 nm range.[57,58] These facts indicate that the wide peak at RT 7–8 min corresponds to intracellular components leaching out of cells due to photodamage of the cell membrane. The above observation further emphasizes the loss of cell membrane integrity.

3.7. Photoinactivation of bacteria in presence of inorganic salts

The photoinactivation of *E. coli* was retarded in the presence of salts, such as 0.1 M of NaH_2PO_4, $NaHCO_3$ and Na_2SO_4 (Fig. SI 3†). As discussed above, ion pair complexation between complex **1** and persulphate is reduced at higher ionic strength, which is not favourable for photoinduced electron transfer between complex **1** and persulphate.[21] Thus, these results indicate that the complete photoinactivation of *E. coli* depends on the composition of ions and ionic strength of the medium, as observed in the photodegradation of MO.

3.8. Effect in simulated ground water

The irradiation of MO in the presence of complex **1** and persulphate in simulated ground water resulted in significant degradation of MO (~80%) (Fig. 6A). In addition, irradiation of bacteria (*E. coli* and *S. aureus*) in the presence of complex **1** and persulphate in simulated ground water also caused complete inactivation of bacteria (Fig. 6B). The slight decrease in percentage of photodegradation of MO when compared with double distilled water could be accounted for by the presence of a variety of inorganic salts and organic matter in simulated ground water. In the case of photoinactivation of bacteria, the relatively less ionic strength of simulated ground water than PBS medium (10 mM) favored complete inactivation. Importantly, the above results reveal that photoactivation of persulphate by complex **1** has the propensity to degrade MO and completely inactivate bacteria in simulated ground water that contained a variety of inorganic ions, and organic matter. As discussed above, both the photodegradation of MO and photoinactivation of *E. coli* were affected in a medium with relatively higher ionic strength and organic content. Therefore, both the photodegradation of MO and photoinactivation of bacteria could be affected in a more complex media than the simulated ground water used in the present study. The inorganic and organic composition of the medium has been shown to affect photolytic water treatment processes such as UV-TiO_2, and the Photo-Fenton process.[6,41]

4. Conclusion

A photolytic process that has the potential to degrade organic contaminants as well as inactivate bacteria in aqueous media has great environmental significance. The present findings

reveal that photochemical activation of persulphate by complex **1** has the potential to degrade azo dyes (methyl orange) as well as inactivate bacteria in aqueous media.

Ruthenium complexes have received interest as potential visible light photosensitizers in environmental studies. These complexes have been used as sensitizers of TiO_2 for the degradation of organic contaminants, and as singlet oxygen sensitizers supported on a solid matrix for solar water disinfection.[59,60] Additionally, ruthenium(II) polypyridyl complexes also have suitable biocompatibility and are studied as photoactive anticancer and antimicrobial agents.[61–63] Although ruthenium complexes are biocompatible, and are required in micromolar amounts for effective photochemical activation of persulphate in the present study, removal of complex from the treated aqueous media would make this system more practicable for actual application to the environment. Moreover, high oxidative conditions could affect the stability of the complex. It is reported that the removal of photosensitiser and its degraded products is important in the photosensitized disinfection of water.[64] Favourably, transition metal ions and their complexes, including $[Ru(bpy)_3]^{2+}$, that are cationic in nature are known to be adsorbed on common adsorbents, such as silica and activated charcoal. Thus these complexes and degraded products could be removed from aqueous media.[65,66] Apart from the use of adsorbents for the removal of photoactive complexes, immobilisation of these molecules on a solid surface is also another possibility of preventing the release of these complexes in water bodies. Development of strategies to immobilise potential photoactive transition metal complexes on solid supports for degradation of bacteria and organic contaminants is currently under progress.

Activation of persulphate is a promising strategy in advanced oxidation process for degradation of organic contaminants.[10–17] Oxidation using persulphate is effective, easy to handle and no toxic byproducts are produced.[10,11,16] The present study enlightens that activation of persulphate by visible light using a photoactive metal complex has the ability to cause degradation of organic contaminants as well as inactivation of bacteria.

Acknowledgements

H. P. acknowledges research grant no. BT/PR133316/GBP/27/251/2009 from Department of Biotechnology (DBT), Government of India. H. P. also acknowledges research support from Aditya Birla Groups, India. G. S. and P. P. acknowledge DBT and Council of Scientific and Industrial Research (CSIR) for fellowships, respectively. We are grateful to Dr Nitin Borkar, Dr Subasranjan Acharya and Vergo Pharma team for TOC measurements. The authors are thankful to Dr Meenal Kowshik, and Dr P. Nandakumar BITS, Pilani, Goa, for providing the bacterial cultures and power meter, respectively. The authors are also thankful to Dr Rahul Mohan, NCAOR (National Centre for Antartic and Ocean Research) for providing the fluorescence microscope and SEM facility.

References

1 D. Zhang, G. Li and J. C. Yu, Inorganic materials for photocatalytic water disinfection, *J. Mater. Chem.*, 2010, **20**, 4529–4536.
2 M. N. Chong, B. Jin, C. W. K. Chow and C. Saint, Recent developments in photocatalytic water treatment technology: a review, *Water Res.*, 2010, **44**, 2997–3027.
3 M. L. Marin, L. Santos-Juanes, A. Arques, A. M. Amat and M. A. Miranda, Organic photocatalysts for the oxidation of pollutants and model compounds, *Chem. Rev.*, 2011, **112**, 1710–1750.
4 G. Ruppert, R. Bauer and G. Heisler, The photo-Fenton reaction – an effective photochemical wastewater treatment process, *J. Photochem. Photobiol., A*, 1993, **73**, 75–78.
5 M. Cho, Y. Lee, H. Chung and J. Yoon, Inactivation of *Escherichia coli* by photochemical reaction of ferrioxalate at slightly acidic and near-neutral pHs, *Appl. Environ. Microbiol.*, 2004, **70**, 1129–1134.
6 A. Moncayo-Lasso, L. E. Mora-Arismendi, J. A. Rengifo-Herrera, J. Sanabria, N. Benitez and C. Pulgarin, The detrimental influence of bacteria (*E. coli*, *Shigella* and *Salmonella*) on the degradation of organic compounds (and *vice versa*) in TiO_2 photocatalysis and near-neutral photo-Fenton processes under simulated solar light, *Photochem. Photobiol. Sci.*, 2012, **11**, 821–827.
7 M. D. Labas, R. J. Brandi, C. S. Zalazar and A. E. Cassano, Water disinfection with UVC radiation and H_2O_2. A comparative study, *Photochem. Photobiol. Sci.*, 2009, **8**, 670–676.
8 N. Klamerth, S. Malato, A. Aguera, A. Fernandez-Alba and G. Mailhot, Treatment of municipal wastewater treatment plant effluents with modified photo-Fenton as a tertiary treatment for the degradation of micro pollutants and disinfection, *Environ. Sci. Technol.*, 2012, **46**, 2885–2892.
9 S. Esplugas, J. Gimenez, S. Contreras, E. Pascual and M. Rodriguez, Comparison of different advanced oxidation processes for phenol degradation, *Water Res.*, 2002, **36**, 1034–1042.
10 T. K. Lau, W. Chu and N. J. D. Graham, The aqueous degradation of butylated hydroxyanisole by UV/$S_2O_8^{2-}$: study of reaction mechanisms *via* dimerization and mineralization, *Environ. Sci. Technol.*, 2006, **41**, 613–619.
11 S. Gokulakrishnan, P. Parakh and H. Prakash, Degradation of Malachite green by potassium persulphate, its enhancement by 1,8-dimethyl-1,3,6,8,10,13-hexaazacyclotetradecane nickel(II) perchlorate complex, and removal of antibacterial activity, *J. Hazard. Mater.*, 2012, **213–214**, 19–27.
12 Y. Q. Gao, N. Y. Gao, Y. Deng, Y. Q. Yang and Y. Ma, Ultraviolet (UV) light-activated persulfate oxidation of sulfamethazine in water, *Chem. Eng. J.*, 2012, **195–196**, 248–253.
13 Y. T. Lin, C. Liang and J. H. Chen, Feasibility study of ultraviolet activated persulfate oxidation of phenol, *Chemosphere*, 2011, **82**, 1168–1172.
14 Y. Deng and C. M. Ezyske, Sulfate radical-advanced oxidation process (SR-AOP) for simultaneous removal of

refractory organic contaminants and ammonia in landfill leachate, *Water Res.*, 2011, **45**, 6189–6194.
15 J. Criquet and N. K. V. Leitner, Degradation of acetic acid with sulfate radical generated by persulfate ions photolysis, *Chemosphere*, 2009, **77**, 194–200.
16 R. H. Waldemer, P. G. Tratnyek, R. L. Johnson and J. T. Nurmi, Oxidation of chlorinated ethenes by heat-activated persulfate: kinetics and products, *Environ. Sci. Technol.*, 2006, **41**, 1010–1015.
17 S. Yang, X. Yang, X. Shao, R. Niu and L. Wang, Activated carbon catalyzed persulfate oxidation of azo dye acid orange 7 at ambient temperature, *J. Hazard. Mater.*, 2011, **186**, 659–666.
18 G. P. Anipsitakis and D. D. Dionysiou, Transition metal/UV-based advanced oxidation technologies for water decontamination, *Appl. Catal., B*, 2004, **54**, 155–163.
19 K. Henbest, P. Douglas, M. S. Garley and A. Mills, Persulphate quenching of the excited state of ruthenium(II) tris-bipyridyl dication: thermal reactions, *J. Photochem. Photobiol., A*, 1994, **80**, 299–305.
20 A. Horvath, Z. Bako, S. Papp and C. S. Keszei, Oxidative quenching of excited $Ru(bpy)_3^{2+}$ with $S_2O_8^{2-}$ at various pH and external magnetic field values, *J. Photochem. Photobiol., A*, 1990, **52**, 271–280.
21 A. L. Kaledin, Z. Huang, Y. V. Geletii, T. Lian, C. L. Hill and D. G. Musaev, Insights into photoinduced electron transfer between $[Ru(bpy)_3]^{2+}$ and $[S_2O_8]^{2-}$ in water: computational and experimental studies, *J. Phys. Chem. A*, 2009, **114**, 73–80.
22 A. L. Kaledin, Z. Huang, Q. Yin, E. L. Dunphy, E. C. Constable, C. E. Housecroft, Y. V. Geletii, T. Lian, C. L. Hill and D. G. Musaev, Insights into photoinduced electron transfer between $[Ru(mptpy)_2]^{4+}$ (mptpy = 4′(4-methylpyridinio)- 2,2′:6′,2″-terpyridine) and $[S_2O_8]^{2-}$: computational and experimental studies, *J. Phys. Chem. A*, 2010, **114**, 6284–6297.
23 X. Y. Yu, Z. C. Bao and J. R. Barker, Free radical reactions involving Cl, Cl_2^-, and SO_4^- in the 248 nm photolysis of aqueous solutions containing $S_2O_8^{2-}$ and Cl^-, *J. Phys. Chem. A*, 2003, **108**, 295–308.
24 J. Costanza, G. Otano, J. Callaghan and K. D. Pennell, PCE oxidation by sodium persulfate in the presence of solids, *Environ. Sci. Technol.*, 2010, **44**, 9445–9450.
25 A. L. Teel, M. Ahmad and R. J. Watts, Persulfate activation by naturally occurring trace minerals, *J. Hazard. Mater.*, 2011, **196**, 153–159.
26 A. Tsitonaki, B. F. Smets and P. L. Bjerg, Effects of heat-activated persulfate oxidation on soil microorganisms, *Water Res.*, 2008, **42**, 1013–1022.
27 S. D. Richardson, B. L. Lebron, C. T. Miller and M. D. Aitken, Recovery of phenanthrene-degrading bacteria after simulated *in situ* persulfate oxidation in contaminated soil, *Environ. Sci. Technol.*, 2010, **45**, 719–725.
28 F. G. Gao and A. J. Bard, Solid-state organic light-emitting diodes based on tris(2,2′-bipyridine)ruthenium(II) complexes, *J. Am. Chem. Soc.*, 2000, **122**, 7426–7427.
29 G. P. Anipsitakis and D. D. Dionysiou, Degradation of organic contaminants in water with sulfate radicals generated by the conjunction of peroxymonosulfate with cobalt, *Environ. Sci. Technol.*, 2003, **37**, 4790–4797.
30 C. Hu, X. Hu, J. Guo and J. Qu, Efficient destruction of pathogenic bacteria with $NiO/SrBi_2O_4$ under visible light irradiation, *Environ. Sci. Technol.*, 2006, **40**, 5508–5513.
31 X. Hu, C. Hu, T. Peng, X. Zhou and J. Qu, Plasmon-induced inactivation of enteric pathogenic microorganisms with $Ag–AgI/Al_2O_3$ under visible-light irradiation, *Environ. Sci. Technol.*, 2010, **44**, 7058–7062.
32 O. Feuerstein, D. Moreinos and D. Steinberg, Synergic antibacterial effect between visible light and hydrogen peroxide on *Streptococcus* mutans, *J. Antimicrob. Chemother.*, 2006, **57**, 872–876.
33 C. S. Enwemeka, D. Williams, S. K. Enwemeka, S. Hollosi and D. Yens, Blue 470 nm light kills methicillin-resistant *Staphylococcus aureus* (MRSA) *in vitro*, *Photomed. Laser Surg.*, 2009, **27**, 221–226.
34 M. Maclean, S. J. MacGregor, J. G. Anderson and G. Woolsey, Inactivation of bacterial pathogens following exposure to light from a 405-nanometer light-emitting diode array, *Appl. Environ. Microbiol.*, 2009, **75**, 1932–1937.
35 C. Arrojado, C. Pereira, J. P. C. Tome, M. A. F. Faustino, M. G. P. M. S. Neves, A. C. Tome, J. A. S. Cavaleiro, A. Cunha, R. Calado, N. C. M. Gomes and A. Almeida, Applicability of photodynamic antimicrobial chemotherapy as an alternative to inactivate fish pathogenic bacteria in aquaculture systems, *Photochem. Photobiol. Sci.*, 2011, **10**, 1691–1700.
36 L. S. Zhang, K. H. Wong, H. Y. Yip, C. Hu, J. C. Yu, C. Y. Chan and P. K. Wong, Effective photocatalytic disinfection of *E. coli* K-12 using $AgBr–Ag–Bi_2WO_6$ nanojunction system irradiated by visible light: the role of diffusing hydroxyl radicals, *Environ. Sci. Technol.*, 2010, **44**, 1392–1398.
37 M. Hartmann, M. Berditsch, J. Hawecker, M. F. Ardakani, D. Gerthsen and A. S. Ulrich, Damage of the bacterial cell envelope by antimicrobial peptides gramicidin S and PGLa as revealed by transmission and scanning electron microscopy, *Antimicrob. Agents Chemother.*, 2010, **54**, 3132–3142.
38 M. Salmon-Divon, Y. Nitzan and Z. Malik, Mechanistic aspects of *Escherichia coli* photodynamic inactivation by cationic tetra-meso(*N*-methylpyridyl)porphine, *Photochem. Photobiol. Sci.*, 2004, **3**, 423–429.
39 S. Kang, M. Herzberg, D. F. Rodrigues and M. Elimelech, Antibacterial effects of carbon nanotubes: size does matter!, *Langmuir*, 2008, **24**, 6409–6413.
40 B. P. Dash and S. Chaudhari, Electrochemical denitrificaton of simulated ground water, *Water Res.*, 2005, **39**, 4065–4072.
41 J. Marugan, R. V. Grieken, C. Pablos and C. Sordo, Analogies and differences between photocatalytic oxidation of chemicals and photocatalytic inactivation of microorganisms, *Water Res.*, 2010, **44**, 789–796.

42 M. G. Antoniou, A. A. de la Cruz and D. D. Dionysiou, Degradation of microcystin-LR using sulfate radicals generated through photolysis, thermolysis and e^- transfer mechanisms, *Appl. Catal., B*, 2010, **96**, 290–298.
43 J. G. Muller, R. P. Hickerson, R. J. Perez and C. J. Burrows, DNA damage from sulfite autoxidation catalyzed by a nickel(II) peptide, *J. Am. Chem. Soc.*, 1997, **119**, 1501–1506.
44 V. Lepentsiotis, J. Domagala, I. Grgic, R. VanEldik, J. G. Muller and C. J. Burrows, Mechanistic information on the redox cycling of nickel(II/III) complexes in the presence of sulfur oxides and oxygen. Correlation with DNA damage experiments, *Inorg. Chem.*, 1999, **38**, 3500–3505.
45 G. T. Gogniat and S. Dukan, TiO_2 photocatalysis causes DNA damage *via* Fenton reaction-generated hydroxyl radicals during the recovery period, *Appl. Environ. Microbiol.*, 2007, **73**, 7740–7743.
46 A. Aboul-Enein and D. Schulte-Frohlinde, Biological deactivation and single-strand breakage of plasmid DNA by photosensitization using tris(2,2′-bipyridyl)ruthenium(II) and peroxydisulfate, *Photochem. Photobiol.*, 1988, **48**, 27–34.
47 L. Bourre, F. Giuntini, I. M. Eggleston, C. A. Mosse, A. J. MacRobert and M. Wilson, Effective photoinactivation of gram-positive and gram-negative bacterial strains using an HIV-1 tat peptide-porphyrin conjugate, *Photochem. Photobiol. Sci.*, 2010, **9**, 1613–1620.
48 G. Jori and S. B. Brown, Photosensitized inactivation of microorganisms, *Photochem. Photobiol. Sci.*, 2004, **3**, 403–405.
49 S. George, M. R. Hamblin and A. Kishen, Uptake pathways of anionic and cationic photosensitizers into bacteria, *Photochem. Photobiol. Sci.*, 2009, **8**, 788–795.
50 A. Minnock, D. I. Vernon, J. Schofield, J. Griffiths, J. Howard Parish and S. B. Brown, Photoinactivation of bacteria. Use of a cationic water-soluble zinc phthalocyanine to photoinactivate both Gram-negative and Gram-positive bacteria, *J. Photochem. Photobiol., B*, 1996, **32**, 159–164.
51 M. Szpakowska, K. Lasocki, J. Grzybowski and A. Graczyk, Photodynamic activity of the haematoporphyrin derivative with rutin and arginine substituents (HpD-Rut_2-Arg_2) against *Staphylococcus aureus* and *Pseudomonas aeruginosa*, *Pharmacol. Res.*, 2001, **44**, 243–246.
52 S. H. Vilhunen and M. E. T. Sillanpaa, Ultraviolet light emitting diodes and hydrogen peroxide in the photodegradation of aqueous phenol, *J. Hazard. Mater.*, 2009, **161**, 1530–1534.
53 J. P. Ghosh, C. H. Langford and G. Achari, Characterization of an LED based photoreactor to degrade 4-chlorophenol in an aqueous medium using coumarin (C-343) sensitized TiO_2, *J. Phys. Chem. A*, 2008, **112**, 10310–10314.
54 Y. Hou, X. Li, Q. Zhao, G. Chen and C. L. Raston, Role of hydroxyl radicals and mechanism of *Escherichia coli* inactivation on Ag/AgBr/TiO_2 nanotube array electrode under visible light irradiation, *Environ. Sci. Technol.*, 2012, **46**, 4042–4050.
55 F. Chen, X. Yang, F. Xu, Q. Wu and Y. Zhang, Correlation of photocatalytic bactericidal effect and organic matter degradation of TiO_2 part I: observation of phenomena, *Environ. Sci. Technol.*, 2009, **43**, 1180–1184.
56 F. Chen, X. Yang and Q. Wu, Photocatalytic oxidation of *Escherischia coli, Aspergillus niger*, and formaldehyde under different ultraviolet irradiation conditions, *Environ. Sci. Technol.*, 2009, **43**, 4606–4611.
57 C. Z. Chen and S. L. Cooper, Interactions between dendrimer biocides and bacterial membranes, *Biomaterials*, 2002, **23**, 3359–3368.
58 D. A. Caminos, M. B. Spesia, P. Pons and E. N. Durantini, Mechanisms of *Escherichia coli* photodynamic inactivation by an amphiphilic tricationic porphyrin and 5,10,15,20-tetra(4-*N*,*N*,*N*-trimethylammoniumphenyl) porphyrin, *Photochem. Photobiol. Sci.*, 2008, **7**, 1071–1078.
59 Y. Cho, W. Choi, C. H. Lee, T. Hyeon and H. I. Lee, Visible light-induced degradation of carbon tetrachloride on dye-sensitized TiO_2, *Environ. Sci. Technol.*, 2001, **35**, 966–970.
60 F. Manjon, M. Santana-Magana, D. Garcia-Fresnadillo and G. Orellana, Singlet oxygen sensitizing materials based on porous silicone: photochemical characterization, effect of dye reloading and application to water disinfection with solar reactors, *Photochem. Photobiol. Sci.*, 2010, **9**, 838–845.
61 B. S. Howerton, D. K. Heidary and E. C. Glazer, Strained ruthenium complexes are potent light-activated anticancer agents, *J. Am. Chem. Soc.*, 2012, **134**, 8324–8327.
62 W. Lei, Q. Zhou, G. Jiang, B. Zhang and X. Wang, Photodynamic inactivation of *Escherichia coli* by Ru(II) complexes, *Photochem. Photobiol. Sci.*, 2011, **10**, 887–890.
63 A. Bolhuis, L. Hand, J. E. Marshall, A. D. Richards, A. Rodger and J. Aldrich-Wright, Antimicrobial activity of ruthenium-based intercalators, *Eur. J. Pharm. Sci.*, 2011, **42**, 313–317.
64 N. A. Kuznetsova, D. A. Makarov, O. L. Kaliya and G. N. Vorozhtsov, Photosensitized oxidation by dioxygen as the base for drinking water disinfection, *J. Hazard. Mater.*, 2007, **146**, 487–491.
65 M. Ogawa, T. Nakamura, J.-i. Mori and K. Kuroda, Luminescence of tris(2,2′-bipyridine)ruthenium(II) cations ($[Ru(bpy)_3]^{2+}$) adsorbed in mesoporous silica, *J. Phys. Chem. A*, 2000, **104**, 8554–8556.
66 P. Zhang, J. Guo, Y. Wang and W. Pang, Incorporation of luminescent tris(bipyridine)ruthenium(II) complex in mesoporous silica spheres and their spectroscopic and oxygen-sensing properties, *Mater. Lett.*, 2002, **53**, 400–405.

RSC Advances

PAPER

Cite this: *RSC Adv.*, 2015, **5**, 31716

Nickel azamacrocyclic complex activated persulphate based oxidative degradation of methyl orange: recovery and reuse of complex using adsorbents†

Gokulakrishnan Subramanian,[a] Pranav Nalawade,[a] Steven J. Hinder,[b] Suresh C. Pillai[cd] and Halan Prakash*[a]

Received 23rd February 2015
Accepted 16th March 2015

DOI: 10.1039/c5ra03350k

www.rsc.org/advances

Adsorbents are useful for the removal of metal complex based catalysts from the reaction medium. Moreover, effective catalysts may be recycled with the use of adsorbents. These facts inspired us to investigate the use of adsorbents for the recovery and reuse of a metal complex that could activate persulphate to effectively degrade an organic pollutant in water. Herein, we report the nickel complex (C1) activated persulphate based degradation of methyl orange (MO) in water and the removal of C1 using activated carbon (AC) and Amberlite (Am) as adsorbents. C1 adsorbed onto AC (C1–AC) was reused in the solid form to activate persulphate and degrade MO without leaching C1 into water. Additionally, solid C1–Am recovered from the degraded MO solution was ion exchanged using sodium chloride to obtain C1, which was reused for MO degradation. The study demonstrates the application of adsorbents such as AC and Am for the adsorptive recovery and reuse of a metal complex based persulphate activator.

Introduction

Adsorption of homogeneous catalysts onto solid supports is useful for the recovery and reuse of catalysts.[1–4] Remarkably, metal complexes adsorbed onto solid supports *via* non-covalent bonding, such as π–π[5,6] and ionic interactions,[2,7] have been shown as reusable solid catalysts for the reduction[7] and oxidation of organic compounds[2,6,8] in the presence or absence of peroxides.

In addition, homogeneous metal ions and complexes are excellent for the activation of peroxo compounds, such as peroxides (hydrogen peroxide and alkyl peroxides)[9,10] and persulphates (peroxydisulphate and peroxymonosulphate),[11–15] to generate highly reactive radical oxidants that cause rapid oxidative degradation and mineralization of organic pollutants in wastewater.[12–21] Particularly, persulphate activation by homogeneous transition metal ions and complexes have gained attention as an advanced oxidation process (AOP) for the degradation of organic pollutants such as dyes,[13,14,16] antibiotics,[17] pesticides,[18] and cyanobacterial toxins[12,20] in water.[21]

Earlier, we reported that complexes, such as a redox active nickel(II) azamacrocyclic complex (C1, Chart 1; L = 1,8-dimethyl-1,3,6,8,10,13-hexaazacyclotetradecane) and a photoredox active $[Ru(II)(bpy)_3]^{2+}$ complex (where bpy = bipyridine), were useful for the activation of persulphate (KPS, potassium persulphate, $K_2S_2O_8$), which effectively degraded persistent, carcinogenic organic dye pollutants in water.[13,14] Homogeneous redox active nickel complex C1 activated the persulphate anion *via* an ion-pair mechanism with the generation of a reactive sulphate radical, a hydroxyl radical and a trivalent nickel 290 nm species that oxidize organic pollutants (reaction (1)–(7)).[13,22,23] It should be noted that transition metal ions and metal complexes are left over in water after the degradation of organic pollutants by the activation of persulphate.

Recovery and reuse of heterogeneous persulphate activators, with minimal release of metal ions during the persulphate activation and degradation of organic pollutants, have been studied. Mainly, these heterogeneous activators were prepared by methods involving wet impregnation, doping, co-precipitation, and calcinations and covalent modifications.[16,24–28]

$$[Ni(II)L]^{2+} + S_2O_8^{2-} \leftrightarrow \underset{\text{ion-pair}}{\{Ni(II)L^{2+} + S_2O_8^{2-}\}} \quad (1)$$

[a]*Department of Chemistry, Birla Institute of Technology and Science, Pilani, K.K. Birla Goa Campus, NH17B, Zuarinagar, Goa, 403 726, India. E-mail: halanprakash@goa.bits-pilani.ac.in*

[b]*The Surface Analysis Laboratory, Department of Mechanical Engineering Sciences, University of Surrey, Guildford, Surrey, GU2 7XH, UK*

[c]*Nanotechnology Research Group, Department of Environmental Sciences, Institute of Technology Sligo, Sligo, Ireland*

[d]*Centre for Precision Engineering, Materials and Manufacturing Research (PEM), Institute of Technology Sligo, Sligo, Ireland*

† Electronic supplementary information (ESI) available. See DOI: 10.1039/c5ra03350k

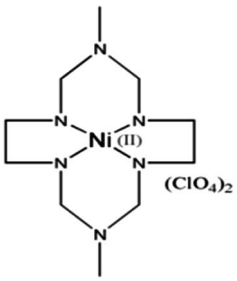

Chart 1 Structure of C1, 1,8-dimethyl-1,3,6,8,10,13-hexaazacyclotetradecane.

$$\{Ni(II)L^{2+} + S_2O_8^{2-}\} \rightarrow [Ni(III)L(SO_4)]^+ + SO_4^{\bullet -} \quad (2)$$

$$[Ni(II)L]^{2+} + SO_4^{\bullet -} \rightarrow [Ni(III)L(SO_4)]^+ \quad (3)$$

$$SO_4^{\bullet -} + \text{organic pollutant} \rightarrow \text{oxidative degradation} \quad (4)$$

$$SO_4^{\bullet -} + H_2O \leftrightarrow OH^{\bullet} + H^+ + SO_4^{2-} \quad (5)$$

$$OH^{\bullet} + \text{organic pollutant} \rightarrow \text{oxidative degradation} \quad (6)$$

$$[Ni(III)L(SO_4)]^+ + \text{organic pollutant} \rightarrow [Ni(II)L]^{2+} + SO_4^{2-} + \text{oxidative degradation} \quad (7)$$

where $[Ni(II)L]^{2+}$ = C1 with nickel in divalent state with absorption maximum at 446 nm; $[Ni(III)L(SO_4)]^+$ = C1 in trivalent form with absorption maximum at 290 nm.

Notably, adsorbents are useful for the removal of metal ions from wastewater and for the easy separation of effective metal based catalysts.[29–31] Moreover, adsorbents may be useful to recycle the effective catalysts,[32–34] as mentioned above. These facts inspired us to employ adsorbents in a metal complex activated persulphate based AOP for the recovery and reuse of the complex.

Earlier, it has been reported that nickel azamacrocylic complexes adsorbed onto solids showed redox reactivity.[35,36] These reports indicated that a nickel azamacrocyclic complex adsorbed onto supports would react with persulphate and act as a reusable solid persulphate activator. Importantly, adsorbents such as activated carbon (AC)[29–31] and Amberlite (Am)[32–34] have been used to recover metal ions from wastewater, and also to recover and reuse metal complex catalysts. Hence, herein, we have investigated a C1 activated persulphate (KPS) based advanced oxidation process (AOP) to degrade a persistent dye pollutant, methyl orange (MO), and the adsorptive recovery and reuse of C1 using the adsorbents AC and Am.

Experimental section

Materials and reagents

Nickel chloride hexahydrate ($NiCl_2 \cdot 6H_2O$), potassium persulphate (KPS, $K_2S_2O_8$), sulphuric acid (H_2SO_4), sodium hydroxide (NaOH), methyl orange, potassium iodide (KI), starch, sodium chloride (NaCl), acetic acid (CH_3COOH), formic acid (HCOOH), hydrochloric acid (HCl), sodium thiosulphate ($Na_2S_2O_3$), potassium dichromate ($K_2Cr_2O_7$), ethyl acetate, tertiary butyl alcohol and ethanol were of guaranteed analytical grade, from SD Fine Chemicals, India. Amberlite^R IR-120 and activated carbon were purchased from SD Fine Chemicals, India. Nitrogen adsorption–desorption based surface area and pore size values of activated carbon were found to be 248.8 $m^2\ g^{-1}$ and 3.5 nm, respectively, while the surface area and pore size values of Amberlite were 42.1 $m^2\ g^{-1}$ and 23.5 nm, respectively. C1 was prepared as reported earlier.[37] Briefly, to a methanolic solution (50 mL) of $NiCl_2 \cdot 6H_2O$ (11.5 g), ethylenediamine 99% (6.8 mL), formaldehyde 36% (20 mL), and methylamine (8.6 mL) were added and stirred at reflux conditions for 24 hours. The resulting orange solution was cooled and filtered. The desired complex was precipitated after adding excess perchloric acid to the filtrate.

For HPLC analysis, acetonitrile (HPLC grade) and Millipore water were used. The stock solutions of MO, complex C1, and KPS were prepared using double distilled water. Simulated ground or natural water was prepared by the addition of following components to distilled water, as reported earlier: $FeNO_3$ (0.24 μm), $NaHCO_3$ (1.2 mM), Na_2SO_4 (0.34 mM), Na_2HPO_4 (0.28 mM), NaCl (0.86 mM) and resorcinol (1 ppm).[14] Freshly prepared KPS solution was used for all the experiments.

Degradation of MO by KPS using C1

For the degradation of methyl orange (MO), an appropriate amount of aqueous MO (20–30 mg L^{-1}) solution was taken with and without C1 (C1 in the range of 12–49 mg L^{-1}), and the reaction was initiated by the addition of the required amount of KPS (5 g L^{-1} to 0.5 g L^{-1}). Reaction volume was maintained at 5 mL, unless otherwise mentioned. The reaction was carried out at room temperature. Initially, the pH of the solution was ~7. The degradation of MO was studied by following the decrease in absorption maximum at 464 nm of MO with respect to time, using a JASCO V-570 UV/VIS/NIR spectrophotometer. The degradation of MO by (i) KPS alone, (ii) KPS and $Ni(II)Cl_2 \cdot 6H_2O$ was performed as a control experiment. Pseudo-first order rate constant (k) for the degradation of MO was determined from the C/C_0 *vs.* time plot. Initial concentrations of C1, KPS and MO were varied and (k) values for the degradation of MO were determined. The optimised condition for MO degradation was determined to be MO (20 mg L^{-1}), C1 (48.3 mg L^{-1}), KPS (1 g L^{-1}), based on the rate constant (k) analysis.

A Shimadzu UFLC Prominence system with SPDM 20A Prominence diode array detector, equipped with Phenomenex C18 HPLC column (250 mm × 4.5 mm, 5 μm), was used for high pressure liquid chromatography (HPLC) analysis. A 70 : 30 (v/v) mixture of ammonium acetate buffer (pH 4.5)/acetonitrile was used as the mobile phase, in isocratic mode, with a flow rate of 1 mL min^{-1}. For each analysis, 100 μL of the sample taken from the appropriate reaction mixture was injected and the degradation of MO was monitored at 464 nm.

A Shimadzu IR-Affinity-1 FTIR spectrophotometer was used for Fourier transform infrared (FTIR) analysis of MO degradation. After the treatment of MO with KPS and C1, the reaction mixture was completely evaporated using a rotary evaporator.

Degraded intermediates present in this dry residue were extracted with ethanol and ethyl acetate, and then evaporated to solid residues for FTIR analysis. In the liquid chromatography mass spectrometry (LCMS) analysis, a Vantage TSQ triple stage quadrupole mass spectrometer (Thermo Fisher Scientific, San Jose, CA, USA) equipped with heated electro spray ionization (HESI) was used. The mass spectrometer is coupled with an Agilent 1290 Infinity UHPLC system (Agilent Technologies India Pvt. Ltd., India). The UHPLC was provided with a column oven (set at 40 °C), an auto-sampler and a thermo-controller (set at 4 °C). A flow-through injection mode equipped with a needle wash system was used (with acetonitrile, 0.1% formic acid) before injection to ensure zero percent carry over problems. The UHPLC system was equipped with a Luna C-18(2) column (4.6 × 150 mm, 5 μm, Phenomenex, Inc.). Mobile phase: Solvent A was 10 mM ammonium acetate containing 0.1% formic acid; and Solvent B was acetonitrile containing 0.1% formic acid. The binary gradient was optimized to get maximum separation (gradient: 5% B at 0 min, 5% B at 3 min, 90% B at 15 min, 0% B at 15–17 min) at a flow rate of 300 μL min^{-1}. Operating conditions were as follows: spray voltage 4000 V; ion transfer capillary temperature 270 °C; source temperature 300 °C; sheath gas 20, auxiliary gas 10 (arbitrary units) and ion polarity negative; full scan analysis 50 to 400 *m*/*z* with the scan time of 500 milliseconds. 10 μL of the sample from appropriate reaction mixture of MO, KPS and C1 was injected after specific time intervals.

A Sievers 900 TOC analyser was used for total organic carbon (TOC) analysis during degradation. An aliquot of 20 mL reaction solution was taken at specific time intervals from the reaction mixture (100 mL) containing MO (20 mg L^{-1}), KPS (1 g L^{-1}) and C1 (48.3 mg L^{-1}) and injected into the TOC analyser.

Redox reaction between C1 (48.3 mg L^{-1}) and KPS (1 g L^{-1}), leading to formation of trivalent nickel 290 nm species, was monitored at its absorption maximum at 290 nm, similar to the reaction of tetraazamacrocyclic nickel complex with ammonium persulphate, as reported by Haines *et al.* (Fig. S1†).[22,23] C1 existing predominantly as trivalent nickel 290 nm species was prepared by incubating the reaction mixture containing KPS and C1 (Fig. S1†).[22,23] Reactivity of trivalent nickel 290 nm species with MO was monitored by following the absorption spectral changes of MO. The concentration of KPS during MO degradation in the presence and absence of C1 was determined by iodometric titration, as reported earlier.[38,39] Tertiary butyl alcohol and ethanol were used as scavengers for sulphate and hydroxyl radicals, as reported earlier.[11,40]

Adsorption of C1 onto activated carbon (AC) and amberlite (Am)

Langmuir and Freundlich adsorption equations were used to determine the adsorptivity (K_F and q_m values) of C1 onto AC and Am.[41,42]

$$\text{Langmuir isotherm: } q_e = \frac{q_m K_a C_e}{1 + K_a C_e}$$

$$\text{Freundlich Isotherm: } q_e = K_F C_e^{1/n}$$

q_e = amount of adsorbate adsorbed on to the adsorbent (mg g^{-1}) at equilibrium; C_e = equilibrium concentration of adsorbate in the solution (mg L^{-1}); $q_{m(L)}$ = Langmuir maximum adsorption capacity (mg g^{-1}); K_a = Langmuir constant (L mg^{-1}); K_F = Freundlich constant indicative of relative adsorption capacity of the adsorbent ($[mg^{1-(1/n)}\ L^{1/n}]\ g^{-1}$); $1/n$ = Freundlich constant, which is indicative of the intensity of adsorption. Freundlich maximum adsorption capacity was determined from the equation $K_F = q_m/{C_0}^{1/n}$, where q_m is Freundlich maximum adsorption capacity (mg g^{-1}), K_F is the Freundlich constant indicative of relative adsorption capacity of the adsorbent ($[mg^{1-(1/n)}\ L^{1/n}]\ g^{-1}$), and C_0 is the initial concentration of adsorbate in the bulk solution (mg L^{-1}).[41,42]

The equilibrium concentration of C1 during adsorption was determined by following the absorption of C1. In the absence of KPS, the concentration of C1 in the divalent state was followed by monitoring the d–d absorption maximum at 446 nm. In the presence of KPS, the concentration of C1 in the trivalent state was followed by monitoring the absorption band maximum around 290 nm.[22,23]

C1–AC was prepared by adding AC (1 g) to 100 mL of C1 (4.25 mM). This suspension was stirred overnight. Supernatant obtained after removing AC was filtered using a 0.45 μM polytetrafluoroethylene (PFTE) membrane filter, and the absorption spectrum of the filtrate was recorded to determine the adsorption. Then, the C1 immobilized onto AC (C1–AC) was removed by filtration and washed thrice with distilled water, and finally dried in a desiccator. The loading of C1 in C1–AC was determined to be 160.6 mg of C1 per gram of AC (16.0%). Similarly, for the preparation of C1–Am, Am (1 g) was added to 50 mL of C1 (4.25 mM). The loading of C1 in C1–Am was determined to be 96.4 mg of C1 per gram of Am (9.64%). X-ray photoelectron spectroscopy (XPS) measurements were carried out using a Thermo Fisher Scientific (East Grinstead, UK) θ probe spectrometer and monochromatic Al-Kα radiation (photon energy 1486.6 eV). The adsorption of MO onto AC was studied by following the absorbance of MO at 464 nm.

Degradation of MO by KPS using C1 adsorbed onto AC (C1–AC) and Am (C1–Am)

The degradation of MO (30 mg L^{-1}) by KPS (1 g L^{-1}) using C1–AC (0.3 g L^{-1}, 16.0% C1 loading)/C1–Am (0.5 g L^{-1}, 9.64% C1 loading) was studied spectrophotometrically, as mentioned above for the homogeneous degradation of MO. The suspension of 0.3 g L^{-1} of C1–AC with 16.0% C1 loading or 0.5 g L^{-1} of C1–Am with 9.64% C1 loading in reaction mixture (5 mL) corresponds to an effective concentration of 48.3 mg L^{-1} of C1, similar to the amount of C1 used in the homogeneous condition. Control experiments (i) bare AC/Am (without C1) and MO in the presence of KPS and (ii) C1–AC/C1–Am and MO in the absence of KPS were performed. Reuse of C1–AC for MO degradation was studied by performing a cyclic degradation experiment in the presence and absence of KPS. After each cycle, C1–AC was removed by centrifugation and reused for the subsequent cycle. Degraded MO solution obtained from each cycle was analysed for the presence of C1 (as nickel) by AAS.

Similarly, the reuse of C1–AC for MO degradation in simulated natural water was also performed. The concentration of C1 in the MO degraded solution was monitored by the determination of nickel content using an atomic absorption spectrometer (AAS) (Perkin Elmer, AAS 400), as well as by following the change in the absorption of C1. Ion exchange (extraction) of C1 that was adsorbed onto Am was performed by eluting with 0.17 M NaCl solution. Degradation of MO using the C1 that was extracted from C1–Am was performed similar to the protocol mentioned above.

Results and discussion

Homogeneous C1 activated persulphate and degradation of MO

Absorption spectral results revealed that the degradation of MO (20 mg L^{-1}) by KPS (1 g L^{-1} to 5 g L^{-1}) was slow and incomplete after 60 min of reaction (Fig. 1A and B). On the other hand, MO (20 mg L^{-1}) was rapidly degraded by KPS (1 g L^{-1}) in the presence of persulphate activator C1 (48.3 mg L^{-1}) within 10 min, with a pseudo-first order rate constant value (k) of 3.9 ± 0.07 s^{-1} (Fig. 2A and 1B). The effects of initial concentrations of MO, KPS and C1 on k value for the degradation of MO were determined (Table 1). k value increased with increase in the initial concentration of C1 and KPS; however, k value decreased with increase in the initial concentration of MO. It was observed that $NiCl_2 \cdot 6H_2O$ (without azamacrocyclic ligand) had no effect on the degradation of MO by KPS, unlike redox active C1 (Fig. 1B). Thus, these results revealed that the persulphate activator C1 is required for the rapid and complete degradation of MO by KPS (1 g L^{-1}) (Fig. 1B and Table 1).

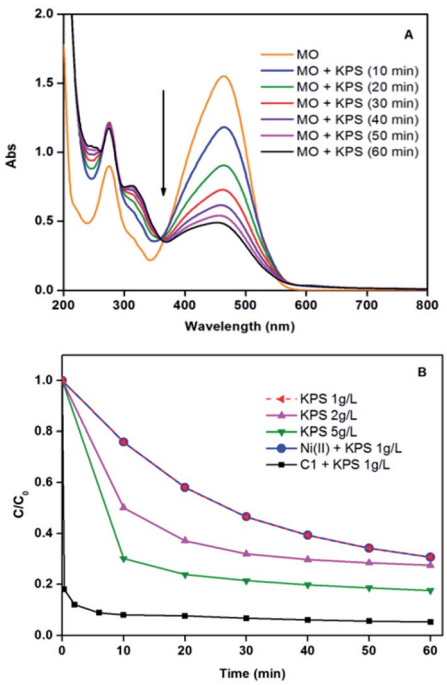

Fig. 1 (A) Absorption spectra showing the degradation of MO by KPS. (B) C/C_0 plot showing the degradation of MO in the presence of KPS, KPS + C1, and $NiCl_2 \cdot 6H_2O$ + KPS. [MO] = 20 mg L^{-1}; [C1] = 48.3 mg L^{-1}; [$NiCl_2 \cdot 6H_2O$] = 23.7 mg L^{-1}.

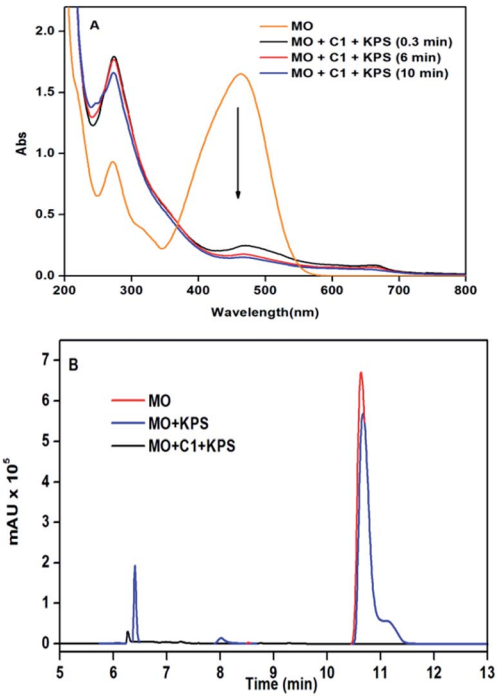

Fig. 2 (A) Absorption spectra showing the degradation of MO by KPS in the presence of C1. (B) HPLC chromatogram of MO (red), MO degraded by KPS (blue), and MO degraded by KPS in the presence of C1 (black). [MO] = 20 mg L^{-1}; [KPS] = 1 g L^{-1}; [C1] = 48.3 mg L^{-1}. Treatment time = 10 min.

Further, the MO peak at retention time 11 min, observed in the HPLC chromatogram, rapidly disappeared in the presence of KPS and C1 (Fig. 2B). However, a prominent MO peak was observed in the presence of KPS alone (Fig. 2B). Thus, the HPLC results also revealed that the degradation of MO by KPS in the presence of C1 was rapid and complete, whereas degradation of MO was slow and incomplete by KPS alone.

The N=N-stretching peak at 1608 cm^{-1} of the azo group was absent from the FTIR spectra of ethanol and ethyl acetate extract residues of MO degraded by KPS in the presence of C1 (Fig. S2†). Moreover, the IR spectra of degraded MO showed

Table 1 Pseudo-first order rate constants determined for the degradation of MO by KPS under different concentrations of MO, C1 and KPS[a]

C1 ppm (mg L^{-1})	KPS (g L^{-1})	MO (mg L^{-1})	Rate constant k (s^{-1})
12.07	1	20	0.55 ± 0.01
24.15	1	20	1.16 ± 0.03
48.3	1	20	3.90 ± 0.07
48.3	0.5	20	1.06 ± 0.03
48.3	2	20	3.82 ± 0.11
48.3	1	50	1.96 ± 0.07
48.3	1	100	0.66 ± 0.02

[a] Room temperature; initial pH ~ 7.

peaks at 3000 cm^{-1} and 2785 cm^{-1} due to –C–H-stretching; 1223 cm^{-1} because of C–N-stretching; 858 cm^{-1} and 1051 cm^{-1} corresponding to aromatic ring vibrations, and 587 cm^{-1} and 692 cm^{-1} due to –C–S- and S=O-stretching, respectively (Fig. S2†).[43–45] These IR results indicated the loss of the characteristic azo group of MO, and transformation to aromatic amine and sulphonated intermediates during degradation.

The total ion chromatogram (TIC) of MO showed a single peak at RT 14.4 min (Fig. S3A†) corresponding to 304 *m*/*z* of MO (Fig. S4†). This MO peak was completely absent in the TIC of MO degraded by KPS in the presence of C1 (Fig. S3D†), whereas a prominent MO peak was observed in the TIC of MO degraded by KPS alone (Fig. S3B†). Some of the degradation intermediates (Fig. S3B–D and S4,† Table 2) of MO observed during the reaction are similar to those reported earlier.[46–48] Degradation intermediates 200 *m*/*z* (RT 12.5 min) and 290 *m*/*z* (RT 13.7 min) disappeared from the TIC of MO degraded by KPS in the presence of C1, within 30 min (Fig. S3C and D†), whereas these peaks were clearly observed in the TIC of MO degraded by KPS alone, even after 60 min (Fig. S3B†).

The loss of MO and the significant reduction in the degraded intermediates by KPS in the presence of C1 indicated that the combination of KPS and C1 could lead to the mineralization of MO. One hour of treatment of MO (20 mg L^{-1}) with KPS (1 g L^{-1}) in the presence of C1 (48.3 mg L^{-1}) caused about 75% reduction of TOC, whereas only 10% TOC reduction was observed after one hour of treatment of MO by KPS alone (1 g L^{-1}). Thus, the significant reduction in the TOC revealed the ability of KPS and C1 to effectively degrade and mineralize MO.

Earlier, Haines *et al.* reported that the reaction between nickel(II) azamacrocyclic complex and ammonium persulphate rapidly generated sulphate radicals and a trivalent nickel 290 nm species *via* an ion-pair mechanism (reaction (1)–(3)).[22,23] The sulphate radical is non-selective and a highly reactive oxidant. It has been shown that the sulphate radical can oxidise a wide variety of organic pollutants (reaction (4)) such as dyes,[13,14,16] antibiotics,[17] pesticides,[18] cyanobacterial toxins,[19,20,49] as well as microbial pollutants[14,15] and toxic metal ions.[50]

Table 2 Proposed degradation intermediates of MO

Min (RT)	Mol. Wt	Proposed structure
11.6	157	
12.5	200	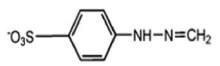
13.66	240	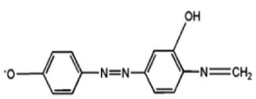
13.7	290	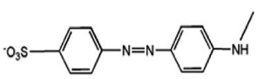

Additionally, sulphate radical also reacts with water in acidic and neutral conditions to produce hydroxyl radical, which has the potential to oxidise organic substrates (reaction (5)).[11,13,21] The rate of degradation of MO by KPS and C1 was retarded in the presence of radical scavengers such as tertiary butyl alcohol and ethanol (Fig. 3 and Table 3), indicating that both sulphate and hydroxyl radicals are involved in the degradation of MO. Similar results were reported for the activation of persulphate using metal ions (Fe^{2+}, Fe^{3+} and Ag^{+}) for the degradation of halocarbon.[11]

Degradation of MO was also observed for the solution that has C1 predominantly as trivalent nickel 290 nm species in the presence of KPS (Fig. S5†). Moreover, it was determined by iodometric titration that about 21% (0.21 g L^{-1}) of KPS was consumed for the degradation of MO (20 mg L^{-1}) by KPS (1 g L^{-1}) in the presence of C1 (48.3 mg L^{-1}) (within 10 min), whereas only 4% (0.04 g L^{-1}) of KPS was consumed for the reaction between MO (20 mg L^{-1}) and KPS (1 g L^{-1}) without C1 (after 60 min of reaction). These results indicate that the trivalent nickel 290 nm species oxidised MO (reaction (7)) and reduced to the divalent state. The resulting divalent C1 could be oxidised by KPS (reaction (1)–(3)), leading to higher consumption of KPS (more than the stoichiometric amount of C1), as revealed by titration experiments.

Earlier it was shown that trivalent nickel complexes could oxidise organic substrates (reaction (7)).[13,51,52] All the above results highlight that C1 has the ability to activate persulphate and cause the degradation of MO, as proposed in the reactions (1)–(7).

Although homogeneous C1 activated KPS and degraded MO, it is important to recover C1 from the solution and reuse. The results on the adsorptive recovery and reuse of C1 using adsorbents for water remediation,[29–34] such as AC and Am, are presented below.

Recovery and reuse of C1 using adsorbents

Adsorption of C1 onto AC and Am adsorbents were determined to follow the Freundlich adsorption isotherm model (Fig. 4 and

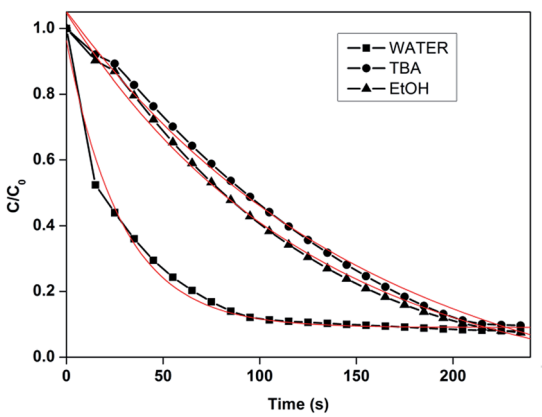

Fig. 3 Effect of radical scavengers on the rate of degradation of MO by KPS and C1. [C1] = 100 μM; [KPS] = 1 g L^{-1}; [MO] = 50 mg L^{-1}; [TBA] = 0.5 M; [ethanol] = 0.5 M.

Table 3 Degradation of MO by C1 activated KPS in the presence of radical scavengers[a]

Scavenger	Pseudo-first order rate constant k (s^{-1})
TBA (0.5 M)	0.38 ± 0.02
Ethanol (0.5 M)	0.47 ± 0.01
None	1.96 ± 0.07

[a] [C1] = 100 (mg L^{-1}); [KPS] = 1 g L^{-1}; [MO] = 50 (mg L^{-1}).

S6†), and their adsorptivity parameters are tabulated (Table 4 and S1†). AAS results revealed the absence of C1 in water (not detectable, and less than 1 mg L^{-1}) after the recovery of C1 using adsorbents. Thus, AC and Am are useful for adsorptive recovery of C1 in the presence of persulphate, in which C1 existed as trivalent nickel 290 nm species (Fig. 2A and S5†), as well as for the recovery of C1 with nickel in divalent state in the absence of persulphate.

The X-ray photoelectron spectrum of C1 adsorbed onto AC (C1–AC) showed peaks at 400.3 eV and 855.9 eV that correspond to the binding energy of nitrogen (N1s) atom and divalent nickel atom of C1 ($Ni2p_{3/2}$), respectively (Fig. 5).[53–59] C1 adsorbed onto Am (C1–Am) also showed similar peaks (Fig. S7†). The ability of solid C1–AC and C1–Am to activate persulphate and degrade MO was investigated, and the results are presented below.

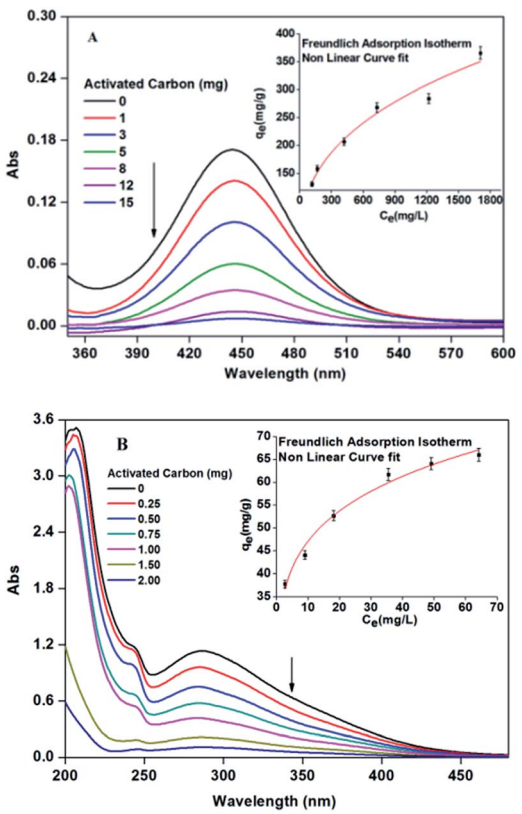

Fig. 4 Adsorption of C1 onto activated carbon without KPS (A) and with KPS (B). Inset shows the non-linear fitting for the Freundlich adsorption isotherm.

Table 4 Freundlich adsorption isotherm parameters for the adsorption of C1 onto Amberlite and activated carbon in the presence and absence of KPS

Freundlich adsorption isotherm					
Adsorbent	Adsorbate	K_F	$1/n$	q_m	R^2
Am	C1[a]	2.27	0.20	6.1	0.989
AC	C1[a]	30.37	0.20	75.8	0.981
Am	C1[b]	8.61	0.33	106.9	0.979
AC	C1[b]	24.06	0.36	375.6	0.964

[a] C1 in presence of KPS. [b] C1 in absence of KPS; $[C1]_0$ = 2.06 g L^{-1} for Am and AC. K_F = Freundlich constant indicative of equilibrium adsorption capacity of the adsorbent ([$mg^{1-(1/n)}$ $L^{1/n}$] g^{-1}); $1/n$ = Freundlich constant indicative of intensity of adsorption; q_m = Freundlich maximum adsorption capacity (mg g^{-1}). R^2 = correlation coefficient.

MO (30 mg L^{-1}) was rapidly degraded by KPS (1 g L^{-1}) in the presence of C1–AC (0.3 g L^{-1}, 16% loaded C1) within 10 min (Fig. 6 A). On the other hand, the degradation of MO (30 mg L^{-1}) by KPS (1 g L^{-1}) in the presence of AC (0.3 g L^{-1} of bare AC without C1) was incomplete even after 60 min of treatment (Fig. 6A).

Further, the adsorption of MO (30 mg L^{-1}) onto C1–AC and AC was determined to be ~9 mg L^{-1} and 12 mg L^{-1}, respectively (Fig. 6A, Table S2†), revealing that the adsorptive removal of MO by C1–AC and AC was incomplete.

It was observed that XPS of C1–AC treated with persulphate showed additional peaks at 401.6 eV and 854.8 eV that correspond to nitrogen (N1s) and trivalent nickel of C1 ($Ni2p_{3/2}$) (Fig. S8†), respectively.[53–59] Moreover, the iodometric titration

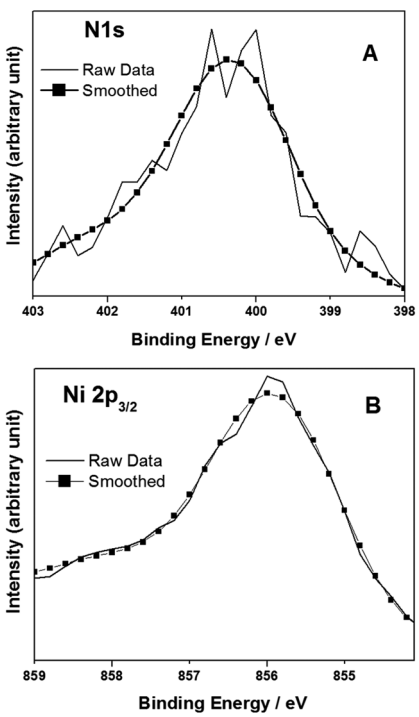

Fig. 5 XPS of C1–AC showing (A) N1s and (B) $Ni2p_{3/2}$ peaks.

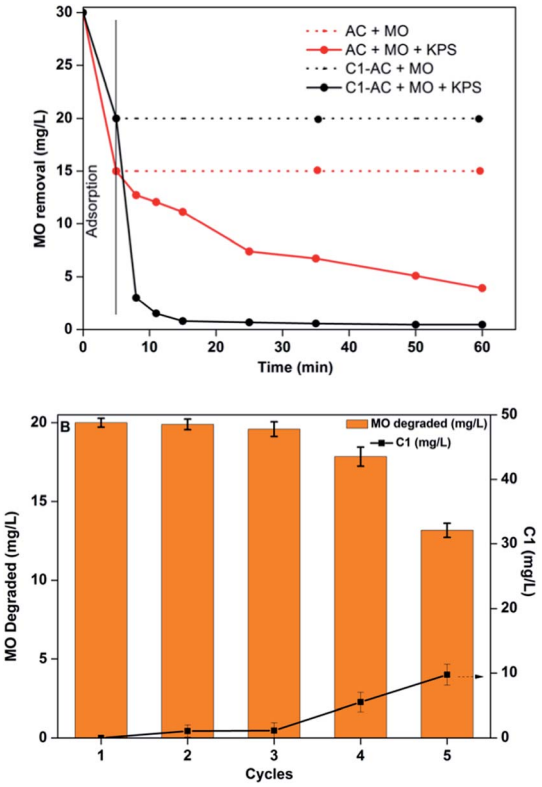

Fig. 6 (A) Plot showing MO degradation by KPS in the presence of AC and C1–AC. [AC] = 0.3 g L^{-1}; [C1–AC] = 0.3 g L^{-1} (16% loading; effective concentration of C1 is 48.3 mg L^{-1}); [KPS] = 1 g L^{-1}. The dotted lines represent the adsorptive removal of MO by AC and C1–AC in the absence of KPS. (B) Reuse of C1–AC. Reuse runs (cycles) for degradation of MO by C1–AC in the presence of KPS, and the corresponding concentration of C1 (in mg L^{-1}) at the end of each cycle in the treated solution. Initial concentration of MO at each cycle is 20 mg L^{-1}.

results, as discussed earlier, also revealed a higher consumption of persulphate (than the stoichiometric amount of C1) during the degradation of MO. All the above results, *i.e.* both the XPS and the iodometric titration results, reveal the redox reaction between C1 in solid form and KPS. C1–AC was reused five times to activate persulphate and degrade MO, in which almost the complete degradation of MO was observed for the first three reuse runs without significant loss of C1 from C1–AC (less than ~1 mg L^{-1} in each reuse run) (Fig. 6B). At fourth and fifth reuse runs, MO degradation was determined to be ~80% and 60%, respectively. Moreover, AAS analysis revealed that there was about 10% (5.52 mg L^{-1}) and 20% (9.7 mg L^{-1}) leaching of nickel from C1–AC into water at the fourth and fifth reuse runs, respectively (Fig. 6B and S9†). The reusability of C1–AC was also observed for the degradation of MO carried out in simulated natural water (Fig. S10†). All the above results reveal that AC is useful to recover C1 and reuse C1 as solid C1–AC.

Although C1 was effectively adsorbed onto Am, the solid C1–Am was not effective in activating persulphate and degrading MO, unlike the solid C1–AC discussed above. It is proposed that the electrostatic repulsion between the negatively charged Am and persulphate anion is not favourable for their interaction to activate the persulphate anion by the C1 adsorbed onto Am.

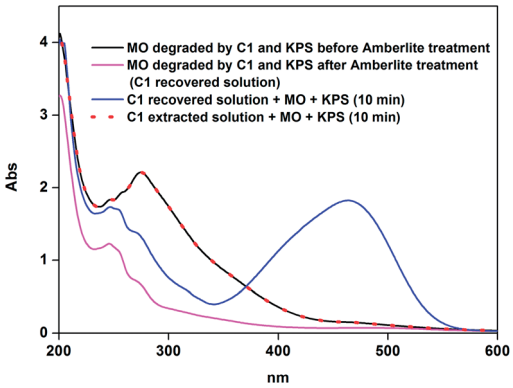

Fig. 7 Reusability of C1 using Amberlite. [MO] = 20 mg L^{-1}; [KPS] = 1 g L^{-1}; [C1] = 48.3 mg L^{-1}; [Am] = 15 mg L^{-1}.

However, the adsorption of C1 onto Am was useful in completely recovering the homogeneous C1 from the degraded MO solution, as revealed by absorption and AAS results (Fig. 7, black and magenta). Further, the recovered C1–Am was ion exchanged using sodium chloride to obtain C1 (>85% (extracted) as determined from AAS), which was reused for MO degradation (Fig. 7, red dotted line).

Almost similar results were also observed for the degradation of MO carried out in simulated natural water (Fig. S11†). Thus, Am was useful in a metal complex activated persulphate based AOP for adsorptive recovery of the complex, and for the reuse of the complex in homogeneous form after the ion exchange process.

Conclusions

In summary, a homogeneous metal complex based persulphate activator, C1, was recovered by adsorption onto AC and Am. C1 adsorbed onto AC (C1–AC) showed the ability to activate persulphate and degrade MO. Moreover, solid C1–AC was reused to activate persulphate and degrade MO without significant leaching of nickel into the solution. Additionally, the recovered C1–Am was ion exchanged to obtain C1, which was reused for MO degradation. These results demonstrate the application of adsorbents to recover and reuse a metal complex based persulphate activator.

Recovery and reuse of a metal complex based persulphate activator is advantageous in persulphate based AOP for the treatment of natural or ground water contaminated with recalcitrant pollutants from industries and other sources. The study draws attention to the application of adsorbents in metal complexes that can activate persulphate based AOP for the removal of metal based persulphate activators from water after the treatment, preventing the entry of metal ions into water bodies. Moreover, the study highlights the recyclability of an effective metal complex based persulphate activator using versatile adsorbents.

Acknowledgements

H.P. acknowledges research grant no. BT/PR133316/GBP/27/251/2009 from Department of Biotechnology (DBT),

Government of India. H.P also acknowledges research support from Aditya Birla Groups, India. G.S acknowledges Council of Scientific and Industrial Research (CSIR) for fellowship. We thank Dr Kannan, CCAMP, NCBS, TIFR, Bengaluru for the ESI-LCMS analysis. We are grateful to Dr Nitin Borkar, Dr Subashranjan Acharya and Vergo Pharma team for TOC measurements. The authors thank Goa State Pollution Control Board, Government of India, for AAS analysis support.

Notes and references

1 J. M. Fraile, J. I. Garcia and J. A. Mayoral, *Chem. Rev.*, 2008, **109**, 360–417.
2 P. Barbaro and F. Liguori, *Chem. Rev.*, 2008, **109**, 515–529.
3 P. McMorn and G. J. Hutchings, *Chem. Soc. Rev.*, 2004, **33**, 108–122.
4 A. F. Trindade, P. M. P. Gois and C. A. M. Afonso, *Chem. Rev.*, 2009, **109**, 418–514.
5 S. Sabater, J. A. Mata and E. Peris, *ACS Catal.*, 2014, **4**, 2038–2047.
6 M. A. Lebedeva, T. W. Chamberlain, M. Schrader and A. N. Khlobystov, *Chem. Mater.*, 2014, **26**, 6461–6466.
7 D. T. Genna, A. G. Wong-Foy, A. J. Matzger and M. S. Sanford, *J. Am. Chem. Soc.*, 2013, **135**, 10586–10589.
8 Q. Zhao, C. Bai, W. Zhang, Y. Li, G. Zhang, F. Zhang and X. Fan, *Ind. Eng. Chem. Res.*, 2014, **53**, 4232–4238.
9 A. S. Novikov, M. L. Kuznetsov, A. J. L. Pombeiro, N. A. Bokach and G. B. Shulâpin, *ACS Catal.*, 2013, **3**, 1195–1208.
10 A. Burg, I. Shusterman, H. Kornweitz and D. Meyerstein, *Dalton Trans.*, 2014, 9111–9115.
11 G. P. Anipsitakis and D. D. Dionysiou, *Environ. Sci. Technol.*, 2004, **38**, 3705–3712.
12 X. He, A. A. de la Cruz, K. E. O'Shea and D. D. Dionysiou, *Water Res.*, 2014, **63**, 168–178.
13 S. Gokulakrishnan, P. Parakh and H. Prakash, *J. Hazard. Mater.*, 2012, **213–214**, 19–27.
14 G. Subramanian, P. Parakh and H. Prakash, *Photochem. Photobiol. Sci.*, 2013, **12**, 456–466.
15 S. Ahn, T. D. Peterson, J. Righter, D. M. Miles and P. G. Tratnyek, *Environ. Sci. Technol.*, 2013, **47**, 11717–11725.
16 Y. Ding, L. Zhu, A. Huang, X. Zhao, X. Zhang and H. Tang, *Catal. Sci. Technol.*, 2012, **2**, 1977–1984.
17 C. Qi, X. Liu, C. Lin, X. Zhang, J. Ma, H. Tan and W. Ye, *Chem. Eng. J.*, 2014, **249**, 6–14.
18 N. S. Shah, X. He, H. M. Khan, J. A. Khan, K. E. O'Shea, D. L. Boccelli and D. D. Dionysiou, *J. Hazard. Mater.*, 2013, **263**, 584–592.
19 M. G. Antoniou, A. A. de la Cruz and D. D. Dionysiou, *Appl. Catal., B*, 2010, **96**, 290–298.
20 X. He, A. A. de la Cruz and D. D. Dionysiou, *J. Photochem. Photobiol., A*, 2013, **251**, 160–166.
21 R. H. Waldemer, P. G. Tratnyek, R. L. Johnson and J. T. Nurmi, *Environ. Sci. Technol.*, 2006, **41**, 1010–1015.
22 R. Haines and J. Rowley, *J. Inclusion Phenom. Macrocyclic Chem.*, 2003, **47**, 25–32.
23 R. I. Haines and S. J. Northcott, *Can. J. Chem.*, 1992, **70**, 2785–2791.
24 Q. Yang, H. Choi, Y. Chen and D. D. Dionysiou, *Appl. Catal., B*, 2008, **77**, 300–307.
25 Y.-H. Guan, J. Ma, Y.-M. Ren, Y.-L. Liu, J.-Y. Xiao, L. Q. Lin and C. Zhang, *Water Res.*, 2013, **47**, 5431–5438.
26 P. R. Shukla, S. Wang, H. Sun, H. M. Ang and M. Tada, *Appl. Catal., B*, 2010, **100**, 529–534.
27 M. Pu, Y. Ma, J. Wan, Y. Wang, M. Huang and Y. Chen, *J. Colloid Interface Sci.*, 2014, **418**, 330–337.
28 Z. Huang, H. Bao, Y. Yao, W. Lu and W. Chen, *Appl. Catal., B*, 2014, **154–155**, 36–43.
29 P. Parakh, S. Gokulakrishnan and H. Prakash, *Sep. Purif. Technol.*, 2013, **109**, 9–17.
30 M. Dabioch, R. Skorek, A. Kita, P. Janoska, K. Pytlakowska, P. Zerzucha and R. Sitko, *Cent. Eur. J. Chem.*, 2013, **11**, 742–753.
31 E. Okoniewska, J. Lach, M. Kacprzak and E. Neczaj, *Desalination*, 2007, **206**, 251–258.
32 P. E. Franco, M. R. T. Veit, C. E. Borba, G. d. C. Gonasalves, M. r. R. Fagundes-Klen, R. Bergamasco, E. A. da Silva and P. Y. R. Suzaki, *Chem. Eng. J.*, 2013, **221**, 426–435.
33 A. Demirbas, E. Pehlivan, F. Gode, T. Altun and G. Arslan, *J. Colloid Interface Sci.*, 2005, **282**, 20–25.
34 M. K. Jha, N. Van Nguyen, J. C. Lee, J. Jeong and J.-M. Yoo, *J. Hazard. Mater.*, 2009, **164**, 948–953.
35 K. V. Gobi and T. Ohsaka, *J. Electroanal. Chem.*, 2000, **485**, 61–70.
36 M. P. Suh, H. R. Moon, E. Y. Lee and S. Y. Jang, *J. Am. Chem. Soc.*, 2006, **128**, 4710–4718.
37 M. P. Suh and S. G. Kang, *Inorg. Chem.*, 1988, **27**, 2544–2546.
38 N. Wahba, M. F. El Asmar and M. M. El Sadr, *Anal. Chem.*, 1959, **31**, 1870–1871.
39 A. Rastogi, S. R. Al-Abed and D. D. Dionysiou, *Appl. Catal., B*, 2009, **85**, 171–179.
40 S. Yuan, P. Liao and A. N. Alshawabkeh, *Environ. Sci. Technol.*, 2013, **48**, 656–663.
41 O. Hamdaoui and E. Naffrechoux, *J. Hazard. Mater.*, 2007, **147**, 381–394.
42 G. D. Halsey, *Adv. Catal.*, 1952, **4**, 259–269.
43 D. Kalyani, S. Phugare, U. Shedbalkar and J. Jadhav, *Ann. Microbiol.*, 2011, **61**, 483–491.
44 Y. P. Chen, S.-Y. Liu, H.-Q. Yu, H. Yin and Q. R. Li, *Chemosphere*, 2008, **72**, 532–536.
45 G. K. Parshetti, A. A. Telke, D. C. Kalyani and S. P. Govindwar, *J. Hazard. Mater.*, 2010, **176**, 503–509.
46 W. Li, D. Li, J. Xian, W. Chen, Y. Hu, Y. Shao and X. Fu, *J. Phys. Chem. C*, 2010, **114**, 21482–21492.
47 W. Li, D. Li, Y. Lin, P. Wang, W. Chen, X. Fu and Y. Shao, *J. Phys. Chem. C*, 2012, **116**, 3552–3560.
48 K. Dai, H. Chen, T. Peng, D. Ke and H. Yi, *Chemosphere*, 2007, **69**, 1361–1367.
49 X. He, A. A. de la Cruz, K. E. O'Shea and D. D. Dionysiou, *Water Res.*, 2014, **63**, 168–178.
50 B. Neppolian, E. Celik and H. Choi, *Environ. Sci. Technol.*, 2008, **42**, 6179–6184.

51 I. Zilbermann, A. Meshulam, H. Cohen and D. Meyerstein, *Inorg. Chim. Acta*, 1993, **206**, 127–130.
52 V. Lepentsiotis, J. Domagala, I. Grgic, R. van Eldik, J. G. Muller and C. J. Burrows, *Inorg. Chem.*, 1999, **38**, 3500–3505.
53 J. Matienzo, L. I. Yin, S. O. Grim and W. E. Swartz, *Inorg. Chem.*, 1973, **12**, 2762–2769.
54 S. Roe, J. Hill and J. Liesegang, *Transition Met. Chem.*, 1985, **10**, 100–106.
55 X. Solans-Monfort, J. L. G. Fierro, L. Hermosilla, C. Sieiro, M. Sodupe and R. Mas-Balleste, *Dalton Trans.*, 2011, 6868–6876.
56 Q. Zhang, J.-P. Ma, P. Wang, Z.-Q. Shi, Y.-B. Dong and R.-Q. Huang, *Cryst. Growth Des.*, 2008, **8**, 2581–2587.
57 V. Etacheri, M. K. Seery, S. J. Hinder and S. C. Pillai, *Inorg. Chem.*, 2012, **51**, 7164–7173.
58 P. Periyat, D. E. McCormack, S. J. Hinder and S. C. Pillai, *J. Phys. Chem. C*, 2009, **113**, 3246–3253.
59 Z. Yang, Y. Miao, T. Wang, X. Liang, M. Xiao, W. Li and Y. Yang, *J. Electrochem. Soc.*, 2014, **161**, H375–H378.